Development of the Mesencephalic Trigeminal Nucleus in the Zebrafish

Dyer, Carlene

Awarding institution:
King's College London

Title: Development of the Mesencephalic Trigeminal Nucleus in the Zebrafish

Author: Carlene Dyer

Development of the Mesencephalic Trigeminal Nucleus in the Zebrafish

By

Carlene J. Dyer

A thesis submitted to Kings College London in part fulfilment of the requirement for the degree of Doctor of Philosophy (PhD)

MRC Centre for Developmental Neurobiology,

Kings College London

December 2011

Abstract

The mesencephalic trigeminal nucleus (MTN) forms part of the monosynaptic trigeminal circuit and is essential for eating and suckling in mammals. Little is known about how the MTN forms. For this thesis I aimed to elucidate the molecular and cellular basis of MTN development. I also aimed to investigate the role of the Fgf and Wnt signalling pathways in MTN development.

The zebrafish was used as a model organism to investigate these aims. Putative MTN cells in zebrafish larvae were retrogradely labelled by applying DiI to the adductor mandibulae, a jaw closing muscle. Labelled axons projected from muscles via the trigeminal ganglion to cell bodies in the dorsal anterior mesencephalon, suggesting that the MTN does innervate jaw muscles in teleosts, contrary to previous studies.

Molecular characterisation of the MTN in zebrafish revealed a similar expression profile as the mammalian MTN. To investigate whether MTN neurons are neural crest-derived, the neural crest was ablated, which resulted in an increase in MTN number. This suggests that the neural crest may play an inhibitory role in MTN development contradictory to previous studies in chick that suggested MTN neurons are derived from the neural crest.

The role of the Fgf and Wnt signalling pathways was investigated by analysis of mutants and drug treatments where the pathways had been genetically or chemically manipulated. Down-regulation of Fgf signalling showed an increase in MTN neuron numbers, suggesting that Fgf signalling from the midbrain/hindbrain boundary inhibits development of the MTN in the midbrain. When the Wnt pathway was up-regulated there was also an increase in MTN neuron number. Based on the results from these experiments a model is proposed, in which Fgf signalling regulates the formation of MTN neurons in a spatial and temporal manner, and Wnt signals from the dorsal roof plate induce the proliferation of MTN precursor cells.

Acknowledgements

I'd like to say a big thank you to my supervisor Robert Knight for giving me the opportunity to work on this interesting project, and for all his support, guidance and enthusiasm.

I would also like to thank my fellow lab partner Kaz Yokoya for his support and encouragement, especially over the writing up months, and to past lab member Arturo D'Angelo for helping me find my way around the lab and teaching me new techniques. Also thank you to temporary members of the Knight Lab who made our small busy lab feel even busier.

Another big thank you goes to all the members of the fish labs in the centre, for helping me with advice and reagents. In particular thank you to Paula, Joao, and Marie for their advice and the use of their transgenic fish lines. Thank you also to Jon Clarke for showing me the electroporation method and for the use of his electroporating equipment.

Another thank you goes to the fish labs at UCL for probes, and the use of some of their fish lines. In particular thank you to Tom Hawkins for welcoming me into the UCL fish group lab and for allowing me to use their injection set up for experiments at UCL. Also thank you to Issac for showing me the best technique to use for retrograde labelling with DiI, and a big thank you to Gaia for giving me the *tfap2c* morpholino, without her I may still be trying to get results from *tfap2a* morpholino injections into *low* mutant fish.

Thank you to everyone at the MRC centre for many conversations which has helped me to progress with my work in some way, and for creating a fantastic working atmosphere to help make the last three years very enjoyable.

Thank you very much to my family Mum, Dad, Jason and Mark, for all their never-ending support and encouragement over the last three years. Lastly, but certainly not least a massive thank you to my partner Scott for his support, encouragement, and unwavering patience.

Table of Contents

List of Figures

page

Chapter 1

Chapter 3

Chapter 4

Chapter 5

Chapter 6

List of Tables

List of Appendices

Abbreviations

AP: anterior-posterior

a.m.: adductor mandibulae

CNCC: Cranial neural crest cells

CNS: Central nervous system

dd: Dorsal diencephalon

DiI: 1,1'-dioctadecyl-3,3,3',3'- tetramethylinocarbocyanine perchlorate

DiD: 1,1′-dioctadecyl-3,3,3′,3′-tetramethylindodicarbocyanine, 4-chlorobenzenesulfonate salt

dpf: Days post fertilisation

DRG: Dorsal root ganglia

DV: dorsal-ventral

GFP: Green fluorescent protein

HRP: Horseradish peroxidase

i.r.: inferior rectus

KWT: Kings Wild Type

l.a.p.: levator arcus palatini

LLF: Lateral longitudinal fasciculus

MHB: midbrain hindbrain boundary

mlf: medial longitudinal fasciculus

MTN: Mesencephalic trigeminal nucleus

NCC: neural crest cell

nIV: Trochlear nerve

nTPC: nuclei of the tract of the posterior commissure

nV: Trigeminal motor neuron

P1: Prosomere 1

PNS: Peripheral nervous system

R2: Rhombomere 2

RB: Rohon-Beard

ss: Somite stage

TPC: Tract of the posterior commissure

TPOC: Tract of the post optic commissure

TTC: Truncated Tetanus Toxin

WGA: Wheatgerm Agglutinin

Chapter 1 – Introduction

Neuronal circuits regulate muscle function by sensing muscle stretch and then modulating motor neuron activity. The development of the neuronal circuits that regulate proprioception in the limb have been extensively studied, but far less is known about the formation of neuromuscular circuits in the head (Arber et al., 2000; Livet et al., 2002; Hippenmeyer et al., 2005). The monosynaptic trigeminal circuit in the head comprises trigeminal afferents from the sensory mesencephalic nucleus of the trigeminal nerve, located in the midbrain, and efferents from the motor nucleus of the trigeminal nerve located in the hindbrain. In amniotes these neurons form a monosynaptic reflex arc with masticatory muscles of the mandibular arch that are formed from the first branchial arch. This circuit is required for conveying information important for controlling the jaw movement and biting force during eating and suckling.

Jaws evolved from the mandibular arch in an ancestral gnathostome following the divergence of agnathans (such as the lamprey) and jawed vertebrates (Pough et al., 2009). Early gnathostomes lacked teeth, and therefore it has been suggested that jaws were initially important for respiration by regulating the flow of oxygenated water to the gills (Butler and Hodos, 2005). Evolution of jaws in gnathostomes altered the way in which animals fed and therefore the way they lived (Mallatt, 1996). The trigeminal nerve is most closely associated with the development of the jaws as it innervates mandibular arch muscles, and is most developed in animals with a prominent snout such as mammals (mouse, cat), birds and alligators; the development of whiskers further expanded the trigeminal system (Butler and Hodos, 2005; Mameli et al., 2010). The trigeminal nerve consists of three branches, the ophthalmic, maxillary and mandibular branches (Figure 1.1). The ophthalmic branch of the trigeminal nerve contains only sensory fibres that supply receptors in the eye orbit. The maxillary branch is also only formed of sensory fibres that supply receptors of the snout and upper jaw. The mandibular branch contains both sensory afferents and motor efferents that innervate the mandibular muscles (adductor mandibulae, lateral and medial pterygoideus and temporalis) that are required for jaw movement. The mandibular muscles form from the first branchial arch (Figure 1.1). The sensory afferents of the mandibular branch of the trigeminal nerve also supply receptors in the skin of the lower jaw.

Figure 1.1 – Peripheral distribution of the trigeminal nerve.

A schematic of a vertebrate head showing the three branches of the trigeminal nerve and the area in the head they innervate. The opthalmic branch innervates the eye orbit, the maxillary branch innervates the perioral area of the nose and upper jaw, and the mandibular branch innervates the mandibular muscles, teeth and perioral area of the lower jaw. am, adductor mandibulae. do, dilator operculi. lap, levator arcus palatini. nV, trigeminal motor nerve.

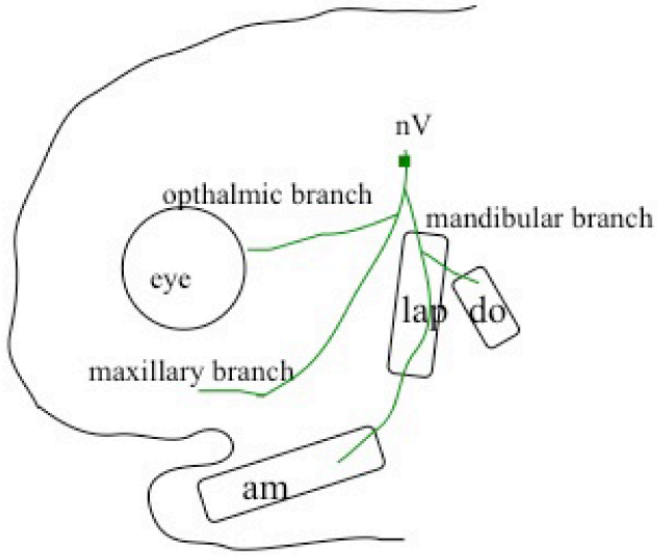

The most intriguing and least characterised component of the trigeminal circuit is the proprioceptive sensory afferent, the mesencephalic trigeminal nucleus (MTN). MTN neurons are unusual because they are located in the dorsal midbrain and rostral hindbrain (mammals only) within the central nervous system (CNS), unlike other adult sensory neurons that are located in the peripheral nervous system (PNS). The MTN are the first born neurons in the dorsal midbrain in vertebrates, and send out a single descending axon from their cell body. Tract tracing studies of the MTN using HRP in amniotes (lobe-finned bony fishes; see Figure 1.3) reveal the MTN innervates extraocular and masticatory muscles, and periodontal ligaments (Alvarado-Mallart et al., 1975; Figure 1.2A). In teleosts (ray-finned bony fishes) and sharks (cartilaginous fishes) however, the MTN does not appear to innervate extraocular or masticatory muscles, but instead innervates the adjacent skin of the jaw (Roberts and Witkovsky, 1975; Luiten, 1979; Figure 1.2B). These differences imply that the ancestral function of the MTN was not to provide proprioception for jaw muscles, and that this was an acquired function within the lobe-finned fish lineage (For phylogenetic trees see Figure 1.3).

Figure 1.2 – Monosynaptic trigeminal circuits in vertebrates

Diagrammatic representation of (A) a monosynaptic trigeminal circuit in the head of amniotes comprised of the mesencephalic trigeminal nucleus (MTN, purple), located in the midbrain (mb) and hindbrain (hb), the mandibular branch of the trigeminal motor nerve (nV, green) and mandibular arch muscles (am, lap, do). The MTN is also shown innervating the eye muscles together with the oculomotor motor nerve (nIII, blue; io, ir, mr, sr) and the trochlear motor nerve (nIV, red; so)(Alvarado-Mallart et al., 1975; Ruggiero et al., 1982). (B) Diagrammatic representation of the monosynaptic trigeminal circuit in the head of shark and fish in which the MTN only innervates the perioral area and teeth (in shark). am, adductor mandibulae. do, dilator operculi. hb,hindbrain. io, inferior oblique. ir, inferior rectus. lap, levator arcus palatini. mb, midbrain. nIII, oculomotor motor nerve. nIV, trochlear motor nerve. nV, trigeminal motor nerve. mr, medial rectus. so, superior oblique. sr, superior rectus.

A

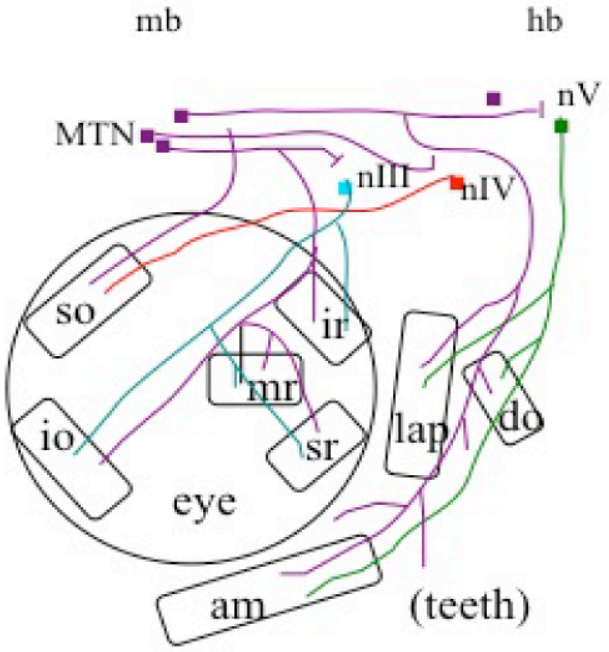
mb
hb
nV
MTN
nIII
nIV
so
ir
mr
io
sr
lap
do
eye
am
(teeth)

B

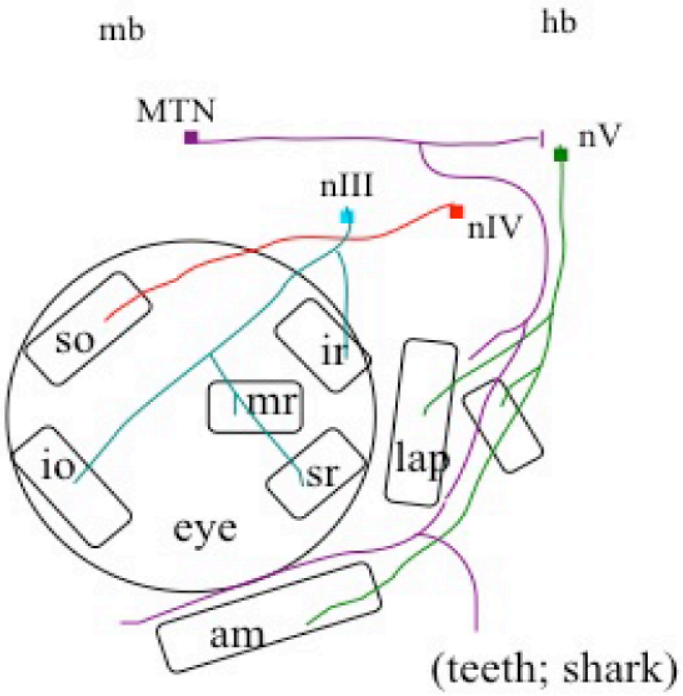
mb
hb
MTN
nV
nIII
nIV
so
ir
mr
io
sr
lap
eye
am
(teeth; shark)

Figure 1.3 – Phylogeny of chordates and ray-finned fish

(A) A phylogenetic tree of the chordates, and (B) phylogenetic tree of the actinopterygian lineage.

A

B

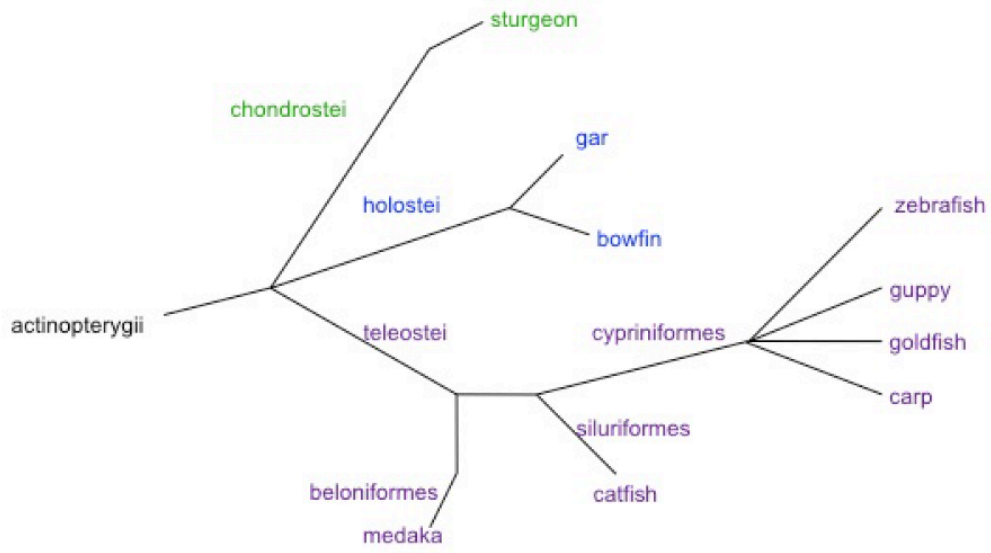

The cellular origin of MTN neurons is controversial, with early studies suggesting it is neural crest derived similar to other sensory neurons present in adult gnathostomes, while later studies did not find a neural crest contribution to the MTN (Narayanan and Narayanan, 1978; Baker et al., 1997a). However differing regions of NCCs were grafted in these experiments. In the earlier experiment early NCCs that have just left the neural tube were transplanted, which may remain closely associated with the neuroepithelium. In the later study migratory NCC that had moved away from the neural tube were transplanted. Therefore NCCs contributing to the MTN may remain closely associated with the neuroepithelium.

Fgf and Wnt signalling from the isthmus play important roles in specifying the regions of the brain (Rhinn and Brand, 2001; Wurst and Bally-Cuif, 2001). The role these signalling pathways play in MTN specification and differentiation from neighbouring cell types is not understood.

A better understanding of MTN development can contribute towards a paradigm for the formation of neuronal circuits, and to show how different sensory neurons are specified depending on the local cues they receive. It can also be used to begin to elucidate how these unusual neurons evolved.

1.1 – Early development of the embryonic brain

The central nervous system (CNS) is derived from the dorsal neuroectoderm (Wilson, 1997). In amniotes the release of molecular signals during gastrulation and neurulation induces the development of the neural plate, which rolls up along the anterior-posterior (AP) axis forming the neural tube (Lumsden and Krumlaf, 1997; Copp et al., 2003). In teleosts the neural tube forms by a different process in which a solid neural rod primordium forms, and undergoes a rearrangement of cells to form the neural tube (Clarke, 2009).

The anterior end of the neural tube swells giving rise to the anlagen of the forebrain, midbrain and hindbrain (Gilbert, 2003). Region specific expression and signalling of developmental control genes along the AP and dorsal-ventral (DV) axis patterns the neural tube, resulting in the refinement of the cellular domains within the brain (Vieira et al., 2010). The boundaries that form during this refinement, leads to the formation of secondary organising centres; the anterior neural ridge, zona limitans intrathalamica (ZLI), and isthmic organiser, which establishes positional information,

giving rise to the cellular diversity and structure of the brain (Houart et al., 1998; Kiecker and Lumsden, 2005; Figure 1.4). Patterning of the brain by specific genes is conserved across the vertebrate phyla revealing an underlying Bauplan (Kiecker and Lumsden, 2005).

Figure 1.4 – Organisation of a general vertebrate brain

Diagrammatic representation of the organisation of a vertebrate brain, indicating the forebrain (tel, telencephalon. di, diencephalon; yellow), midbrain (light blue) hindbrain (green) and the positions of the organisers (dark blue) that pattern the brain (anterior neural ridge (ANR), zona limitans intrathalamica (ZLI) and isthmus).

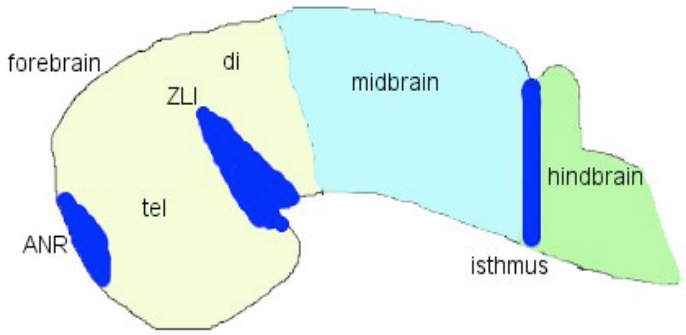

1.1.1 – Important cues required during gastrulation for early formation of the embryonic brain

In vertebrates, neural induction begins at mid gastrula stage of embryogenesis, as neural organising centres instruct neighbouring cells to become nervous system as opposed to epidermis (Streit et al., 2000). The neural organising centre was identified from transplant studies, in which the dorsal lip of the blastopore from one newt species was grafted into a ventral region of a different newt species during gastrulation (Spemann and Mangold, 1924). This led to the induction of host ventral tissues to change their fate from epidermis to become neural tube, and dorsal mesodermal tissue (Gilbert et al., 2003). The transplanted tissue also organised host and donor tissues to form a secondary embryo with clear anterior – posterior (AP) and dorsal – ventral (DV) axes. Similar transplants have been carried out in chick, and more

recently in mouse and zebrafish, which also resulted in the induction of ectopic neural plate, and subsequently a partial new embryonic axis (Waddington, 1933; Beddington 1994; Shih and Fraser, 1996). Such co-ordination by this transplanted tissue led to it being termed 'the organiser' in amphibians. These organising centres are present in most vertebrates. In teleosts, it is called 'the shield', in mammals it is called 'the node' and in birds 'Hensen's node' (Schier and Talbot, 1998; Boettger et al., 2001).

The default model for neural induction suggests that ectodermal cells are defaulted to differentiate into neural fates, but these are inhibited by bone morphogenetic proteins (BMPs), causing epidermal cells to form instead (Hemmati-Brivanlou and Melton, 1997). The organiser emits BMP antagonists; noggin, follistatin and chordin, which allows neural induction to occur in cells in the region of this organiser, specifying neural plate formation (Wilson and Hemmati-Brivanlou, 1997).

More recently however, earlier initiation factors of neural induction have been suggested (Beddington and Robertson, 1998; Streit et al., 2000). These studies propose that neural induction starts at the beginning of gastrulation, by FGF signalling from a population of organizer precursors at the posterior margin of the embryo (Streit et al., 2000). Therefore the later suppression of BMP signalling by the organiser acts to maintain neural differentiation (Vieira et al., 2010).

1.1.2 – Important cues required during early neurulation

Once neural induction is initiated by the suppression of BMP and the expression of Hox genes, the neural plate is specified and neurulation begins (Hooiveld et al., 1999; Linker and Stern, 2004). Neurulation is defined as the set of morphogenetic movements that result in the formation of the neural tube, and subsequently the future brain and spinal cord (Lowery and Sive, 2004). Two forms of neurulation occur in amniotes, these are primary and secondary neurulation. During primary neurulation the neural plate invaginates to form a neural groove which closes to form the neural tube (Schoenwolf and Smith 1990). Secondary neurulation is restricted to the caudal region of the trunk, and proceeds by the initial formation of a solid neural rod which cavitates to form the neural tube (Papan and Campos-Ortega, 1994). In teleosts secondary neurulation occurs to form the entire neural tube (Papan and Campos-Ortega, 1994).

In teleosts the anterior regions of the neural plate, that will form prospective forebrain, midbrain and hindbrain, is a multi-layered structure three – six cells deep

(Clarke, 2009). Above the neural plate is an enveloping layer (EVL) which is a monolayer of epithelial cells that surrounds the entire embryo during gastrulation, to protect the embryo from trauma (Sagerstrom et al., 2005). The neural plate cells converge towards the dorsal midline and invaginate to form a neural keel, which condenses through further convergence to form a solid neural rod primordium (Kimmel et al., 1994). Wnt/Planar cell polarity (PCP) signalling is required for the convergence of neural plate cells to the midline (Clarke, 2009). This has been demonstrated in Wnt/PCP mutants, in which neural plate convergence is delayed and fails to merge completely, generating a duplicate neural keel and subsequently duplicated neural tubes (Clarke, 2009). N-cadherins are also required to complete convergence of the neural plate (Hong and Brewster, 2006).

Once the neural plate cells have converged to the dorsal midline, they are positioned horizontally along the mediolateral axis with many cell bodies and cell processes lying across the midline (Concha and Adams, 1998). These cells re-arrange and become polarised in a process called C-division (crossing-division; Tawk et al., 2007). During C-division neural plate cells divide mediolaterally to form daughter cells with mirror image apical-basal polarity and morphology (Clarke, 2009). As the cells divide one daughter cell remains in the ipsilateral side of the neural keel, while the other daughter cells crosses the midline and integrates into the contra-lateral neuroepithelial layer (Concha and Adams, 1998; Ciruna et al., 2006). Pard3, a PDZ scaffolding protein, is required to mediate midline crossing and establish cell polarity (Macara, 2004; Tawk et al., 2007). During C-division, Pard3 is localised to the cleavage furrow between daughter cells, and both inherit Pard3 expression at their apical poles (Tawk et al., 2007). The apical ends of the daughter cells expressing Pard3, line the lumenal surface of the neural tube (Clarke, 2009). The formation of mirror-symmetric apical-basal cells and their rearrangement during C-division are important for formation of the lumen within the neural tube.

In non-teleost vertebrates during primary neurulation the underlying axial mesoendoderm signals the ectodermal cells above to elongate into columnar neural plate cells (Smith and Schoenwolf, 1989; Keller 1992). The axial mesoendoderm regulates DV polarity of the developing neural plate resulting in the expression of the ventralising factor *Shh* in the floor plate. Signalling from the organiser through the plane of the ectodermal epithelium regulates AP regionalisation by secreting BMP antagonists (Vieira et al., 2010).

The changes in cell shape, together with intrinsic movements of the epidermal

and neural plate regions during convergent extension, results in the lengthening and bending of the neural plate. Wnt/PCP signals promote the convergence of neural progenitors towards the dorsal midline (Wallingford et al., 2002). As the neural plate bends, hinge regions form, where the neural plate contacts the surrounding tissue (Colas and Schoenwolf, 2001). For example the floor plate contacts the mesoendoderm, which secretes Wnt antagonists and therefore patterns ventral brain structures, in particular within the presumptive forebrain (Wilson and Houart, 2004).

During the continued folding of the neural plate, it becomes regionalised by early developmental control genes. The neural plate is specified ventrally by *Shh* expression (encoding a secreted signalling protein), the presumptive basal plate expresses *Six3*, while the more dorsal alar plate expresses dorsalising transcription factor *Nkx6.1*. The expression of homeodomain transcription factors *Otx2* and *Gbx2* regulates AP regionalisation in the brain (Rubenstein and Shimamura, 1998). *Otx2* is expressed from the anterior limit of the neural plate to the posterior border of the presumptive midbrain hindbrain boundary (MBH), and *Gbx2* is expressed in the posterior region of the neural plate in the presumptive hindbrain (Rhinn and Brand 2001).

As convergent extension continues, this causes the formation of neural folds, which meet at the dorsal midline. This causes the detachment of the epidermal ectoderm from each fold of its ipsilateral neuroepothelial partner, which fuses together with the adjacent epidermal ectoderm (Vieira et al., 2010). The neuroepithelial layers also fuse, resulting in the closure and formation of the roof plate, of the neural tube (Vieira et al., 2010). The roof plate expresses BMPs which now act as dorsalising factors (Nguyen et al., 2000).

Once the neural tube has formed in vertebrates, the earliest subdivisions of the brain develop from the most anterior end, that expands and swells along the mediolateral axis, giving rise to vesicles representing the anlagen of the forebrain, midbrain and hindbrain (Lumsden and Krumlauf, 1996; Figure 1.4). Region specific expression of developmental control genes within these anlagen result in the refinement of these domains (Lumsden and Krumlauf, 1996). AP regionalisation within the neural tube is initially regulated by the expression of *Otx2* and *Lim1* (Rubenstein and Shimamura, 1998). Subsequently Fgfs, retinoic acid and Wnts further regulate AP regionalisation and act as posteriorising factors (Gamse and Sive, 2000; Wilson and Houart, 2004); and specific homeodomain transcription factors (*eng2/3*) maintain the separate forebrain, and midbrain domains (Figure 1.4; Scholpp et al., 2003).

1.1.3 – Development of the forebrain

The forebrain develops at the most anterior/rostral end of the neural tube. The regionalisation of this domain begins during the formation of the neural plate. In response to neural induction, a small number of cells form at the anterior end of the neural plate. These initially express *Otx2*, and then *Fgf8*, which causes the reduction of *Otx2* expression in these cells, but not in the surrounding cells. This *Fgf8* expressing domain is closely associated with tissues expressing *Bmp4* and *Shh* (Crossley et al., 2001). It is believed that the decreased BMP suppression in this region allows for the formation of these cells, which form the secondary organiser; the anterior neural ridge (ANR), that regulates telencephalic regionalisation (Wilson and Houart, 2004; Figure 1.5). The ANR was first identified in zebrafish, by transplanting a group of anterior ectodermal cells from the presumptive anterior forebrain to more posterior regions (Houart et al., 1998). This resulted in the ectopic expression of telencephalic markers *dlx2* and *emx1*, indicating that these cells produce a signal that can induce gene expression required for forebrain development (Houart et al., 1998). The ANR has been shown to pattern the forebrain in other species as well. In chick the ANR appears to regionalise the telencephalon by the initial expression of *Fgf8*, which inhibits *Otx2* and *Emx2* expression (Crossley et al., 2001). Mouse studies have shown that *Otx2* and *Six3* are required in order for a cellular response to signals from the ANR (Tian et al., 2002). *Fgf8* also induces *FoxG1*, which plays an important role in the proliferation of telencephalic precursors (Shimamura and Rubenstein, 1997; Storm et al., 2002). *Shh*, the ventralising factor, is expressed close to the ANR, and represses the expression of *Gli3* allowing for the formation of the telencephalon. The ANR also secretes Wnt antagonists, such as Frizzled Related Protein (sFRP) Tlc, to promote telencephalic development. Studies in mice in which forebrain precursor *Six3* was knocked out, reveals a loss of Wnt inhibition that subsequently results in a loss of telencephalic tissue (Lagutin et al., 2003). A similar loss is seen in the Zebrafish *masterblind* (*mbl*) mutant, which has a mutation in the Wnt inhibitor scaffolding protein *axin1* (van de Water et al., 2001). These *mbl* mutants exhibit a loss of the telencephalon, and the diencephalon is expanded anteriorly (Heisenberg et al., 2001). These experiments show that Wnts need to be antagonized to maintain ventral forebrain structures.

More caudally to the ANR, a wedge shaped expression of *Wnt8B* in the forebrain anlage, with anterior expression of *Six3* and the posterior expression of *Irx3* either side, appears to pre-pattern another secondary organiser called the zona limitans

intrathalamica (ZLI) (Kiecker and Lumsden, 2005; Figure 1.5). The ZLI is required for formation of the diencephalon, and expresses *Shh* which in turn induces *Dlx2* and *Sox14*, required for forming the prethalamus and thalamus respectively (Kiecker and Lumsden, 2004; Scholpp et al., 2006).

Figure 1.5 – Patterning of the forebrain by the ANR and the ZLI organisers
Diagrammatic representation of the signals from the anterior neural ridge (ANR, blue) organiser that pattern the telencephalon, and the signals from the zona limitans intrathalamica (ZLI, blue) that pattern the diencephalon.

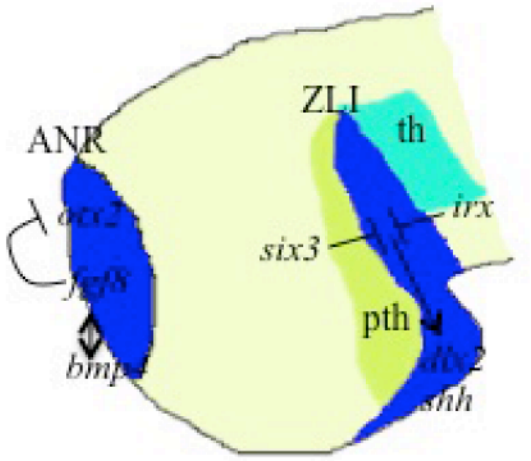

After the forebrain has been patterned in zebrafish, it is comprised of the rostrally located telencephalon and eyes, the hypothalamus located ventrally, and the diencephalon, that is located more caudally. Within the diencephalon is the ventral and dorsal thalamus, with the ZLI located between them, and the pre-tectum (Wilson and Houart, 2004; Figure 1.5).

Early studies investigating forebrain development led to the proposal of the prosomeric model which suggested the forebrain consisted of six subdivisions called prosomeres, three in the telencephalon and three in the diencephalon (Rubenstein et al., 1994). Later fate-mapping studies of the chick forebrain, showed no lineage restriction in the telencephalon, so this prosomeric model has been revised to suggest that there are only prosomeres in the diencephalon (Puelles and Rubenstein, 2003). However there is evidence for lineage restrictions between diencephalic and mesencephalic cells in chick suggesting there is a boundary between the forebrain and midbrain (Larsen et al., 2001).

1.1.4 – Development of the midbrain and isthmic organiser

The isthmic organiser is located at the midbrain hindbrain boundary (MHB) and is required for the formation and maintenance of the midbrain and hindbrain in vertebrates (Rhinn and Brand, 2001). Early expression of *Otx2* in the anterior region of the neural plate up to the presumptive MHB, and *Gbx2* expression posterior to this, is important for the formation of the isthmic organiser in amniotes (Joyner et al., 2000; Wurst and Bally-Cuif, 2001). In zebrafish, *gbx2* is expressed much later at 90% epiboly and is only required to maintain the isthmus (Kikuta et al., 2003). Instead *gbx1* is expressed early in the prospective hindbrain during mid gastrulation at 60% epiboly (Rhinn and Brand, 2001). *otx2* and *gbx1* expression are independently established, and their domains initially overlap by 3-4 cells (Rhinn et al., 2003). As gastrulation proceeds *otx2* and *gbx1* expression abuts, as they repress one another causing the refinement of their expression domains (Rhinn et al., 2003). The interface between *otx2/gbx1* is the equivalent to *Otx2/Gbx2* in amniotes and establishes the isthmic organiser at the MHB (Rhinn and Brand, 2001; Rhinn et al., 2009; Figure 1.7a).

Studies in mice have demonstrated the importance of *Otx2* and *Gbx2*, in the formation of the isthmic organiser, and therefore midbrain development. In *Otx2* null mutant mice, brain structures rostral to rhombomere 3 fail to develop (Ang et al., 1996). The ectopic expression of *Otx2* in the anterior hindbrain results in the posterior shift of the MHB (Broccoli et al., 1999). In *Gbx2* null mutant mice the opposite occurs, the anterior hindbrain fails to develop, and is re-specified as midbrain, which expands posteriorly as shown by ectopic *Otx2* expression (Millet et al., 1999; Rhinn and Brand, 2001). Similarly *gbx1* loss of function studies in zebrafish reveal a posterior shift in the MHB (Rhinn et al., 2009). Conversely over-expression of *gbx1* represses *otx2* causing an anterior shift in MHB formation, and a reduction in forebrain and midbrain (Rhinn et al., 2009).

At the interface of *otx2* and *gbx1* expression in the presumptive MHB, *pax2.1 (Pax2* in mouse and chick) expression is activated at 80% epiboly. Shortly after *pax2.1* is expressed, it induces the expression of *eng2/3* (*En1* in mouse and chick), *wnt1* and *fgf8* which results in the formation of the isthmic organiser (Rhinn and Brand, 2001). The isthmic organiser specifies *pax2.1* (*Pax2*) and *eng2/3* (*En1*) expression in the midbrain that inhibits *pax6* expression in this region, maintaining midbrain identity (Wurst and Bally-Cuif, 2001; Scholpp et al., 2003; Figure 1.7b). An *Fgf8* gradient along the AP axis of the midbrain and hindbrain also forms. In the hindbrain this causes the

inhibition of *Hox* genes in rhombomere 1. The expression of specific *Hox* genes along the AP axis of the hindbrain specifies rhombomeric segmentation and is controlled by graded retinoic acid signalling (Kiecker and Lumsden, 2005).

Analysis of *no isthmus* (*noi*) mutants in zebrafish (mutant for *pax2.1*) indicates the importance of *pax2.1* in the formation of the isthmus, as they lack posterior midbrain, MHB and cerebellum (Lun and Brand, 1998). *eng2/3* is lost in *noi* mutants revealing its expression is dependent on *pax2.1*, unlike *fgf8* and *wnt1* which are initially expressed. *fgf8* and *wnt1* expression are later lost in *noi* indicating that *pax2.1* and *eng2/3* are required to maintain their expression (Lun and Brand, 1998). Similarly in *acerebellar* (*ace*) zebrafish mutants, in which *fgf8* expression is reduced, *pax2.1*, *eng2/3* and *wnt1* are expressed early on (from 80% epiboly), but not maintained (from 6 ss/10 hpf) (Reifers et al., 1998; Jaszai et al., 2003). *ace* mutants lack the MHB and cerebellum, and the AP identity of the midbrain is disrupted, shown by mapping defects of retinal ganglion cell (RGC) axons on the optic tectum and loss of rostral midbrain structure (Lee et al., 1997; Picker et al., 1999). These studies indicate that later in embryonic development, the expression territories of *fgf8*, *wnt1*, and *eng2/3* and *pax2*, become interdependent and establish a positive regulatory feedback loop (Wurst and Bally-Cuif, 2001; Figure 1.6). This feedback loop maintains the organising activity at the MHB, and the rostrocaudal identity of the midbrain and anterior hindbrain (Lee et al., 1997).

Figure 1.6 – Patterning the midbrain by the isthmic organiser

Diagrammatic representation of (A) the formation of the midbrain hindbrain boundary (MHB) which forms at the interface of *otx2* and *gbx1* expression, and (B) the regulatory feedback loop between *fgf8* (green), *wnt1* (blue), *pax2.1* and *eng2/3* which maintains the organising activity of the isthmus required for specifying and maintaining the rostro-caudal identity of the midbrain (mb). fb, forebrain.

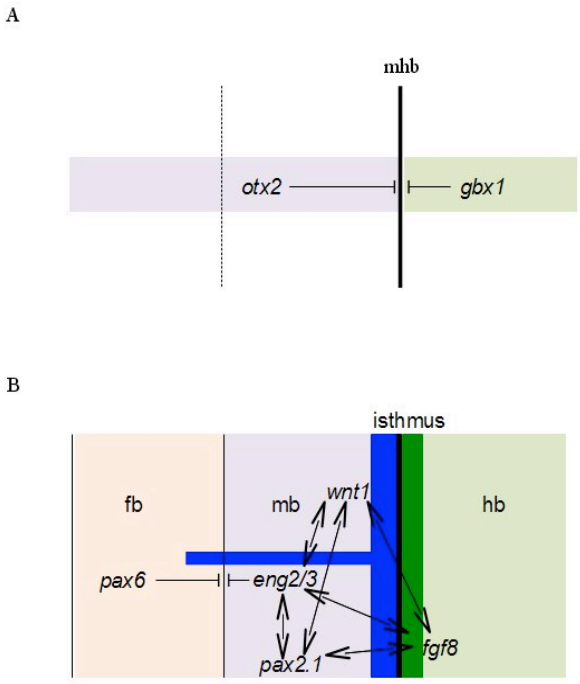

fgf8 expression at the MHB mediates organising activity of the isthmus. This has been shown in *ace* mutants where the absence of *fgf8* leads to the loss of the isthmus/MHB (Brand et al., 1996). A role for *Fgf8* in conferring A-P polarity in the midbrain and formation of the cerebellum has also been demonstrated by the ectopic expression of Fgf8 protein in the diencephalon of chick, which induces the midbrain and cerebellum (Crossley et al., 1996; Martinez et al., 1999). In contrast, when *Fgf8* is reduced in mice, the isthmus and cerebellum fail to develop, and posterior mesencephalic cells develop into anterior midbrain (Basson et al., 2009). When *Wnt1* is ectopically expressed in rhombomere 1, there is no induction of midbrain formation, further indicating the importance of *Fgf8* in the formation of the isthmus (Panhuysen et al., 2004). The ectopic expression of *pax2.1* (*Pax2*) and *eng2/3* (*En1*) in the diencephalon of zebrafish or chick leads to the induction of *fgf8* and *wnt1*, and the repression of forebrain specific marker *pax6.1* (*Pax6*) (Okafuji et al., 1999; Wurst and

Bally-Cuif, 2001).

The forebrain midbrain boundary is maintained by the specific expression of homeodomain protein *pax6.1* (*Pax6*) in the diencephalon, and *pax2.1* (*Pax2/5*) in the mesencephalon (Scholpp and Brand 2003). This maintenance of the boundary has been demonstrated in mice lacking *Pax6* function, in which the midbrain expands anteriorly into presumptive forebrain territory (Mastick et al., 1997). Conversely when *pax2.1* function is lost in zebrafish *noi* mutants, the posterior forebrain expands into the midbrain territory; shown by the extended expression of forebrain marker *pax6* (Scholpp and Brand, 2003). The nucleus of posterior commissure (nTPC), which lies at the diencephalic mesencephalic boundary (DMB), and is used as an anatomical landmark for this boundary, is extended in size (Scholpp and Brand 2003).

In mouse the loss of *Pax2/5* also resulted in an expansion of the forebrain and posterior commissure, and therefore a shift in the DMB (Schwarz et al., 1999). Synergistic interactions between *fgf8* and *engrailed* homeodomain transcription factors are also required to maintain midbrain fate, and therefore also maintain the DMB (Scholpp et al., 2003). Analysis of zebrafish where *eng2/3* function is lost but *pax2.1* is unaffected, reveals a similar phenotype to *noi* mutants in which *pax2.1* is lost, with the extended expression of *pax6* into midbrain territory. These results show that *pax2.1* inhibits *pax6.1* expression via the activation of *eng2/3* (Scholpp and Brand, 2001; Scholpp et al., 2003). Conversely the over-expression of *eng2/3* in zebrafish causes a suppression of of *pax6* expression in the forebrain and the midbrain extends anteriorly.

The boundaries (DMB, MHB) that form between these lineage restricted compartments, are required to prevent intermingling of cells fated to contribute to the different parts of the embryo. These boundaries also provide positional information to adjacent populations of cells for normal brain development (Kiecker and Lumsden, 2005). Once the midbrain has been patterned in zebrafish it is comprised of the optic tectum located dorsally and the tegmentum located ventral to the tectum.

1.1.5 – Neurogenesis

Neurogenesis is the process that controls the formation of neurons. The molecular mechanisms controlling neurogenesis are conserved among vertebrates and invertebrates (Blader et al., 2004). Neurogenesis was first characterised by analysis of the specification of the *Drosophila* peripheral nervous system (PNS) (Campos-Ortega,

1993). Pre-pattern genes define populations of cells called pro-neural clusters that express pro-neural basic helix loop helix (bHLH) proteins, within which neuronal progenitors are selected (Blader et al., 2004; Geling et al., 2004). The Delta/Notch signalling system causes lateral inhibition that determines which cells become neuronal progenitors resulting in them undergoing neuronal differentiation (Lewis, 1996; Figure 1.7A). Both Delta and Notch are single pass transmembrane proteins. Delta expressed in one cell binds to Notch in its neighbouring cell which induces cleavages in both the extracellular and cytoplasmic domains (Artavanis-Tsakonas et al., 1995; figure 1.7B). The cleaved cytoplasmic tail of Notch then migrates to the nucleus and activates transcriptional repressors (e.g. her5) which inhibit the activity of proneural genes (Haddon et al., 1998; Geling et al., 2004; Figure 1.7B). In these Notch activated cells Delta expression is also reduced, creating a positive feedback loop in which the cells inhibiting their neighbours are not inhibited themselves.

Figure 1.7 – The Delta/Notch signalling pathway

A diagrammatic representation of (A) Delta/Notch signalling in pro-neural clusters, causing lateral inhibition that determines which cells undergo neuronal differentiation. (B) A diagrammatic representation of the Delta/Notch signalling pathway. Delta (purple) displayed on the surface of one cell binds to Notch (green) on the surface of a neighbouring cell, which induces the extracellular and cytoplasmic cleaving of Notch. The cleaved Notch tail migrates to the nucleus and activates transcriptional repressors which inhibit the activity of proneural genes.

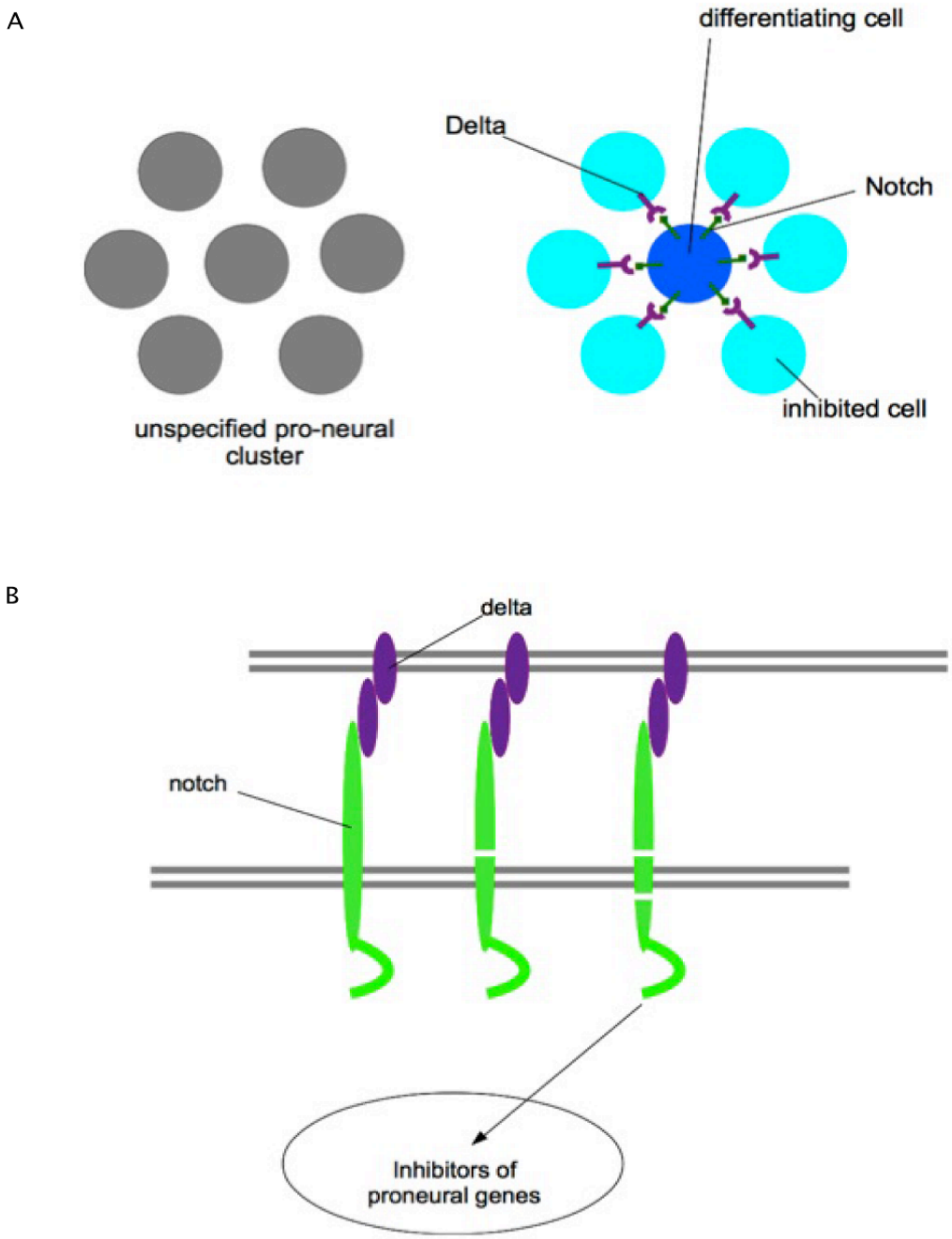

Studies of vertebrate neurogenesis reveal similar regulatory mechanisms to those identified in *Drosophila* (Chitnis, 1999). Neurogenic genes in vertebrates include bHLH *Atonal* (*Ath*) and *achaete-scute* related genes *Neurogenin1* (*Ngn1*) and *NeuroD* which are pro-neural (Blader et al., 1997; Ninkovic et al., 2005). Other neurogenic genes such as *Hairy/E*(*Spl*) transcription factors inhibit neurogenesis (Geling et al., 2004). Studies have shown that *Ngn1* positively regulates the expression of *NeuroD*, which is required for neuronal differentiation, and HuC which encodes an RNA binding protein expressed in post-mitotic neurons (Kim et al., 1996; Kageyama and Nakaniski, 1997). In mouse and zebrafish *neuroD* expression follows *ngn1* expression throughout the rostrocaudal axis (Sommer et al., 1996; Korzh et al., 1998). Ectopic expression of *Ngn1* in frog causes the ectopic expression of *NeuroD* positive cells, and overexpression of *ngn1* in zebrafish induces ectopic expression of HuC (Ma et al., 1996; Kim et al., 1997). In contrast, double ablation of *Ngn1/2* in mice mutants results in the loss of *NeuroD* (Ma et al., 1999).

A region of progenitor cells termed the intervening zone (IZ), located at the MHB, plays an important role in controlling neurogenesis in the midbrain and hindbrain domains in vertebrates (Geling et al., 2003). The IZ indirectly inhibits neurogenesis via the bHLH transcription factors (*Hairy/E* transcription factors *Hes1* and *Hes3* in mouse) which form and maintain the IZ, independent of Notch signalling (Ninkovic et al., 2008). Zebrafish homologues of mouse *Hes1* and *Hes3*; *her5* and *her11*, have a similar role in forming and maintaining the IZ (Ninkovic et al., 2008). At 70% epiboly, *her5* is expressed in the entire midbrain hindbrain anlage (Tallafuss and Bally-Cuif, 2003). During development *her5* expression regresses towards the MHB and becomes restricted to the IZ in the isthmus, allowing for neurogenesis to occur. Analysis of *Tg*(*her5PAC:EGFP)* transgenic fish revealed that restriction of *her5* begins from 3 ss in the ventral mesencephalon. By 16 ss this restriction accelerates with the dorsal regression of *her5* too, which is completed by 24 hpf, when *her5* expression is limited to the isthmus (Tallafuss and Bally-Cuif, 2003). In *ace* and *noi* zebrafish mutants molecular markers of the MHB are lost, resulting in the premature and accelerated posterior regression of *her5* (Geling et al., 2003). This indicates that the inhibition of neurogenesis by *her5* is regulated by Fgf signalling at the isthmus (Tallafuss and Bally-Cuif, 2003). The antagonistic regulation of neurogenesis by the Notch signalling pathway and Hairy/E transcription factors are essential for controlling numbers of neuronal cell types and for morphogenesis of the nervous system (Kageyama and Nakanishi, 1997).

Most recently micro-RNA's have been identified that block the translation of *fgf8*, which in turn reduces *her5* expression to promote neurogenesis (Coolen and Bally-Cuif, 2009). miR-9 is expressed from 20 – 24 hpf in the telencephalon and spreads throughout the CNS, with the exception of the MHB, as development progresses (Leucht et al., 2008). This has led to the hypothesis that miR-9 acts to refine the MHB by regulating MHB correct positioning, spatial restriction and the coincidence of MHB patterning and neurogenesis inhibition activities (Leucht et al., 2008).

1.2 – Anatomy, function and connectivity of the MTN

1.2.1 – Anatomy of the MTN

The mesencephalic trigeminal nucleus (MTN) comprises sensory neurons located in the dorsal mesencephalon in vertebrates, and extends into the rostral hindbrain of mammals (Weinberg, 1928). In mammals, more than 70% of MTN neurons are located in the rostral hindbrain (Lazarov, 2007). The cell bodies of the MTN are large (frog 10µm, Pratt and Aizenman, 2009; goldfish, 20µm-40µm, Puzdrowski et al., 1988; Shark, 39µm-56µm, Witkovsky and Roberts, 1975; rat, Ruggiero et al., 1982; chick, 15µm-20µm, Sanchez et al., 2002) and generally oval in shape.

The numbers of MTN cell bodies in the mesencephalon (and hindbrain in mammals) vary between species. Early studies in the carp to locate the MTN, showed it is comprised of 20-25 cells each side of the brain in the dorsal mesencephalic tegmentum, caudal to the posterior commissure (Luiten, 1979). In smaller teleosts such as the guppy, as few as 10 – 16 cells in each side of the brain in the dorsal mesencephalic tegmentum have been identified (Pombal et al., 1997; goldfish, 8 – 12, Puzdrowski et al., 1988). The numbers of MTN cell bodies in the zebrafish has not been classified; Only one previous study has identified MTN neurons in the zebrafish, and this briefly described them as located in the midbrain, similar to amniotes (Kimmel et al., 1985). In shark (catshark) the number of MTN neurons has been shown to range from 1063-1102 each side of the brain (Witkovsky and Roberts, 1975). In amniotes the number of MTN neurons has been shown to range from 400 to several thousand (newborn mouse ~ 1500 Hinrichsen and Larramendi, 1969; cat, 639-1489, Dault and Smith, 1969).

MTN neurons are the first neurons born in the dorsal midbrain in vertebrates; they arise either side of the midline in chick from stage 14 (22 ss), and in mouse at E8.5 (10 ss) (Stainier and Gilbert, 1990; Stainier and Gilbert, 1991; Chedotal et al,, 1995). In

mouse, MTN neurons initially form in the rostral mesencephalon and as development proceeds they then form caudally in the mesencephalon and pons (Stainier and Gilbert 1990; Stainier and Gilbert, 1991). These early born MTN neurons send out single descending processes to pioneer the dorsal longitudinal tracts (Stainier and Gilbert, 1990; Hunter et al., 2001).

The first sets of tracts to develop serve as a scaffold on which most later tracts form, to create the networks on which neural function depends (Easter and Taylor, 1989). In cartilaginous fishes (catshark, Kuratani and Horigome, 2000), amphibians (*Xenopus*, Anderson et al., 2000) and amniotes (mouse, Mastick and Easter, 1996; alligator, Pritz, 2010), two parallel longitudinal axon tracts form. The dorsal tract is formed of the tract of the postoptic commissure (TPOC) and the supraoptic tract (SOT) that arises in the telencephalon, and continues to the descending tract of the mesencephalic nucleus of the trigeminal nerve (dtmesV; Figure 1.8).

The TPOC originates from somata at the base of the optic stalk and within the thalamus (Easter et al., 1993; Nural and Mastick, 2004). The supraoptic tract is formed from neurons of the supraoptic nucleus in the olfactory bulb (Hatton and Yang, 1989). The ventral tract is formed by the mammilotegmental tract (MMT) and continues to the medial longitudinal fasciculus (MLF). The MMT arises from neurons of the mammillary nuclei in the posterior hypothalamus, and the MLF arises from neurons of the vestibular nuclei (Purves et al., 2001; Hayakawa and Zyo, 1989). In amniotes these tracts project caudally from the prosencephalon to the rhombencephalon (Easter et al., 1993; Figure 1.8).

In contrast, in teleosts there is only one longitudinal tract, except at the level of the rhombencephalon where the dorsal longitudinal tract forms (DLT; Ishikawa et al., 2004). The DLT is formed from axons of Rohon Beard (RB) and trigeminal ganglion neurons (Ross et al., 1992). In teleosts the dtmesV has not been identified, and the TPOC and SOT in the prosencephalon appears to belong to the ventral longitudinal tract (Ishikawa et al., 2004; Wilson et al., 1990; Ross et al., 1992; Figure 1.8). Similarly a single tract located ventrally has been described in the primitive agnathan vertebrate the Sea Lamprey (Huard et al., 1999). This single axon tract is conserved in teleosts, with the exception of medaka and guppy, which possess a dorsal mesencephalic tract (DMT; Ishikawa et al., 2004; Pombal et al., 1997; Figure 1.8). The DMT in medaka has been described as comparable to the dtmesV in mouse, due to its similar location and early development (Barreiro-Iglesias et al., 2008). In Lamprey, a dorsal tract develops in the hindbrain, where projections from dorsal cells (DC) give rise to the dorsolateral

longitudinal fascicle (DLL) (Barreiro-Iglesias et al., 2008).

Figure 1.8 - Typical axonal tracts in fish, amniotes and agnathans

Diagrammatic representation of the early axonal tracts that form in (A) lamprey, (B) zebrafish, (C) medaka, (D) catshark, and (E) mouse. The location of the MTN and the tract it forms is not clearly known in zebrafish. AC, anterior commissure. DC, dorsal cells. DDT, dorsal diencephalic tract. DLT, dorsal longitudinal tract. DmesV, descending tract of the mesencephalic nucleus of the trigeminal nerve. DMT, dorsal mesencephalic tract. DVDT, dorso-ventral diencephalic tract. FR, fasciculus retroflexus. HC, habenular commissure. IN, isthmic nucleus, MLF, medial longitudinal fasciculus. MTT, mamillo-tegmental tract. POT, postoptic commissure. SM, stria medullaris. SOT, supraoptic tract. TAC tract of the anterior commissure. THC, tract of the habenular commissure. TmesV, tract of the mesencephalic nucleus of the trigeminal nerve. TPOC, tract of the postoptic commissure. Taken from Barreiro-Iglesias et al., 2008.

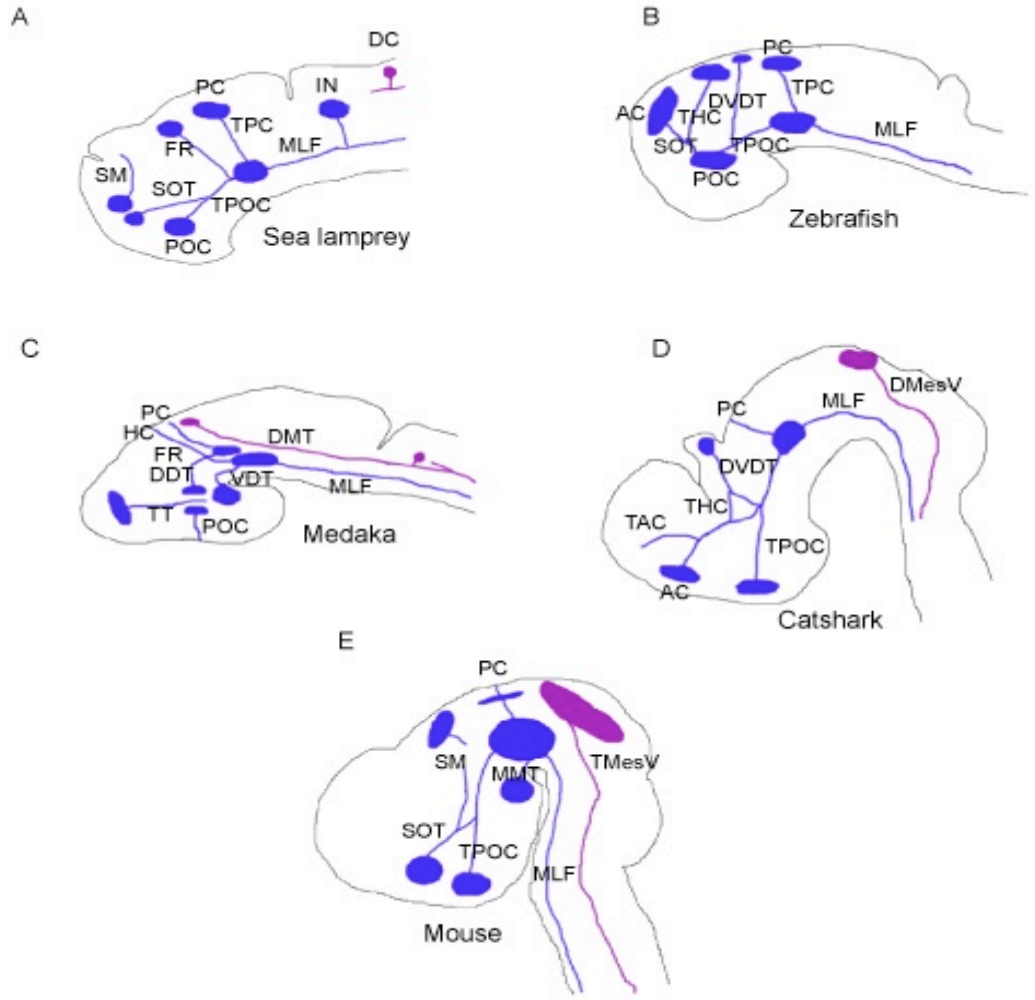

Previous studies in chick have identified the MTN by analysis of BEN (a cell adhesion molecule) expression, and from labelling neurofilament in axons of the brain (Chedotal et al., 1995; Hunter et al., 2001). MTN cell bodies were observed in most of the dorsal mesencephalon, but were absent in the caudal mesencephalon (Chedotal et al., 1995). They showed that MTN cell bodies send out ventral projections, which turn 90^{o} to pioneer the lateral longitudinal fasciculus (LLF), a dorsal descending tract. The axons of the MTN then pass through the isthmus, at the MHB to rhombomere 2 in the hindbrain, where they then exit with the mandibular branch of the trigeminal motor neuron (MoV), and grow along this to the mandibular arch muscles that they innervate (Figure 1.9).

Figure 1.9 – Axonal pathways of the MTN in chick

Diagrammatic representation of the axon tracts of the MTN that pioneer the lateral longitudinal fasciculus in chick. Adapted from Hunter et al., 2001.fb, forebrain. nV, nucleus of the trigeminal motor nerve.

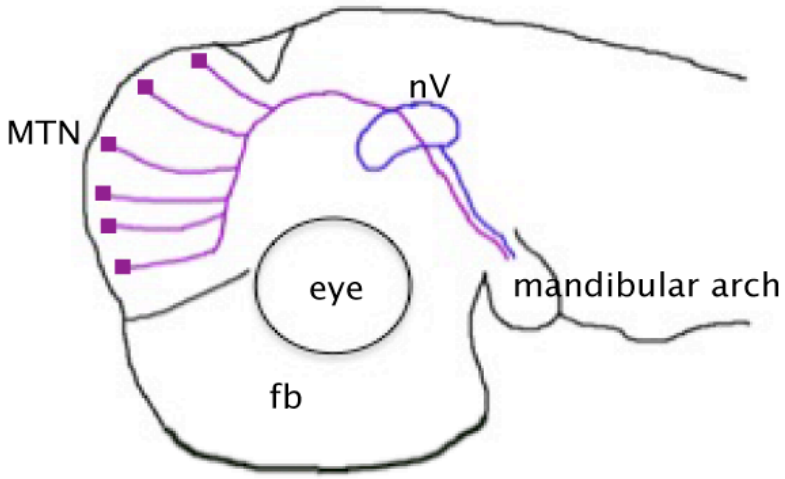

Other cell types located near the MTN are the nuclei of the posterior commissure (nTPC) located at the DMB, and tectal cells within the mesencephalon, that both have a role in vision (Hemsley and Savage 1987; Scholpp et al., 2003). The nTPC are pre-tectal nuclei, some of which include the interstitial nucleus of Cajal (NIC), and their ascending axons form the posterior commissure (PC) as they project contralaterally to the oculomotor nucleus (Carpenter et al., 1970; Partsalis et al., 1994; Stanic et al., 2010). The role of nTPC in visual functioning was identified by creating lesions along the PC, which resulted in an impairment of vertical eye movements and eyelid retraction

(Carpenter et al., 1970; Partsalis et al., 1994). How the MTN is specified differently to neighbouring nTPC and tectal neurons is not understood.

In some previous studies in chick and fish, the MTN has been classified as nTPC (zebrafish, Scholpp and Brand 2003; birds, Manni et al., 1965; Azzena and Pamieri 1967). In chick and mouse some cell bodies of the anterior MTN are located among the nTPC (Mastick and Easter, 1996). In fish and selachians (shark) MTN appear to be restricted to the anterior dorsal midbrain, and extend from the region of the posterior commissure (Weinberg, 1928). In trout and bowfin the anterior region of the MTN have been seen to lie among the fibres of the posterior commissure (Weinberg 1928).

1.2.2 – Connectivity and function of the MTN

Axonal tracing studies of neuronal projections of the MTN in amniotes, showed that as the MTN projection reaches the motor nucleus of the trigeminal nerve, the MTN neuron bifurcates giving rise to a central branch and a peripheral descending branch (Pratt and Aizenman, 2009). The central projection enters the trigeminal motor nucleus, where it makes excitatory synaptic connections with jaw-closing motor and premotor neurons (Bae et al., 1996). This has also been identified in shark and carp (Roberts and Witkovsky, 1975; Luiten, 1979). Neurons of the MTN have also been reported to make synaptic connections with motor nuclei of other cranial nerves, the facial (VII), vagal (X) and hypoglossal (XII) in rats (Zhang et al., 2005; Luo et al., 2006). In mammals the majority (80-90%) of the MTN descending branches have been seen to ipsilaterally innervate spindles in the jaw closing muscles (Alvarado-Mallart et al., 1975; Lazarov, 2007). The remaining descending branches appear to be periodontal pressoreceptors that respond to forces on the teeth (Byers et al., 1986). The MTN has also been reported to innervate the eye muscles in some species (cat, Byers et al., 1986; frog, Hiscock and Straznicky, 1982; lungfish, von Bartheld, 1992). In shark and teleosts, MTN does not appear to innervate the mandibular muscles, instead it innervates the perioral area and teeth. This has been shown in shark by stimulating the jaw-opening and closing muscles which failed to cause a measured response in the MTN. However a response in the MTN was measured after mechanical stimulation to the perioral skin and teeth. Similarly in carp and guppy, HRP application to different masticatory and eye muscles resulted in no retrograde labelling of MTN, but application to the perioral skin

did label the MTN.

In mammals the MTN appears to be topographically positioned according to the tissues it innervates. In rat, neurons innervating the teeth were concentrated in the caudal MTN in the hindbrain, while neurons innervating muscle were distributed throughout the MTN in the midbrain and hindbrain (De et al., 2005a). Similarly in cat, neurons innervating the teeth were located in the caudal MTN in the hindbrain, and neurons innervating the muscle were concentrated in the midbrain MTN (Alvarado-Mallart et al., 1975). No topographic distribution within the MTN has been identifed in agnathans and shark.

In the agnathan vertebrate the Sea Lamprey a dorsal tract develops in the hindbrain, where projections from dorsal cells (DC) give rise to the dorsolateral longitudinal fascicle (DLL) (Barreiro-Iglesias et al., 2008). It has been suggested that DCs are homologues of mammalian mesencephalic trigeminal neurons that form the dtmesV in vertebrates (Anadon, 1989; Northcutt, 1979). In amniotes 70% of the MTN neurons are also positioned in the hindbrain, while the remaining 30% are located in the mesencephalon (Ruggiero et al., 1982; Lazarov 2007). The MTN has not been identified in the hindbrain of teleosts and shark. DCs are also comparable to MTN cell bodies because they are one of the earliest cells to arise in the brain, and they send axons through the trigeminal nerve (Barreiro Iglesias et al., 2008). There may be some MTN cell bodies in the mesencephalon in the lamprey, as a small number of cells were retrogradely labelled in the midbrain, after injection of cobalt-lysine into the motor nucleus of the trigeminal nerve (Huard et al., 1999). The trigeminal motor neurons innervate unique muscles that control the rhythmical movement of the sucker in parasitic lamprey, therefore these putative MTN cells labelled in the midbrain may also innervate these unique muscles (Huard et al., 1999).

Tract tracing studies where the ophthalmic branch of the trigeminal motor nerve was retrogradely labelled also labels MTN neurons, implying MTNs form synapses to this branch too (Alvarado-Mallert et al., 1975; Matesz, 1981). It has been shown, from physiological data in rats, that MTN neurons make soma-somatic contacts to one another (Paik, 2005). This may explain the cell clustering of the MTN among vertebrates (Hinrichsen and Larramendi 1969; Rokx and Van Willigan, 1988).

It has also been suggested that in some species (rat, cat) the MTN neurons receive synaptic inputs from various brainstem structures on their somata and on their terminals within the trigeminal nucleus (rat, Matesz, 1981; cat, Bae et al., 1996; Lazarov, 2007). Therefore this input may be used to control the excitability of the cells,

which potentially occurs by membrane depolarisation (Lazarov, 2007). In mice axonal tracing studies of the locus coeruleus (LC) neurons have shown that they project to the MTN and potentially form synapses with them, identified by the presence of synapse like swellings on LC axons in the vicinity of the MTN cells (Takahashi et al., 2010). The LC is located medially to the MTN and is a major source of noradrenaline in the brain (Takahashi et al., 2010). The LC sends axons to different brain regions, such as the hypothalamus and amygdala, therefore playing an important role in aggressive behaviour and response to stressful situations (Foote et al., 1983). Other retrograde tracing studies of cortical neurons in mice have also identified LC axons projecting to MTN cell bodies (Iida et al., 2010). These results imply that the LC regulates the bite strength, by modifying MTN cell activity (Takahashi et al., 2010). MTN cell activity may be modified by the release of noradrenaline from LC cells (Takahashi et al., 2010).

Responses from visual stimuli or stimuli to the optic nerve, have also been recorded in MTN in tadpoles, suggesting that MTN neurons receive input from either retinal ganglion cells (RGC's) or tectal neurons (Pratt and Aizenman, 2009). MTN neurons were also found to innervate the ipsilateral tentacle, a sensory organ in the mouth of premetamorphic tadpoles (Pratt and Aizenman, 2009). Therefore MTN neurons may play an integrative role in which slow visual input via RGC's or tectal neurons enhances the tentacle driven output of MTN, required for the tadpoles to filter feed (Pratt and Aizenman, 2009). The expression of drebrin, an actin binding post-synaptic protein that has been implicated in the formation of synapses, in the rat MTN supports these studies that suggest the MTN neurons receive synaptic inputs from RGCs or tectal neurons (Park et al., 2009).

It is unclear whether MTN neurons are excitatory or inhibitory. Different studies investigating the chemical neuroanatomy of MTN reveal it exhibits a broad variety of chemical neurotransmitters for synaptic transmission. Physiological studies have shown that MTN neurons are depolarised by exogenous application of glutamate and GABA respectively (Hayar et al., 1997; Pelkey and Marshall, 1998). This plasticity of MTN suggests it may be an integrating centre in circuits underlying the reflex control of a variety of oral and facial movements (Copray et al., 1990; Lazarov, 2007).

1.3 – The development of sensory neurons

1.3.1 – Sensory neuron diversity; a comparison with the MTN

The sensory division of the peripheral nervous system (PNS) conveys information about the external environment to the central nervous system (CNS). In the trunk these sensory neurons lie in clusters in the dorsal root ganglia (DRG), and are located outside the CNS. DRGs are organized metamerically along the ventrolateral edges of the spinal cord (Raible and Ungos, 2006). In the head, most sensory neurons lie in the cranial sensory ganglia, with the exception of the mesencephalic trigeminal nucleus (MTN), which is located within the CNS in the midbrain. Studies in frog and zebrafish have identified primary sensory neurons, called Rohon Beard (RB) neurons, which are thought to be homologous to dorsal cells (DCs) found in the spinal cord of the sea lamprey (Northcutt, 1979; Lamborghini 1980; Anadon, 1989). These are located within the CNS, along the dorsolateral spinal cord (Lamborghini 1980; Clarke et al., 1984). The RB neurons (and DCs) are mechanoreceptors that convey sensory information before replacement by DRGs (Clarke et al., 1984).

1.3.1.1 – The development of peripheral somatosensory neurons in the trunk

There are four types of DRG sensory neurons, these are; mechanoreceptors, which convey mechanical sensations, e.g. touch; proprioceptors, (a subclass of mechanoreceptors) that innervate muscles and convey the sense of limb movement and position; nociceptors which convey pain; and thermoreceptors which are required to detect hot and cold stimuli (Raible and Ungos, 2006).

The four types of sensory neurons within the DRG exhibit different morphological phenotypes to one another. Nociceptive neurons are small and tend to have unmyelinated fibers, and are positioned dorsomedially within the DRG (Raible and Ungos, 2006). In contrast, proprioceptive and mechanoreceptive neurons are large and have myelinated fibres, and are positioned ventrolaterally within the DRG (Marmigere and Ernfors, 2007). MTN neurons are thought to convey mechano-proprioceptive information from the mandibular muscles (Luiten 1977; Jüch, 1981). MTN neurons are similar to proprioceptive and mechanoreceptive DRG neurons because they also have large cell bodies. However MTN neurons are unipolar, unlike DRG neurons which are

pseudo-unipolar. DRG neurons initially send out two processes. These processes are brought together during development by the elongation of cytoplasm from the cell body, which gives rise to the appearance of a single process (Takahashi and Ninomya, 1987).

In mouse, proprioceptive sensory neurons innervate muscle spindles. Muscle spindles are stretch sensitive mechanoreceptors that lie in parallel with skeletal muscle fibres, that are innervated by proprioceptive sensory neurons (Hunt, 1990). Muscle spindles are comprised of a fusiform (wide in the middle and tapers toward the end) capsule, that contains distinct intrafusal muscle fiber types with stereotypically arranged nuclei (Hunt, 1990). In fish, muscle receptors are less specialised compared to those in mammals, and muscle spindles have not been identified (Billintijin, 1975; Maeda et al., 1983). Proprioceptive sensory neurons also form synaptic connections to motor neurons, and motor neurons innervate extrafusal muscle fibres (Hippenmeyer et al., 2007). Together these components form monosynaptic circuits. ETS transcription factors and zinc finger transcription factors are required for development of these spinal reflex arcs (Arbor et al., 2000). ETS family gene *Pea3*, is expressed in motor neurons and some proprioceptive sensory neurons, while another ETS family gene *Er81* is expressed in proprioceptive neurons. *Er81* together with EGF family protein *Neuregulin1* (*nrg1*) define motor neuron pools and their corresponding sensory afferents. *Er81* and *nrg1* induce ETS family genes *Erm* and *Pea3*, and Egr family gene *Egr3* in intrafusal muscle fibers which specifies their differentiation into muscle spindles (Hippenmeyer et al., 2007). *Erm* is also required for the formation of extrafusal muscle fibres (Hippenmeyer et al., 2007).

All sensory neurons of the DRG are derived from neural crest cells (NCC). NCCs are a population of multi-potent cells that arises at the border of the neural plate and non-neural ectoderm during gastrulation (Baker et al., 1997b; Huang and Saint-Jeannet, 2004). Initial neural crest induction is dependent on a gradient of BMP activity that is established in the ectoderm, and Wnt activity in the presumptive epidermis (Aybar et al., 2002). After induction, NCC undergo an epithelial to mesenchymal transition, and delaminate from the neuroepithelium of the neural tube (Barembaum and Bronner-Fraser, 2005). They then migrate away from the neural tube in a rostrocaudal wave and differentiate into a broad range of derivatives in the head, trunk, enteric system and heart (Huang and Saint-Jeannet, 2004; Barembaum and Bronner-Fraser, 2005). The overall pattern of this migration appears to be similar among different species, with some exceptions. For example in mammals the migration of NCCs begins before the neural tube has closed. In chick, zebrafish and *Xenopus*, migration only

begins after closure of the neural tube (Santagati and Rijli, 2003; Huang and Saint-Jeannet, 2004). NCCs in the trunk form sensory and sympathetic ganglia, non-neuronal cells such as satellite cells of peripheral nerves, and pigment cells.

The Delta/Notch signaling pathway controls neurogenesis in NCCs, and this occurs in two waves (Wakamatsu et al., 2000). The early phase of neurogenesis in neural crest results in the expression of both *Ngn1* and *Ngn2*, which specifies neural crest to differentiate into early forming DRG neurons; those involved in proprioception that have the furthest to migrate (Andermann et al., 2002; Raible and Ungos, 2006). During the second phase of neurogenesis *Ngn1* alone is required, and NCC inhibited during this phase go on to differentiate into non-neural glial cells (Wakamastsu et al., 2000). In zebrafish only *ngn1* has been identified. *ngn1* appears to have the same function of both mammalian *Ngn1* and *Ngn2* (Andermann et al., 2002). After the specification of RB neurons, the fate of NCCs is specified by *ngn1* in another wave of neurogenesis, which specifies neural crest to form either sensory neurons or glial cells in the DRG when neurogenesis is inhibited in NCCs.

1.3.1.2 – The development of peripheral somatosensory neurons in the head

In the head some sensory neurons are neural crest derived, while many others arise from specialised regions of the embryonic ectoderm, called neurogenic placodes (Graham and Begbie, 2000). Placodes are discrete regions of thickened columnar epithelium in the head induced by the neural tube (Baker and Bronner-Fraser, 2001). Some placodes such as the otic and epibranchial form in the ectoderm adjacent to the neural tube, while others such as the olfactory and trigeminal placodes originate in the neural folds (Begbie et al., 2002). Cranial sensory neurons are specified within these placodes which they delaminate from and migrate, guided by NCCs, to where the sensory ganglia of the trigeminal, facial, glossopharyngeal and vagal nerves form (Baker and Bronner-Fraser, 2001; Begbie et al., 2002). Therefore cranial sensory ganglia are derived from both neural crest and placodal cells, unlike DRG neurons that are only derived from neural crest (D'Amico-Martel and Noden, 1983). The placodes contribute large sensory neurons to the distal lobes of the ganglion, and neural crest contributes smaller sensory neurons to the proximal ganglia (Baker and Bronner-Fraser, 2001). In comparison to DRG neurons in the trunk, cranial sensory ganglia convey more specialised sensory information such as taste, hearing and balance (Begbie et al., 2002).

However, like DRG neurons, they are positioned in the peripheral nervous system.

1.3.1.3 – The development of central somatosensory neurons in the trunk

RB neurons are primary neurons that are some of the earliest neuronal cell types to arise during development, similar to MTN neurons. RB neurons are mechanoreceptors that convey sensory information from the skin (Clarke et al., 1984). They begin to develop during gastrulation before the neural tube has closed, and MTN develop from stage 10 1/2 in frog (Lamborghini 1980; Pratt and Aizenman, 2009; Kollros and Thiesse, 1985). Both RB neurons and MTN also have large cell bodies (frog RB neurons 15-25μm and MTN 10μm; zebrafish RB neurons approx 35μm; Pratt and Aizenman, 2009; Clarke et al., 1984). Retrograde labelling of zebrafish RB neurons with HRP, shows they are bipolar and have two long thin ipsilateral longitudinal highly branched axons, one ascending and the other descending (Bernhardt et al., 1990). This is in contrast to MTN cell bodies that are unipolar.

Unlike DRG neurons, RB neurons are not derived from NCCs. In the trunk of zebrafish, pre-migratory neural crest and RB primary sensory neurons arise from a common progenitor pool in an equivalence domain at the lateral edge of the neural plate (Knecht and Bronner-Fraser, 2002). After initial induction of prospective NCCs at the neural plate border by BMP and Wnt signalling, further intercellular signals are required for the complete specification of NCC, distinguishing them from neighbouring RB neurons (Aybar, 2002).

Delta/Notch signalling is required to segregate the specification of neural crest and RB neurons from their common progenitor pool (Cornell and Eisen 2000). Progenitor cells with high *deltaA* expression on progenitor cells causes the activation of the Notch signalling pathway in neighbouring cells, which inhibits the expression of neurogenic genes, i.e. *ngn1* (Cornell and Eisen 2000; Cornell and Eisen, 2002; Figure 1.10). Therefore these neighbouring cells become neural crest as they are unable to differentiate into RB sensory neurons. Those cells expressing high levels of *deltaA* form RB neurons because the Notch signalling pathway is not activated in these cells, therefore they still express *ngn1* and can undergo neurogenesis (Cornell and Eisen 2002).

Figure 1.10 - Segregation of neural crest cells and RB neurons from their common progenitors by Delta/Notch signalling

Diagrammatic representation of (A) neurulation in the zebrafish (taken from Papan and Campos-Ortega, 1994), and (B) the differentiation of RB neurons and NCC from their common progenitor via lateral inhibition by Delta/Notch signalling which inhibits ngn1 and therefore inhibits differentiation into RB neurons. EVL, enveloping layer.

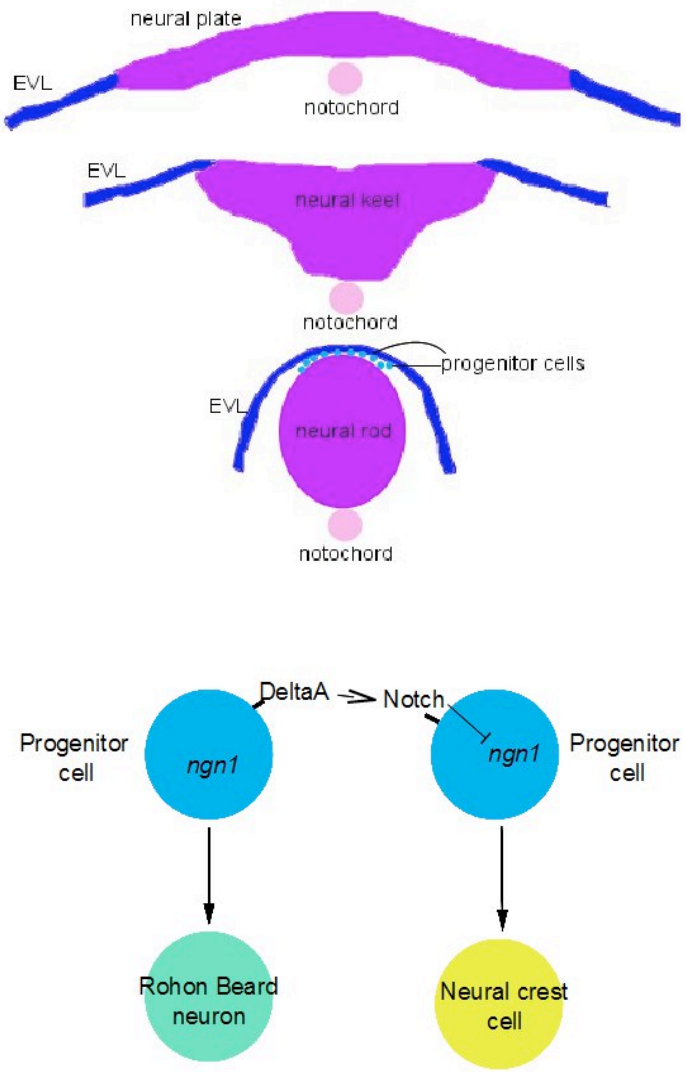

The importance of the Delta/Notch signalling pathway has been demonstrated in *deltaA* mutant zebrafish. When *deltaA* expression is lost, more RB neurons form at the expense of neural crest. The reduction in neural crest was identified by reduced expression of neural crest markers and the lack of trunk neural crest derivatives (Cornell

and Eisen, 2000). In contrast, when *ngn1* expression is lost, causing the inhibition of neurogenesis, the number of RB neurons are reduced/lost. Trunk neural crest formation is restored when *ngn1* activity is reduced in embryos with reduced Delta/Notch signalling (Cornell and Eisen 2002).

Studies using zebrafish mutant *narrowminded*, which has a mutation in the *prdm1* gene (homologue of mammalian *Blimp1*) reveals a genetic link between the formation of neural crest and RB sensory neurons (Artinger et al., 1999; Olesnicky et al., 2010). *prdm1* is expressed at the neural plate border where NCC and RB neurons form. Co-expression studies reveal that *foxd3* expressed in NCC, and *huC* expressed in all RB neurons, are co-expressed with the *prdm1* at the neural plate border (Hernandez-Lagunas et al., 2005). In *nrd* mutants, all RB neurons are absent, and NCC and their derivatives are reduced (Hernandez-Lagunas et al., 2005). This indicates the importance of *prdm1* in the formation of NCC and RB progenitor cells.

Analysis of *prdm1* expression in BMP mutants reveals that BMP signalling is required to induce expression of *prdm1* (Hernandez-Lagunas et al., 2005; Roy and Ng, 2004). In turn *prdm1* initiates *ngn1* expression, which is required for neurogenesis and therefore the formation of RB neurons (Rossi et al., 2009). This has been shown in crosses between *nrd* mutants and *Tg(ngn1:gfp)* transgenic zebrafish, which resulted in the loss of *ngn1* expression (Blader and Struhle, 2003). However, overexpression of *ngn1* in *nrd* mutants rescues RB neuronal formation in these mutants (Rossi et al., 2004).

1.3.1.4 – The development of central somatosensory neurons in the head

There are only a few centrally located somatosensory neurons in the head. These somatosensory neurons all appear to be associated with the trigeminal nerves, and in lower vertebrates are homologous to the MTN. In the agnathan sea lamprey, dorsal cells (DC) are positioned in the hindbrain. These DCs are proposed to be MTN homologues, due to their peripheral axonal projections that follow alongside the trigeminal motor nerve, to the muscle and skin of the mouth that they innervate (Anadon et al., 1989; Barreirio-Iglesias et al., 2008). Similarly in hagfish a population of large neurons lie in the dental fascicle of the trigeminal tract and may be associated with the trigeminal nerves and homologous to the MTN (Ronan, 1988). In gnathostomes the MTN is centrally located within the midbrain, and also in the hindbrain in mammals

(Wienberg, 1928; Ruggiero et al., 1982). In teleosts and shark the MTN has been shown to innervate the skin around the mouth and teeth (Roberts and Witkovsky, 1975; Luiten, 1979; Pombal et al., 1997; Puzdrowski et al., 1988), and in mammals the MTN also innervates the mandibular muscles (Alvarado-Mallart et al., 1975; Byers et al., 1986).

Unlike the peripheral somatosensory neurons in the head, that are known to be derived from either CNCCs or placodes, the origin of the MTN is unclear. Early grafting studies in which mesencephalic neural crest from quail was transplanted into duck hosts, have shown that MTN is derived from neural crest (Narayanan and Narayanan, 1978). In this study they transplanted NCCs that had just left the neural tube, but were still closely associated with the neuroepithelium (Baker et al., 1997a). More recent grafting studies, using early and late migrating mesencephalic neural crest transplanted from quail into chick, showed there was no contribution of neural crest to MTN neurons (Baker et al., 1997a). The absence of MTN neurons in these later grafting studies may imply that MTN are formed from NCCs that stay closely associated with the neuroepithelium.

1.3.1.5 – Development of sensory neurons in invertebrates

The cell bodies of sensory neurons in invertebrates are commonly located in the PNS, like DRG neurons in vertebrates (Braunig and Hustert, 1980). Sensory neurons in invertebrates are not neural crest derived; NCCs are thought to be unique to vertebrates (Holland et al, 1996).

The PNS in *Drosophila* is relatively simple and is populated by two major classes of sensory neuron; type one which have a single dendritic terminal and are ciliated, and type two that have multiple dendrites but no ciliary structures (Mill, 1976; Jarman 1998).

Type one innervates two forms of sensory organs, these are external organs and chordotonal organs (Mill, 1976; Tobin and Bargmann, 2004). External organs are mechanoreceptors and chemoreceptors, usually associated with an external cuticular structure such as a bristle (Jarman and Ahmed, 1998). Chordotonal organs are generally internal proprioceptors that are stretch receptors, similar to the muscle spindles in vertebrates (Jarman and Ahmed, 1998). Type two sensory neurons are not associated with specialised sensory structures, and are believed to convey nociceptive information, due to their naked dendrites that resemble vertebrate nociceptors (Jarman, 2002; Tobin

and Bargmann).

Type one and two sensory neurons are most commonly bipolar in morphology, however some multipolar cells have been identified. These are different to the unipolar morphology of MTN neurons. There are two distinct structures of type one proprioceptive sensory neurons, some exhibit long dendrites that reach the surface of the embryo. Others have short stubby dendrites that remain subepidermal. As in vertebrates, invertebrate sensory neurons are specified by the expression of proneural transcription factors of the bHLH class. *Atonal* is required for the specification of sensory neurons that innervate chordotonal organs, and *achaete-scute* specifies sensory neurons that innervate external organs (Jarmann, 2002).

In some insects and crustaceans the presence of sensory cell bodies in the CNS has been described (Braunig and Hustert, 1980; Alexandrowicz and Whitear, 1957). In insects (cockroach; locust) proprioceptive sensory cell bodies innervating stretch receptors in the metathoracic leg have cell bodies in the CNS (Braunig and Hustert, 1980; Collin, 1981). This is similar to MTN neurons that are also located in the CNS. The cephalochordate amphioxus, a non-vertebrate basal chordate, has intramedullary sensory cell bodies that are also located in the CNS (Bone, 1960). These intramedullary sensory cells are thought to be homologous to RB neurons as they appear early in the development of the amphioxus, and then disappear as development progresses (Bone 1960).

1.3.2 – Specification of sensory neuronal sub-types

Studies investigating the development of sensory neurons have led to the identification of important genes required for the specification and diversity of sensory neurons. The generation of DRG neurons in progenitor cells are controlled by two bHLH pro-neural transcription factors *Ngn1* and *Ngn2* in mice (Kramer et al., 2006). *Ngn2* is required for early neurogenesis, while *Ngn1* is involved in early and late neurogenesis (Baker and Bronner-Fraser, 2001; Andermann et al., 2002). In *Ngn1* null mice all nociceptive neurons are lost, and numbers of other sensory neurons are reduced. In *Ngn2* null mice, sensory neuron development was only delayed (Ma et al., 1999). This indicates that *Ngn1* can act as a substitute for *Ngn2* activity (Ma et al., 1999). In zebrafish, only a single neurogenin gene (*ngn1*) has been identified which appears to have the same function as both *Ngn1* and *Ngn2* in amniotes (Andermann et

al., 2002).

The different types of sensory neurons can not only be distinguished by their morphologies, but also by the expression of neurotrophic factors and their corresponding receptors (Chen and Frank, 1999). Signalling by neurotrophins (NT-3, NT4, BDNF, NGF) through trk receptors (TrkA/B/C), plays an important role in the survival of these specific sensory neuronal populations (Matsuo et al., 2000; Oakley and Karpinski, 2002). The diversification of sensory neurons is controlled by Runt-related transcription factors (*Runx1/2/3*) that repress the expression of Trk receptors (Inoue et al., 2008).

TrkA is expressed in nociceptive and thermoceptive neurons, which require nerve growth factor (NGF) for their survival. *TrkB* is expressed in mechanoreceptive neurons, which require brain derived neurotrophic factor (*BDNF*) or *neurotrophin-4* (*NT4*) for their development (Kramer et al., 2006). *TrkC* is expressed in proprioceptive neurons, which require *neurotrophin-3* (*NT3*) for survival and muscle innervation, which has been shown using *TrkC* and *NT3* knockout mice (Fan et al., 2000). In *TrkC* and *NT3* null mice there was a complete loss of proprioceptive sensory neurons, and subsequently their muscle spindles in the limb were also absent (Matsuo et al., 2000).

MTN neurons express *TrkC* (Fan et al., 2000); However in *TrkC* null mice there was only a reduction in the number of MTN, and their muscle spindle primary endings (Matsuo et al., 2000). Similarly when NT3 function is lost there was a reduction (50-60%), but not a complete loss of MTN (Fan et al., 2000; Matuso et al., 2000). These studies showed that while the MTN appears to require *NT3/TrkC* signalling for normal numbers of neurons to develop, another mechanism is involved which rescues the surviving MTN neurons which then innervate muscles normally. Analysis of *TrkB* expression in wild type mice revealed 90% of MTN neurons co-express with *TrkC* and *TrkB* (Fan et al., 2000). Analysis of *NT3/NT4* double knockouts, that are the corresponding signalling neurotrophins to *TrkB* and *TrkC*, revealed a further reduction (68%) in MTN, while *NT3/NT4/BDNF* triple knockouts resulted in the loss of all MTN neurons (Fan et al., 2000). Therefore this showed that in *TrkC* and *NT3* null mice, *NT4* and *BDNF* were able to partially rescue MTN development and survival.

1.3.3 – Molecular expression in sensory neurons

In chick and mouse several genes are expressed in the MTN, these are; a pou

domain transcription factor, *Brn3a* in chick and mouse (Hunter et al., 2001; Xiang et al., 1995); a paired homeodomain transcription factor, *Drg11* (Wang et al., 2007); a zinc finger transcription factor, egr2 in mouse (De et al., 2005); a LIM homeodomain transcription factor *Isl1* (Fedtsova et al., 2001; Sun et al., 2008); and T-cell leukemia translocation homeobox gene *Tlx3* (Logan et al., 1998). These genes are expressed in DRG neurons in mouse/chick, RB neurons in zebrafish and in some of the cranial ganglia in chick (Fedtsova and Turner, 1997; McCormick et al., 2007; Wang et al., 2007; Blentic et al., 2011).

Brn3a is expressed in post-mitotic sensory neurons in the dorsal neural tube of the spinal cord and sensory ganglia (He 1989; Fedtsova and Turner, 1997). *Brn3a* is also expressed in post-mitotic neurons in the tectum and tegmentum, including MTN neurons (Fedtsova and Turner, 2001). Studies in mice reveal that *Brn3a* is required for the development of somatosensory systems (Xiang et al., 1996). In *Brn3a* null mice there is a reduction in number of neurons in the trigeminal ganglia and neurons in the brain, such as a loss of MTN, and there are defects in axonal growth (Ichikawa et al., 2005; Eng et al., 2001). *Brn3a* null mutant mice exhibit impaired suckling and limb co-ordination, shown by a lack of response to stimulations, and the inability to right themselves (Xiang et al., 1996). *Runx3* and *TrkC* expression are absent in *Brn3a* null mice, while *TrkA* and *TrkB* is initially expressed in neurons, but many of these later undergo cell death (Huang et al., 1999). *Runx3* and *TrkC* are required for the formation of mechanoreceptive neurons (Inoue et al., 2008). These results suggest that the development of mechanoreceptive somatosensory systems is regulated by *Brn3a* via the promotion of *Runx3* expression, and therefore *TrkC* expression (Dykes 2010; Eng et al., 2004). Overexpression of *Brn3a* caused the activation of apoptotic repressor *bcl-2* in trigeminal neurons, suggesting that *Brn3a* also acts to protect these neurons from apotosis (Ensor 2001).

Egr2 plays an essential role in hindbrain development (De et al., 2005a). Analysis of *Egr2* mutant mice revealed an initial increase in the number of MTN neurons in the caudal MTN cell population in the hindbrain at E15, but by birth half the number of MTN neurons were present compared to wild type mice (De et al., 2005b). MTN neurons were visualised by their unique large size, and expression of *Brn3a*. These results suggest that *Egr2* regulates the period and extent of apoptosis in MTN neurons, to control their final numbers (De et al., 2005b). However this may be specific to mammals, as the MTN is not seen in the hindbrain of non-mammalian vertebrates.

Isl1 is expressed in many differentiating sensory and motor neuronal

populations (Ericson 1992; Korzh 1993). Within the midbrain *Brn3a* and *Isl1* are generally expressed in distinct separate groups of midbrain neurons, with the exception of MTN (Fedtsova and Turner, 2001). *Isl1* is expressed in MTN neurons from a later stage, compared to *Brn3a*. Both are co-expressed from stage 17 in chick and E15 in mouse (Hunter et al., 2001; Fedtsova and Turner, 2001). *Isl1* null mice are unable to survive past E11.5 because their development arrests at E9.5. Earlier analysis at E8.5 using molecular markers of motor neurons, showed no expression, revealing motor neurons failed to differentiate, indicating the importance of *Isl1* for motor neuron differentiation (Pfaff et al., 1996). *Isl1* conditional knockouts (CKO), which avoids early embryonic death, were analysed for the effects on sensory development. In these mice initial neurogenesis was normal in the sensory ganglia, but by E12.5 excess apoptosis occurred (Sun et al., 2008). The expression of *TrkA*, *TrkB* and *Runx1*, markers of neurons mediating pain and touch were reduced, but *TrkC* and *Runx3*, markers of proprioceptive neurons were unaffected. Therefore *Isl1* regulates the specification of sensory neuronal subtypes (Sun et al., 2008).

Most recently zebrafish *lullaby* mutants, in which zebrafish orthologue of *isl1* is truncated, were analysed for the effects on development of the primary sensory neurons RB neurons (Tanaka et al., 2011). In these mutants, defects are seen in the axonal outgrowth of all classes of spinal motor neurons. The *llb* mutation also affects the outgrowth of RB axons too, though other sensory neurons such as the trigeminal ganglia are not affected differently to that observed in the trigminal ganglia of mouse *Isl1* CKO.

Drg11 is expressed in DRG neurons, dorsal spinal cord neurons, and in MTN neurons of the mouse (Wang et al., 2007). *Drg11* is also transiently expressed in primary mechanoreceptive sensory neurons RB neurons in zebrafish (McCormick et al., 2007). *Drg11* is required for nociceptive circuit assembly in the spinal dorsal horn, and for survival of nociceptive DRG neurons (Chen et al., 2001; Rebelo et al., 2006). Studies in *Drg11* null mice have shown abnormal spatio-temporal patterning of axonal projections of nociceptive DRG neurons to the dorsal spinal cord (Chen et al., 2001). These mice also showed a reduced sensitivity to noxious stimuli, which reflects the abnormal development of axonal projections.

Analysis of MTN development in *Drg11* null mice from E10.5, revealed that MTN neurons also initially form and are present in normal numbers, determined by retrograde labelling with DiI applied to the first branchial arch (Wang et al., 2007). By E13.5, the majority of MTN neurons were lost, but the trigeminal nerve developed

normally. A marker for apoptotic cells, cleaved caspase3, was used to determine whether loss of MTN neurons were due to an increase in cell death. More cleaved caspase3 positive cells were observed in *Drg11* null mice compared to wild type (Wang et al., 2007). This suggests that *Drg11* is required for later stages of MTN development to sustain neuronal survival, and for normal muscle innervation; similar to the requirement of *Drg11* for normal formation of projections from nociceptive sensory neurons to their central targets in the spinal cord (Chen et al., 2001).

1.4 – Aims and objectives

The monosynaptic trigeminal circuit in the head comprises trigeminal afferents from the sensory mesencephalic nucleus of the trigeminal nerve, and efferents from the motor nucleus of the trigeminal nerve. Together these neurons innervate mandibular arch muscles and regulate jaw movement during eating/suckling and talking. The most intriguing, and least characterised component of this circuit is the MTN.

The aim of this thesis is to characterise the development of the MTN in zebrafish. Zebrafish are an ideal model organism to investigate how development occurs because they are transparent, therefore cells can easily be visualised *in vivo*. In particular live imaging of transgenic zebrafish can be performed due to their relatively fast early embryonic development. Zebrafish are also easy to genetically manipulate through gene over-expression, or knockdown of gene function using morpholino antisense oligonucleotides.

Previous studies have identified MTN neurons in all vertebrates, implying it was present in the jawed vertebrate ancestor, but it is not clear if its development is conserved between fish and amniotes. This is as little is known about the molecular profile of MTN neurons during development or how they are formed.

The cellular origin of MTN is controversial. Some studies suggest that it is derived from neural crest similar to other adult vertebrate sensory neurons, while others do not, suggesting MTN neurons are more similar to RB neurons, found in both vertebrate and invertebrate chordates Finally, the signals MTN neurons receive that causes their specific differentiation, distinguishing them from neighbouring neurons (nTPC, tectal cells) is not clear.

Specific aims for this thesis were;

i) **Identify the location of the MTN in zebrafish**. MTN neurons have not been clearly identified in zebrafish.

ii) **Characterise the expression of molecular markers in MTN neurons in zebrafish**.

1.To determine conservation of MTN neurons between fish and amniotes

2.To investigate the similarities and differences between MTN neurons, RB primary sensory neurons and DRG neurons.

iii) **Determine the cellular origin of MTN**. Some studies suggest that MTN neurons are derived from NCC, while other studies suggest MTN are not neural crest derived.

iv) **Characterise the signalling pathways required for the specification and development of MTN neurons**. The Fgf and Wnt signalling pathways play an important role in the patterning and specification of the midbrain, but their roles during MTN development are not known. The MTN are the most anteriorly derived midbrain neurons and most studies of midbrain patterning have focussed on tectal neurons.

Chapter 2 – Materials and Methods.

2.1 – Materials.

2.1.1 - Common Reagents and Buffers.

DEPC-water (Diethyl Pyrocarbonate) – 0.1% DEPC added to sterile water and autoclaved.

Phosphate buffered Saline (PBS) – one PBS tablet (Oxoid Ltd) dissolved in 100ml H20, autoclaved and stored at room temperature.

PBS-Tween (PBT): PBS containing 0.1% (v/v) Tween 20.

PBT-TritonX-100 and dimethyl sulphide (PBDT): PBS containing 0.1% (v/v) Tween 20, 1% (v/v) TritonX-100 and 0.1% DMSO (v/v).

4% Paraformaldehyde (PFA): 4g PFA in 100ml PBS, adjusted to pH7.4 with NaOH, aliquoted and stored at -20^{o}C.

Trichloroacetic acid (TCA) – 1% TCA in 15ml MQH_2O.

2.1.2 – Bacterial Culture Media.

Luria Bertoni (LB) medium – 1% tryptone, 0.5% yeast extract, 0.5% NaCl dissolved in distilled water and autoclaved.

LB Ampicillin (LB-amp) medium – LB medium with 50ml/ml ampicillin.

LB Kanamycin (LB-kan) medium – LB medium with 50ml/ml kanamycin.

LB agar plates with 2.5% agar, once cooled, ampicillin/kanamycin was added to a final concentration of 50µg/µl (or 60µg/ml if kanamycin) before media was poured into a 10mm diameter sterile petri dish and allowed to cool. Plates were stored, inverted at 4^{o}C.

2.1.3 – In Situ Hybridisation Solutions.

Proteinase-K: lyophilised enzyme reconstituted in dH_2O to a stock concentration of 10mg/ml, aliquoted and stored at -20^{o}C.

20x SSC: 3M NaCl, 0.3M tri-sodium citrate, adjusted to pH4.5 with citric acid (from Fisher Scientific).

2x SSC – 20x SSC and MQH_2O

0.2SSC - 20x SSC and MQH_2O

MABT – 1M maleic acid in MQH_2O pH using sodium hydroxide tablets and 5M sodium hydroxide solution to pH7.2.

Hybridisation Buffer without tRNA: 50% formamide, 20x SSC, 0.1% tween-20, 1M citric acid pH6.0

Hybridisation Buffer with tRNA: hybridisation buffer without tRNA, Heparin 50ug/ml, tRNA 500µg/ml

In situ hybridisation block 'Thisses Block': PBT containing 2% sheep serum and 2mg/ml BSA.

In situ hybridisation block: 1M Maleic acid (pH 7.5) and 10% Boehringer block diluted to 1% in MABT.

Fluorescent in situ hybridisation block 'Holley Block': 150mM maleic acid, 100mM NaCl (pH7.5), 2% Boehringer blocking reagent.

Alkaline phosphatase (APT) buffer: 1M Tris/HCl (pH 9.5), 1M $MgCl_2$, 1M NaCl, 10% Tween-20 and dH_2O

Fast red developing solution: Roche fast red tablets, dissoved in 2ml 1M Tris/HCl (pH8.2).

Staining solution – APT buffer containing 2.25µl nitroblue tetrazolium chloride (NBT) 50mg/ml, and 1.75µl 5-bromo-4-chloro-3-indolyl-phosphate (BCIP) 50mg/ml

2.1.4 – Immunohistochemistry Solutions.

TSA fluorescent substrate (FITC, Cy3, Cy5 PerkinElmer): Flourophore tyramide reconstituted in 120µl DMSO.

3% H_2O_2: 30% H_2O_2 diluted in MQH_2O.

HRP substrate: PBS containing 1ul TSA fluorescent substrate, 1µl 3% H_2O_2

1% Newborn calf serum (NBCS) block/PBT: 10% newborn calf serum diluted in PBT.

1% NBCS/PBT/2% triton-x: PBT containing diluted 10% NBCS and 2% triton-x.

DAB Solution: 0.05% diaminobenzidine, 1% dimethyl sulfoxide in 0.05 M PO4 buffer, pH 7.3. in 5ml H20

2.1.5 – Zebrafish Buffers.

10x Embryo Medium (E3) – 2.87g NaCl, 0.13g KCl, 0.48g $CaCl_2 2H_2O$, 0.82g MgSO47H_2O, in 1litre MQH_2O and autoclaved.

Tricaine (ethyl 3-aminobenzoate): 400mg/ml of tricaine powder was dissolved in 90ml MQH_2O, and 2.1ml tris (pH9.0). Hydrochloric acid was added to adjust to final pH7.0. Volume adjusted to 100mls and stored at 4^oC. 4ml was used in 100ml fish water/E3 PTU to anaesthetise fish.

Low melting (LM) agarose in MQH_2O – 1.5% low melting point dissolved in MQH_2O.

Fish water – system fish water with 4 drops of methylene blue.
0.003% Phenylthiourea (PTU)/E3 – 0.3% PTU heated to 60^oC with stirring to dissolve,

diluted to 0.003% in embryo medium.

0.3% 1-phenyl-2-thiourea in 10% Hanks saline.

2.1.6 – Pharmacological Reagents.

SU5402 (Calbiochem) – 500µg powder, resuspended in 42µl DMSO giving a stock concentration of 40mM. Stored in 10ul aliquots at -20^{o}C. Used at 50µM.

BIO (Sigmaaldrich) – 5mg powder, resuspended in 35µl DMSO giving a stock concentration of 40mM. Stored in 10µl aliquots at -20^{o}C. Used at 4µM.

Alsterpaullone (Calbiochem) – 1mg powder, resuspended in 120ul DMSO giving a stock concentration of 20µM. Used at 10µM

2.1.7 - Anterograde and retrograde labelling dyes

1,1'-dioctadecyl-3,3,3',3'- tetramethylinocarbocyanine perchlorate (DiI): reconstituted in 1ml ethanol to make stock solution of 50mg/ml. Working concentration of DiI at 1mg/ml.

3,3′-dioctadecyloxacarbocyanine perchlorate (DiD) – reconstituted in 1ml ethanol to make stock solution of 50mg/ml

2.1.8 – Gel Electrophoresis.

TAE (50x) - 0.8M Tris base, 40mM EDTA, set to pH8.2 with glacial acetic acid.

TAE (1x) – 50x TAE diluted in MQH_2O

Agarose Gel (1%)- agarose power dissolved in 1x TAE, when cooled one drop of Ethidium Bromide was added and solution poured into agarose gel mould and left to

set at room temperature under extraction hood.

2.2 – Methods

2.2.1 - Embryos/fish maintenance

Embryos were obtained from Kings College London fish facility and raised at 28.5^{o}C in fish water and 0.003% phenyl-2-thiourea (PTU). Embryos were staged according to Kimmel et al (1995), in somites or in hours post fertilisation (hpf) at 28.5^{o}C for 24 hpf and older embryos.

2.2.2 – Fixation methods

Fish were euthanised by adding 5-10ml tricaine to the water they were contained in, in the petri dish. Fish were fixed at the required stages at 4^{o}C in 4% paraformaldehyde (PFA; in PBS) overnight for use with in situ hybridisation and most antibodies, unless stated otherwise

2.2.3 – Transgenic and mutant fish lines

For this study the following transgenic fish lines were used: Neuronal marker *Tg(1.4dlx4-dlx6:eGFP)* (Zerucha et al., 2000). Marker of sub-population of neural crest *Tg(foxd3:GFP)* (Gilmour et al., 2002). Wnt antagonist *Tg(hsp70l:dkk1-GFP)* (Aman and Piotrowski, 1998), successful HS was analysed by GFP expression. Post-mitotic neuronal marker *Tg(huC:eGFP)* (Park et al., 2000). Marker of a sub-population of neural crest *Tg(sox10:eGFP)* (Carney et al., 2006).

For this study the following mutant fish lines were used: *Fgf8* mutant *acerebellar (ace)* (Haftner et al., 1996; Brand et al., 1996). *ace* mutants were identified at 24hpf by the absence of the cerebellum and an enlarged tectum. *sox10* neural crest mutant *colourless* (*cls*) (Kelsh and Eisen, 2000). *cls* mutants were identified at 26 hpf by the absence of pigment in the skin. *tfap2a* neural crest mutant *lockjaw* (*low*) (Li and Cornell, 2007). *low* mutants were identified by the absence of pigment in the skin.

Axin1 mutant *masterblind* (*mbl*) (Heisenberg et al., 1996). *mbl* mutants were identified by the significant reduction in eye size. *Pax2.1* mutant *no isthmus* (*noi*) (Lun and Brand, 1998). *noi* mutants were identified by the absence of cerebellum and dorsal posterior tectum.

2.2.4 - Zebrafish Microinjections

Injections were carried out under a stereoscope microscope (Nikon) using 0.5mm diameter borosilicate glass capillaries containing microfilament (World Precision instruments). Needles were pulled in a Flaming/Brown micropipetter puller (Sutter Instruments, model P-87) using programme number 3 (heat, 690; pull, 140; velocity, 120; time, 150). The needle was back-filled by placing it upside down for approximately 10 minutes, into a 1.5ml eppendorf tube containing the DNA/RNA/morpholino required to inject, to allow for sufficient time to back-fill the needle. The needle was mounted onto a micromanipulator connected to a picospritzer (Intracel). The needle was calibrated by clipping the end using forceps, and the droplet size measured using an eyepiece graticule (Pyser-SGI Ltd). Depending on the size of the droplet the injection pressure of the picospritzer was altered. Calibrating the needle meant that a consistent droplet size was administered to every embryo.

Embryo's were either mounted into indented columns in an agarose gel attached to a petri dish so that the gel was submerged in fish water, or lined up along the edge of a glass slide in a petri dish. Mounting embryo's along the edge of a glass slide meant that more embryo's could be mounted and therefore more numbers could be injected.

After injecting, the embryo's were transferred from the injection plate into a petri dish containing fish water and incubated at 28.5^{o}C and left to develop until the required stage. A plate of non-injected controls was also kept.

2.2.5 - Zebrafish Morpholino Injections

The *tfap2c* and *foxd3* morpholinos were purchased from Gene Tools. Upon receiving the lyophilised *tfap2c* and *foxd3* morpholinos, a stock solution of 2mM was made for each by reconstituting the morpholinos in sterile water and stored at -20^{o}C.

An aliquot of *tfap2a* morpholino at a stock solution of 3mM was kindly given by Gaia Gestri from UCL. For each injected morpholino the optimum working concentration was determined by injecting a series of dilutions into embryos at the 1-4 cell stage. *tfap2a* morpholinos were injected at a working concentration of 0.75mg/ml in 1ng droplet. *tfap2c* morpholinos were injected at a working concentration of 0.5mg/ml in 1ng droplet. *foxd3* morpholinos were injected at a working concentration of 1mg/ml in 1ng droplet. For the partial ablation of neural crest *tfap2a* morpholino was injected at a working concentration of 0.4mg/ul in 1ng droplet, and *tfap2c* morpholino was injected at a working concentration of 0.2mg/ul in 1ng droplet.

Embryos were mounted for injection as previously described in section 2.2.4 and injected at the 1-4 cell stage. Embryos were then placed into a petri dish containing fresh fish water and left in the 28^{o}C incubator to develop until the required stage of 26 hpf when they were fixed in 4% PFA overnight at 4^{o}C.

Table 2.1 – Zebrafish morpholino sequences

Morpholino name	Morpholino sequence	Working concentrations
tfap2a	GAAATTGCTTACCTTTTTTGATTAC	0.75mg/ml and 0.4mg/ml
tfap2c	TCTGACATCAACTCACCTGAACATC	0.5mg/ml and 0.2mg/ml
foxd3	CACTGGTGCCTCCAGACAGGGTCAT	1mg/ml

2.2.6 – Gel Electrophoresis

For analysing DNA and RNA probes, 1% gels were prepared by adding 0.5g of agarose to 50ml of 1x TAE buffer. The mixture was heated in the microwave in a glass flask and stirred occasionally until the agarose had fully dissolved. The flask was cooled until hand hot and one drop (10µl) of ethidium bromide (10mg/ml) was added and the contents left to set at room temperature under an extractor hood in a gel casting mould with inserted gel combs.

Once the gel had set, the combs were removed and transferred to an

electrophoresis tank filled with 1x TAE buffer. 5µl of 1kb ladder was loaded into the first well, then in the subsequent wells 1-2µl of DNA/RNA was mixed with 1µl loading dye (NEB) Once the gel was loaded, the gel was run at 120mV for 30 minutes. The bands were visualised on a UV trans-illuminator and photographed with a gel camera.

2.2.7 – Preparation of plasmid DNA

DNA plasmids were transformed (see later section) into bronze DH5a competent E.coli, plated onto Ampicillin/Kanamycin LB plates and left at 37^{o}C overnight. Colonies were picked and cultured overnight in 2ml LB broth containing Ampicillin/Kanamycin. Minipreps to recover the plasmid DNA were carried out using the promega miniprep kit. Concentrations were determined by spectrophotometry.

2.2.8 – Sequencing

All DNA sequencing was sent to Gene Service Ltd, UCL London.

2.2.9 – Wholemount Zebrafish Immunohistochemistry

2.2.9.1 – Fixation methods

Fish were fixed at the required stages at 4^{o}C in 4% PFA overnight for use with in situ hybridisation and most antibodies with the exception of parvalbumin (PV) and acetylated tubulin (at later stages). For labelling with Isl1, fish were fixed for two hours at room temperature in 4% PFA. Where fish were fixed at the required stages in 4% PFA overnight at 4^{o}C, they were then washed four times in PBT for 5 minutes and then put through 25%, 50%, 75% and 100% methanol series and stored at -20^{o}C.

For labelling with parvalbumin and actetylated tubulin, fish were fixed in 2% trichloroacetic acid for 1 hour at room temperature.

2.2.9.2 – Standard wholemount Immunohistochemistry

Standard procedures were used for antibody labelling as described by Wilson et al., 1990. Embryos were permeablised by either 0.1% Trypsin (in PBS), 10µg/ml Proteinase-K (in PBS) or six 30 minute washes with PBS/2% TritonX-100. Washes were made in PBT (PBS/0.1% Tween 20), and blocked in either 10% new born calf serum (NBCS) in PBT or 10% NBCS/PBT/2% TritonX-100 for 1 hour. For primary incubations, anti-GFP antibody was diluted 1:500, HuC (Molecular Probes) was diluted 1:200, Isl1 (39.4D5/40.2D6 Developmental Studies Hybridoma Bank/Jessell) was diluted 1:200, and wheatgerm agglutinin (Sigma) was diluted 1:200. Dilutions were made in block (NBCS/PBT or 10% NBCS/PBT/2% Triton-X). For secondary incubations the corresponding conjugated antibody was used as stated in the manufacturer's information for each primary antibody, these were IgG1, IgG2b or anti-rabbit (Southern Biotech) diluted 1:500. To visualise antibody labelling larvae were incubated in HRP substrate: PBS containing tyramide signal amplification (TSA) fluorescent substrate (FITC/Cy3/Cy5) and 3% H_2O_2 for 30 minutes in the dark. Where more then one antibody was used, the HRP of the previous antibody was inactivated by 10 minutes' incubation with 0.1M HCl.

Zebrafish larvae for labelling with parvalbumin (Sigma) or acetylated tubulin (Sigma) were fixed for one hour in 2% trichloroacetic acid (TCA) and then permeabilised for 7 minutes at -20^{o}C with acetone. To kill the endogenous peroxidase activity they were incubated in 3% H_2O_2/MeOH at room temperature for 1 hour. To increase the permeablisation the larvae were treated with 0.1% trypsin for various times depending on their age of fixation. After permeablisation washes were all made in PBT/1% DMSO/0.1% TritonX-100 (PBTD), and blocked in 10% NBCS/PBTD. For the primary incubations PV (Sigma) antibody was diluted in 1:200, and acetylated tubulin (Sigma) antibody was diluted in 1:200. For secondary incubations IgG1 and IgG2b respectively were diluted 1:500 in block. Images were collected on an Olympia or Zeiss confocal microscope.

Table 2.2 – Primary antibodies used

Antibody	Company	Volume	Secondary
Acetylated Tubulin	Sigma	1 in 200	IgG2b (Southern Biotech)
Anti-GFP	AMS	1 in 500	anti-rabbit (Southern Biotech)
HuC	Molecular Probes	1 in 500	anti-rabbit (Southern Biotech)
Isl1	Developmental Studies Hybridoma Bank	1 in 200	IgG2b (Southern Biotech)
Parvalbumin	Sigma	1 in 200	IgG1 (Southern Biotech)
Wheatgerm agglutinin	Sigma	1 in 200	anti-rabbit (Southern Biotech)

2.2.9.3 – Alcian Blue Labelling

Alcian Blue was used to stain cartilage. Alcian Blue solution was made by mixing 20mg Alcian Blue with 70ml of 100% ethanol, and 30ml acetic acid. 3 dpf embryos were fixed in 4% PFA overnight at 4^{o}C. They were then washed three times in PBT for 5 minutes and then put through 25%, 50%, 75% and 100% ethanol series in 5 minute steps. Embryos were then placed in 5ml of fresh Alcian Blue solution and left overnight at room temperature on a shaking incubator. The stain was then removed and washed twice in PBT.

2.2.10 – Retrograde and Anterograde tracing experiments

2.2.10.1 – Retrograde labelling by application using tungsten needle or injection

To trace the MTN neurons 1,1'-dioctadecyl-3,3,3',3'-tetramethylindocarbocyanine perchlorate (DiI, Biotium) crystals were applied to the adductor mandibulae muscle using a sharp tungsten needle.

Before labelling was achieved a variety of conditions were tested, these were:

1) Retrograde labelling of live fish at 3 dpf, 4 dpf and 5 dpf respectively by either injecting DiI into the a.m. of approximately 60 fish or DiI application to the a.m. muscle using a sharp tungston needle. 2) Retrograde labelling of fixed fish at 3 dpf, 4 dpf and 5 dpf respectively by DiI injection, or application using a sharp tungston needle, to the a.m. muscle. 3) Anterograde labelling of live fish at 3 dpf and 5 dpf by either injection of DiI or application using a sharp tungston needle to the dorsal anterior mesencephalon. 4) Anterograde labelling of fixed fish at 3 dpf and 5 dpf as before by either injection of DiI or application using a sharp tungston needle to the dorsal anterior mesencephalon.

The successful condition that was used was the following: DiI was dissolved in 1ml 100% proof ethanol. Approximately 5ml DiI was pipetted onto a glass slide and while the ethanol evaporated a sharp tungston needle was dipped into the solution collecting DiI crystals. Crystals were then applied to the adductor mandibulae muscle of freshly fixed fish in 4% PFA, pinned to Sylgard by sharpened tungston wire. After application fish were removed and left for several days in PBS at 4^{o}C. Images were collected on a Nikon confocal microscope.

2.2.10.2 – Anterograde and Retrograde labelling by Electroporation

An alternative method used to trace MTN neurons was by electroporation. 1mm diameter borosilicate glass capillaries, with no microfilament (world precision instruments), needles were pulled in a Flaming/Brown micropipetter puller (Sutter Instruments, model P-87) using the following parameters; heat, 670; pull, 120; velocity, 100; time, 150. The needles were filled with Dextran or 100ng/ml *huC:tdtom* using a needle filling pipette tip.

Live 5 dpf wild type larvae were anaesthetised and individually moved by a glass pasteur pipette into an eppendorf containing molten 1.5% low melting (LM) agarose that had been kept at 50^{o}C. The embryo was then transferred from the molten LM agarose by the glass pasteur pipette to the right hand side of a glass slide chamber and mounted in lateral orientation using manipulation needles. (The chamber was made using araldite, and shaped in a figure of 8 with a gap in the middle, see figure). The LM agarose droplet containing the oriented embryo was left to set. Once the droplet was set, the chamber was carefully filled with fish water and placed onto the stage of a UV compound microscope. A silver electrode, connected to the negative

terminal of an electric current box was placed in the left hand side of the chamber so that it was in contact with the fish water. A needle filled with Dextran was mounted onto a micromanipulator containing a silver wire connected to a positive terminal of an electric current box. The silver wire was checked to make sure it was in contact with the Dextran liquid. The needle was carefully lowered to penetrate the a.m. muscle and 2-3 one second electric pulses were applied. (Machine setting for electroporation; Frequency – 200, Delay – N/A, Duration – 20, Velocity – 3).

The fish were removed from the chamber and placed in a petri dish filled with fish water to recover, and left 2 – 4 hours for the Dextran to actively be transported along the axons. The fish were then re-anaesthetised and mounted in LM agar on concave slides and placed onto a confocal microscope (Nikon) stage and analysed for successful retrograde labelling.

For anterograde labelling, *Tg(1.4dlx4-dlx6:eGFP)* transgenic fish were mounted dorsally into a chamber as previously described. The tip of a needle filled with *huC:tdtom* was placed next to dorsal GFP+ neurons in the dorsal midbrain and 2 – 3 one second pulses were applied. The fish were then placed back into a petri dish, and after 2, 4, and 12 hours analysed using a confocal microscope to check for successful labelling of GFP+ cells and axons.

2.2.11 - Wholemount Zebrafish In Situ Hybridisation

2.2.11.1 - Probe Linearisation

Plasmids were linearised with the appropriate restriction enzyme (New England Biolabs) overnight using the manufacturer's recommended temperature and conditions. Plasmids and restriction enzymes used are listed in the table below. The linearised template DNA was purified by phenol/chloroform extraction and then used to synthesize Digoxygenin (DIG) or Fluorescein (FP) labelled antisense probes.

Table 2.3 – Zebrafish *in situ* probes used.

Gene	Source	Restriction enzyme	Transcription enzyme
axin2	Corinne Houart, Kings College	*KpnI*	SP6

	London (KCL)		
Brn3a	Anthony Graham, KCL	*ApaI*	SP6
cxcr4b	Holger Knaut, New York University School of Medicine	*EcoRI*	T3
dlx2	TS	*BamHI*	T7
drg11	James Cohon	*notI*	T3
egr1	gene service	*SmaI*	T7
egr2	gene service	*PstI*	T7
egr3	gene service	*SmaI*	T7
eng2	TS	*XhoI*	T7
eph4a	Steffen Scholpp, KCL	-	-
er81	Silvia Arber, Columbia University, New York	*XhoI*	T3
erm	Ivor Mason, KCL	*NotI*	T7
etv5	Silvia Arber, Columbia University, New York	*EcoRI*	T7
fgf8	TS	*EcoRI*	SP6
foxd3	TS	*BamHI*	T7
GADI	TS	*NcoI*	SP3
GFP	TS	*BamHI*	T3
gsh1	Steffen Scholpp KCL	-	-
huC	Corinne Houart, KCL	*SacI*	T7
isl1	Hitoshi Okamoto,RIKEN Brain Science Institute, Japan	*XbaI*	T3
ngn1	Corinne Houart, KCL	*XhoI*	T7
Pax6.1	Steffen Scholpp, KCL	-	-
pax7	Steffen Scholpp, KCL	-	-
pea3	Ivor Mason, KCL	*XhoI*	T7

runx3	gene service	*BamHI*	T7
snail2	TS	*XhoI*	T3
sox10	Robert Kelsh, University of Bath	*salI*	T7
tlx3a	gene service	*BglI*	T7
trkC	Stella Martin, Boston University School of Medicine	*EcoRI*	T7
vglut1	Shin-ichi Higashijima, State University of New York	*ClaI*	T3
vglut2.1a	Shin-ichi Higashijima, State University of New York	*EcoRI*	T3
vglut2.1b	Shin-ichi Higashijima, State University of New York	*HindIII*	T3
vglut2.1c	Shin-ichi Higashijima, State University of New York	*EcoRI*	T3
vglut2.2a	Shin-ichi Higashijima, State University of New York	*HindIII*	T3
vglut2.2b	Shin-ichi Higashijima, State University of New York	*HindIII*	T3
vglut2.2c	Shin-ichi Higashijima, State University of New York	*EcoRI*	T3
Wheatgerm Agglutinin	Yoshihiro Yoshihara, RIKEN Brain Science Institute, Japan	*HindIII*	T3
wnt1	Corinne Houart, KCL	*BamHI*	SP6

2.2.11.2 - Probe Transcription

For riboprobe synthesis linearized template DNA was mixed with DIG rNTP labelling mix, 10x transcription buffer, RNase inhibitor and the appropriate RNA polymerase to generate an antisense probe. See table above for the RNA polymerase used for each probe. For those where SP6 RNA polymerase was used, the reaction was incubated at 40^{o}C. Where T3 and T7 RNA polymerase were used, the reaction was incubated at 37^{o}C.

The riboprobe was precipitated in 4M LiCl and 100% ethanol at -20^{o}C overnight. This was extracted by centrifuging at 13000rpm for 10 minutes to obtain the RNA pellet and then 70% ethanol was added which was removed after centrifuging for a further 5 minutes. The pellet was left to dry for no more then 5 minutes and then re-suspended in hybridisation buffer ready for in situ hybridisation. For fluorescein labelled probes, the same method was used but in the RNA synthesis reaction Fp labelling mix (Roche) was added in place of the DIG rNTP labelling mix. Before precipitation the Fp labelled probe was purified through ProbeQuant G-50 Micro Column (Amersham Pharmacia).

2.2.10.3 - Wholemount Single In Situ Hybridisation

Single in situ hybridisation was performed as described by Thisse and Thisse, 2008. Fish were fixed as described in sections 2.2.2 and 2.2.9.1, and stored in methanol. To prepare embryos, those stored in methanol at -20^{o}C were put through reverse methanol series, washed four times in PBT for 5 minutes and permeated in 10µg/ml proteinase K. Larvae stages 24 hpf, 30 hpf, 48 hpf and 72 hpf were used therefore permeation times were 1 minute, 5 minutes, 10 minutes and 45 minutes respectively. These were then re-fixed in 4% PFA for 20 minutes and then washed a further four times in PBT for 5 minutes. For hybridisation of probe, larvae were pre-hybridised in hybridisation buffer without tRNA for approximately 2 hours at 62^{o}C. This was then replaced with hybridisation buffer with tRNA and the antisense probe at a dilution of 1:200ml and incubated overnight at 62^{o}C. The larvae were washed in an increasing series of hybridisation buffer dilutions in 2x standard saline citrate (SSC) at 62^{o}C for 15 minutes, two washes in 0.2x SSC alone and then in a series of decreasing SSC dilutions in PBT for 10 minutes per dilution wash. To detect DIG labelled probe,

larvae were hybridised in 1% 'Thisses' block for 2 hours at room temperature. Blocking agent was made using PBT containing 2% sheep serum and 2mg/ml BSA. The block was replaced with alkaline phosphatase-conjugated anti-digoxigenin antibody antibody at 1:10,000 in Thisses block and incubated overnight at 4^{o}C. After further four 30 minute washes in PBT at room temperature, hybridised embryos were equilibrated in APT buffer three 5 minute washes. Larvae were transferred into multi-well dishes and the DIG labelled probe was developed in 4-nitro blue tetrazolium chloride (NBT) at 1:250 and 5-bromo-4-chloro-3-indolyl-phosphate 4-toluidine (BCIP) stain at 1:1000 in APT buffer. To monitor degree of staining, larvae were checked every hour. After developing they were washed twice in PBT and then PBS and left in 4% PFA overnight at 4^{o}C to stop the reaction.

2.2.11.4 - Wholemount Zebrafish Double In Situ Hybridisation

Double in situ hybridisation was performed similar to the Thisse protocol described in section 2.2.11.3 with the following changes: the larvae were washed in a series of decreasing SSC dilutions in MABT. To detect DIG labelled probe, larvae were hybridised in 1% block for 2 hours at room temperature. Blocking agent was made using autoclaved 1M maleic acid (pH to 7.5) and Boehringer block to 10%, this was further diluted in 2% MABT. The block was replaced with alkaline phosphatase-conjugated anti-digoxigenin antibody antibody at 1:1000 in 1% block and incubated overnight at 4^{o}C. After further four 30 minute washes in MABT at room temperature, hybridised embryos were equilibrated in APT buffer with three 5 minute washes and developed in NBT/BCIP stain as described in section 2.2.11.3.

After developing in NBT/BCIP, larvae were washed in five 5 minute washes in MABT. They were then prepared for fluorescein detection by 10 minute incubation in 0.1M glycine (pH2.2) with 0.1% Tween-20 to remove the aDIG antibody and blocked at room temperature in 1% block for 2 hours as before. This was replaced with aFp at 1:10,000 in 1% block and incubated at 4^{o}C overnight. After 4x 30 minute washes in MABT, larvae were equilibrated for 10 minutes in 0.1M Tris-HCl (pH8.2) with 0.1% Tween-20, and then stained in Fast Red (Roche) to detect the fluorescein label. One fast red tablet was dissolved in 2ml 0.1M Tris-HCl (pH8.2) with 0.1% Tween-20 by vigourously shaking for 2 minutes and filtered using a 0.2mm filter. Developing with fast red is relatively slow, so larvae were left in fast red at 4^{o}C

overnight to develop. After staining they were washed in 2x 5 minute MABT and 2x 5 minute PBS washes and the reaction stopped in 4% PFA.

2.2.11.5 - Fluorescent In Situ Hybridisation

Fluorescent in situ hybridisation was performed as described by Holley et al. The protocol is similar to that described in 2.2.11 for single in situ hybridisation by Thisses et al on day one until the pre-hybridisation step.

For hybridisation of probe, larvae were pre-hybridised in hybridisation buffer with tRNA for approximately 5 minutes, at 55^{o}C or 65^{o}C respectively depending on whether an antibody was to be used after the fluorescent in situ hybridisation. This was then replaced with pre-hybridisation buffer without tRNA for 1 hour, and then replaced with antisense probe at a dilution of 1:50 and incubated overnight at 55^{o}C/65^{o}C.

The larvae were washed in a series of washes of: 50% pre-hybridisation buffer and 50% 2x SSC, 2% SSC alone for two 15 minutes, and then 0.2% SSC for 30 minutes at 55^{o}C/65^{o}C. To detect the probe, larvae were hybridised in Holley block for approximately 1 hour at room temperature. Holley blocking reagent was made using 150mM maleic acid, 100mM NaCl (pH 7.5) and 2% Boehringer reagent. The block was replaced with a-DIG-POD (roche) antibody used at 1:200 in Holley block and incubated overnight at 4^{o}C.

After a further four 20 minute washes in maleic acid buffer containing 0.5mM HCl and 100mM NaCl pH to 8.2. Hybridised embryos were equilibrated in PBS with two 5 minute washes. To detect the probe Cy3/FITC (PerkinElmer) fluorescent substrate was added to dilutant buffer (Promega) at 1:50 and left to develop for 45-60 minutes. Larvae were washed in PBS for a further two 5 minute washes and then analysed under a UV stereoscope (Nikon) to detect successful fluorescent labelling of probe.

2.2.12 – Microscopy

2.2.12.1 - Analysis of In Situ Hybridisation

Zebrafish were put through glycerol series of 25%, 50% and finally 75% glycerol (in PBS). Their yolks were removed using a fine needle (for those mounted in a dorsal orientation). The embryos were then placed on a glass slide and oriented in a dorsal, ventral or lateral position, with modelling clay as platforms before being covered with a glass coverslip. The embryos were viewed using a Zeiss compound microscope (Zeiss Axioscope R) and photographs were taken using a mounted Nikon Cad pol990 digital camera and using the Openlab programme. Fluorescent in situ larvae were viewed using Nikon stereoscope to screen for the clearer labelled fish, and imaged using the Nikon confocal microscope.

2.2.12.2 - Timelapse Microscopy

HuC:GFP fish were left at 22^{o}C overnight to slow down their development so they could be imaged from 18ss. Fish embryo's expressing the GFP were de-chorionated and anaesthetised. Live anaesthetised fish were individually moved by a glass pasteur pipette into an eppendorf tube containing molten 1.5% low melting (LM) agarose that had been kept at 50^{o}C. The embryo was then transferred from the molten LM agarose by the glass pasteur pipette to a glass slide chamber and mounted in a dorsal orientation using manipulation needles. The LM agarose droplet containing the oriented embryo was left to set. Once the droplet was set, the chamber was carefully filled with fish water and placed onto the confocal stage. The embryo could now be imaged for long periods of time without the water drying up. After imaging, the zebrafish embryo was carefully released from the set agarose droplet and returned to a petri dish containing fresh fish water and PTU. Timelapse microscopy was carried out using the Nikon confocal microscope

2.2.12.3 - Making glass chambers for timelapse imaging

To a glass slide a thin wall of modelling clay approximately 5mm high was

placed 5mm away from the outer edge all around the slide. Another thin wall of modelling clay was pushed firmly along the outer edge of the slide on top of aluminium foil so that there were no gaps between the edge of the slide and the aluminium foil underneath. Into the 5mm gap between the two moulds, Araldite was carefully poured. The araldite was left to set for 24 hours. Once the araldite was set, the modelling clay was peeled away and the chamber washed ready for mounting embryos in the centre of the glass slide chamber for timelapse imaging.

2.2.13 - Generation of constructs

2.2.13.1 – PCR amplification

The following clones were used: a 669bp *XbaI* fragment of truncated WGA cDNA subcloned into pBluescript (Yoshihara et al., 1999), a 2.466kb fragment of TTC containing an eGFP fusion protein subcloned into pGEX-4T-2 (Sapir et al., 2004), and a 3.9kb *α-actin* promoter subcloned into pBluescript (Higashijima et al., 1997). The Promega mini prep protocol was used to recover the plasmid. Primers were designed for the *TTC* to include the *XbaI* restriction site for insertion into the *XbaI* multiple cloning site of the pminiTol2 (Balciunas et al., 2006) vector and to incorporate all of the eGFP fusion protein. The following primers were used for the *TTC:eGFP* sequence: primer F1
TA*tctaga*GGCCACCATGAGCAA and primer R1
TA*tctaga*TCATCAATTTCGGCTGC.

Primers were designed to the *a-actin* promoter to include the *BglII* restriction site for insertion into the pminiTol2 vector at the *BglII* multiple cloning site for the WGA construct, and *MscI* for the *TTC* construct. The following primers were used for the α-actin sequence to insert into the *WGA:Tol2* construct: α-actin primer F1 TA*agatct*GGGCCTGGTAATATC and α-actin primer R1
TA*agatct*CCACATCCTGCTGTA. To insert the a-actin promoter sequence into the TTC:Tol2 construct the same primers were used except the *BglII* sequence was substituted with the *Msc1* sequence *tggcca*.

The *TTC* and *α-actin* were PCR amplified from TTC:eGFP pBS and α-actin pBS respectively using KAPA HiFi biosystems. 0.5μl of each of the forward primer and reverse primer (10μM) were added to a 50μl mix containing a final concentration of: 5x KAPA HiFi buffer, 0.2mM dNTPs (25mM), 2μl of cDNA template plasmids (as

described above), dH_2O and 0.5µl KAPA HiFi polymerase. The PCR was run on the following program:

98°C for 2 minutes

(98°C for 20 seconds, 56.9 °C for 15 seconds, 68°C for 2 minutes) x 35 cycles

68 °C for 5 minutes

4 °C indefinitely

Table 2.4 – Primer sequences

Gene	Forward primer sequence	Reverse primer sequence
a-actin	TA*agatct*GGGCCTGGTAATATC	TA*agatct*CCACATCCTGCTGTA
TTC:eGFP	TA*tctaga*GGCCACCATGAGCAA	TA*tctaga*TCATCAATTTCGGCTGC

2.2.13.2 - Restriction Digest

For insertion of *WGA* and *TTC* into pminiTol2, each was digested with *XbaI* using the following reaction mix: mini-prep DNA for WGA and Tol2, or TTC PCR, 10x buffer, 10x BSA, dH_2O and then left at 37°C overnight according to manufacturers instructions for *XbaI* restriction enzyme. For insertion of *α-actin* into *WGA:Tol2* both were digested with *BglII* and for insertion of α-actin into *TTC:Tol2* both were digested with *MscI*. The same reaction mix and conditions were used as before. The vectors were treated with Calf Inositol Phosphatase (New England Biolabs) for 1 hour at 37°C to remove the phosphates to prevent the vector from self-ligating, and then heated to 65°C for 20 minutes to stop the reaction. All digests were gel extracted according to Qiagen gel extraction protocol. The concentration of DNA extracted was measured by spectrometer.

2.2.13.3 - Ligation

An overnight ligation reaction at 4°C was set up using 10x ligation buffer, insert (left out in the control reaction) and vector DNA, dH_2O and T4 DNA ligase (Roche). Three conditions for each ligation were used, these were a control containing no insert to determine the degree of self-ligation, a reaction ratio of 1:1 and a 3:1 of insert to vector.

2.2.13.4 – Transformation

Ligation products were transformed into DH5α by incubation of ligate mixed with DH5α cells on ice for 20 minutes, then heat shocked for 45 seconds at 42^{o}C and a further 5 minute incubation. To recover the cells they were incubated at 37^{o}C on an agitator in LB for 1 hour and then centrifuged at 4000rpm for 10 minutes and the remaining LB discarded. Cells were carefully resuspended in surplus LB and plated onto agar plates containing 60ml/mg ampicillin and incubated at 37^{o}C overnight. Colony growth was compared between the three conditions and 10-20 colonies were picked from the 3:1 condition and grown overnight in LB at 37^{o}C on an agitator. A mini prep was performed on each colony using the Promega mini-prep kit protocol. A diagnostic was then performed to determine whether the plasmid recovered contained the required insert. To test for *WGA* or *TTC* insert into pminiTol2, *XbaI* was used, to test for α-actin insert into *WGA:Tol2 BglII* was used, and to test for α-actin insert into TTC:Tol2 *MscI* was used. If the insert is present two bands will be seen when run on a 1% gel, one at the length of the vector and the other at the length of the insert. The orientation of the insert was determined by choosing enzymes that digested in the vector close to the insert at the 5' end and digested in the insert towards the 3' end. If the predicted band sizes from this digestion are seen then the insert is in the correct orientation. To confirm this, identified plasmids were sent off for sequencing. The finished construct generated was then injected into zebrafish embryos at the one cell stage.

2.2.13.5 – Generation of tol2 RNA

Transposase RNA, used to inject with the TTC or WGA tol2 contstruct, was synthesised using the mMessage machine protocol (Ambion).

2.2.13.6 - Plasmid DNA and RNA injection

WGA and *TTC* were diluted to 100ng/µl in dH_2O and 6% phenol red. 100ng/µl of tol2 RNA was added to each of these. The DNA and RNA were then used to inject into zebrafish embryos at the one cell stage. Injected embryos were placed in

fish water and left in incubator at 28.5^{o}C until fixation using 4% PFA at 30hpf, 72hpf or 5dpf respectively.

2.2.14 - Zebrafish Drug Treatments

Drug treatments using fgfr1 inhibitor SU5402 (Calbiochem), and gsk3β inhibitor BIO (SigmaAldrich), were carried out. Both drugs were received as a lyophilised solid, and were reconstituted in DMSO to a stock concentration of 40mM. Each drug was aliquoted and stored at -20^{o}C. To determine the best working concentration for both drugs a series of concentrations were tested, and the larvae examined for toxicity and degree of death. The optimum working concentration for SU5402 was 40μM, and for BIO was 4μM. To reach the required working concentration the drugs were diluted in 1ml 1x embryo media by vortexing briefly. For controls, fish for each drug were treated in the equivalent concentration of DMSO diluted in embryo media.

Shortly before drug treatments the embryo chorions at 5 ss or 10 ss were torn so that the drug could come in contact with the embryo more easily. Embryos were not completely de-chorionated because at these early stages this tended to be too rough and resulted in the embryo dying. Approximately 15-20 embryos were carefully transferred, using a glass pasteur pipette, into an eppendorf containing the drug or DMSO control, adding as little extra liquid as possible so that the drug was not diluted further. The embryo's in the drug were then transferred by a pasteur pipette to one well in a 12 well plate. To stop the embryo's sticking to the bottom of the well, the wells had been pre-lined with 1ml 1.5% LM agarose and left for a short while to set. Once both controls and drug treated fish had been transferred to the plate it was covered with foil to keep out any light, as the drugs are light sensitive, and left in the 28^{o}C incubator until 24hpf. At 24hpf the embryos were completely de-chorionated, anaethetised and then fixed in 4% PFA.

Fgf signalling was partially down regulated using SU5402 drug treatments at a working concentration of 20μM, in conjunction with a partial ablation of neural crest (see section 2.2.4).

Table 2.5 – Pharmacological inhibitors

Drug	Company	Stock concentration	Working concentration
SU5402	Calbiochem	40mM	40µM and 20µM
BIO	Sigmaaldrich	40mM	4µM

2.2.15 – Heat shock induction of *Tg(hsp70l:dkk1-GFP)*

Heat shock treatments were carried out using *Tg(hsp701:dkk1-GFP)* transgenic fish (Aman and Piotrowski, 1998). To determine the best stage to heat-shock a series of stages were tested and the larvae examined for toxicity and degree of death. The stage at which heat-shock treatments proved to be less toxic, because they were able to survive to 24 hpf, was 15 ss. Embryos were left in the 28^{o}C incubator until 15 ss when they were removed and transferred into a 50ml falcon tube containing fish water and placed in a water bath set to 37^{o}C for 1 hour. The embryos were then transferred back into a petri dish and into the 28^{o}C incubator until 24 hpf, when effective inhibition of Wnt signalling was confirmed by GFP expression by analysis under a UV stereoscope (Nikon). GFP negative embryos were used as a control. At 24 hpf embryos were de-chorionated, anaesthetised and then fixed in 4% PFA.

2.2.16 – Quantification of MTN cell numbers

Counts of total MTN and posterior commissure cell numbers in zebrafish embryos were performed on in situ hybridised embryos at 24 hpf or 26 hpf labelled for drg11 or isl1. 10 embryos were mounted in a dorsal orientation and cell numbers counted for each condition to get 'n' numbers.

To determine whether there was any difference in cell numbers between mutants/treated compared to controls, the average number was calculated. These values were plotted in a graph and the standard error of the mean was also plotted.

Students paired T-test was used to analyse the statistical significance of the data sets. This test calculated the probability (*p*) of the null hypothesis (i.e that there is

no significant difference between the control and the experimental groups). A two-tailed test was used, so a *p* value of less then *0.001* was taken to be statistically significant.

Results

Chapter 3 – Characterisation of the MTN in the Zebrafish

3.1 Introduction

There has been a limited number of studies into the development of the mesencephalic trigeminal nucleus (MTN). While previous investigations have identified the location of the MTN in many vertebrates, little is actually understood about its development. MTN cell bodies are positioned along the dorsal mesencephalon in fish and amniotes, and also in the rostral hindbrain of mammals (Luiten, 1979; Pombal et al., 1997; Ruggiero et al., 1982). HRP axonal tracing studies of the MTN in vertebrates reveal that they innervate the skin and perioral area of the jaw, and the mandibular arch muscles in mammals (cat, Alvarado-Mallart et al., 1975). HRP axonal tracing studies of the MTN in teleosts and shark revealed that they also innervated the skin and perioral area of the jaw, but found that MTN neurons did not innervate the mandibular arch muscles. In mammals the nucleus is topographically arranged, with perioral associated neurons concentrated in the caudal hindbrain, while muscle associated neurons are distributed throughout the midbrain (Alvarado and Mallart, 1975; Ruggiero et al., 1982; De et al., 2005).

In this chapter, I describe the identification and location of the MTN in zebrafish, in the dorsal mesencephalon similar to other vertebrates. The MTN has been characterised in other teleosts such as the carp and medaka, but not clearly in zebrafish (Luiten, 1979; Pombal et al., 1997). These studies identified the location of MTN neurons by retrograde labelling with dextrans and HRP dyes applied to the trigeminal nerve (Luiten and Van der Pers, 1977; Luiten, 1979). Dextrans are not ideal to use for labelling the MTN in zebrafish because: they are not fixable, they have to be applied directly to a severed neuron, and only work in live fish because they are actively transported.

To identify the location of MTN in zebrafish I have used a lipohilic dye called DiI to retrogradely label MTN axons from the mandibular arch muscles that they innervate. Fluorescent lipophilic dyes are a good tool to use for labelling axons because they work in fixed tissue as they are not actively transported along the axons (Honig and Hume, 1986; Perrin and Stoeckli, 2000). They are distributed along the axon by diffusion along the plasma membrane instead, so these lipophilic dyes do not have to be applied directly to a severed neuron.

After identifying the location of MTN cell bodies in larval zebrafish I then aimed to identify genes expressed in the MTN in zebrafish. *In situ* hybridisation was used to assess zebrafish orthologues of genes previously shown to be expressed in the MTN in chick and mouse (*brn3a*, *drg11*, *isl1*; Hunter et al., 2001; Wang et al., 2007). Interestingly, these genes are also expressed in Rohon-Beard (RB) neurons and dorsal root ganglia (DRG). This leads to the intriguing question of how genetically similar proprioceptive MTN are to other sensory neurons, RB neurons and DRGs. Genes expressed in proprioceptive DRGs and RB neurons were also analysed for their expression in MTN, such as *trkC* and *runx3* (Williams et al., 2000; Park and Saint-Jeannet, 2010). Neuronal specific genes *huC* and *ngn1* were also analysed for their expression in MTN, in order to determine at which stage MTN neurons and adjacent neurons undergo neurogenesis in the midbrain (Park et al., 2000; Andermann et al., 2002). The expression analysis of genes expressed in MTN in the zebrafish revealed a conservation between different vertebrates. This data was also used to compare the similarities and differences in gene expression between MTN, RB neurons and DRGs, to understand how similar they are to one another.

To ascertain the axonal trajectories of MTN neurons and their origin in their brain, developing neurons were analysed by time-lapsed microscopy of *Tg(huC:eGFP)*. I used this to compare MTN axonal patterns and origin in zebrafish, to other species.

In summary I present data that reveals MTN patterning, innervation of head muscles, and gene expression profile is conserved between teleosts and amniotes.

3.2 Results

3.2.1 - Retrograde labelling with DiI reveals MTN cell bodies are located in the dorsal anterior mesencephalon.

To identify the location of MTN cell bodies in larval zebrafish, axons contacting muscles in the mandibular arch were retrogradely labelled by applying the lipophilic dye, DiI. Axons contacting the adductor mandibulae (a.m.) muscle were labelled in this manner, by applying DiI directly to the muscle. Labelling of axons was optimised in 5 days post fertilisation (dpf) larvae as it was not possible to obtain labelling in animals at earlier stages (see materials and methods). At earlier stages, the MTN may not yet have innervated the muscles in which DiI was applied. DiI labelled cell bodies were approximately 10μm in diameter (Figure 3.2.1H and I). The number of

cell bodies labelled varied between fish (approximately 2-7 cells per fish; Appendix 1), and reflects the varying amount of DiI applied to the muscle. MTN cell bodies were labelled in the dorsal-lateral region of the anterior mesencephalon (20/50 embryos had labelled cells in the dorsal mesencephalon, while the remaining embryos had no labelled cells) superficial to the tectum, similar to the location of MTN described in amniotes (Hiscock and Straznicky, 1982, 1986; Mastick and Easter, 1996) (Figure 3.2.1; Appendix 1).

In teleosts the MTN has not been found to innervate the jaw muscles, therefore the MTN neurons could be innervating the skin adjacent to the muscle in zebrafish, and would be labelled by DiI applied to the muscle (carp, Luiten, 1979; guppy, Pombal et al., 1997). However in the DiI applications where no cells had been labelled (30/50 embryos), the DiI had been unsuccessfully applied to the muscle, and appeared restricted to the skin overlying the muscle instead (data not shown). This implies that in zebrafish, neurons of the MTN do innervate the jaw muscles, in contrast to previous nerve tracing studies in teleosts (carp, Luiten, 1979; guppy, Pombal et al., 1997). Axons growing from the MTN cell bodies are apparent in the dorsal midbrain and take a medio-lateral route to the midbrain hindbrain boundary (MHB), into the hindbrain. Branching of the MTN axons can be seen close to the MTN cell bodies in the midbrain (Arrowhead; Figure 3.2.1I). After bifurcation, both branches appear to follow the same path into the hindbrain (Figures 3.2.1A-G, and I). It is unclear where these branches project to when they enter rhombomere two (R2) of the hindbrain, due to bright DiI labelling in the motor nuclei [nucleus] of the trigeminal nerve (nV). In chick, one MTN branch synapses to the nV cell body while the other branch follows the mandibular process of the nV out of R2, and down to the mandibular arch muscles that they innervate (Hiscock and Straznicky, 1986). These connections between the MTN, nV and mandibular muscles, form the monosynaptic trigeminal circuit (Zhang et al., 2005).

Successful labelling of MTN cell bodies in the dorsal mesencephalon means it is likely one branch of the MTN does innervate the a.m., but this branch cannot be seen due to the bright labelling of the the nV that also innervates the a.m. The nV can be clearly followed up into the hindbrain (Figure 3.2.1A-C).

When applying DiI to the a.m. muscle, occasionally adjacent eye muscles were also accidentally labelled, such as the inferior rectus (i.r.) (8/20). This resulted in the retrograde labelling of other nuclei, e.g. the oculomotor nucleus (nIII), (located in the ventral midbrain; blue arrowhead, Figure 3.2.1G and Figure 3.2.2D and F; Appendix

1), which innervates the i.r. (Higashijima et al., 2000; Chandrasekhar, 2004; Chilton and Guthrie 2004). The location and numbers of MTN neurons labelled within the dorsal anterior mesencephalon were unchanged when DiI was applied to both a.m. and i.r. muscles compared to fish where DiI was applied to the a.m. alone. This reveals that the labelling of the i.r. did not have any affect on the results.

The MTN is the only mesencephalic nucleus that innervates jaw muscles in amniotes (Lazarov and Usunoff, 2003). The location of labelled neurons in zebrafish in the mesencephalon is conserved with the location of MTN in amniotes, which strongly implies that these are also MTN neurons. In contrast to previous studies in teleosts, which failed to find any innervation of jaw muscles by the MTN neurons, the MTN appears to innervate the jaw muscles in zebrafish.

Figure 3.2.1.1 – Application of DiI to the adductor mandibulae muscle retrogradely labels MTN neurons.

Confocal images of 5 dpf zebrafish in which DiI crystals were applied to the adductor mandibulae (a.m, asterisk). A-C) Lateral views revealing the DiI labelling of the motor nucleus of the trigeminal nerve (V), and MTN neurons located in the dorsal anterior mesencephalon (white arrows). D-F) Dorsal views of the same 5 dpf zebrafish seen in A-C, showing the retrograde labelling of MTN neurons (white arrows). G) A lateral view of 5 dpf zebrafish where many MTN cell bodies have been traced by the DiI. Blue arrow indicates retrograde labelling of the motor nucleus of the oculomotor nerve. H) A higher magnification of G, revealing MTN cell bodies and their axonal projections. I) A higher magnification focussing on MTN neurons labelled with DiI, and their axonal branching (white arrowhead) a short distance from the cell body. J) A schematic of the lateral view of a zebrafish head, showing the locations of the adductor mandibulae (a.m), levator arcus palatini (l.a.p) and dilator operculi (d.o) at 5 dpf. K) A schematic of the dorsal view of a zebrafish head at 5 dpf. a.m, adductor mandibulae. d, diencephalon. d.o, dilator opperculi. l.a.p, levator arcus palatini. mb, midbrain. tg, trigeminal ganglion. V, motor nucleus of the trigeminal nerve.

Scale bars; A - G = 100 μm, H = 10 μm, and I = 20 μm

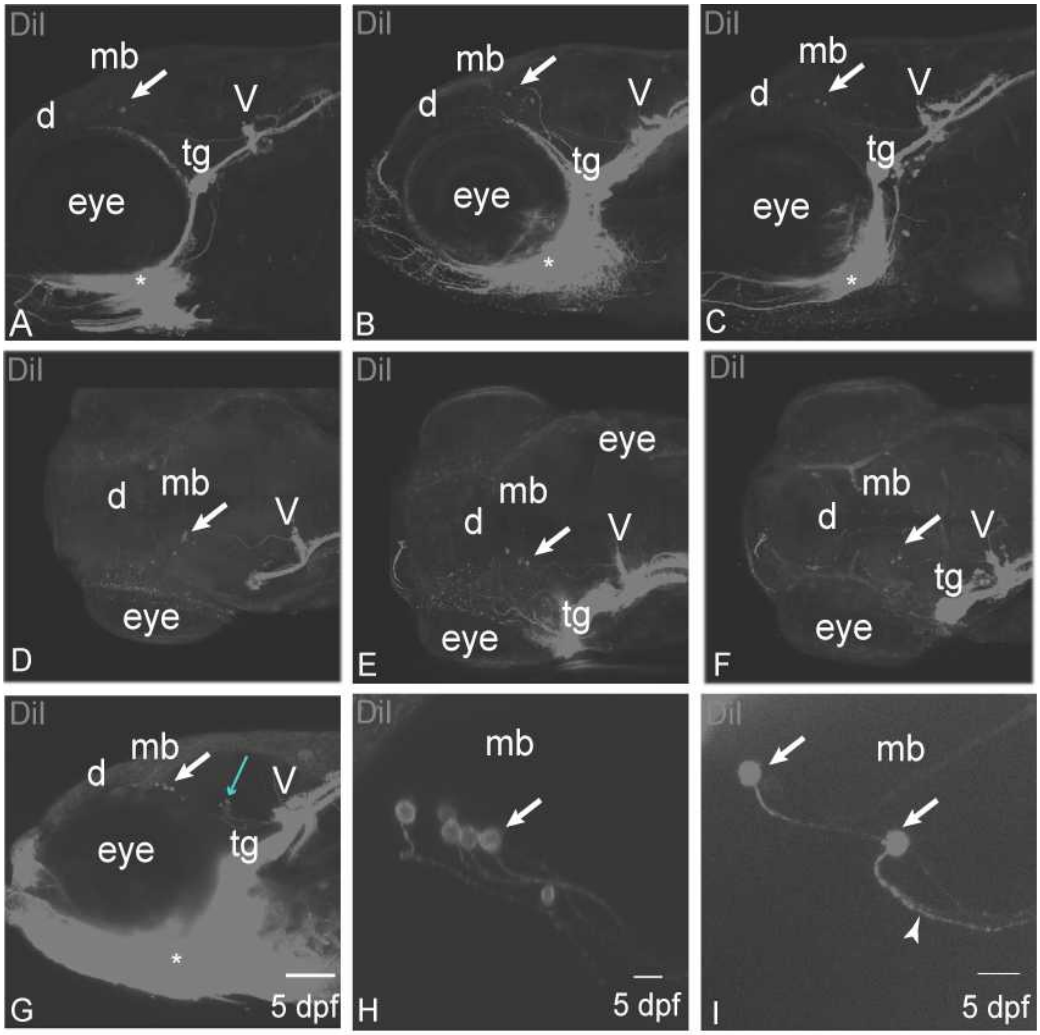
DiI
mb
d
V
tg
eye
*
A
B
C
D
E
F
G
H
I
5 dpf

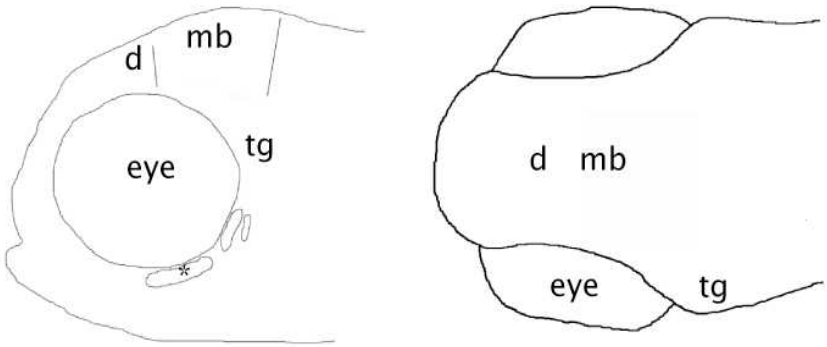
d
mb
eye
tg
*
d mb
eye
tg

Figure 3.2.1.2 - Application of DiI to the adductor mandibulae muscle retrogradely labels MTN neurons.

Confocal images of 5 dpf zebrafish in which DiI crystals were applied to the adductor mandibulae (a.m. asterisk). (A – N) Lateral views showing the DiI labelling of the nucleus of the trigeminal motor nerve (V), and MTN neurons located in the dorsal anterior mesencephalon (white arrows). In some cases the nucleus of the oculomotor motor nerve (III) was labelled too (D, F, H, I, K, N), but the location and numbers of MTN neurons labelled were unchanged compared to animals in which DiI labelled the nucleus of the trigeminal motor nerve alone (A – C, E, G, J, L, M). (O) Diagrammatic representation of a lateral view of the zebrafish head. d, diencephalon. III, oculomotor nucleus. mb, midbrain. tg, trigeminal ganglion. V, nucleus of the trigeminal motor nerve

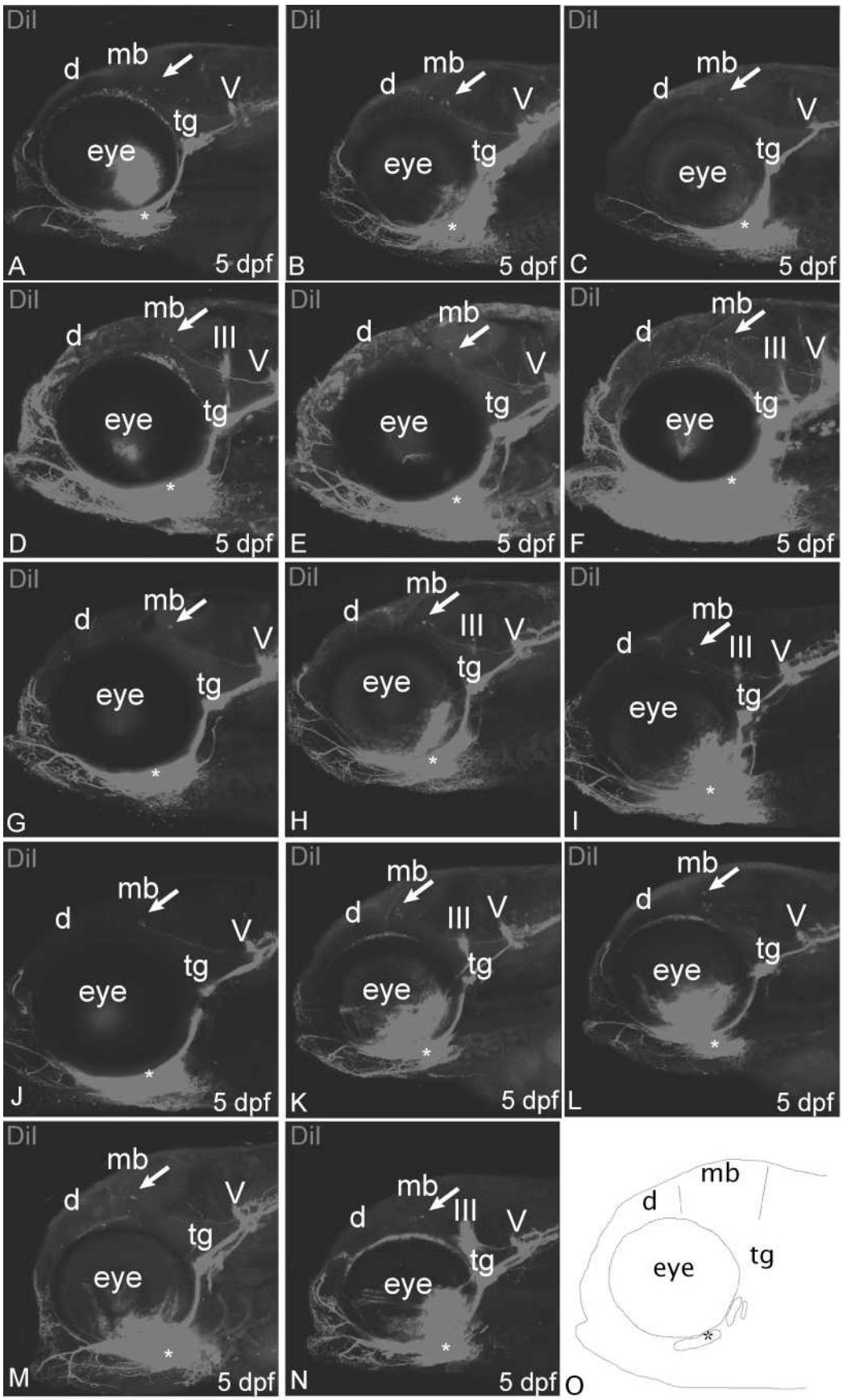
DiI
mb
d
V
tg
eye
III
*
A
B
C
D
E
F
G
H
I
J
K
L
M
N
O
5 dpf

3.2.2 – Retrograde labelling of different muscles reveals co-labelling in most MTN cell bodies.

To determine whether MTN neurons form a topographically organised map relative to the muscles that they innervate two lipophilic dyes were applied to different muscles. If there are different populations of MTN, they may respond differently to molecular signals, during their development, in order to target the correct muscle. As before DiI was applied to the a.m. at 5dpf (Figure 3.2.2A and G, asterisk). In the same fish DiD was applied to the lavator arcus palatini (l.a.p.) located near to the eye (Figure 3.2.2B and H, asterisk).

Imaging of the MTN, by confocal microscopy, showed that when DiI and DiD were applied to different muscles in the same fish, both resulted in the co-labelling of the mandibular branch of the trigeminal motor neuron and the trigeminal ganglia (Figure 3.2.2). MTN cell bodies were labelled with DiI or DiD in the dorsal anterior mesencephalon (12/12). In fish where both DiI and DiD labelled MTN (6/12), most MTN neurons labelled with DiI were also co-labelled with DiD (5/6, Figure3.2.2F, white arrow). In one fish where MTN were labelled with DiI, there was one MTN labelled with DiD alone (1/6) (Figure 3.2.2L, arrowhead). In most cases where co-labelling was seen in MTN cell bodies (4/6), the application regions of the DiI and DiD appeared to overlap, where DiD was also seen in the a.m. This may then result in MTN innervating the a.m. also being labelled with DiD. Occasionally DiI or DiD had also accidentally been applied to the dorsal operculi (d.o).

From these results I am unable to discriminate if MTN innervate muscles in a topographic fashion, due to imprecision of the labelling technique. It would be more ideal to use genetically encoded constructs expressed in specific muscles, to label axons.

Figure 3.2.2 – Application of DiI and DiD to different mandibular arch muscles shows co-labelling in most MTN neurons.

Lateral views of 5 dpf zebrafish showing, A) the application point of DiI crystals to the adductor mandibulae (a.m.) muscle and B) the application point of DiD crystals to the levator arcus palatini (l.a.p.) muscle, within the same fish. The muscles are indicated with an asterisk. C) A merge of both A and B. D) A higher magnification of C, showing the DiI labelling of MTN neurons in the dorsal anterior mesencephalon. Both the motor nucleus of the oculomotor nerve (III) and trigeminal nerve (V) are also labelled with DiI. E) A higher magnification of C, showing the DiD labelling of MTN neurons in the dorsal anterior mesencephalon. F) A merge of both D and E, showing that some MTN have been retrogradely labelled with both DiI and DiD (white arrow).G) Another example of the application point of DiI, and H) DiD to mandibular arch muscles. I) A merge of both G and H. J) A higher magnification of I showing DiI, and K) DiD labelled MTN. L) A merge of both J and K, showing that some MTN neurons are again co-labelled with both DiI and DiD, while one MTN cell body has been retrogradely labelled with DiD alone (white arrowhead). III, motor nucleus of the oculomotor nerve. mb, midbrain. V, motor nucleus of the trigeminal nerve.

Scale bars; C and I = 100μm, and F and L = 50μm

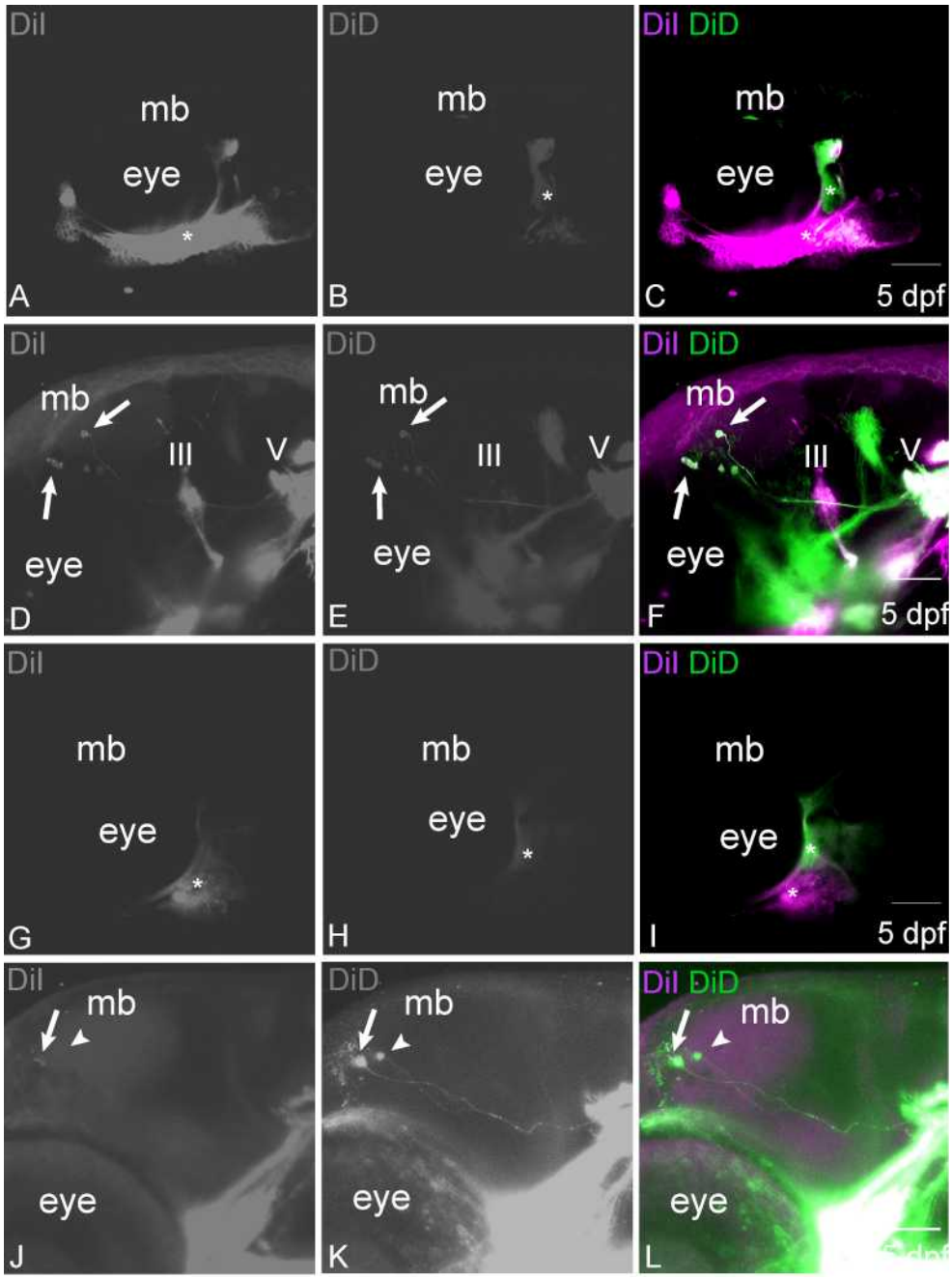
DiI
mb
eye
A
DiD
mb
eye
B
DiI DiD
mb
eye
C
5 dpf
DiI
mb
III
V
eye
D
DiD
mb
III
V
eye
E
DiI DiD
mb
III
V
eye
F
5 dpf
DiI
mb
eye
G
DiD
mb
eye
H
DiI DiD
mb
eye
I
5 dpf
DiI
mb
eye
J
DiD
mb
eye
K
DiI DiD
mb
eye
L

3.2.3 – Generation of genetically encoded tracers of neuronal circuits.

To visualise MTN neurons and the other components that form the monosynaptic trigeminal circuit, two plasmids were generated using a muscle specific promoter α-actin (see materials and methods; Higashijima et al., 1997). The first construct expressed the pan-synaptic protein; wheatgerm agglutinin (WGA; Yoshihara et al., 1999). WGA is transported in the axons and dendrites of neurons in both anterograde and retrograde directions (Yoshihara et al., 1999). It is a trans-synaptic protein so it can be transferred between neurons at synapses, therefore labelling neuromuscular circuits. The second construct expresses a retrogradely transported protein; truncated tetanus toxin (TTC; Coen et al., 1997). The TTC is fused to a green fluorescent protein (GFP) enabling live in vivo imaging of axons (Sapir et al., 2001). TTC is taken up by nerve endings at neuromuscular junctions and it is then transported along the axon of the motor nerve in vesicles until it reaches the cell body that it labels (Coen et al., 1997).

Zebrafish injected with either α-actin:WGA or α-actin:TTC-EGFP plasmids at the one cell stage, were analysed for any expression of the WGA or EGFP at 33 hpf and 50 hpf respectively. *WGA* gene expression was seen in muscle fibres in the zebrafish trunk (Figure 3.2.3A – C). The protein expression in WGA injected fish was assessed by labelling with anti-WGA. Many different conditions were tested, but this did not result in any labelling of the protein. *TTC* expression was also seen in cells in the trunk, but this appeared as isolated patches (Figure 3.2.3D - E). Labelling of TTC-EGFP protein in the injected fish revealed aggregations of EGFP expression localised to the Golgi in trunk muscles (data not shown). No EGFP was seen in any axons, suggesting that the TTC was unable to retrogradely label axons innervating the muscles. The patchy appearance of the GFP suggested that the protein may be undergoing degradation or is sequestered in the cell.

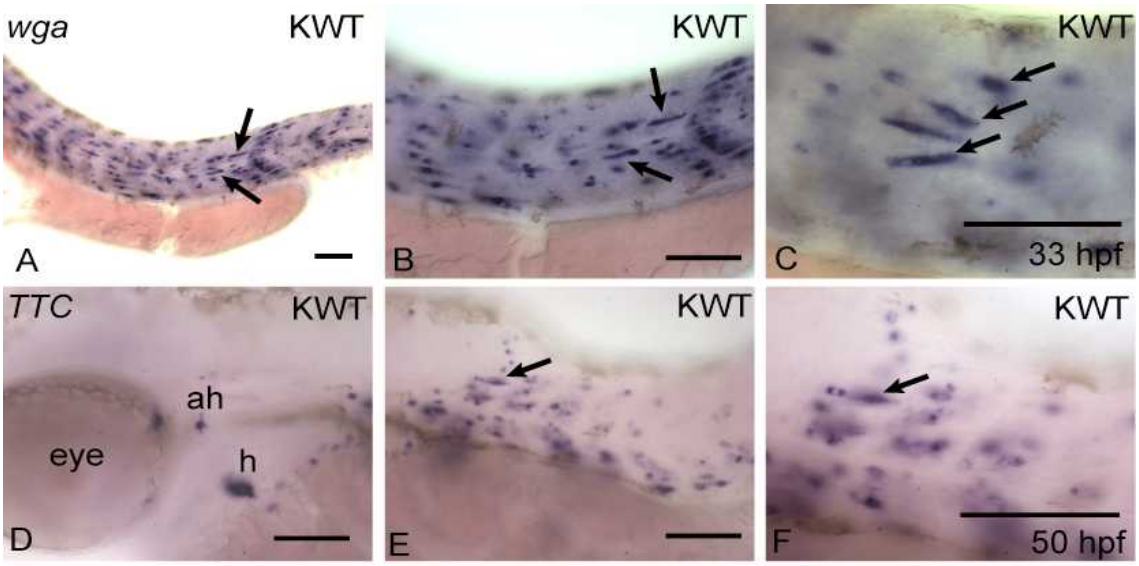

Figure 3.2.3 – Expression of α-actin:TTC and α-actin:WGA constructs

Dorsal views of the zebrafish. A) *WGA* expression in the trunk at 33 hpf, controlled by the muscle specific promoter α-actin. B) a higher magnification of A. C) a higher magnification of B, *WGA* expression can be seen in individual muscle cell fibers. D) *TTC* expression in an eye muscle, hyoid arch muscle (adductor hyomandibulae, ah) in the head, and in the heart (h) at 50 hpf (based on zf anatomy Schilling and Kimmel, 1997), and E) in the trunk muscles (arrows). *TTC* expression is also controlled by the muscle specific promoter α-actin. F) A higher magnification of E. ah, adductor hyomandibulae. h, heart. KWT, Kings Wild Type.

Scale bars; 100μm

3.2.4 – *Tg(1.4dlx4-6:GFP)* is expressed in a subset of MTN cell bodies labelled with DiI.

In the transgenic line *Tg(1.4dlx4-6:GFP)*, GFP is expressed in neurons of the dorsal mesencephalon, where MTN cell bodies are located (Ellies et al., 1997). To determine whether *Tg(1.4dlx4-6:GFP)* transgenic fish could be used as a tool to follow MTN development, MTN were compared to GFP in the midbrain.

As before DiI was applied to the a.m. muscle in fixed *Tg(1.4dlx4-6:GFP)* transgenic fish at 5dpf. A number of GFP+ cells in the dorsal mesencephalon were retrogradely labelled by DiI (25/100 fish, 2-4 cells per fish) (Figure 3.2.4.1A, B and E-H). However not all the DiI labelled cells in the dorsal anterior mesencephalon were GFP+ (approximately 1-3 per fish) (Figure 3.2.4.1G and H). This may reflect heterogeneity between MTN neurons, or variability in the expression of the transgene. Therefore the *Tg(1.4dlx4-6:GFP)* transgenic line was not ideal for following MTN development. There were also many other GFP+ cell bodies in the dorsal mesencephalon, such as tectal cells (Ellies et al., 1997; Figure 3.2.4.1C and D). This would cause further problems in following MTN development, because differentiating between various cell types and their axons would be difficult.

MTN cells labelled with DiI alone (magenta), and MTN GFP+ cells co-labelled with DiI (yellow), were plotted onto a schematic diagram to topographically map these apparent sub-populations of MTN neurons (Figure 3.2.4.2, see materials and methods). MTN GFP+ cells co-labelled with DiI did not map to a specific area within the dorsal anterior mesencephalon. This shows there is no organisation of these sub-populations; or that the random locations of GFP+ MTN cells within the dorsal anterior mesencephalon is due to variation in the expression of the transgene.

A composite from the DiI labelling of MTN neurons was assembled (see materials and methods) (Figure 3.2.4.2). Cell bodies are shown located in the dorsal anterior mesencephalon, and their axons grow peripherally to the hindbrain (Hunter et al., 2001; Hiscock and Straznicky, 1982). A short distance away from the cell body the axon bifurcates sending one branch to rhombomere two in the hindbrain. Based on MTN anatomy in amniotes this branch may synapse with the motor nucleus of the trigeminal nerve (unclear from DiI labelling in zebrafish) (Hiscock and Straznicky, 1986). The other branch grows down to the mandibular arch muscles with the mandibular branch of the trigeminal nerve. The DiI labelling of MTN and nV are consistent with these neurons forming a circuit to the a.m. muscle, similar to that noted

in amniotes but in contrast to previous observations in teleosts (Luiten, 1979; Lazarov and Usenoff, 2003).

Figure 3.2.4.1 – *Tg(1.4dlx4-6:GFP)* is expressed in a subset of MTN cell bodies retrogradely labelled with DiI

Views of *Tg(1.4dlx4-6:GFP)* transgenic 5 dpf zebrafish where DiI crystals were applied to the adductor mandibulae (asterisk) to trace MTN neurons. A) Lateral and B) dorsal view showing the DiI labelling of; MTN cell bodies (white arrow, co-labelled with GFP+ cells; white arrowhead DiI labelled MTN cell bodies alone) and their axons in the dorsal mesencephalon, and the oculomotor (III; A only) and trigeminal nucleus (V). The expression of GFP+ cells in the tectum and the telencephalon (t) can also be seen C) A higher magnification of A, and D) a higher magnification of B showing the DiI labelling of MTN cell bodies and their axons in the dorsal mesencephalon. E) A higher magnification of A, and F) a higher magnification of B showing the expression of GFP+ cells in the tectum. G) a merge of both C and E, and H) A merge of both D and F, showing the co-labelling of DiI and GFP in some MTN cell bodies (white arrow; number of co-labelled MTN = 2). III, oculomotor nucleus. d, diencephalon. mb, midbrain. t, telenecephalon. tg, trigeminal ganglion. V, trigeminal nucleus.

Scale bars; A – F = 100μm, and G and H = 50μm

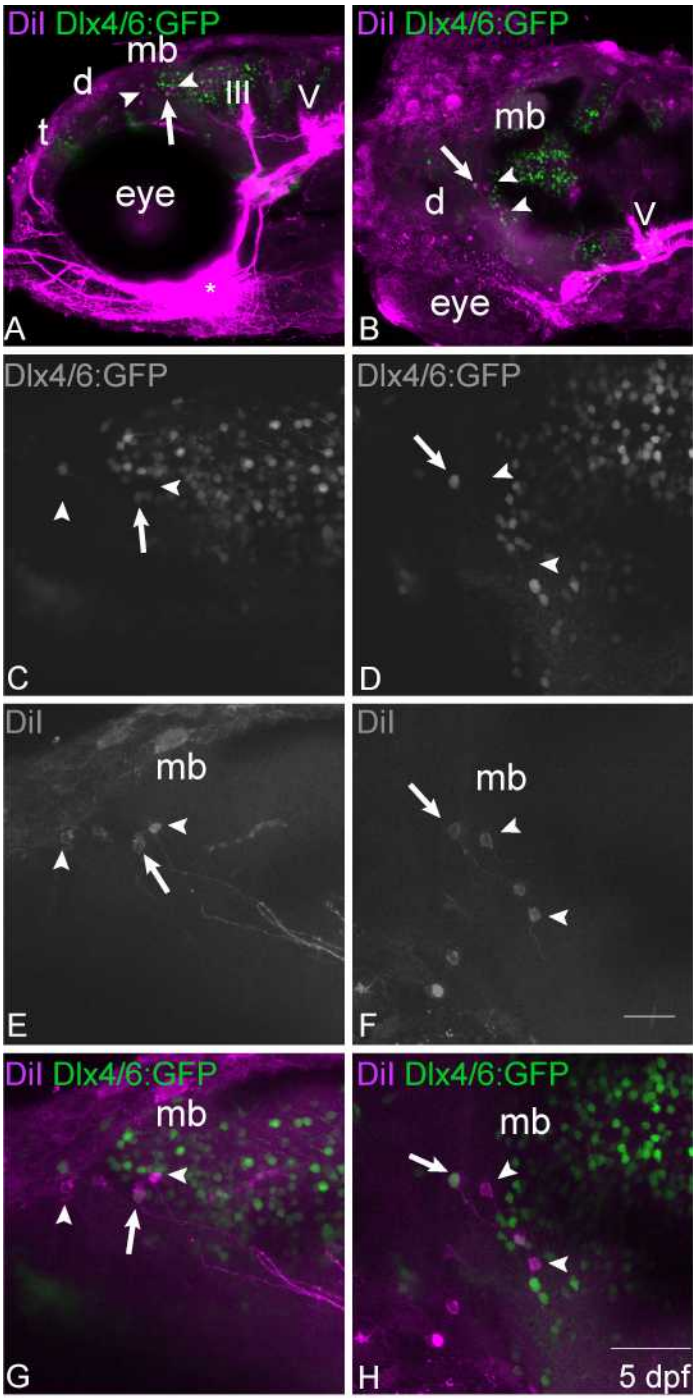
DiI Dlx4/6:GFP
mb
d
III
V
t
eye
*
A
DiI Dlx4/6:GFP
mb
d
V
eye
B
Dlx4/6:GFP
C
Dlx4/6:GFP
D
DiI
mb
E
DiI
mb
F
DiI Dlx4/6:GFP
mb
G
DiI Dlx4/6:GFP
mb
H
5 dpf

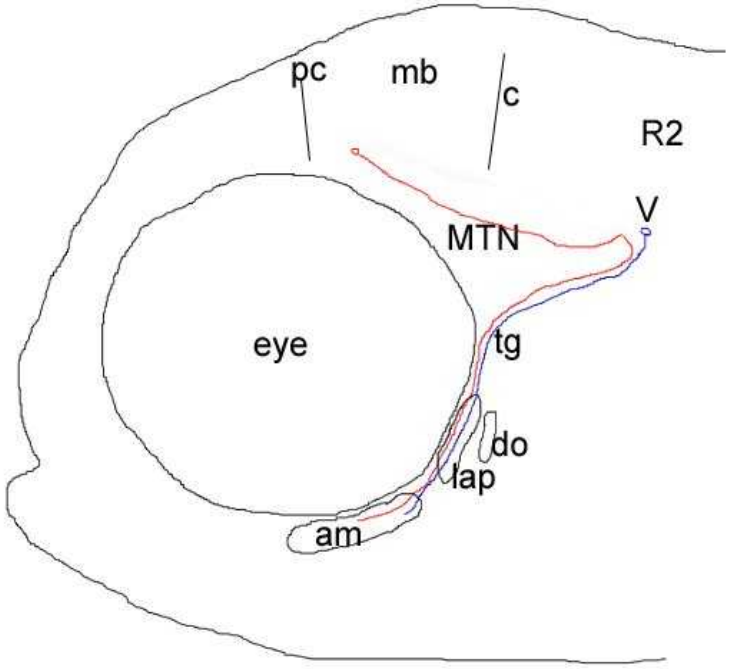

Figure 3.2.4.2 – Diagrammatic representation of DiI labelling of the monosynaptic trigeminal circuit in 5 dpf larval zebrafish

The diagrammatic representation of the monosynaptic circuit in zebrafish at 5 dpf is based on data from retrograde labelling with DiI (n = 45). The axonal path of the trigeminal motor nucleus (V) from rhombomere 2 (r2) in the hindbrain, to the adductor mandibulae (a.m) muscle is shown. MTN cell bodies are shown in the dorsal anterior mesencephalon with axons branching a short distance from the cell body, which then follow a path into the midbrain (mb; from traces of axons in lateral images of DiI labelled 5 dpf zebrafish). One axonal branch of the MTN is shown to form a presumptive synapse with the nucleus of the trigeminal motor nerve (V) and the other branch takes a similar path as the neurons from the motor nucleus of the trigeminal nerve (V) to innervate the a.m. (based on data from previous studies by Hiscock and Straznicky, 1986, and; Lazarov and Usenoff, 2003). a.m, adductor mandibulae. c, cerebellum. do, dilator operculi. lap, levator arcus palatini. mb, midbrain. MTN, mesencephalic trigeminal nucleus. pc, posterior commissure. R2, rhombomere 2. tg, trigeminal ganglion. V, trigeminal motor nucleus.

3.2.5 – Retrograde labelling with dextran and anterograde labelling with *huC:tdTomato*

Alternative methods were used for following the development of MTN neurons, to identify the axonal pathways they take, these were: Injection of dextran into mandibular arch muscles, electroporation of dextran and *huC:tdTomato* plasmids into the midbrain where MTN cell bodies lie, and kaede photoconversion at the level of the MTN in the midbrain. Injection of dextran into the a.m. and l.a.p. only resulted in the labelling of the motor nucleus of the trigeminal nerve (Figure 3.2.5.1). Dextran and *huC:tdTomato* plasmid were electroporated into MTN cell bodies in the *Tg(1.4dlx4-6:GFP)* line. While some dorsal cells were successfully electroporated with *huC:tdtomato* DNA (4/40 fish), they appeared to be tectal cells, identified by their axonal projections (Meek and Schellart, 1978) (Figure 3.2.5.2).

Kaede is a photoconvertable protein that is initially green until a UV light is directed onto it, which causes a change in colour to red (Hatta et al., 2006). If the area photoconverted was small enough, then the cell body and its axon can be traced. In order to photoconvert MTN, the relative positions of MTN neurons in the zebrafish mesencephalon were measured by calculating the average distances of DiI labelled cell bodies, from anatomical landmarks (Figure 3.2.5.3 and Figure 3.2.5.4). Despite attempts to photoconvert individual neurons in the areas where MTN arise, many cells were uncaged. Therefore MTN neurons could not be differentiated from other neurons.

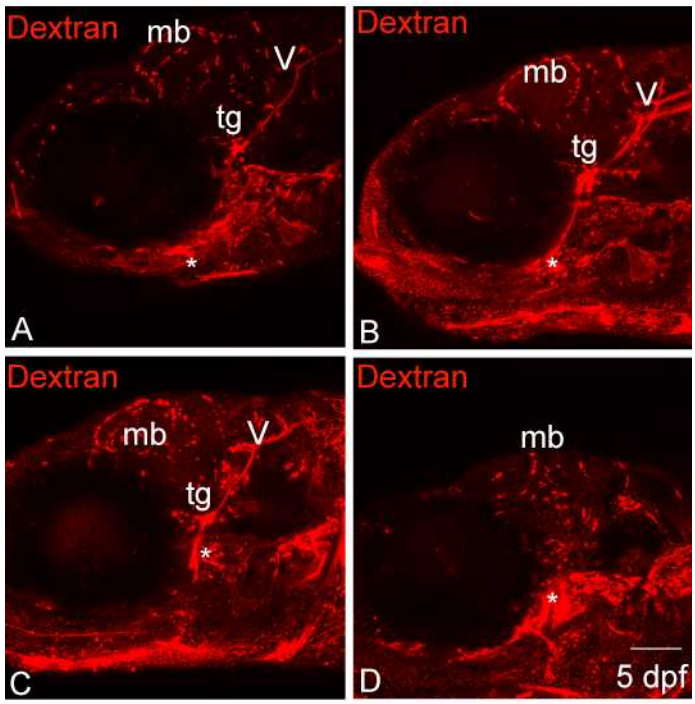

Figure 3.2.5.1 – Injection of Dextran into mandibular arch muscles to retrogradely label MTN

Lateral views of 5 dpf zebrafish where A, B) dextran was injected into the adductor mandibulae (a.m.) and C, D) the levator arcus palatini (l.a.p.), showing labelling of the trigeminal motor nucleus (V) (except for D). Muscles are indicated by asterisks. mb, midbrain. tg, trigeminal ganglion. V, trigeminal nucleus. Scale bar = 100μm

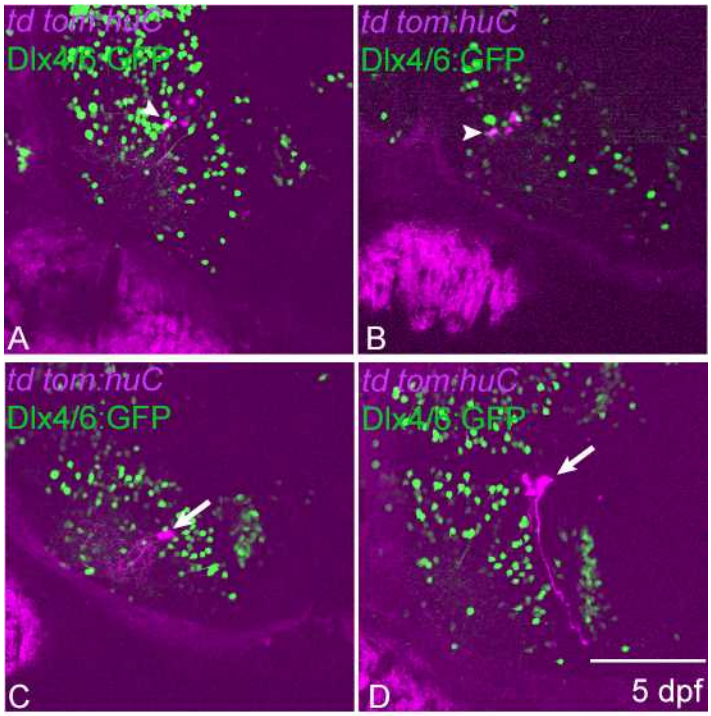

Figure 3.2.5.2 – Electroporation of *huC:tdTomato* into *Tg(1.4dlx4-6:GFP)* cells in the anterior mesencephalon

Dorsal views of *Tg(1.4dlx4-6:GFP)* 5 dpf zebrafish electroporated with *huC:tdTomato* (magenta). (A, B) Co-expression of *huC:tdTomato* with GFP (white arrowheads) indicates successful electroporation of a GFP+ cell, but no axonal projections can be seen. (C and D) tdtom:huC expression in an electroporated tectal cell, with anterograde labelling of axons (white arrow) (identified by descriptions of tectal cell morphology by Meek and Schellart, 1978).

Scale bar = 50μm

animal number	top of eye to bottom most cell	top of eye to top most cell	back of eye to most posterior cell	back of eye to most anterior cell	tip of head to most anterior cell
1	80.1	109	47.01	78.06	149
2	21	50	53.93	67.63	195.12
3	19.03	53	67	89.08	164
4	21	60.92	49	72.03	200
5	31.02	47	80.03	111	177.1
6	29.35	74.03	49.01	105.02	226
7	26.06	65.01	49	107.02	235.03
8	19	48.01	26.63	59.03	245.03
9	37.45	90.73	52	109	186
10	16	45.01	29	55.04	255.05
11	37	63.4	42	94.02	217
12	50.06	65	38.01	65	248.03
Total	387.07	771.11	582.62	1011.93	2497.36
Average	32.26	64.26	48.55	84.33	208.11
Standard deviation	18.02	19.24	52.01	20.72	34.91
Standard error of the mean	5.2	5.56	4.26	5.98	10.08

Figure 3.2.5.3 – Distances of DiI labelled cell bodies from anatomical landmarks in the zebrafish head.

Distances from anatomical landmarks; the eye and cerebellum (c) were measured (number of zebrafish = 15) detailing MTN localisation in the dorsal anterior mesencephalon.

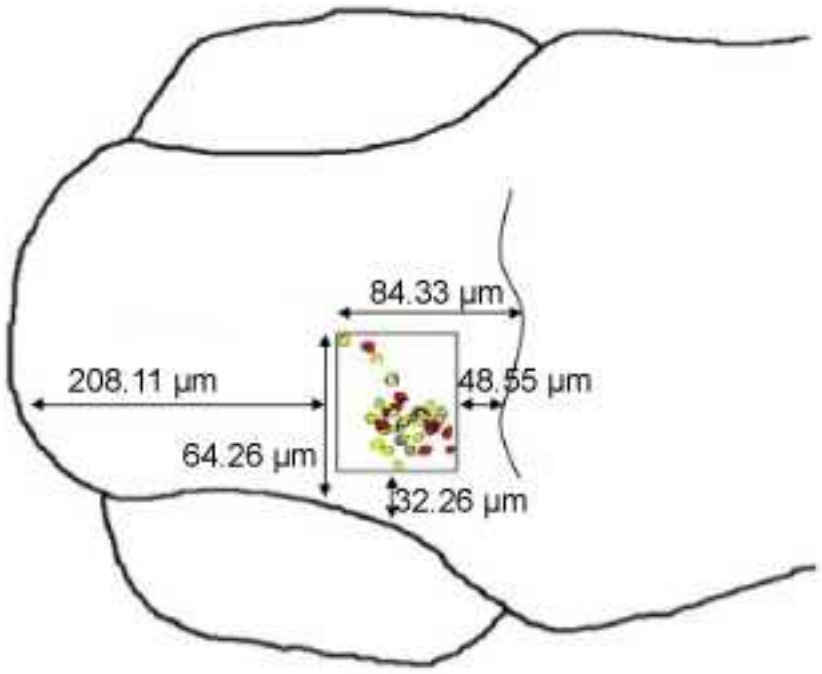

Anatomical landmarks	Average distances of MTN cell bodies from anatomical landmarks
Top of eye to most lateral cell	32.26 ± 5.20
Top of eye to most medial cell	64.26 ± 5.56
Back of eye to most posterior cell	48.55 ± 4.26
Back of eye to most anterior cell	84.33 ± 5.98
Tip of head to most anterior cell	208.11 ± 10.08

Figure 3.2.5.4 – A diagrammatic representation of DiI labelled MTN cell bodies showing MTN localisation and distances from anatomical landmarks in the zebrafish head.

A topographic map of MTN cell bodies labelled with DiI alone (red), and GFP+ cell bodies co-labelled with DiI (green), from DiI labelled *Tg(1.4dlx4-6:GFP)* zebrafish at 5 dpf (number of zebrafish = 25). This shows that there is no clustered organisation of these apparent sub-populations. Average distances from anatomical landmarks; the eye and cerebellum (c) were measured (number of zebrafish = 15) detailing MTN localisation in the dorsal anterior mesencephalon. Scale bar = 100µm

3.2.6 – Neuronal genes *huC* and *ngn1* are both expressed in MTN.

The specification of MTN neurons was assessed by looking at the expression of neuronal regulatory genes *huC* and *ngn1* (Park et al., 2000; Andermann et al., 2002). All sensory neurons express *huC* and *ngn1* and they are required for neuronal differentiation. *huC* encodes an RNA-binding protein homologous to *Drosophila* elav (Park et al., 2000). *ngn1* is a bHLH transcription factor. *huC* and *ngn1* were assessed because they are early markers of neurogenesis and can, therefore be used to determine where and when MTN arise.

A series of zebrafish embryonic stages, from 18 ss to 5 dpf, were used to examine the expression patterns of *huC* and *ngn1* to investigate whether they are expressed in MTN cell bodies. At 18 ss there is no *huC* or *ngn1* expression in MTN cell bodies, but they are expressed in other cells in the brain (data not shown). *HuC* is expressed in the telencephalon, early epiphysis cells and putative nTPC (Park et al., 2000). Similarly *ngn1* is expressed in some cells of the telencephalon, the nTPC, and also ventrally in the pre-tegmentum, similar to that described in previous studies (Korzh et al., 1998). By 22 ss (20 hpf) both *huC* and *ngn1* are expressed in a small number of early putative MTN cell bodies in the dorsal anterior mesencephalon (Figure 3.2.6A – D). At 24 hpf *huC* and *ngn1* are expressed in many neuronal cell bodies covering the dorsal mesencephalon, similar to the locations of MTN along the dorsal midbrain in chick and mouse (Hunter et al., 2001; Mastick and Easter, 1996) (Figure 3.2.6E - H). The most posteriorly distant *huC* expressing neuronal cell bodies from the nTPC are located more posteriorly, compared to the furthermost MTN cell bodies expressing *brn3a*, *drg11*, *isl1*, *tlx3* and *trkC* at 24 hpf (Figure 3.2.5.2; Figure 3.2.6E, F). By 48 hpf *huC* expression is no longer specific to dorsal cells in the mesencephalon, instead they are expressed throughout the tectum in the midbrain (Figure 3.2.6I, J). In contrast, *ngn1* expression is lost in the midbrain, and is now restricted to the dorsal diencephalon (Figure 3.2.6K, L).

Figure 3.2.6 – Expression of neuronal genes *huC*, and *ngn1* in zebrafish

(A) Lateral, and (B) dorsal views of a zebrafish head at 20 hpf, showing *huC* expression in epiphysis (e), nuclei of the tract of the posterior commissure (nTPC, black arrowhead), telencephalon, MTN cell bodies and other dorsal cells in the mesencephalon. (C) Lateral, and (D) dorsal views of a zebrafish head at 20 hpf, showing *ngn1* expression in nTPC (black arrowhead), pre-tegmentum, dorsal telencephalon, and dorsal cells in the mesencephalon, some of which may include expression in MTN cell bodies. (E) Lateral, and (F) dorsal views of a zebrafish head at 24 hpf, showing *huC* expression in cerebellum (c), epiphysis (e), nuclei of the tract of the posterior commissure (nTPC), telencephalon, MTN cell bodies and other dorsal cells in the mesencephalon. (G) Lateral, and (H) dorsal views of a zebrafish head at 24 hpf, showing *ngn1* expression in nTPC, pre-tegmentum, dorsal telencephalon, and dorsal cells in the mesencephalon, some of which may include expression in MTN cell bodies. (I) Lateral, and (J) dorsal views of a zebrafish head at 48 hpf, showing *huC* expression is no longer restricted to dorsal cells of the mesencephalon, with expression in the whole tectum. *huC* is also expressed in regions of the telencephalon. (K) Lateral, and (L) dorsal views of *ngn1* expression at 48 hpf, showing continued expression in dorsal cells of the tectum (t), dorsal telencephalon, and it is also now expressed in the dorsal hindbrain. c, cerebellum. e, epiphysis. KWT, Kings Wild Type. mb, midbrain. pt, pretectum. t, tectum. tel, telencephalon.

Scale bar = 100 μm

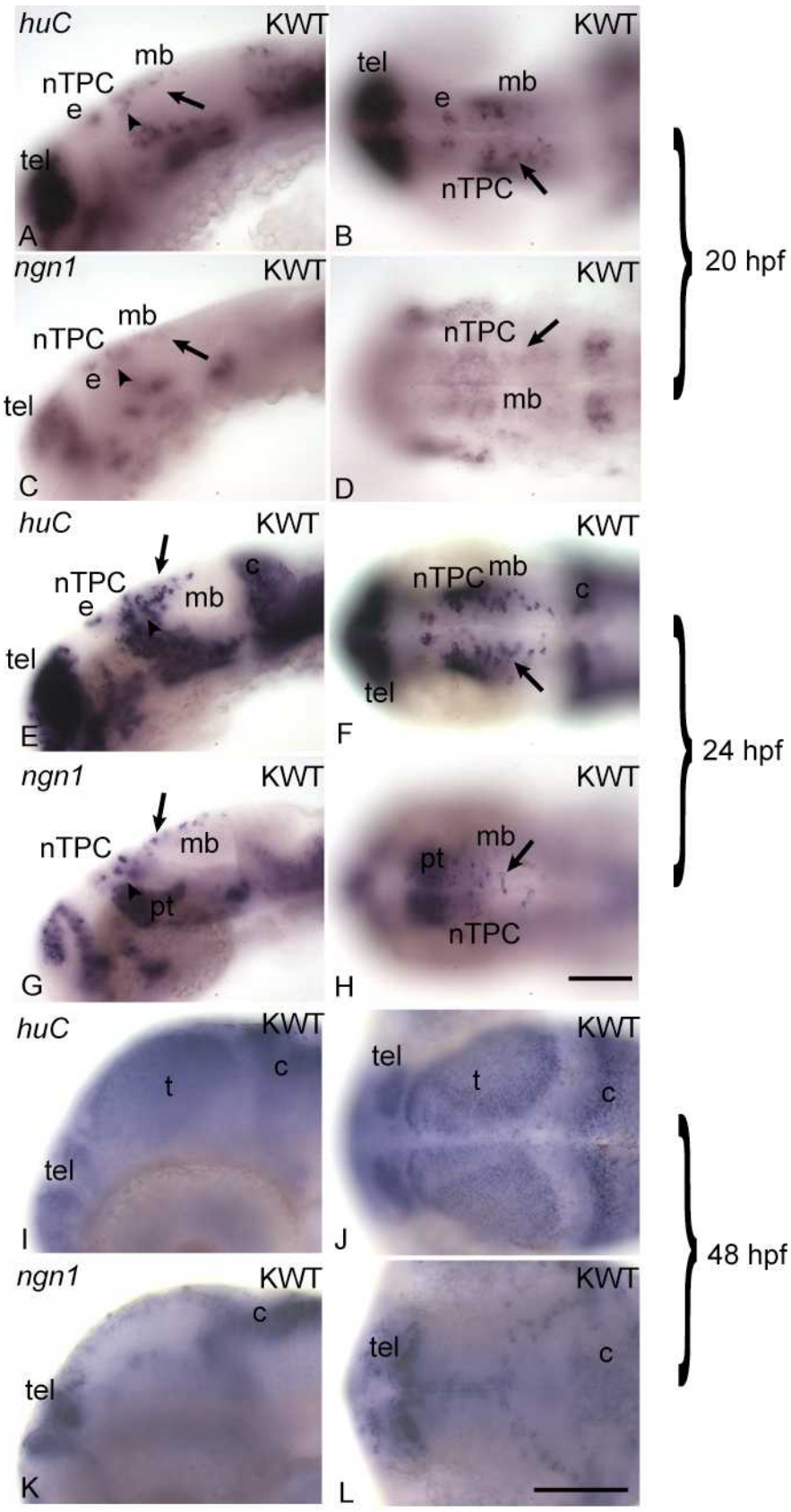
huC
KWT
mb
nTPC
e
tel
A
KWT
tel
e
mb
nTPC
B
20 hpf
ngn1
KWT
mb
nTPC
e
tel
C
KWT
nTPC
mb
D
huC
KWT
nTPC
e
mb
c
tel
E
KWT
nTPC
mb
c
tel
F
24 hpf
ngn1
KWT
nTPC
mb
pt
G
KWT
mb
pt
nTPC
H
huC
KWT
t
c
tel
I
KWT
tel
t
c
J
48 hpf
ngn1
KWT
c
tel
K
KWT
tel
c
L

3.2.7 – MTN neurons express *brn3a*, *drg11*, *isl1*, and *tlx3* during development

Little is known about the molecular profile of MTN neurons during development, therefore candidate genes were investigated for their expression in the MTN. *Brn3a*, *Drg11*, and *Isl1*, are expressed in the MTN of chick and mouse ((Hunter et al., 2001; Ichikawa et al., 2005; Wang et al., 2007). Likewise the proprioceptive markers, *TrkB* and *TrkC* are expressed in amniote MTN (Fan et al., 2000). Proprioceptive markers *Runx3* and *Tlx3* were also analysed for their expression in MTN (Logan et al., 1998; Park and Saint-Jeannet, 2010). Zebrafish orthologues of these genes were identified (except *TrkB*) and their expression analysed during midbrain development. A series of zebrafish embryonic stages from 18 ss to 5 dpf were used to examine the expression patterns of *brn3a*, *drg11*, *isl1*, *runx3*, *tlx3* and *trkC,* to assess whether they are expressed in MTN cell bodies.

In chick, MTN cells are born from stage 14 or 22 ss (Hamburger and Hamilton., 1951; Chedotal et al., 1995). In 18 ss zebrafish no expression was seen in the dorsal anterior mesencephalon for any of the analysed genes. *Isl1* was expressed more anteriorly in the epiphysis, located in the dorsal diencephalon, and in the nuclei of the tract of the posterior commissure (nTPC) (Korzh et al., 1993; data not shown). nTPC are positioned dorsally in a row along the forebrain-midbrain boundary, anterior to MTN cell bodies, and have an elongated/oval shape (Chitnis and Kuwada, 1990). At 22 ss (20 hpf) in some of the zebrafish there were a very small number of large rounded cells, located laterally in the dorsal anterior mesencephalon expressing *isl1* (Figure 3.2.7.1E and F). This implies that putative MTN cells differentiate to form MTN from 20 hpf (22 ss), similar to that described in chick (Chedotal et al., 1995). While there is little or no expression in prospective MTN cells at 20 hpf (20 ss), *brn3a*, *drg11*, *isl1,* and *tlx3a*, were expressed in the nTPC, trigeminal ganglia, and dorsal cells in the spinal cord (Korzh et al., 1993; Langenau et al., 2002; McCormick et al., 2007; Sato et al., 2007; Figure 3.2.7.2). Expression of *isl1* persists in the epiphysis from 20 hpf to 72 hpf.

By 24 hpf, *brn3a*, *drg11*, *isl1*, and *tlx3* are all expressed in putative MTN cells in the dorsal anterior mesencephalon (Figure 3.2.7.2A - H), similar to expression in chick and mouse MTN (Hunter et al., 2001; Ichikawa et al., 2005; Wang et al., 2007). *trkC* expression commences in the brain at stage 24 hpf, and is expressed in the epiphysis and in a region of cells in the posterior diencephalon near to the forebrain/midbrain boundary where the nTPC are situated (Martin et al., 1998; Scholpp et al., 2003). No *trkC* expression was seen in putative cells of the MTN. *runx3*

expression was seen in the skin and was not detected in MTN (data not shown).

At 30 hpf there is little change to the expression in the forebrain and midbrain, of the genes analysed. By 48hpf, however, only *drg11*, *isl1*, and *tlx3* expression persist in some MTN cell bodies (Figure 3.2.7.3C – H). At this MTN cell bodies are more lateral relative to the midline, and in a less dorsal location. By 48 hpf *brn3a* is expressed in many tectal cells in the anterior tectum. *brn3a* also becomes localised specifically to the early developing habenula in the dorsal diencephalon, as previously described in zebrafish (Bianco et al., 2008) (Figure 3.2.7.3A and B). *trkC* expression can be seen in the whole tectum in the midbrain (Martin et al., 1998) (Figure 3.2.7.3I and J). At 72 hpf only *drg11* is expressed in a few MTN cells in the dorsal anterior mesencephalon, until 5dpf when *drg11* expression is lost (Figure 3.2.7.4C and D).

From the expression analysis in this section, *drg11* and *isl1* were identified as the best molecular markers of the MTN. This was because these were seen to be expressed in the MTN over the longest time periods and labelled the MTN clearly. In the following sections of this thesis drg11 or isl1 has been used to visualise the MTN in zebrafish.

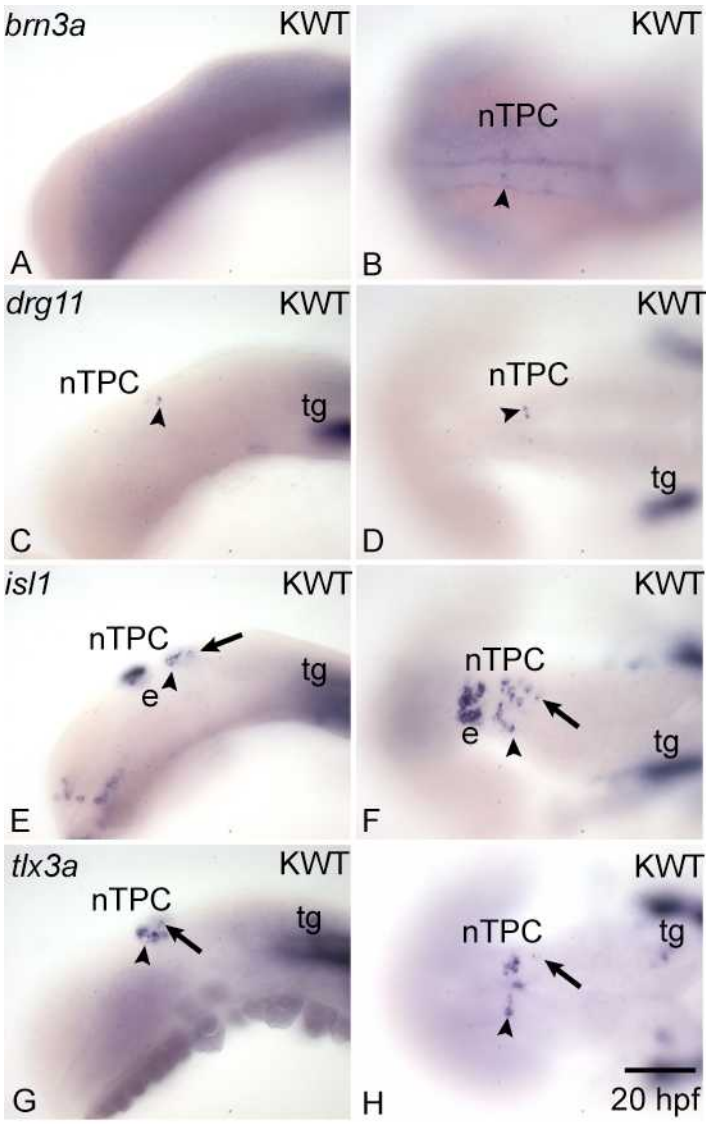

Figure 3.2.7.1 – Expression of *brn3a*, *drg11*, *isl1, tlx3* and *trkC* in 20 hpf zebrafish

(A) Lateral, and (B) dorsal views of a zebrafish head at 20 hpf, showing *brn3a* expression in the nucleus of the tract of the posterior commissure (nTPC) (seen in B only, black arrowhead). (C) Lateral, and (D) dorsal views showing *drg11* expression in nTPC (black arrowhead) and trigeminal ganglion (tg). (E) Lateral, and (F) dorsal views showing *isl1* expression in epiphysis (e), MTN (black arrows), nTPC (black arrowhead), telencephalon (seen in E only) and tg. (G) Lateral, and (H) dorsal views showing *tlx3a* expression in MTN cell bodies (black arrows), nTPC (black arrowhead) and tg. e, epiphysis. KWT, Kings Wild Type. nTPC, nucleus of the tract of the posterior commissure. tg, trigeminal ganglion.

Scale bar = 100 μm

Figure 3.2.7.2 – Expression of *brn3a*, *drg11*, *isl1*, *tlx3* and *trkC* in 24 hpf zebrafish.
(A) Lateral, and (B) dorsal views of a zebrafish head at 24 hpf, showing *brn3a* expression in MTN cell bodies (black arrows), nucleus of the tract of the posterior commissure (nTPC, black arrowhead), and the trigeminal ganglia (tg) (seen in A only). (C) Lateral, and (D) dorsal views showing *drg11* expression in MTN cell bodies (black arrows), nTPC (black arrowhead) and tg. (E) Lateral, and (F) dorsal views showing *isl1* expression in epiphysis (e), MTN (black arrows), nTPC (black arrowhead), telencephalon (seen in E only) and tg. (G) Lateral, and (H) dorsal views showing *tlx3a* expression in MTN cell bodies (black arrows), nTPC (black arrowhead) and tg. (I) Lateral, and (J) dorsal views showing *trkC* expression in epiphysis, nTPC (black arrowhead) and telencephalon, but not in MTN cell bodies. e, epiphysis. KWT, Kings Wild type. mb, midbrain. nTPC, nucleus of the tract of the posterior commissure. tg, trigeminal ganglion.
Scale bar = 100 μm

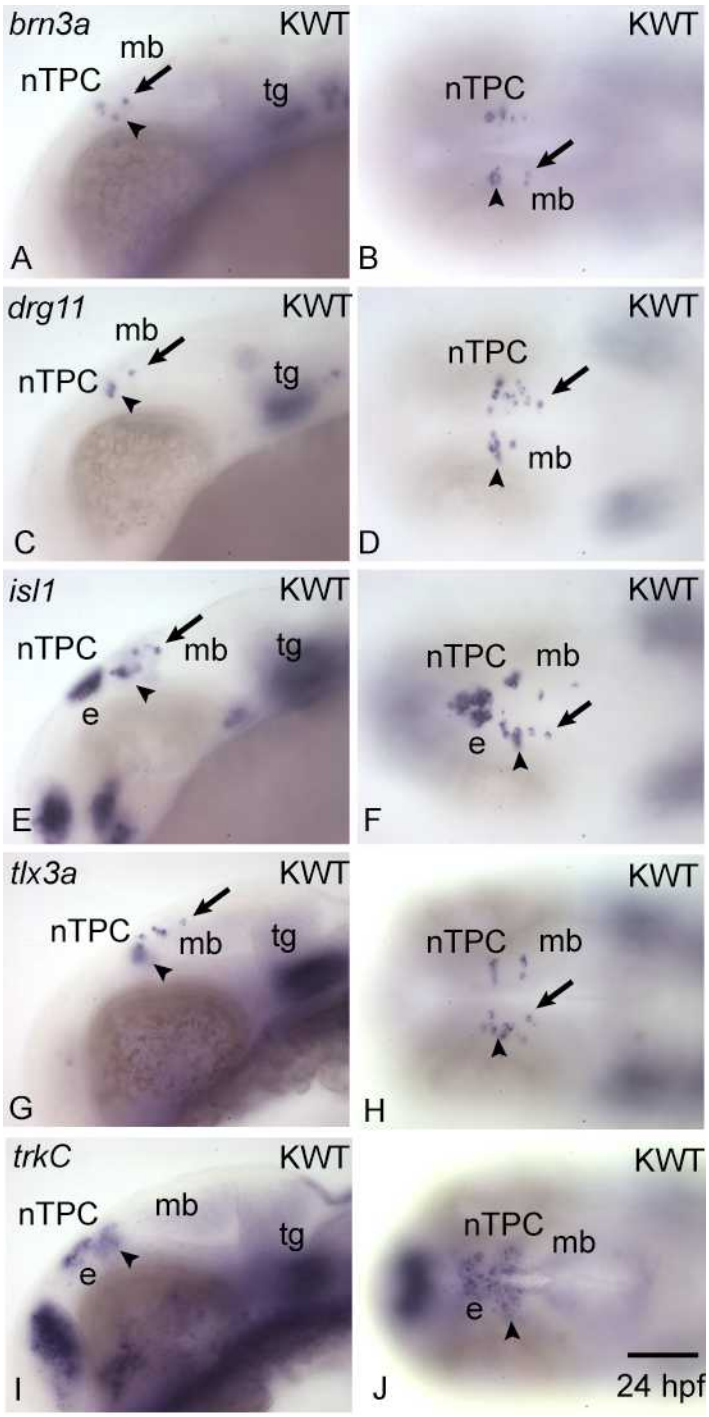
brn3a
KWT
mb
nTPC
tg
A
KWT
nTPC
mb
B
drg11
KWT
mb
nTPC
tg
C
KWT
nTPC
mb
D
isl1
KWT
nTPC
mb
tg
e
E
KWT
nTPC
mb
e
F
tlx3a
KWT
nTPC
mb
tg
G
KWT
nTPC
mb
H
trkC
KWT
nTPC
mb
tg
e
I
KWT
nTPC
mb
e
J
24 hpf

Figure 3.2.7.3 – Expression of *brn3a*, *drg11*, *isl1, tlx3* and *trkC* in 48 hpf zebrafish.
(A) Lateral, and (B) dorsal views of a zebrafish head at 48 hpf, showing *brn3a* expression in the nucleus of the tract of the posterior commissure (nTPC), anterior region of the tectum (t), habenula (ha) and the vestibuloacoustic ganglia (seen in A only). *brn3a* expression may still be present in MTN cell bodies but is obscured by the general expression in anterior tectal cells. (C) Lateral, and (D) dorsal views showing the continued expression of *drg11* in MTN cell bodies (black arrows), nTPC and tg. (E) Lateral, and (F) dorsal views showing the continued expression of *isl1* in epiphysis (e), hypothalamus (h), MTN (black arrows), nTPC, telencephalon (seen in E only) and tg. (G) Lateral, and (H) dorsal views showing *tlx3a* is still expressed in MTN cell bodies (black arrows), nTPC and tg. *Tlx3a* expression is also now seen in the hindbrain region. (I) Lateral, and (J) dorsal views showing low level expression of *trkC* in the tectum and telencephalon. c, cerebellum. e, epiphysis. h, hypothalamus. ha, habenula. mb, midbrain. nTPC, nucleus of the tract of the posterior commissure. t, tectum. tel, telencephalon. tg, trigeminal ganglion.
Scale bar = 100 μm

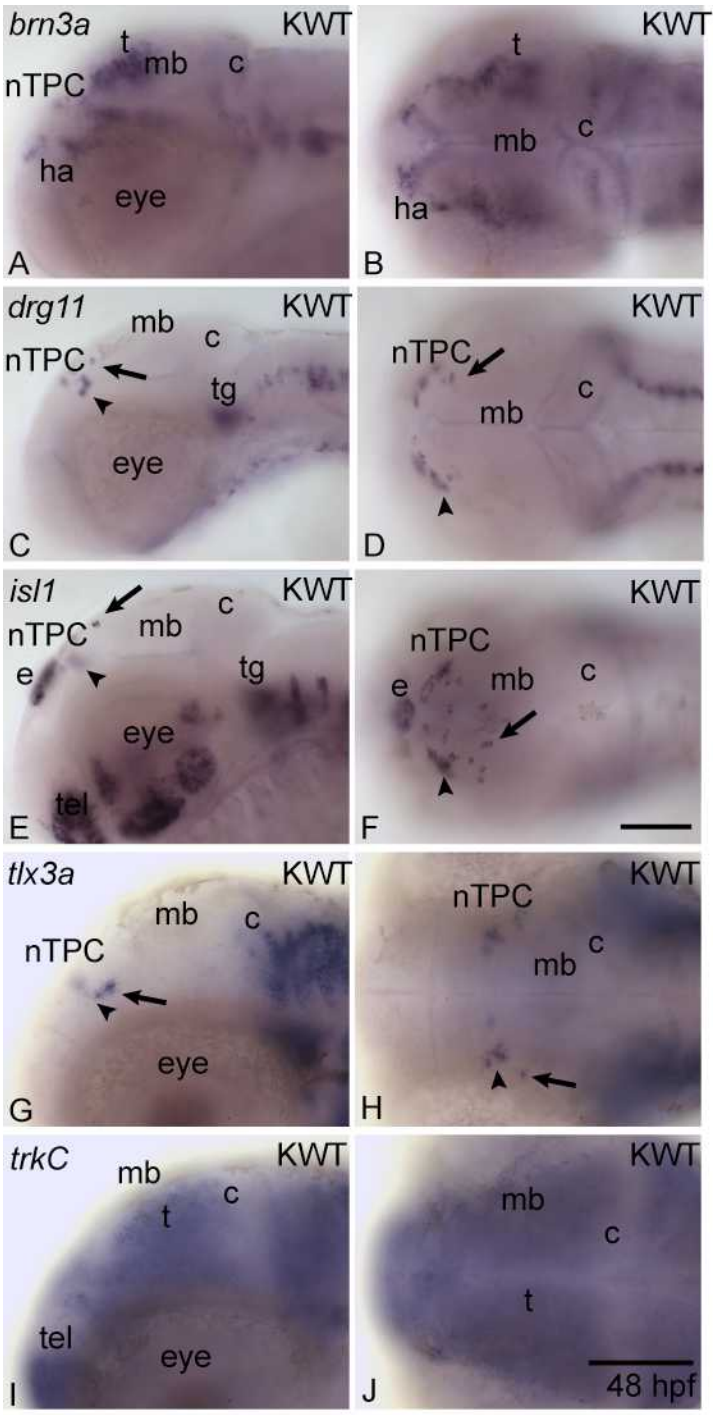
brn3a
KWT
t
mb
c
nTPC
ha
eye
A
KWT
t
c
mb
ha
B
drg11
KWT
mb
c
nTPC
tg
eye
C
KWT
nTPC
c
mb
D
isl1
KWT
c
nTPC
mb
e
tg
eye
tel
E
KWT
nTPC
e
mb
c
F
tlx3a
KWT
mb
c
nTPC
eye
G
KWT
nTPC
c
mb
H
trkC
KWT
mb
c
t
tel
eye
I
KWT
mb
c
t
J
48 hpf

Figure 3.2.7.4 – Expression of *brn3a*, *drg11*, *isl1*, *tlx3* and *trkC* in 72 hpf zebrafish

(A) Lateral, and (B) dorsal views of a zebrafish head at 72 hpf, showing *brn3a* expression in the habenula (ha) and the whole tectum (t). (C) Lateral, and (D) dorsal views showing continued *drg11* expression in MTN cell bodies (black arrows), and nTPC (black arrowheads). *Drg11* is also now strongly expressed in the tegmentum (teg). (E) Lateral, and (F) dorsal views showing continued *isl1* expression in epiphysis (e), MTN (black arrows), nTPC (black arrowheads), and newly expressed in the eye. (G) Lateral, and (H) dorsal views showing continued *tlx3a* expression in MTN cell bodies (black arrows), and nTPC (black arrowheads). (I) Lateral, and (J) dorsal views showing low level expression of *trkC* in the brain. ha, habenula. KWT, Kings Wild Type. nTPC, nucleus of the tract of the posterior commissure. t, tectum. teg, tegmentum

Scale bar = 100 μm

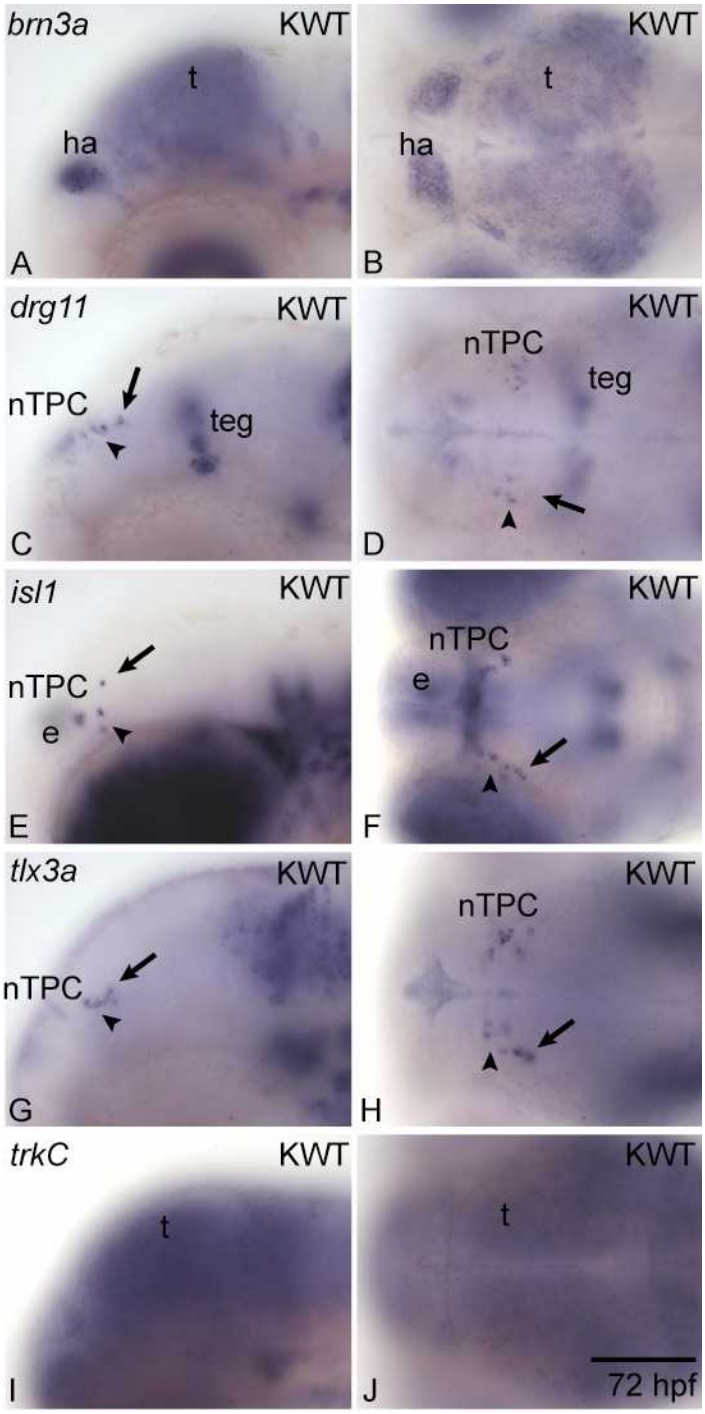
brn3a
KWT
t
ha
A
KWT
t
ha
B
drg11
KWT
nTPC
teg
C
KWT
nTPC
teg
D
isl1
KWT
nTPC
e
E
KWT
nTPC
e
F
tlx3a
KWT
nTPC
G
KWT
nTPC
H
trkC
KWT
t
I
KWT
t
72 hpf
J

3.2.8 – Molecular analysis shows MTN cell bodies expressing *drg11* and *isl1* are located in the dorsal anterior midbrain

By 10 ss, the brain compartments of the zebrafish brain are no longer responsive to positional cues, so general patterning of the zebrafish brain is complete (Scholpp et al., 2003). To show that *drg11* and *isl1* are expressed in the midbrain, double in situ hybridisation was performed using midbrain markers *pax7* and *gsh1*, and forebrain markers *pax6* and *epha4* at 24 hpf (Scholpp et al., 2003; Cheeseman and Eisen, 2004). *Pax6* and *drg11* co-expression was observed in nTPC neurons, but not in the more posterior MTN neurons at 24 hpf (Figure 3.2.8.1A - C). Similarly *pax6* and *isl1* co-expression was observed in nTPC but not in MTN neurons (Figure 3.2.8.2A, B). In *pax7* labelled fish, the more posterior MTN cell bodies expressing *drg11* and *isl1*, are seen to be restricted to the midbrain (Figure 3.2.8.1J – L, Figure 3.2.8.2G, H). Interestingly these cells are located extremely dorsally, in a region of the midbrain where there is little *pax7* expression.

The borders of the zebrafish brain compartments, at 24 hpf, were traced to show their location at this time point, and the position of MTN cell bodies which are seen in the dorsal anterior midbrain (Figure 3.2.8.3).

Figure 3.2.8.1 – The relative positions of MTN cell bodies expressing *drg11* compared to forebrain and midbrain markers in 24 hpf zebrafish

(A) Dorsal, and (B) lateral views of a zebrafish head at 24 hpf, showing the relative positions of cells in the nucleus of the tract of the posterior commisssure (nTPC), and MTN neurons expressing *drg11* (black arrows), compared to the expression of forebrain marker *pax6*. (C) A higher magnification of B, showing that the nTPC is located at the forebrain-midbrain boundary. MTN cell bodies expressing *drg11* can be seen posterior to the expression of forebrain marker *pax6*. (D) Dorsal, and (E) lateral views of a zebrafish head, showing the relative positions of nTPC, and MTN cell bodies expressing *drg11*, compared to the expression of forebrain and tegmentum (teg; E only) marker *eph4a*. (F) A higher magnification of E, similar to C. (G) Dorsal, and (H) lateral views of a zebrafish head, showing the relative position of the nTPC, and MTN cell bodies expressing *drg11*, compared to the expression of the pre-tectal (pt) marker *gsh1*. (I) A higher magnification of H, showing the nTPC and MTN are located dorsal to *gsh1* expression in the ventral midbrain. (J) Dorsal and (K) lateral views of a zebrafish head, showing the relative position of the nTPC, and MTN cell bodies expressing *drg11*, compared to the expression of tectal (t) marker *pax7*. (L) A higher magnification of K, showing that some MTN cell bodies are located in the tectum. Cells of the nTPC are located anterior to *pax7* expression. d, diencephalon. nTPC, nucleus of the tract of the posterior commissure. pt, pre-tectum t, tectum. tel, telencephalon. vz, ventricular zone. Scale bars = 100μm

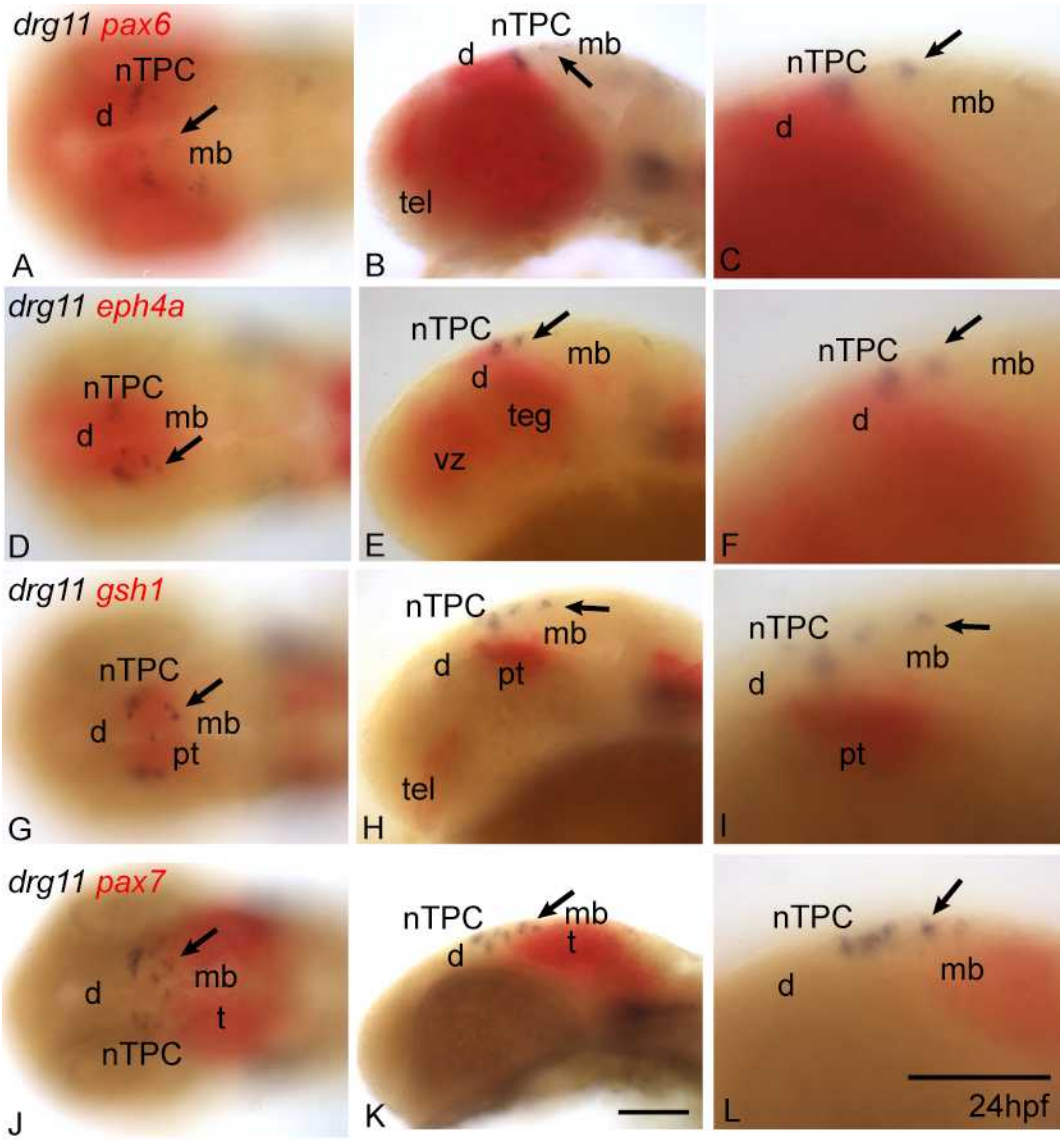
drg11 pax6
nTPC
d
mb
A
nTPC
d
mb
tel
B
nTPC
mb
d
C
drg11 eph4a
nTPC
d
mb
D
nTPC
mb
d
teg
vz
E
nTPC
mb
d
F
drg11 gsh1
nTPC
d
mb
pt
G
nTPC
mb
d
pt
tel
H
nTPC
mb
d
pt
I
drg11 pax7
d
mb
t
nTPC
J
nTPC
mb
d
t
K
nTPC
d
mb
24hpf
L

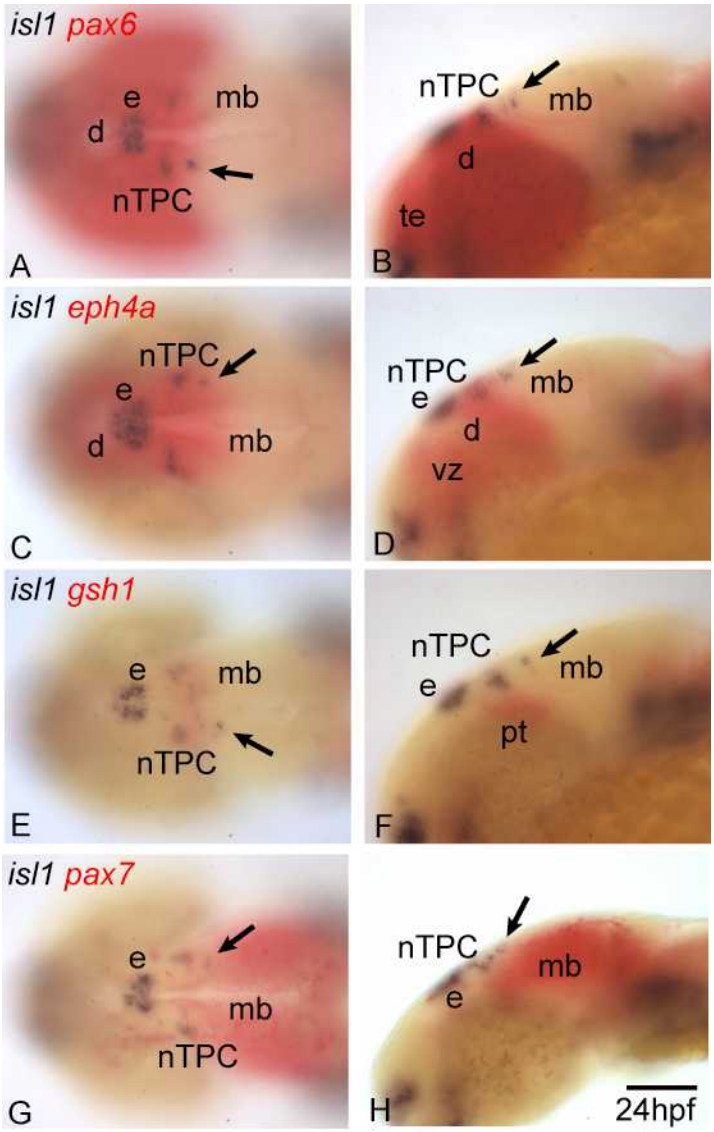

Figure 3.2.8.2 – The relative positions of MTN cell bodies expressing *isl1* compared to forebrain and midbrain markers in 24 hpf zebrafish

Dorsal and lateral views of a zebrafish head at 24 hpf, showing the relative positions of cells in the nucleus of the tract of the posterior commissure (nTPC), and MTN neurons expressing *isl1* (black arrows), compared to the expression of forebrain markers (A, B) *pax6*, and (C, D) *eph4a*. MTN cell bodies expressing *isl1* can be seen posterior to *pax6* and *eph4a* expression, and nTPC are located at the forebrain-midbrain boundary. Dorsal, and lateral views of a zebrafish head, showing the relative positions of nTPC, and MTN cell bodies expressing *drg11*, compared to the expression of (E, F) pre-tectum (pt) marker *gsh1*, and (G, H) tectum (t) marker *pax7*. Some MTN cell bodies are co-localised with *pax7* in the tectum, while others and the nTPC are located more dorsal and anterior to *pax7*. d, diencephalon. e, epiphysis. KWT, Kings wild type. mb, midbrain. nTPC, nucleus of the tract of the posterior commissure. pt, pre-tectum. t, tectum, tel, telencephalon, vz, ventricular zone. Scale bar = 100µm

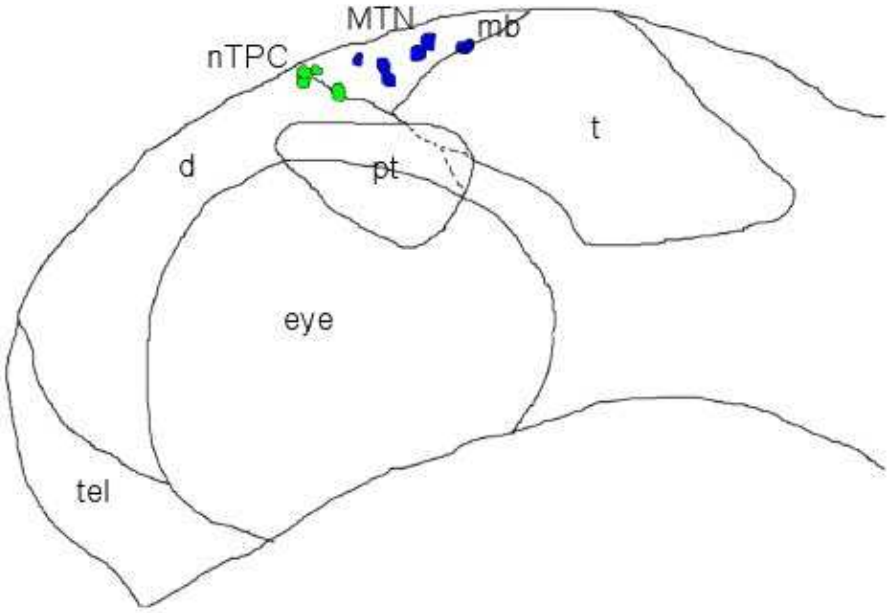

Figure 3.2.8.3 – Diagrammatic representation of the separate brain regions to show the relative locations of MTN and nTPC

The expression data shown in Figure 3.2.8.1. was traced onto a schematic to show the separate brain regions in a 24 hpf zebrafish, defined by the specific gene expressions. The nTPC are located at the forebrain-midbrain boundary. MTN cell bodies are located in a dorsal region of the midbrain and are seen posterior to forebrain markers, but anterior to tectal markers in the midbrain. d, diencephalon. mb, midbrain. nTPC, nucleus of the tract of the posterior commissure. pt, pre-tectum. t, tectum. tel, telencephalon.

3.2.9 – ETS genes and zinc finger genes characteristic of mammalian sensory neurons are not expressed in zebrafish MTN

In mice, the sensory neurons that form monosynaptic circuits in the body, express specific transcription factors important for correct formation of the circuit (Chen et al., 2003). These include ETS family genes *Er81* and *Pea3* expressed in proprioceptive sensory neurons and Egr zinc finger family gene *Egr3* expressed in muscle spindles with *Er81* (Arber et al., 2001; Tourtellotte et al., 2001). The expression profile of ETS genes in the developing midbrain was analysed to determine if these transcription factors may be required for the development of the trigeminal monosynaptic circuit, and to identify genes expressed in MTN in later stages of development. The Egr zinc finger gene family was assessed for expression in MTN due to reports of *egr2* regulating the timing and extent of apoptosis in the MTN (De et al., 2005).

A series of zebrafish embryonic stages from 30 hpf to 72 hpf were analysed for *egr1*, *egr3*, *er81*, *etv5* and *pea3* expression in the head. The expression profiles for *egr1*, *er81*, *etv5* and *pea3* were the same as previously described (Close et al., 2002; Roussigne and Blader, 2006). There was no expression of *egr1*, *egr3*, *er81*, *etv5*, and *pea3* in MTN cell bodies at any of the stages analysed (Figure 3.2.9.1 and 3.2.9.2).

Figure 3.2.9.1 – Expression of *egr1*, *egr3*, *er81*, *etv5*, and *pea3* in 48 hpf zebrafish
(A) Lateral, and (B) dorsal views of a zebrafish head at 48 hpf, showing *egr1* expression in the tectum (t) and telencephalon (tel) (C) Lateral, and (D) dorsal views showing *egr2* expression in the epiphysis (e). (E) Lateral, and (F) dorsal views showing *egr3* expression in telencephalon (shown in E only). (G) Lateral, and (H) dorsal views showing *er81* expression in epiphysis (e), tectal cells and faint expression in the telencephalon (shown in E only). (I) Lateral, and (J) dorsal views showing *etv5* expression in cerebellum, epiphysis, and peripheral located cells above the eye. (K) Lateral, and (L) dorsal views showing *pea3* expression in cerebellum (c), epiphysis (e; K only), eye, tegmentum (teg; K only), ventral telencephalon (tel) and trigeminal ganglion (tg). c, cerebellum. e, epiphysis. KWT, Kings wild type. mb, midbrain. t, tectum. teg, tegmentum. tel, telencephalon. tg, trigeminal ganglion. Scale bars = 100μm

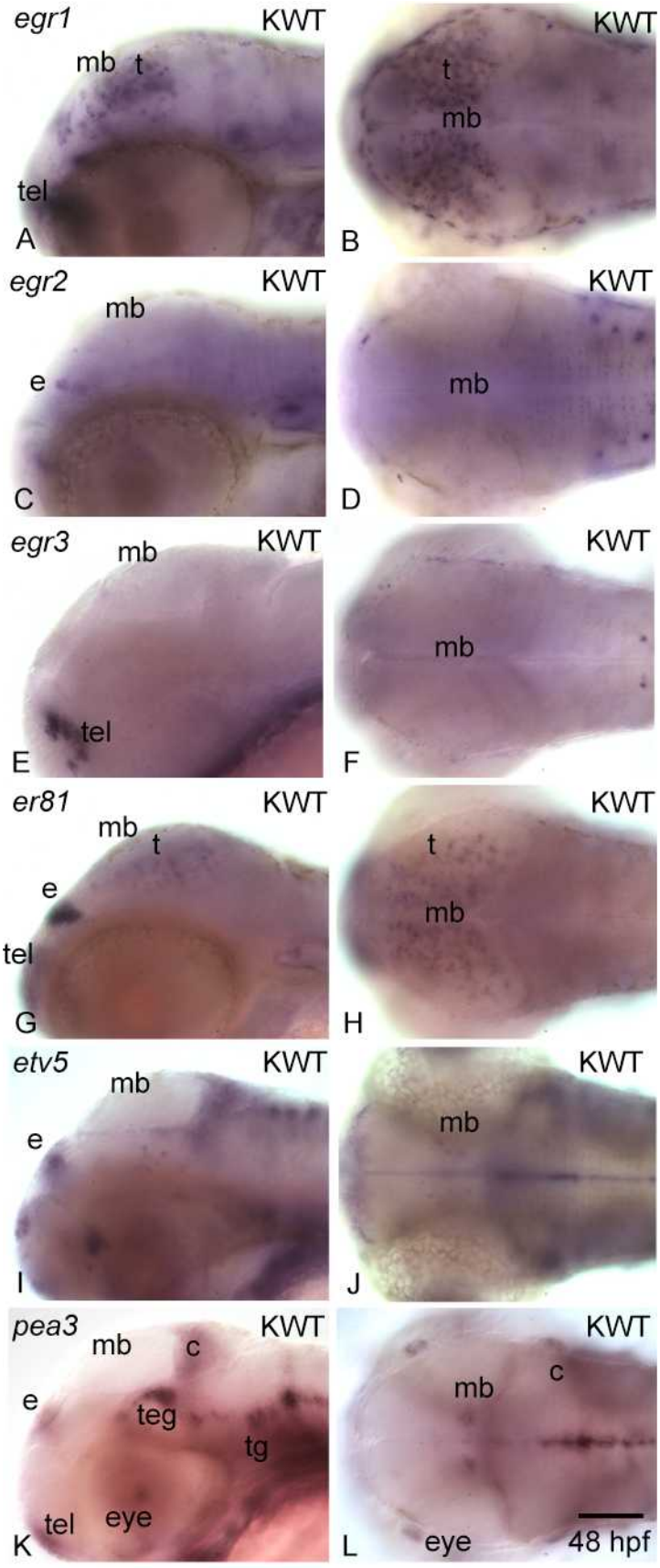
egr1
KWT
mb
t
tel
A
KWT
t
mb
B
egr2
KWT
mb
e
C
KWT
mb
D
egr3
mb
KWT
tel
E
KWT
mb
F
er81
KWT
mb
t
e
tel
G
KWT
t
mb
H
etv5
KWT
mb
e
I
KWT
mb
J
pea3
KWT
mb
c
e
teg
tg
tel
eye
K
KWT
mb
c
L
eye
48 hpf

Figure 3.2.9.2 – Expression of *egr1*, *egr3*, *er81*, *etv5*, and *pea3* in 72 hpf zebrafish

(A) Lateral, and (B) dorsal views of a zebrafish head at 48 hpf, showing egr1 expression in the tectum (t) and telencephalon (tel). (C) Lateral, and (D) dorsal views showing that *egr2* is no longer expressed in the head at this stage. (E) Lateral, and (F) dorsal views showing *egr3* expression in habenula (ha), some tectal cells and in the ventral tegmentum (teg; E only). (G) Lateral, and (H) dorsal views showing *er81* expression is now limited to the epiphysis (e; G only). (I) Lateral, and (J) dorsal views showing *etv5* is faintly expressed in the dorsal diencephalon, and dorsal cerebellum. (K) Lateral, and (L) dorsal views showing *pea3* expression in dorsal cerebellum (c) and trigeminal ganglion (tg). c, cerebellum. e, epiphysis. ha, habenula. KWT, Kings wild type. mb, midbrain. t, tectum. teg, tegmentum. tel, telencephalon. tg, trigeminal ganglion. Scale bar = 100μm

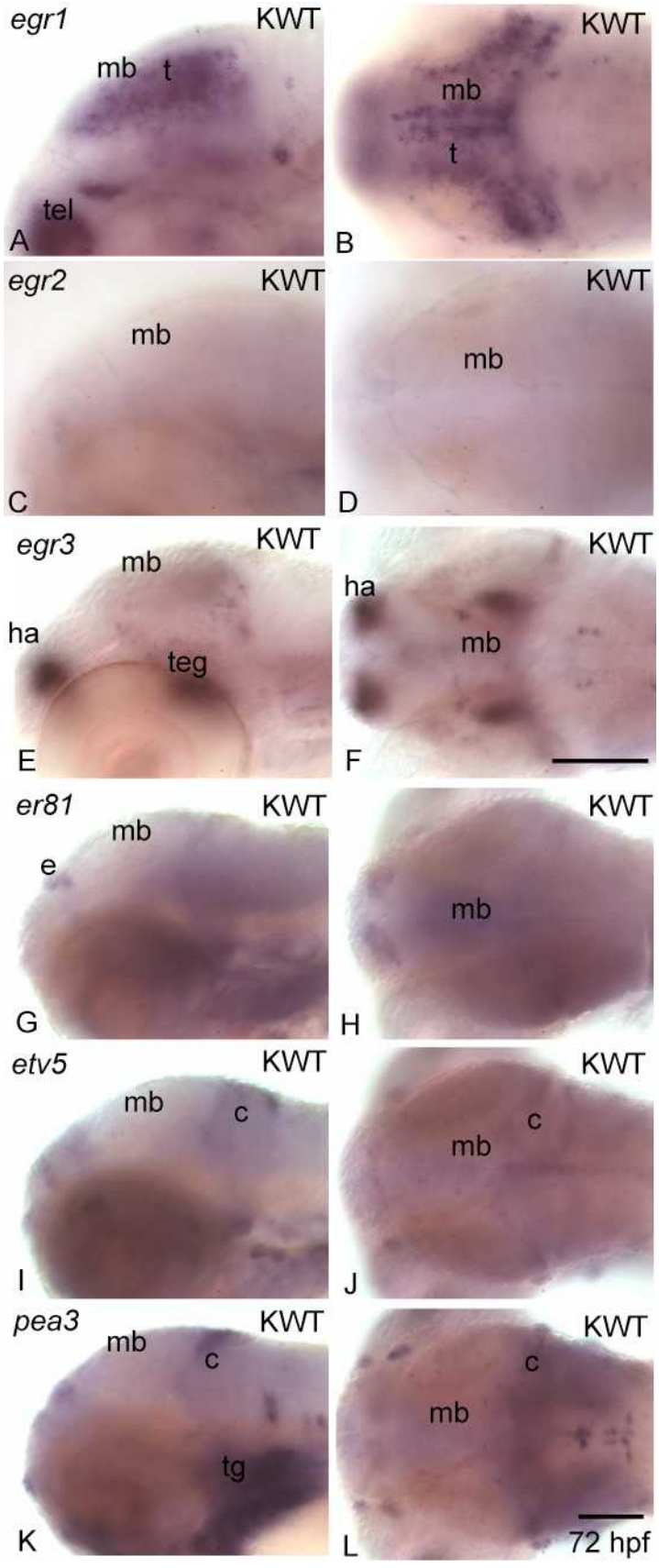
egr1
KWT
mb
t
tel
A
KWT
mb
t
B
egr2
KWT
mb
C
KWT
mb
D
egr3
KWT
mb
ha
teg
E
KWT
ha
mb
F
er81
KWT
mb
e
G
KWT
mb
H
etv5
KWT
mb
c
I
KWT
c
mb
J
pea3
KWT
mb
c
tg
K
KWT
c
mb
L
72 hpf

3.2.10 – Glutamatergic genes *vGlut1* and *vGlut2a-c*, and gabaergic genes *gad1* are expressed in the midbrain by 48hpf

The numerous studies that have investigated the neurotransmitter type of MTN, shows that MTN exhibits a variety of chemical neuromessengers for synaptic transmission (Lazarov, 2007). Some studies suggest that they are glutamatergic, while others suggest they are gabaergic (Chandler, 1989; Copray et al., 1990).

To identify the neurotransmitter type of MTN in zebrafish, in situ hybridisation was carried out to analyse the expression of *GAD1* a marker of inhibitory GABAergic neurons, and vesicular glutamate transporter *vGlut1* and *vGlut2a-c* markers of excitatory glutamatergic transmitters. At 30 hpf g*ad1*, *vGlut1* and *vGlut2a-c* expression are limited to the forebrain (Figure 3.2.8A – D, and data not shown for; *gad1*, *vGlut1* and *vGlut2a*), until 48 hpf where general expression was seen in the ventral brain region (Figure 3.2.8E - G). By 72 hpf this expression was extended to the dorsal midbrain (*vGlut2a*; *gad1* Figure 3.2.8H and J). *gad1*, *vGlut1* and *vGlut2a-c* expression specific to MTN neurons could not be seen, therefore these markers could not be used to follow MTN development at later stages. To elucidate the neurotransmitter type of MTN, further gene analysis is required.

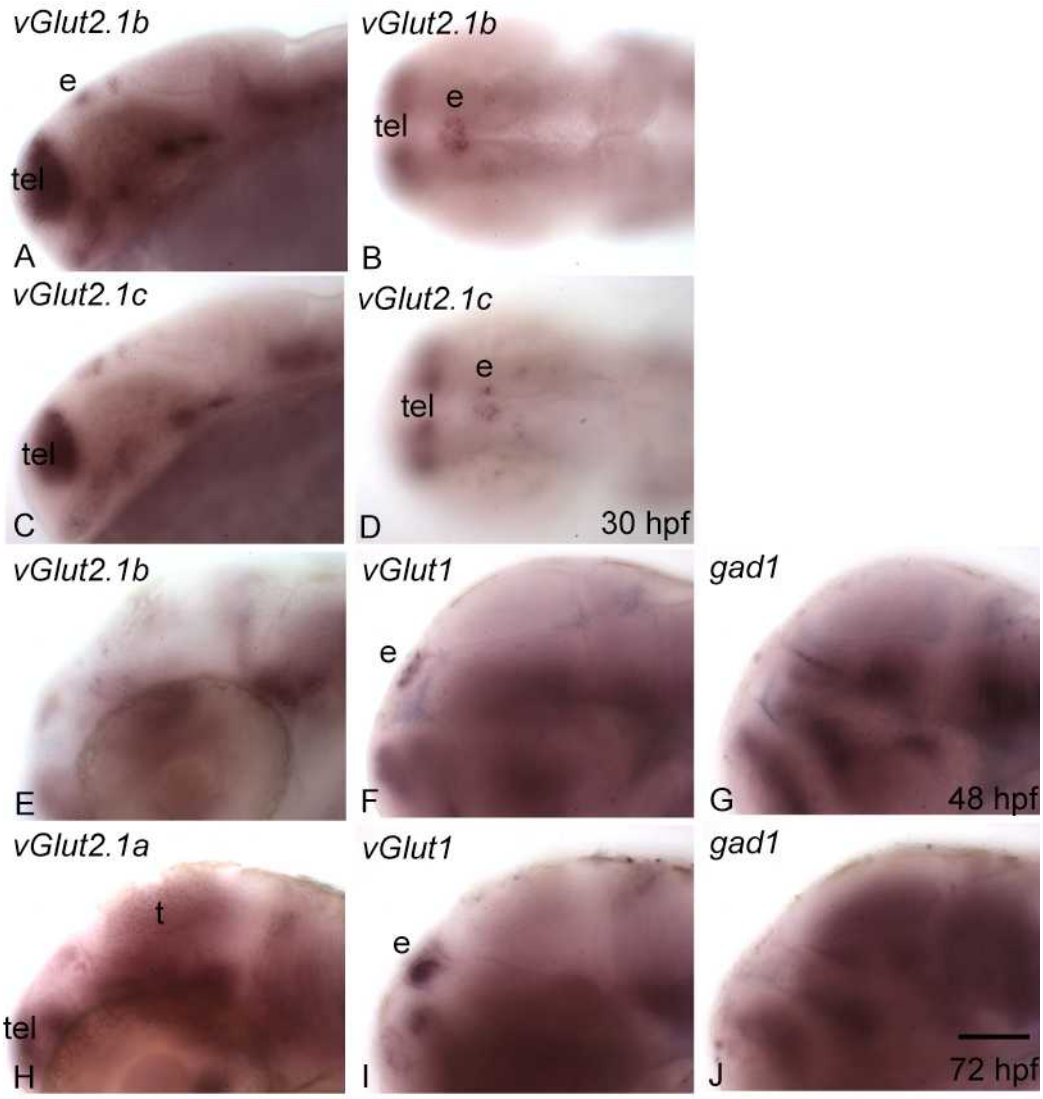

Figure 3.2.10 – Expression of markers of glutamatergic and gabaergic cells in zebrafish

(A) Lateral, and (B) dorsal views of a zebrafish head at 30 hpf, showing *vGlut2.1b* expression in epiphysis (e), nuclei of the tract of the posterior commissure (nTPC; black arrowhead) and telencephalon (tel). (C) Lateral, and (D) dorsal views showing *vGlut2.1c* expression, which is comparable to *vGlut2.1b* expression in A and B. (E) Lateral view of zebrafish at 48 hpf, showing *vGlut2.1b,* (F) *vGlut1* and (G) *gad1* expression in ventral brain regions (telencephalon, tel; tegmentum, teg – F and G only) and the epiphysis (e) (Shown in F only). (H) Lateral view of a zebrafish at 72 hpf, showing *vGlut2.1a* expression in the ventral brain and also in the tectum (t). (I) Lateral view of a zebrafish at 72 hpf, showing *vGlut1* expression comparable to its expression at 48 hpf. (J) lateral view of a zebrafish at 72 hpf, showing the expression of *gad1* now extended dorsally and can be seen in the tectum (t). e, epiphysis. KWT, Kings wild type. mb, midbrain. nTPC, nucleus of the tract of the posterior commissure. t, tectum. teg, tegmentum. tel, telenephalon. tg, trigeminal ganglion. Scale bar = 100µm

3.2.11 – *Tg(1.4dlx4-6:GFP)* is co-expressed with *drg11* and *isl1* in MTN cell bodies

To test if cell bodies labelled with *brn3a*, *drg11*, *isl1*, *tlx3* and *trkC* in the dorsal mesencephalon are MTN neurons, *drg11* and *isl1* expression were compared to the *Tg(1.4dlx4-6:GFP)* transgenic line. I have previously shown that DiI applied to the a.m. in *Tg(1.4dlx4-6:GFP)* fish labels a population of GFP+ MTN cell bodies. Putative molecular markers of MTN could not be directly compared to DiI labelled cell bodies, because the molecular markers were no longer expressed at 5 dpf stage. Therefore to see if there is co-localisation between *drg11* and GFP+ cells in the dorsal mesencephalon of these transgenic fish, double *in situ* hybridisation was carried out at 48 hpf and 72 hpf. This showed that *drg11* expression co-localises with GFP+ cells in the dorsal anterior mesencephalon (Figure 3.2.11.1; arrow), in a similar region to GFP+ cells labelled with DiI at 5 dpf. Fluorescent in situ analysis for *isl1* expression in GFP+ cells at 24 hpf, also revealed co-expression between *isl1* and GFP+ in cells in the dorsal anterior mesencephalon (Figure 3.2.11.2C and F).

These results suggest that the dorsal cell bodies expressing *brn3a*, *drg11*, *isl1*, *tlx3* and *trkC* in the midbrain at 24 hpf are likely to be MTN cell bodies. This is as GFP+ cells are also expressed in this region, and are later co-labelled with DiI from retrograde labelling studies.

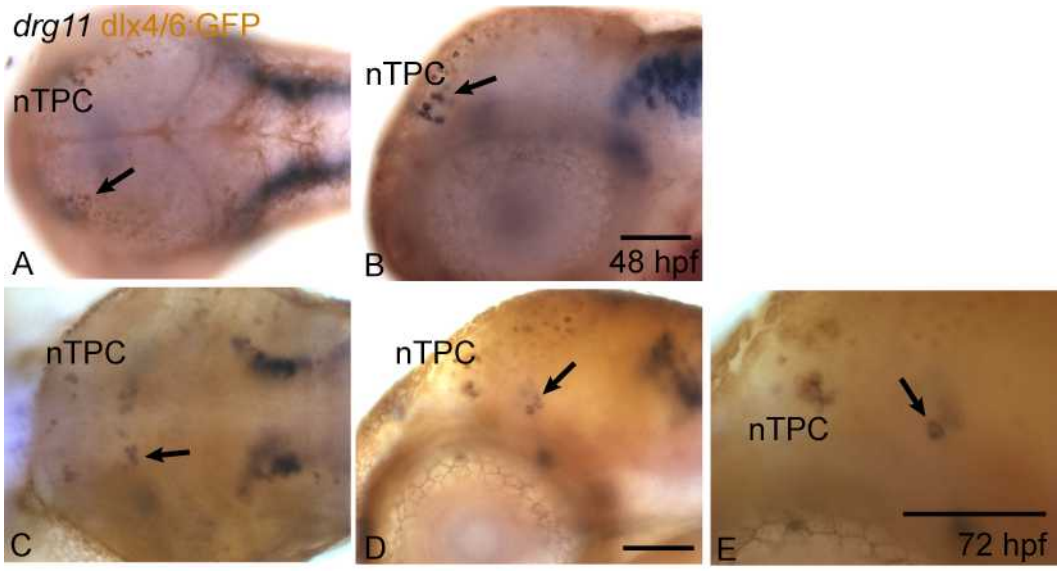

Figure 3.2.11.1 – Co-labelling of neurons with *drg11* and *Tg(1.4dlx4-6:GFP)* in the mesencephalon

(A) Dorsal and (B) lateral views of GFP expression in *Tg(1.4dlx4-6:GFP)* transgenic animals at 48 hpf, compared to *drg11* expression. Co-labelling can be seen between *drg11* and GFP positive cells in MTN cell bodies (black arrows) in the dorsal anterior mesencephalon. Co-labelling is also seen in the nTPC. (C) Dorsal and (D) lateral views of 72 hpf *Tg(1.4dlx4-6:GFP)* transgenic zebrafish, compared to drg11 expression. Co-labelling can be seen between *drg11* and GFP positive cells in MTN cell bodies (black arrows) in the dorsal anterior mesencephalon, similar to A and B. (E) A higher magnification of D. mb, midbrain. nTPC, nucleus of the tract of the posterior commissure. Scale bars = 100μm

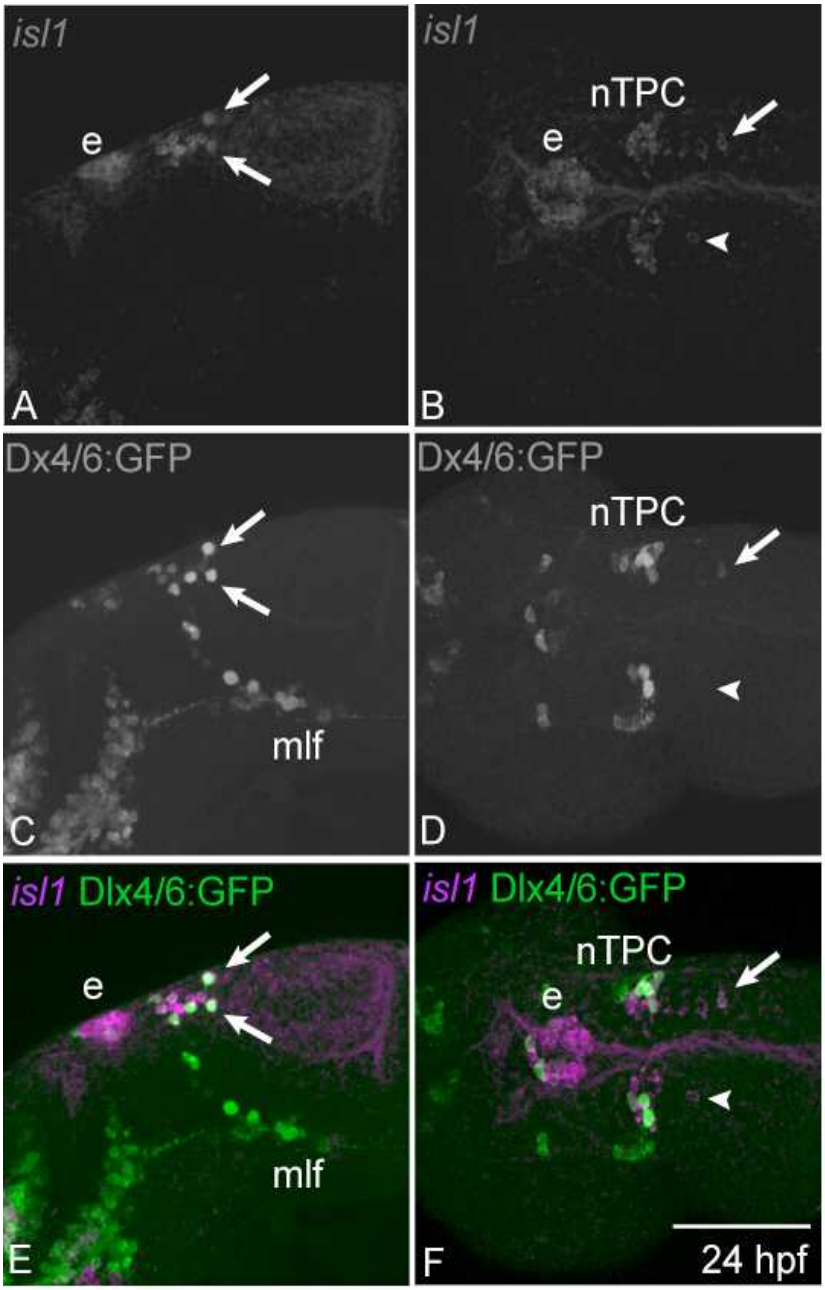

Figure 3.2.11.2 – Co-labelling between *isl1* and *Tg(1.4dlx4-6:GFP)* can be seen in some MTN cell bodies

Lateral image showing (A) *isl1* expression, (C) *Tg(1.4dlx4-6:GFP)* expressing cells in the zebrafish at 24 hpf. (E) a merge of A and C. Co-labelling can be seen between isl1 and GFP in MTN cell bodies. Dorsal view of *Tg(1.4dlx4-6:GFP)* transgenic zebrafish at 24 hpf, showing (B) isl1 expression, (D) GFP+ cells, and (F) a merge of B and D. Co-labelling can be seen between *isl1* and GFP in MTN cell bodies (white arrow) in the dorsal anterior mesencephalon, similar to E, while other MTN cell bodies are seen to only express *isl1* (white arrowhead). e, epiphysis. mlf, medial lateral longitudinal fasciculus. nTPC, nucleus of the tract of the posterior commissure.

Scale bar = 50 μm

3.2.12 – Anti-acetylated tubulin labels the major axon tracts of the early zebrafish brain

Immunohistochemistry was used to identify axons of the MTN and their axonal pathways. Anti-acetylated tubulin, an antibody to a cytoskeletal protein, was used to label the axons, and anti-Isl1 was used to label MTN cell bodies (Peters and Vaughn, 1967; Piperno and Fuller, 1985). By 24 hpf the basic scaffolding of the major axon tracts of the developing zebrafish brain has formed and MTN cell bodies express *isl1* (Sub-section 3.2.7; Wilson et al., 1990).

As the MTNs are primary neurons (and express *isl1*), it is likely that axons of MTN develop at 25hpf. In chick the MTN is one of the earliest neurons to develop (Chedotal et al., 1995). In Figure 3.2.12.1A, MTN neurons are clearly seen in the dorsal anterior mesencephalon, along with nTPC at the forebrain-midbrain boundary labelled by anti-Isl1. The trigeminal ganglia are also labelled by Isl1, and axons of the ganglia grow anteriorly and dorsally. Axons can be seen growing out of MTN cell bodies laterally and ventrally, towards the tegmentum, where the many axon bundles of the tract of the post-optic commissure (TPOC), and tract of the posterior commissure (TPC) accumulate to form the ventral tract, the medial longitudinal fasciculus (mlf) (Chitnis and Kuwada 1990, Wilson et al., 1990; Figure 3.2.12.1C and F; Figure 3.2.12.2, 3D projections of acetylated tubulin v Isl1). It appears that that the MTN axons do not fasciculate with the TPC, instead they grow down more posterior to, and alongside, the TPC (Figure 3.2.12.1C and G; Figure 3.2.12.2). The path MTN neurons take when they reach the mlf is unclear, because it is hard to distinguish between the different ventral axonal tracts. However from the dorsal MTN axonal trajectories seen from retrograde labelling with DiI (Sub-section 3.2.1), MTN neurons may turn shortly before reaching the mlf and form their own tract dorsal to the mlf, similar to that previously described in mouse, chick and catshark (Mastick and Easter, 1996; Kuratani and Horigome, 2000; Hunter et al., 2001)

Neuronal development was also assessed at 48 hpf and 72 hpf by labelling with anti-acetylated tubulin alone, but I was unable to discriminate between MTN axons and those of other neurons at these later stages (Figure 3.2.11.3).

In summary, anti-acetylated tubulin labelling of axons and anti-Isl1 labelling of MTN cell bodies, reveals that the axons of the MTN grows ventrally toward the MLF in a separate tract alongside the TPC.

Figure 3.2.12.1 – Acetylated tubulin can be used to visualise the pathway of MTN axons.

Lateral views of a zebrafish head at 25 hpf showing (A) Isl1 expression, (C) acetylated tubulin labelling, and (E) a merge of A and C. The TPC, axonal projections of neurons from the trigeminal ganglia, and the ventral tracts; the tract of the post-optic commissure (TPOC) and the medial longitudinal fasciculus (mlf), can be seen from the labelling with acetylated tubulin. Dorsal views of a zebrafish head at 25 hpf showing (B) Isl1 expression, (D) acetylated tubulin (a-tub) labelling, and (F) a merge of B and D. MTN cell bodies (white arrows) are labelled by the expression of Isl1. Axons can be seen projecting from MTN cell bodies in an anterior direction towards the periphery and tract of the posterior commissure (TPC, white arrowhead), labelled by acetylated tubulin. The TPC and axons of epiphysal cells (e) are also shown by labelling with acetylated tubulin e, epiphysis. mlf, medial longitudinal fasciculus. nTPC, nuclei of the tract of the posterior commissure. tg, trigeminal ganglion. TPC, tract of the posterior commissure.

Scale bar; E = 100 μm, F = 50 μm

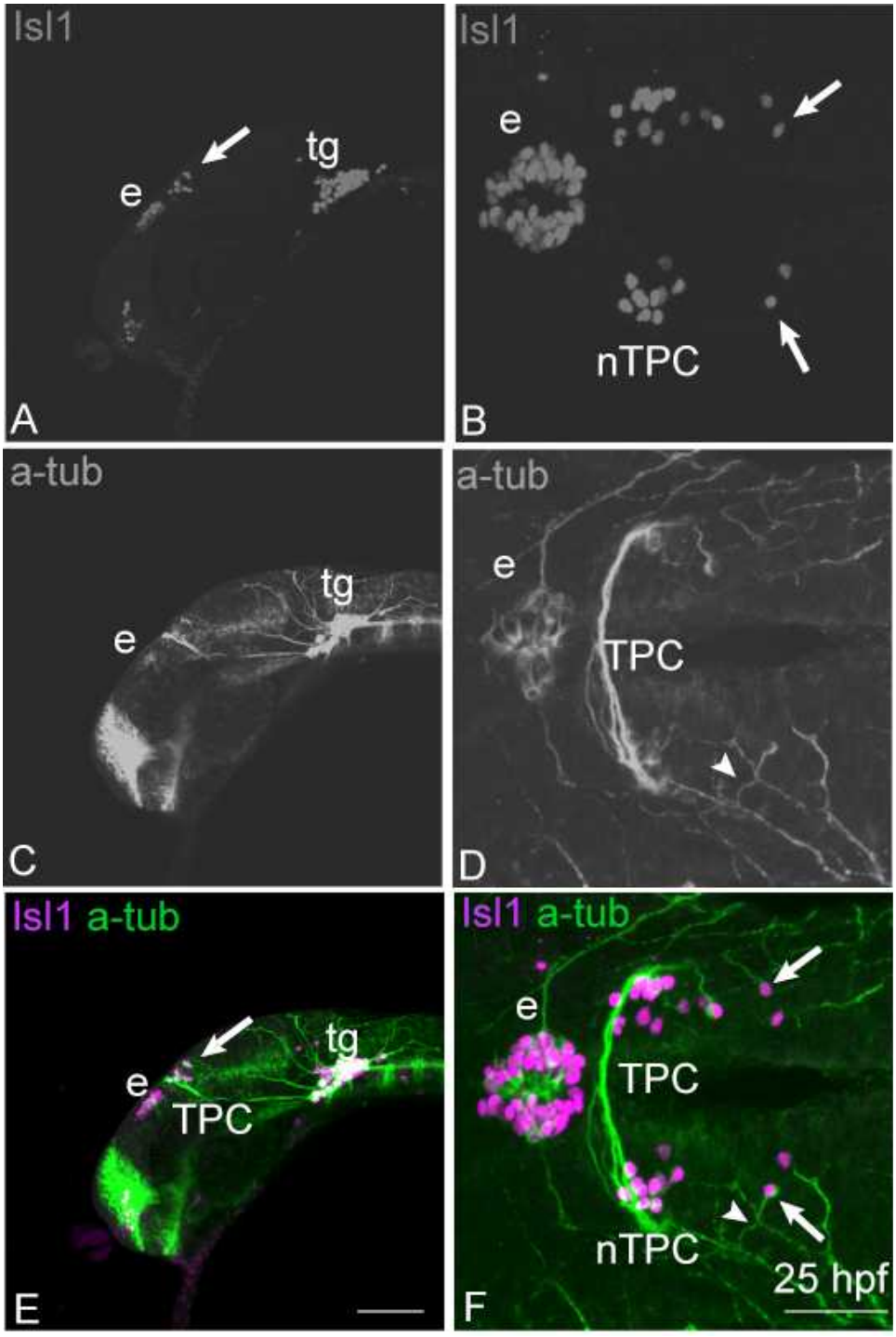
Isl1
tg
e
A
Isl1
e
nTPC
B
a-tub
tg
e
C
a-tub
e
TPC
D
Isl1 a-tub
tg
e
TPC
E
Isl1 a-tub
e
TPC
nTPC
25 hpf
F

Figure 3.2.12.2 - 3D projections of a zebrafish head labelled with acetylated tubulin to visualise the pathway of MTN axons.

Dorsal views of a zebrafish head at 25 hpf showing (A) Isl1 expression, (B) acetylated tubulin (a-tub) labelling, and (C) a merge of A and B. MTN cell bodies (white arrows) are labelled by the expression of Isl1.(C' and C'') 3D projections of C shows the pathway of MTN axons. Axons (white arrowheads), labelled by acetylated tubulin, can be seen projecting from MTN cell bodies in an anterior direction towards the periphery and tract of the posterior commissure (TPC, white arrowhead).

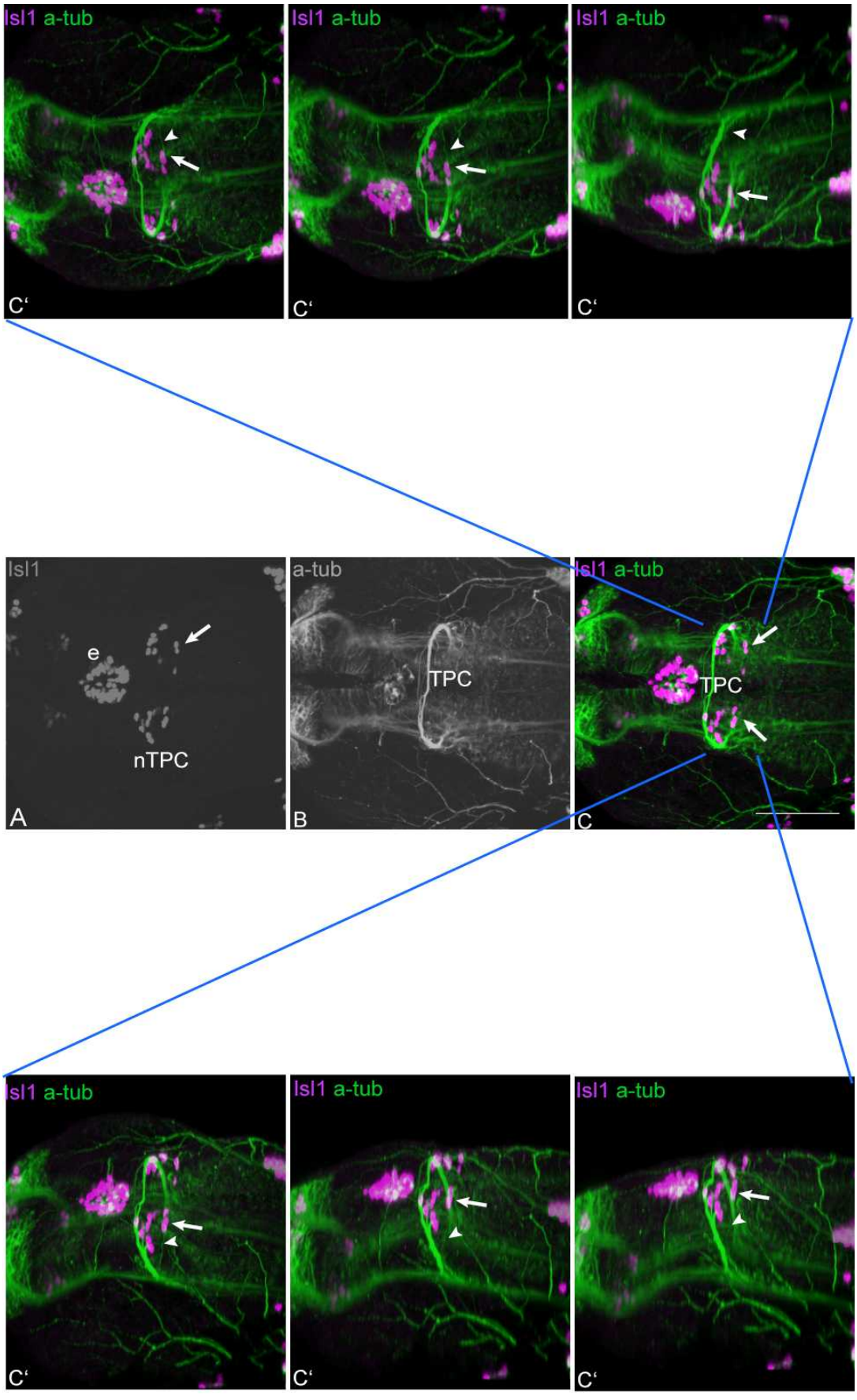
Isl1 a-tub
C‘
Isl1 a-tub
C‘
Isl1 a-tub
C‘
Isl1
e
nTPC
A
a-tub
TPC
B
Isl1 a-tub
TPC
C
Isl1 a-tub
C‘
Isl1 a-tub
C‘
Isl1 a-tub
C‘

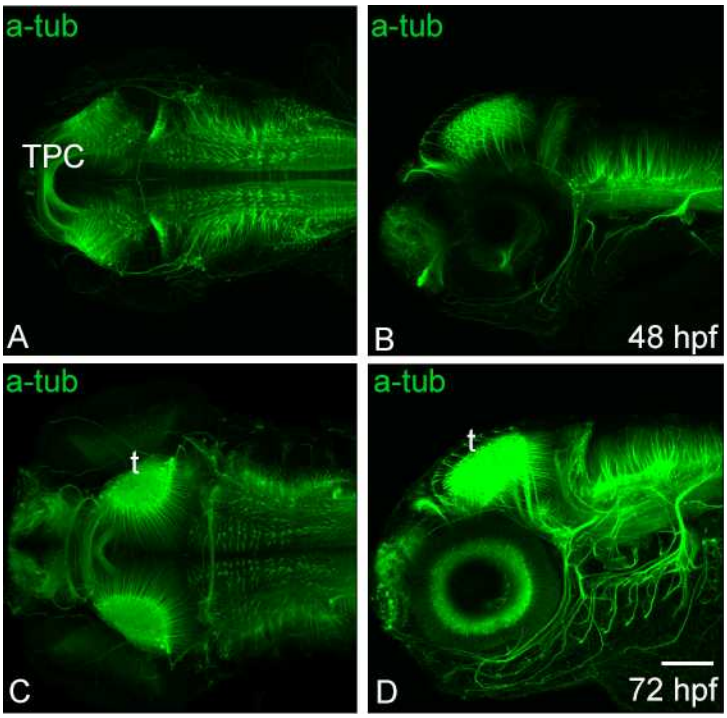

Figure 3.2.12.3 – Anti-acetylated tubulin labels the major axon tracts in the zebrafish brain

(A) Dorsal and (B) lateral views of a 48 hpf zebrafish stained with acetylated tubulin antibody (a-tub), labelling the developing axonal tracts within the brain. (C) Dorsal and (B) lateral views of a 72 hpf zebrafish stained with acetylated tubulin, labelling more developed axon tracts within the brain. t, tectum. TPC, tract of the posterior commissure.

Scale bar = 100 μm

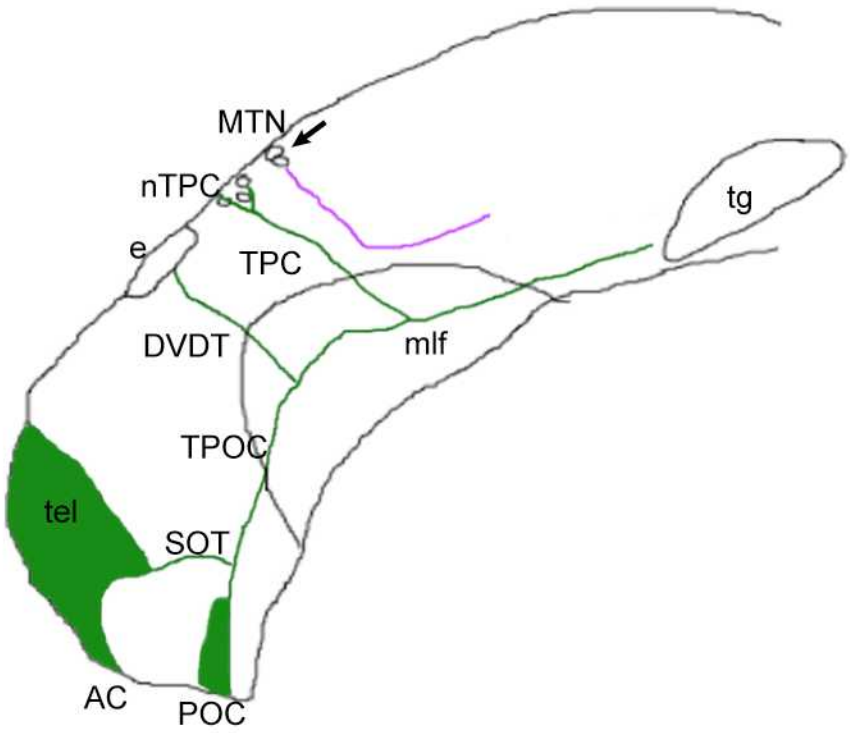

Figure 3.2.12.4 – Diagrammatic representation of the axonal pathway of MTN neurons at 24 hpf.

A diagrammatic representation of the tract MTN neurons form, based on data from the analysis of MTN axonal pathways using immunohistochemistry and DiI labelling. Axons (magenta) are shown projecting ventrally from MTN neuronal cell bodies (Black arrow) in a separate tract alongside the TPC, towards the MLF. Before reaching the mlf they turn 90º in a posterior direction, and grow towards the hindbrain, parallel and dorsal to the mlf. ac, anterior commissure. DVDT, dorso-ventral diencephalic tract. e, epiphysis. mlf, medial longitudinal fascicle. nTPC, nucleus of the tract of the posterior commissure. SOT, supraoptic tract. tel, telencephalon. tg, trigeminal ganglion. TPC, tract of the posterior commissure. TPOC, tract of the postoptic commissure.

3.2.13 – HuC is co-expressed with Isl1 in MTN cell bodies

huC is expressed in many dorsal midbrain neurons in the zebrafish by 24 hpf, however only the HuC protein is an indicator of post-mitotic neurons and is essential for their differentiation (Zhao et al., 2006). Expression of the *huC* gene does not indicate that the protein is present. I have shown this by comparing *huC* gene and protein expression using fluorescent in situ hybridisation and anti-Hu, which revealed that while *huC* is expressed in all dorsal neurons at 24 hpf, the HuC protein is more restricted to some dorsal neurons (Figure 3.2.12.1).

To show that MTN neurons express HuC, 24 hpf *Tg(huC:eGFP)* transgenic fish were labelled with anti-Isl1 and anti-GFP. Co-expression between Isl1 and GFP+ cells in *Tg(huC:eGFP)* was seen in MTN neurons in the dorsal anterior mesencephalon (Figure 3.2.12.2C and F). Isl1 and GFP were also co-expressed in the nTPC, and epiphysal cells. Fluorescent in situ hybridisation comparing *drg11* expression with GFP cells in *Tg(huC:eGFP)* show co-expression in MTN, in the dorsal anterior mesencephalon, similar to the co-expression seen between Isl1 and GFP+ MTN neurons (Figure 3.2.12.2I).

The expression of HuC protein in MTN neurons in *Tg(huC:eGFP)* transgenic fish indicates that this line can be used to visualise early MTN development.

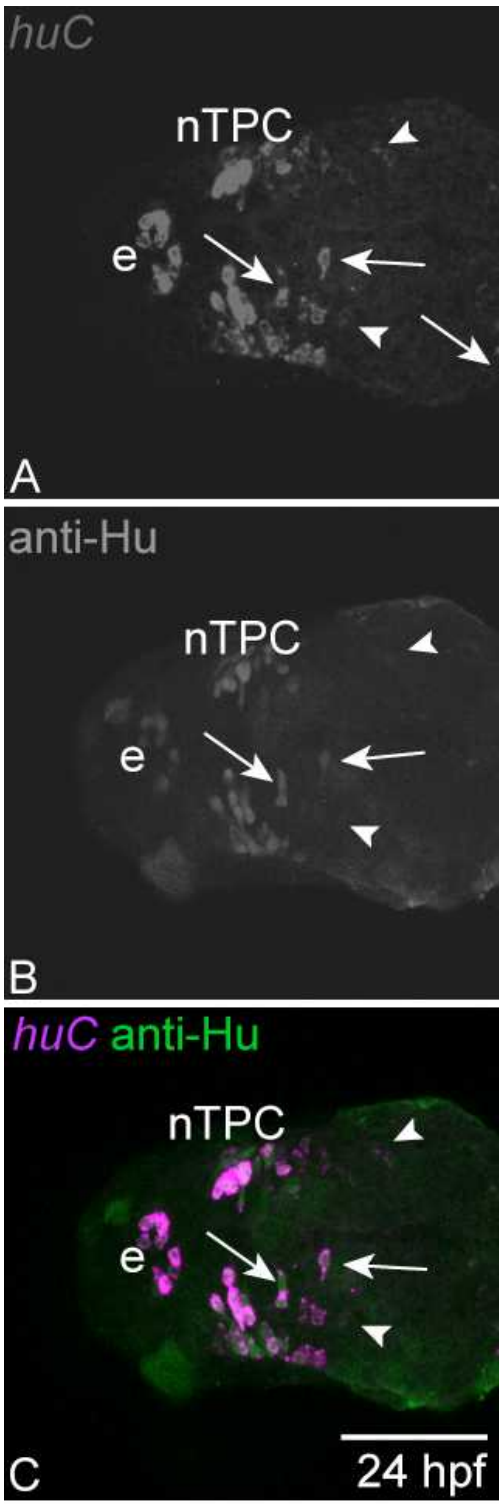

Figure 3.2.13.1 – *huC* is expressed in more dorsal mesencephalic cells relative to expression of the HuC protein

Dorsal views of a zebrafish head at 24 hpf showing (A) *huC* expression, (B) anti-Hu expression and (C) a merge of A and B. anti-Hu is seen co-expressed with *huC* (white arrows). *huC* is also expressed alone in dorsal mesencephalic cells (white arrowhead). e, epiphysis. nTPC, nucleus of the tract of the posterior commissure. Scale bar = 100 μm

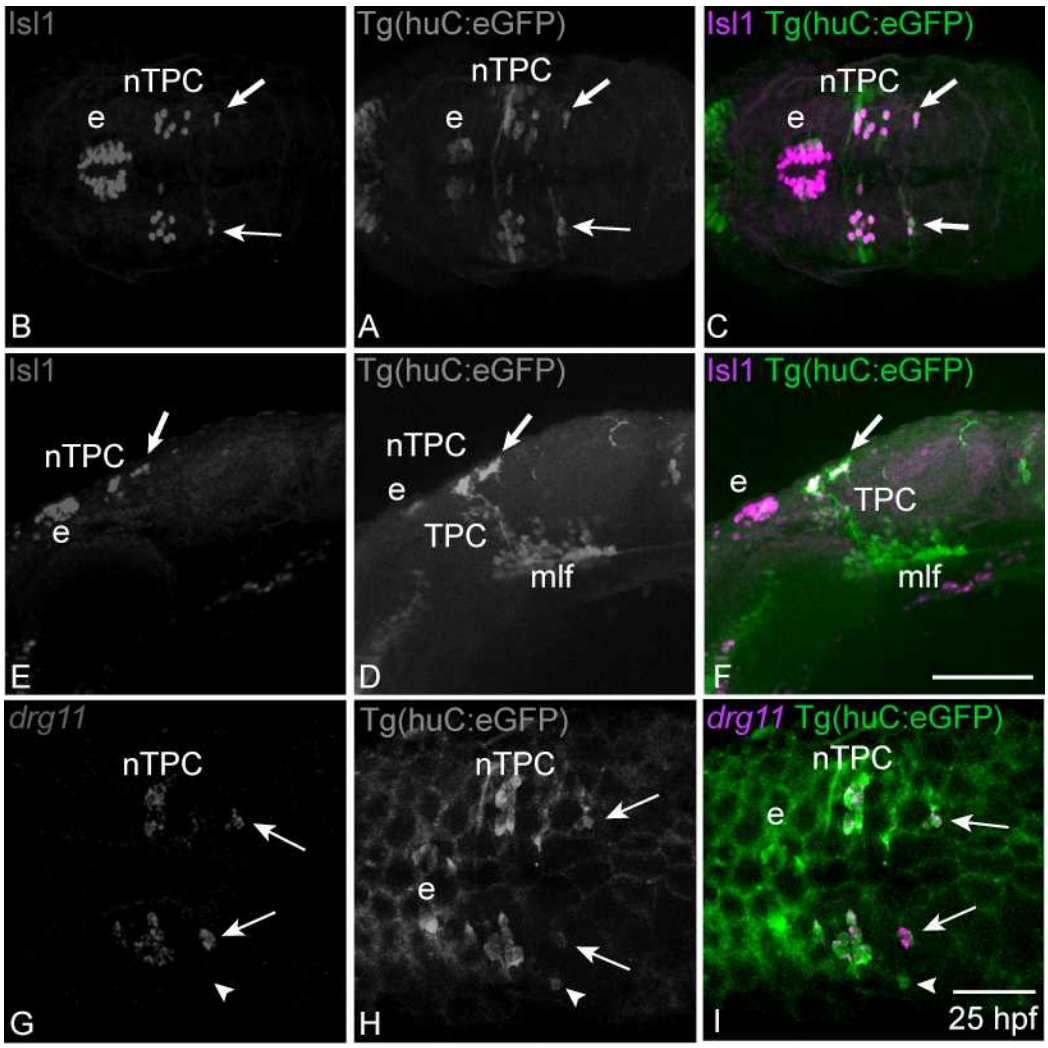

Figure 3.2.13.2 – Co-expression between *drg11* and GFP can be seen in MTN neurons in *Tg(huC:eGFP)* larvae

Dorsal views of a zebrafish head at 25 hpf showing (A) Isl1 expression, (B) *Tg(huC:eGFP)* expression, and (C) a merge of A and B. MTN cell bodies (white arrows) are labelled by the expression of Isl1. Co-expression between Isl1 and HuC:GFP is seen in MTN cell bodies (white arrows), nucleus of the tract of the posterior commissure (nTPC) and epiphysis (e). Lateral views of a zebrafish head at 25 hpf showing (D) Isl1 expression, (E) *Tg(huC:GFP)*, and (F) a merge of D and E. Co-expression between Isl1 and *Tg(huC:GFP)* in MTN cell bodies is shown (white arrow). GFP is also seen in the tract of the posterior commissure (TPC), and the medial longitudinal fasciculus (mlf). Dorsal views of a zebrafish head at 25 hpf showing (G) *drg11* expression, (H) *Tg(huC:eGFP)*, and (I) a merge of G and H. Co-expression between *drg11* and *Tg(huC:eGFP)* in MTN cell bodies and nTPC is shown (white arrow). e, epiphysis. mlf, medial longitudinal fasciculus. nTPC, nucleus of the tract of the posterior commissure. TPC, tract of the posterior commissure. Scale bar = 50 μm

3.2.14 – *Tg(huC:eGFP)* can be used to follow early MTN development

In order to determine where MTN neurons are born in the brain, the *Tg(huC:eGFP)* transgenic line was used (Park et al., 2000). In this line GFP is expressed in all differentiating neurons (Park et al., 2000). A timelapse of *Tg(huC:eGFP)* transgenic fish from 18ss, (before MTN cell bodies first arise), until approximately 36hpf, was performed to follow the early development of MTN cell bodies. At 18ss HuC expression is limited to cells in the telencephalon and epiphysis (Figure 3.2.14.1A). By 20 ss, HuC is also expressed more posteriorly in the nTPC at the forebrain midbrain boundary (Figure 3.2.14.1B; white arrowhead). Ventrally the pioneering axons of the MLF are growing through the tegmentum and into the hindbrain (Figure 3.2.14.3).

As development progresses to around 20 hpf (22 ss) MTN cell bodies begin to form, located posteriorly to the nTPC (Figure 3.2.14.1C; white arrow). They appear to be born along the midline of the dorsal anterior mesencephalon and then move laterally in a dynamic manner. By 24 hpf axons can be seen growing out from MTN cell bodies, with a leading growth cone finding a ventral path slightly posterior to the TPC (Figure 3.2.14.1F; white asterisk; Figure 3.2.14.2B'). At 24 hpf, further MTN cell bodies are still forming, and later their axons can also be seen growing in a similar way (Figure 3.2.14.1F, blue arrow; Figure 3.2.14.1I, blue asterisk; Figure 3.2.14.2). During this time the axons pioneering the mlf and TPC have significantly increased in their numbers (Chitnus and Kuwada, 1990). This makes following the ventral path of the MTN axons impossible using this transgenic line as they cannot be distinguished from other axons in the mlf.

Figure 3.2.14.1 – Developmental stages of early MTN development in *Tg(huC:eGFP)* transgenic fish

Dorsal views taken from a timelapse of *Tg(huC:eGFP)* transgenic zebrafish between 18 ss to 32 hpf, to follow early MTN development. (A) GFP expression is seen in cells of the epiphysis at 18 ss. MTN cells bodies have not yet begun to differentiate, and are still not formed by (B) 21ss. Nuclei of the tract of the posterior commissure (nTPC) are beginning to develop (white arrowhead). (C) At 22 ss MTN cell bodies (white arrow) are seen (by HuC expression) to differentiate, arising near to the midline. nTPC continue to form. (D) At stage 23 ss, and (E) 29 ss, more nTPC and MTN cell bodies form (white arrows). (F) By 24 hpf, axons can be seen growing from MTN cell bodies towards the periphery (white asterisk), while more MTN cell bodies continue to form (blue arrow). (G) between 26 hpf and (H) 27 hpf, growth cones of the growing axons are seen (white asterisk), as they continue to grow and project posteriorly towards the tract of the posterior commissure (TPC). During this time the nTPC grows. (I) At 27.5 hpf another axon can be seen growing from a later born MTN cell body, which continues to grow between (J) 28 hpf and (K) 29 hpf, also taking a posterior path towards the periphery and the TPC. (L) By 32 hpf the formation of MTN and their axons appear to be complete. e, epiphysis.

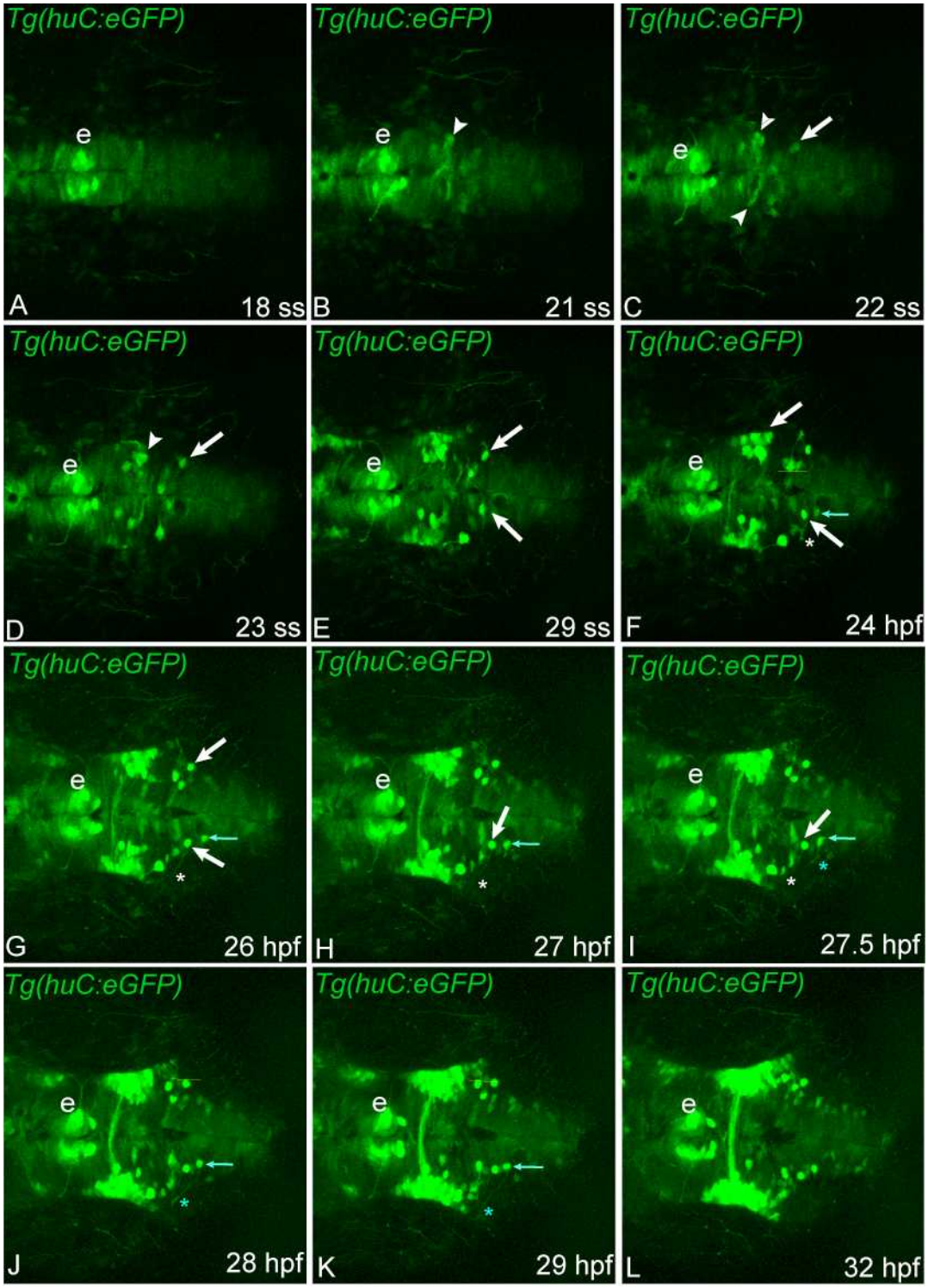
Tg(huC:eGFP)
e
A
18 ss
Tg(huC:eGFP)
e
B
21 ss
Tg(huC:eGFP)
e
C
22 ss
Tg(huC:eGFP)
e
D
23 ss
Tg(huC:eGFP)
e
E
29 ss
Tg(huC:eGFP)
e
*
F
24 hpf
Tg(huC:eGFP)
e
*
G
26 hpf
Tg(huC:eGFP)
e
*
H
27 hpf
Tg(huC:eGFP)
e
*
I
27.5 hpf
Tg(huC:eGFP)
e
*
J
28 hpf
Tg(huC:eGFP)
e
*
K
29 hpf
Tg(huC:eGFP)
e
L
32 hpf

Figure 3.2.14.2 – Higher magnification of developmental stages of early MTN development in *Tg(huC:eGFP)* trangenic fish.

Dorsal views taken from a timelapse of *Tg(huC:eGFP)* transgenic zebrafish between 29 ss to 28 hpf, to follow early MTN development. (A) Image E from Figure 3.2.13 at stage 29 ss. (A') A higher magnification of A, showing an MTN cell body arising near to the midline. An axon can be seen growing from the MTN cell body (white asterisk). (B) Image F from Figure 3.2.12 at 24 hpf. (B') A higher magnification of B, in which the axon (asterisk) has grown further from the MTN cell body (white arrow) towards the periphery, while more MTN cell bodies continue to form (blue arrow). (C) Image G from Figure 3.2.12 at 26 hpf. (C') A higher magnification of C in which growth cones of the growing axon are seen (white asterisk) as it continues to grow and project posteriorly towards the tract of the posterior commissure (TPC). (D) Image I and (E) J from Figure 3.2.13 at 27.5 hpf and 28 hpf. (D') A higher magnification of D, and (E') E, in which another axon (blue asterisk) can be seen growing from a later born MTN cell body (blue arrow), also taking a posterior path towards the periphery and the TPC.

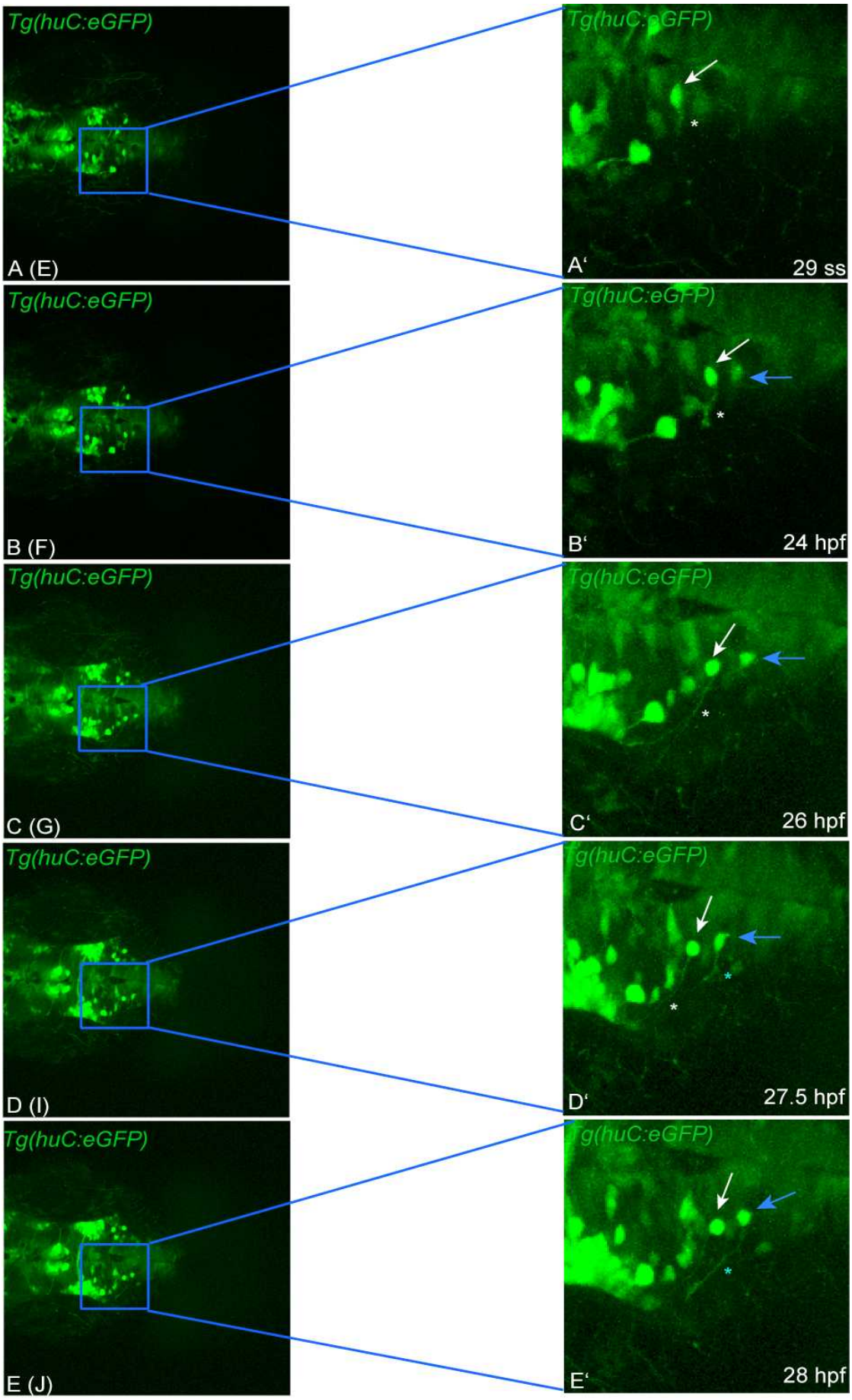
Tg(huC:eGFP)
A (E)
Tg(huC:eGFP)
A‘
29 ss
Tg(huC:eGFP)
B (F)
Tg(huC:eGFP)
B‘
24 hpf
Tg(huC:eGFP)
C (G)
Tg(huC:eGFP)
C‘
26 hpf
Tg(huC:eGFP)
D (I)
Tg(huC:eGFP)
D‘
27.5 hpf
Tg(huC:eGFP)
E (J)
Tg(huC:eGFP)
E‘
28 hpf

Figure 3.2.14.3 - Developmental stages of the pioneering axons of the tract of the post-optic commissure and the medial lateral longitudinal fasciculus in *Tg(huC:eGFP)* transgenic fish.

(A – L) Ventral views taken from a timelapse of *Tg(huC:eGFP)* transgenic zebrafish between 18 ss to 32 hpf, following the development of pioneering axons of the, tract of the post-optic commissure (TPOC), medial longitudinal fasciculus (mlf) and from the trigeminal ganglia. During this time the axons of the mlf and tract of the posterior commissure (TPC) significantly increase in their numbers. Axons from the trigeminal ganglia can also be seen growing out towards the periphery. mlf, medial longitudinal fasciculus. tg, trigeminal ganglion. tpoc, tract of the post-optic commissure.

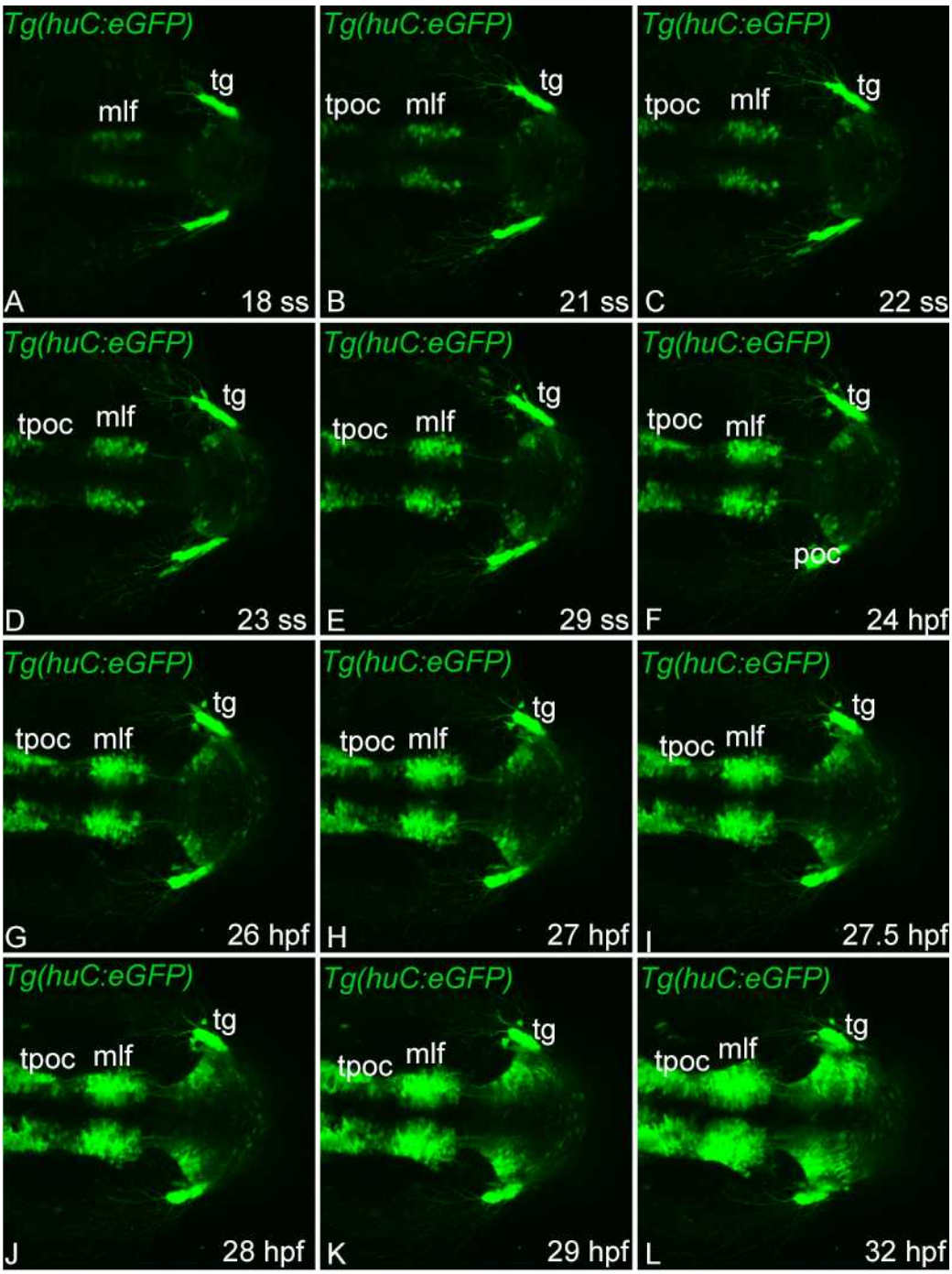
Tg(huC:eGFP)
tg
mlf
A
18 ss
Tg(huC:eGFP)
tg
tpoc
mlf
B
21 ss
Tg(huC:eGFP)
tpoc
mlf
tg
C
22 ss
Tg(huC:eGFP)
tg
tpoc
mlf
D
23 ss
Tg(huC:eGFP)
tg
tpoc
mlf
E
29 ss
Tg(huC:eGFP)
tg
tpoc
mlf
poc
F
24 hpf
Tg(huC:eGFP)
tg
tpoc
mlf
G
26 hpf
Tg(huC:eGFP)
tg
tpoc
mlf
H
27 hpf
Tg(huC:eGFP)
tg
tpoc
mlf
I
27.5 hpf
Tg(huC:eGFP)
tg
tpoc
mlf
J
28 hpf
Tg(huC:eGFP)
tg
tpoc
mlf
K
29 hpf
Tg(huC:eGFP)
tg
tpoc
mlf
L
32 hpf

3.3 – Summary

In this chapter I have shown that MTN cell bodies are located in the dorsal anterior mesencephalon. This data supports the previously described location of MTN cell bodies in amniotes (Stainier and Gilbert 1990; Chedotal et al., 1995). I have also shown that MTN neurons innervate the jaw muscles in zebrafish, contradicting previous studies in teleosts (carp, guppy, medaka) that found MTN neurons only innervated the skin and perioral area of the jaw (Luiten. 1979; guppy/medaka paper). Potentially DiI labelling of the muscle could retrogradely label MTN neurons innervating the skin around the muscle. However when DiI was applied to the skin alone no cells were labelled.

Once the MTN location in the zebrafish was confirmed I then characterised MTN neuronal development using zebrafish orthologues of genes expressed in MTN of other species (Hunter et al., 2001; Ichikawa et al., 2005; Wang et al., 2007). This revealed that zebrafish MTN express *brn3a*, *drg11*, *tlx3* and *isl1*, similar to amniote MTN neurons. *TrkC* has previously been described as expressed in the MTN in mouse, but I did not see *trkC* expression in the zebrafish MTN. ETS transcription factors *pea3* and *er81*, and zinc finger domain genes *egr1*, *egr2* and *egr3* were also not expressed in zebrafish MTN. Previous studies have shown that the MTN in mice are responsive to *egr2*, which has a role in cell survival within the MTN in mice, however this is not a cell autonomous phenotype.

To determine when MTN neurons are born I characterised the expression of *huC* and *ngn1* in MTN. Timelapse imaging of *Tg(huC:eGFP)* identifed MTN cell bodies first arising from the dorsal midline in the mesencephalon at 22 ss. This time point is comparable to when they are described to first appear in the chick at stage 14, but later than that described in mouse when they arise from E8.5 (10 ss) suggesting a conservation of early MTN development (Hamburger and Hamilton 1951; Stainier and Gilbert, 1990; Hunter et al., 2001;).

Using axonal markers acetylated tubulin and *Tg(huC:eGFP)* transgenic larvae, I have begun to show early MTN axonal projections in the embryonic zebrafish (Park et al., 2000). MTN neurons appear to grow towards the tract of the posterior commissure and then follow it down towards the mlf. However it is unclear whether MTN neurons grow parallel to the mlf in a putative LLF or dtmesV, similar to that which has previously been described in other amniotes and teleosts (Mastick and Easter, 1996; Hunter et al., 2001; Ishikawa et al., 2004).

Chapter 4: Candidate signalling pathways required for MTN development

4.1 – Introduction

The aim of this chapter was to identify signalling pathways important for MTN development. Fgf and Wnt signalling pathways were focussed on because they play an important role in patterning the dorsal brain and are therefore likely to be important for MTN specification (Wurst and Bally-Cuif, 2001).

The role of Fgf signalling during MTN development has been investigated in only one previous study (Hunter et al., 2001). Hunter et al (2001) showed in chick that the up-regulation of Fgf resulted in the formation of more MTN neurons. The role of Wnt during MTN development has not been analysed before. The Fgf and Wnt pathways have been studied extensively, however, for their roles in patterning the forebrain, midbrain and hindbrain in a range of species, during development (Suzuki-Hirano and Shimogori, 2009; Seidensticker and Behrens, 2000).

To test the roles of Fgf and Wnt signalling during MTN development, I analysed the affects on MTN cell numbers in mutants with altered Wnt or Fgf signalling and in larvae that had been treated with drugs to manipulate these pathways. I also analysed the affects on nTPC neuronal cell numbers that are located at the forebrain – midbrain boundary anterior to MTNs, and express similar genes. The nTPC neurons were analysed to investigate the specificity of cellular responses to Fgf and Wnt signalling in the dorsal midbrain.

4.2 – Results

4.2.1 – *fgf8* and *wnt1* are expressed at the isthmus and in the dorsal diencephalon

To determine where Fgf and Wnt signalling molecules are expressed during MTN development, the expression of *fgf8* and *wnt1* relative to *drg11* expression were analysed during midbrain development at 20 hpf, when the first MTN neurons are born. *wnt1* and *fgf8* are both expressed at the midbrain hindbrain boundary in one of the organising centres of the brain, the isthmus, and in the dorsal diencephalon (Figure 4.2.1), as previously documented (Suzuki-Hirano and Shimogori, 2009). w*nt1*

expression is localised along the dorsal midline of the midbrain (Figure 4.2.1A and B). No MTN cell bodies are yet present, but *drg11* expression can be seen in the nTPC. However, in the previous chapter I have shown that the Fgf target gene *pea3* is not expressed in MTN neurons, suggesting that Fgf signalling may not be required for MTN development.

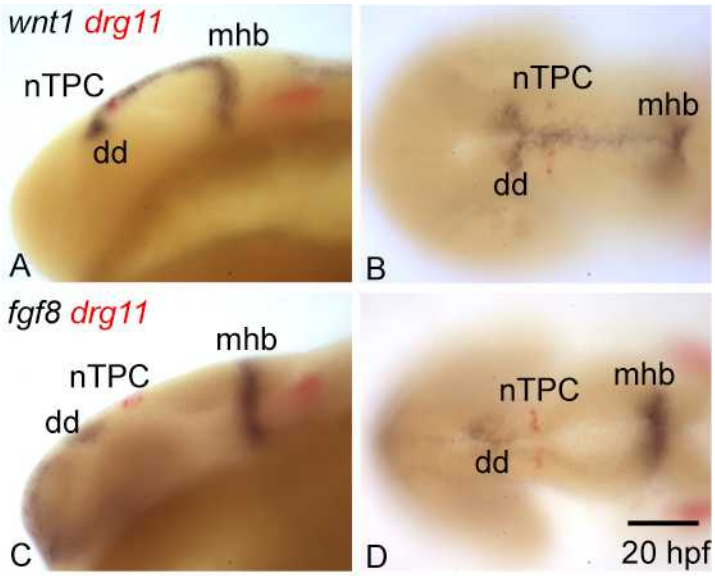

Figure 4.2.1 – *wnt1* and *fgf8* expression relative to *drg11* expression at 20 hpf
(A) lateral and (B) dorsal views of a zebrafish head at 20 hpf showing *wnt1* expression (black/purple) in the dorsal diencephalon (dd), along the dorsal midline and at the midbrain – hindbrain boundary (mhb). *drg11* (red) is expressed in the nuclei of the tract of the posterior commissure (nTPC) anterior to the dorsal diencephalon (dd). (C) Lateral and (D) dorsal views if a zebrafish head at 20 hpf showing *fgf8* expression in the dorsal diencephalon (dd) and at the midbrain hindbrain boundary. dd, dorsal diencephalon. mhb, midbrain – hindbrain boundary. nTPC, nucleus of the tract of the posterior commissure.
Scale bar = 100 μm

4.2.2 – Inhibition of the Fgf signalling pathway with SU5402 causes an increase in MTN numbers

The role of Fgf signalling on MTN development was tested by applying the FgfR1 inhibitor SU5402 to down-regulate Fgf signalling (Mohammadi et al., 1997). SU5402 inhibits the Fgf signalling pathway by binding to the Fgf receptor, preventing the intracellular signalling cascade that allows the transcription of Fgf target genes.

Figure 4.2.2.1 – Schematic of the Fgf signalling pathway

A diagrammatic representation of the Fgf signalling pathway showing the transmembrane Fgf receptor. Upon binding of a ligand to the Fgf receptor, the intracellular domain is phosphorylated, which in turn leads to a phosphorylation signalling cascade allowing ERK to enter the nucleus and induce the transcription of Fgf target genes. Taken from Alberts et al, 2002.

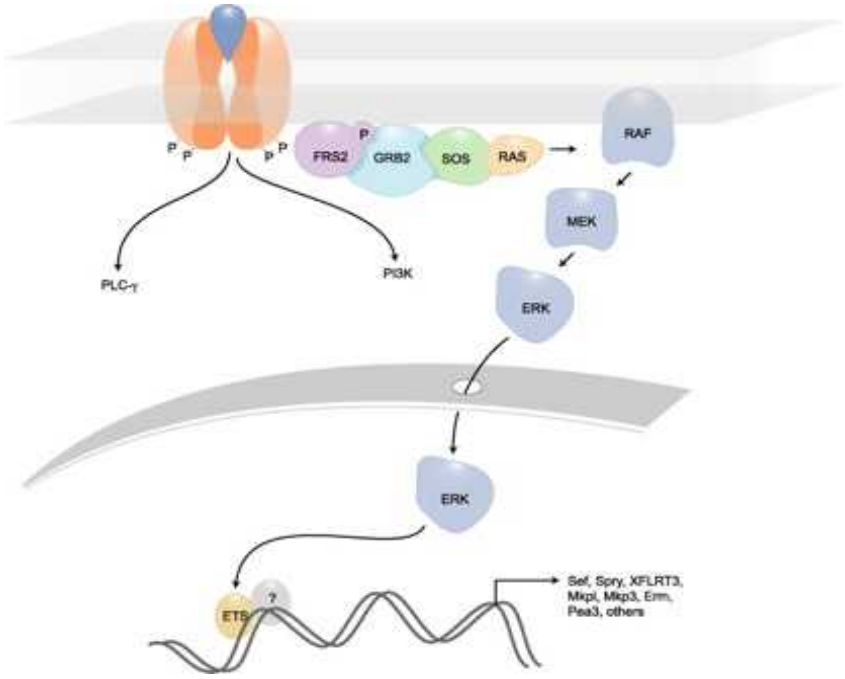

Fish were treated at 5 ss and 10 ss to see whether this slight difference in timing drastically affected the results. At 5 ss the brain is still being patterned and therefore treatment with SU5402 may cause changes in the boundaries of the brain compartments (Scholpp et al., 2003). By 10 ss, the brain compartments appear to have been specified, with no cellular transfer between the boundaries (Kiecker and Lumsden, 2005),

therefore SU5402 should no longer affect brain compartmentalisation. Changes in MTN numbers in SU5402 treated fish at 5 ss could reflect changes to brain boundaries. In contrast, at 10 ss, any changes in MTN numbers are presumed to be due to a specific affect of loss of Fgf signalling on MTN development.

Fish that had been treated with 40uM SU5402 from 5 ss and 10 ss respectively, to 24 hpf, were labelled with *pea3*, an ETS transcription factor which is a target gene of Fgf signalling (Molina et al., 2007). This revealed that treatments at both 5 ss and 10 ss resulted in a complete loss of *pea3* expression, showing that Fgf signalling was successfully inhibited (Raible and Brand, 2001; Figures 4.2.2.4F, H; Figure 4.2.2.5F). In DMSO treated controls, *pea3* expression is unaffected (Figures 4.2.2.4E, G, and 4.2.2.5E).

Fish treated with SU5402 at 5 ss or 10 ss, were labelled with either *drg11* or *isl1* to visualise the MTN cell bodies. Two genes were analysed to confirm that any difference between numbers in treated and controls were due to a specific effect on MTN formation, and not individual gene expression. In SU5402 treated fish there was an increase in MTN neurons in the dorsal anterior mesencephalon relative to MTN numbers in DMSO controls (Figure 4.2.2.4A-D, Figure 4.2.2.5A-D). Some MTN neurons were also located more posteriorly in SU5402 treated fish (Brackets, Figure 4.2.2.4B,D and Figure 4.2.2.5B, D). An increased number of nTPC cells in SU5402 (10 ss) treated fish, compared to DMSO controls, could also be seen.

MTN neurons and nTPC expressing *drg11* or *isl1* were counted and plotted onto graphs (MTN table and graph, Figure 4.2.2.2; nTPC table and graph, Figure 4.2.2.3; Raw data tables Appendices 1.1A, B and 1.2A; see materials and methods). The mean number of *drg11+* MTN neurons per fish (± S.E.M.) was 9.6 ± 0.52 for fish treated with SU5402 from 5 ss (n=10), significantly higher than the 6.5 ± 0.48 seen for DMSO controls (n=10) (*p< 0.002*; Student's t-test; Figure 2.2.2.2). The mean number of *drg11*+ MTN neurons per fish (± S.E.M.) was 10.8 ± for fish treated with SU5402 from 10 ss (n=10) significantly higher than the 4.80 seen for DMSO controls (n=10) (*p< 0.000010*; Students t-test; Figure 4.2.2.2). Similarly the mean number of *isl1*+ MTN neurons per fish (± S.E.M.) was 13.9 for fish treated with SU5402 from 10 ss, significantly higher than the 8.2 ± seen for DMSO controls (n=10) (*p< 0.0000001*; Student's t-test; Figure 4.2.2.2). This is similar to the results obtained by counting neurons expressing *drg11*, where an increase in MTN cell bodies

was seen, which confirms that the increase in numbers is not specific to *drg11* expressing MTN neurons.

The number of MTN neurons expressing *isl1* in both controls and treated fish were higher then the numbers of MTN neurons expressing *drg11*. Cell counts of nTPC expressing *drg11* or *isl1*, also revealed an increase in the number in the SU5402 treatments relative to the controls, but Students t-test revealed this was not statistically significant where $p<0.001$ (Figure 4.2.2.3).

Down-regulation of the FGF signalling pathway by SU5402 drug treatments at 5 ss and 10 ss, resulted in a significant increase in the numbers of MTN neurons in the midbrain, and a posterior expansion in their positions in the dorsal mesencephalon. These results suggest that Fgf signalling inhibits MTN formation.

Figure 4.2.2.2 – Inhibition of the Fgf signalling pathway with SU5402 causes a significant increase in the number of MTN cell bodies expressing *drg11* and *isl1*

(A) Table showing the mean numbers of MTN cell bodies counted per zebrafish in DMSO control compared to treated zebrafish (n = 10), and the p values showing the difference is statistically different (*0.001*). (B) Graph showing the differences in MTN numbers, and standard error of the mean, in DMSO controls (blue) compared to SU5402 treated animals (purple) labelled with *drg11*.

A)

Condition	Mean MTN number in DMSO controls	Mean MTN number in SU5402 treated	MTN T-Test p value (*0.001*)	Significance
SU5402 – treatment from 5 ss – *drg11*	6.5 (± 0.48)	9.6 (± 0.52)	0.002000	**
SU5402 – treatment from 10 ss – *drg11*	4.8 (± 0.25)	10.8 (± 0.51)	0.000010	***
SU5402 – treatment from 10 ss – *isl1*	8.2 (± 0.71)	13.9 (± 0.5)	0.0000001	***

B)

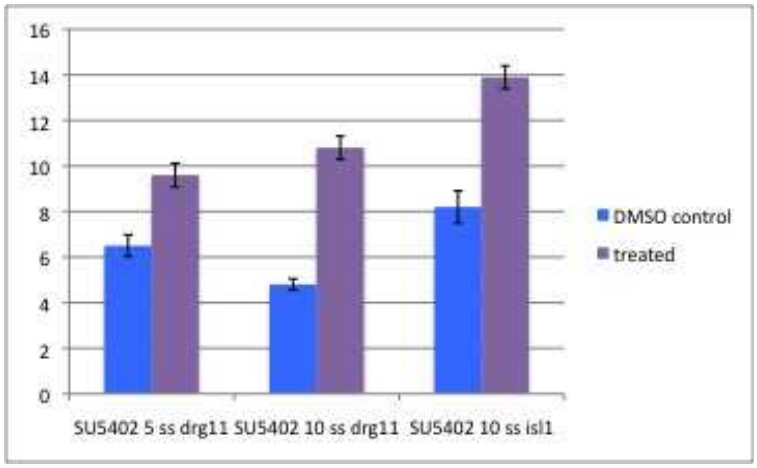

Figure 4.2.2.3 – Down-regulation of the Fgf signalling pathway with SU5402 does not cause a significant increase in the number of nTPC cell bodies expressing *drg11* and *isl1*.

(A) Table showing the mean number of nTPC cell bodies counted per zebrafish in DMSO control compared to treated zebrafish (n = 10), and the p values showing no significant difference (*0.001*). (B) Graph showing the differences in nTPC numbers, and standard error of the mean, in DMSO controls (blue) compared to SU5402 treated animals (purple).

(A)

Condition	mean nTPC number in wild type	mean nTPC number in mutants	nTPC T-Test p value (*0.001*)	Significance
SU5402 – treatment from 5 ss – *drg11*	8.4 (± 0.90)	8.3 (± 0.47)	0.922	none
SU5402 – treatment from 10 ss – *drg11*	11.6 (± 0.54)	13.3 (± 0.52)	0.075	none
SU5402 –treatment from 10 ss – *isl1*	10.9 (± 0.72)	14.1 (± 1.13)	0.04	*

(B)

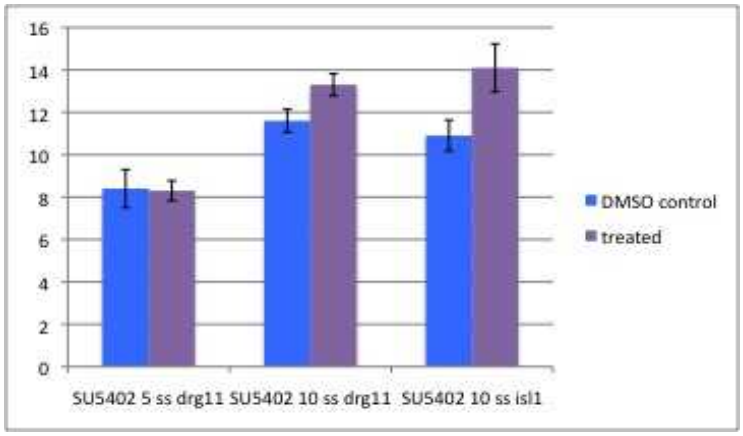

Figure 4.2.2.4 – Inhibition of the Fgf signalling pathway by SU5402 drug treatment results in an increase in the number of MTN neurons expressing *drg11*

(A) Lateral and (C) dorsal views of a DMSO control treated zebrafish from 5 ss to 24 hpf, displaying unaffected *drg11* expression in MTN in the dorsal anterior mesencephalon (bracket; black arrows), nucleus of the tract of the posterior commissure (nTPC) and trigeminal ganglia. (B) Lateral and (D) dorsal views of an SU5402 treated zebrafish from 5 ss to 24 hpf, revealing an increase in the number of MTN (black arrows) expressing *drg11* in the dorsal mesencephalon. Brackets indicate the posterior extension in the location of furthest MTN cell bodies from the nTPC. *drg11* expression is lost from the trigeminal ganglia (tg). (E) Lateral and (G) dorsal view of a DMSO treated zebrafish from 5 ss to 24 hpf displaying unaffected *pea3* expression, while (F) a lateral and (H) dorsal view of an SU5402 treated zebrafish reveals an absence of *pea3*, indicating a down-regulation of Fgf signalling. (I) Lateral and (K) dorsal views of DMSO control treated zebrafish from 10 ss to 24 hpf, displaying unaffected *drg11* expression (brackets; black arrows), similar to A and C. (J) Lateral and (L) dorsal views of an SU5402 treated zebrafish from 10 ss to 24 hpf, revealing an increase in MTN numbers expressing *drg11*, and a posterior extension in their location in the dorsal mesencephalon. mb, midbrain. mhb, midbrain hindbrain boundary. nTPC, nucleus of the tract of the posterior commissure. tg, trigeminal ganglion.

Scale bar = 100 μm

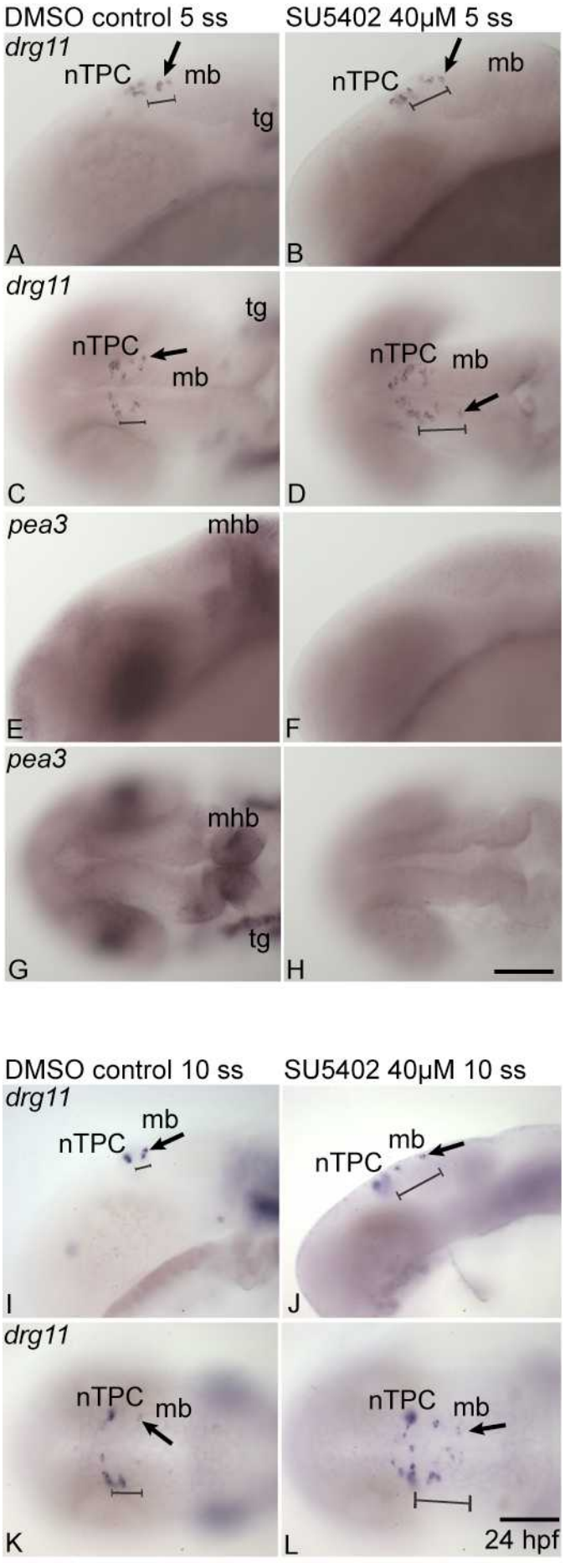
DMSO control 5 ss
SU5402 40μM 5 ss
drg11
nTPC
mb
tg
A
B
drg11
tg
nTPC
mb
C
nTPC
mb
D
pea3
mhb
E
F
pea3
mhb
tg
G
H
DMSO control 10 ss
SU5402 40μM 10 ss
drg11
mb
nTPC
I
mb
nTPC
J
drg11
nTPC
mb
K
nTPC
mb
L
24 hpf

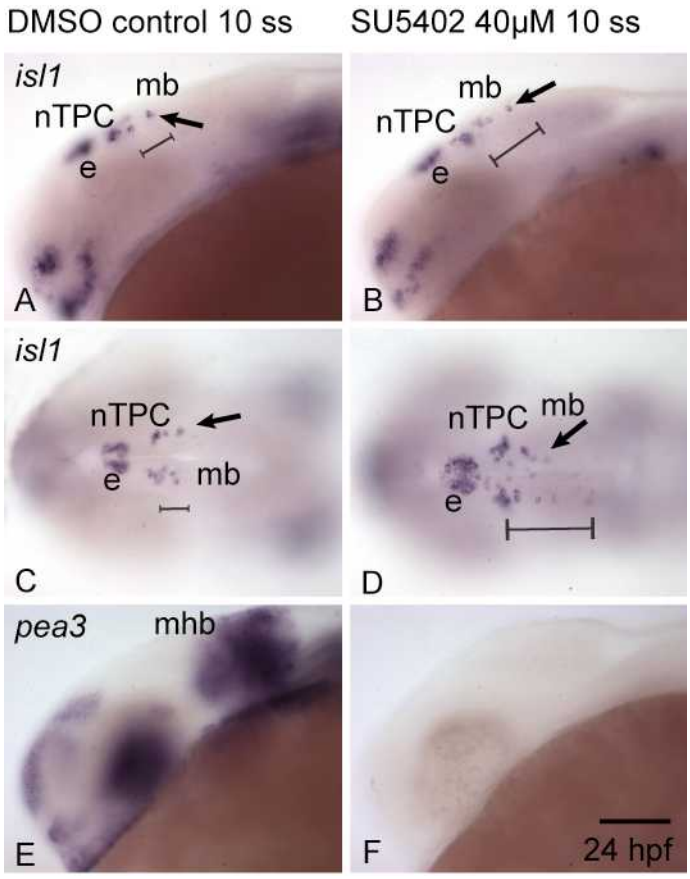

Figure 4.2.2.5 – Inhibition of the Fgf signalling pathway by SU5402 drug treatment results in an increase in the number of MTN neurons expressing *isl1*

(A) Lateral and (C) dorsal views of a DMSO control treated zebrafish from 10 ss to 24 hpf, displaying unaffected *isl1* expression in MTN in the dorsal anterior mesencephalon (bracket; black arrows), and nucleus of the tract of the posterior commissure (nTPC). (B) Lateral and (D) dorsal views of an SU5402 treated zebrafish from 5 ss to 24 hpf, revealing an increase in the number of MTN (black arrows) expressing *isl1* in the dorsal mesencephalon. Brackets indicate the posterior extension in the location of furthest MTN cell bodies from the nTPC. (E) Lateral view of a DMSO treated zebrafish from 5 ss to 24 hpf showing unaffected *pea3* expression, while (F) a lateral view of an SU5402 treated zebrafish reveals an absence of *pea3*, indicating a down-regulation of Fgf signalling. e, epiphysis. mb, midbrain. mhb, midbrain hindbrain boundary. nTPC, nucleus of the tract of the posterior commissure.

Scale bar = 100 µm

4.2.3 – Down-regulation of the Fgf signalling pathway in mutants causes an increase in MTN numbers

I have shown in the previous section, that when Fgf is down-regulated there is an increase in the number of MTN cell bodies. To determine whether the increase in MTN cell numbers is a general response to the down-regulation of Fgf signalling, or specific to the SU5402 drug treatment, mutant fish in which Fgf signalling is down-regulated were also analysed. Mutant fish lines *acerebellar* (*ace*) and *no isthmus* (*noi*) were used. *noi* is a *pax2.1* mutant (Reifers et al., 1998). *pax2.1* has a role in initiating and maintaining the isthmus and the identity of the mesencephalon (Wurst and Bally-Cuif, 2001). In *noi* mutants the inactivation of the *pax2.1* gene results in the failure of the midbrain and isthmus primordium to develop normally from gastrula stage onwards (Lun and Brand, 1998)**.** *ace* is an *fgf8* mutant (Brand et al., 1996). *fgf8* is required to maintain *pax2.1* expression and the midbrain hindbrain boundary (Reifers et al., 1998). While the isthmus initially forms in *ace* mutants, it is not maintained due to the absence of *fgf8*. In *ace* mutants the cerebellum fails to develop and the tectum is enlarged (Jaszai et al., 2003). Since *pax2.1* is initially expressed in *ace* mutants, the midbrain is able to develop normally, until the stage when *pax2.1* needs *fgf8* to maintain its expression. Therefore the *ace* midbrain phenotype is not as extreme as the *noi* midbrain phenotype.

ace and *noi* mutants, and wild type siblings were labelled with *drg11* and *isl1* at 24hpf (Figures 4.2.3.3 and 4.2.3.4). *ace* mutants can be phenotypically distinguished from wild type siblings by the absence of the cerebellum (Brand et al., 1996) (asterisk, Figure 4.2.3.3B and D). *noi* can be distinguished from siblings due to a small reduction in midbrain size and again a loss of the cerebellum (Brand et al., 1996; Figure 4.2.3.4B and D).

drg11 and *isl1* expression in wild type siblings were the same as previously described. In both *ace* and *noi* mutants an increase in the number of MTN cell bodies can be seen in the dorsal mesencephalon (Figures 4.2.3.3 and 4.2.3.4). Furthermore MTN from the nTPC are also located more posteriorly in the midbrain, compared to wild type siblings (black brackets, Figures 4.2.3.3B and D; 4.2.3.4B and D). The number of nTPC at the forebrain-midbrain boundary in mutants, was also increased compared to wild type siblings. These nTPC were clustered together and stop at the diencephalic boundary, unlike the MTN neurons that extended over a larger area than normal. Collectively these results are similar to the results when embryonic zebrafish

were treated with SU5402.

MTN and nTPC neurons expressing *drg11* or *isl1* were counted, and the mean numbers for each condition were plotted onto graphs (MTN table and graph, Figure 4.2.3.1; nTPC table and graph, Figure 4.2.3.2; Raw data tables Appendices 1.1C, D, and 1.2B, C; see materials and methods). Mean MTN numbers per fish were higher in *ace* and *noi* mutants (*ace*, *drg11* 23.6, *isl1* 19.2; *noi*, *drg11* 19.3, *isl1* 18.9) relative to MTN numbers per fish in wild type siblings (*ace*, *drg11* 10.5, *isl1* 8.3; *noi*, *drg11* 6.8, *isl1* 7.6), the same as the results from down-regulating Fgf signalling by SU5402 treatments. Students t-test revealed that the difference in MTN numbers in wild type siblings compared to mutants, was statistically significant for both *ace* (*drg11* $p = 0.000032$; *isl1* $p = 0.000003$) and *noi* (*drg11* $p = 0.0000001$; *isl1* $p = 0.0000001$) where $p < 0.001$ (Figure 4.2.3.1).

Quantification of MTN development reveals that MTN number is negatively regulated by Fgf signalling. Temporal abrogation of Fgf signalling from 10 ss results in an increase in MTN number and these are often ectopically located in the posterior midbrain. Likewise in *ace* and *noi* mutants, which show graded losses of Fgf signalling from the isthmus, more MTN are observed in ectopic locations of the midbrain. Both *ace* and *noi* show a much stronger MTN phenotype than SU5402 treated fish; there are many more MTN neurons in *ace* and *noi*, than in SU5402 treated fish (Figure 4.2.2.2 and Figure 4.2.3.1).

Analyses of MTN neuronal development following Fgf signalling down-regulation by SU5402 drug treatment, or in mutant fish, reveals an increase in MTN number, and a posterior expansion in their positions in the dorsal mesencephalon. This showed that the increase in MTN numbers when fish were treated with SU5402 to down-regulate Fgf signalling was not specific to the drug treatment. These results suggest further that Fgf signalling inhibits MTN formation.

Figure 4.2.3.1 – Down-regulation of the Fgf signalling pathway causes a significant increase in the number of MTN cell bodies expressing *drg11* and *isl1*

(A) Table showing the mean numbers of MTN cell bodies counted per zebrafish in wild type siblings compared to mutant zebrafish (n = 10), and the p values showing the difference is statistically different (*0.001*). (B) Graph showing the differences in MTN numbers, and standard error of the mean, in wild type siblings (blue) compared to *ace* mutants (purple). (C) Graph showing the differences in MTN numbers, and standard error of the mean, in wild type siblings (blue) compared to *noi* mutants (purple).

A)

Condition	Mean MTN number in wild type	Mean MTN number in mutants	MTN T-Test p value (*0.001*)	Significance
ace – drg11	6.5 (± 0.34)	13.4 (± 0.42)	0.000032	***
noi – drg11	6.8 (± 0.53)	19.3 (± 0.94)	0.0000001	***
ace – isl1	7.5 (± 0.54)	14 (± 0.49)	0.000003	***
noi – isl1	7.6 (± 0.4)	18.9 (± 0.57)	0.0000001	***

B)

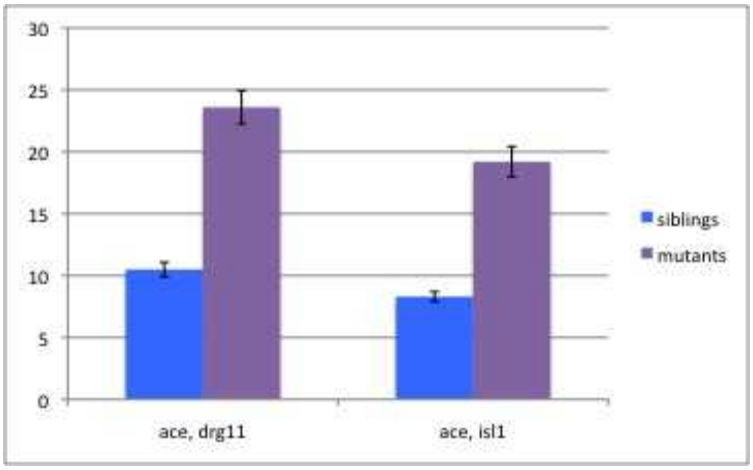

C)

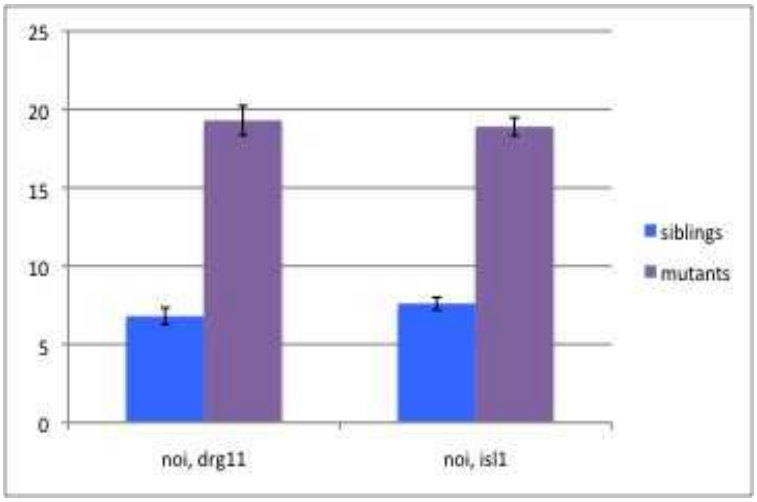

Figure 4.2.3.2 – Down-regulation of the Fgf signalling pathway does not cause a significant increase in the number of nTPC cell bodies expressing *drg11* and *isl1.*

(A) Table showing the mean number of nTPC cell bodies counted per zebrafish in wild type siblings compared to mutant zebrafish (n = 10), and the p values showing no significant difference (*0.001*). (B) Graph showing the differences in nTPC numbers, and standard error of the mean, in wild type siblings (blue) compared to mutant animals (purple).

(A)

Condition	Mean nTPC number in wild type	Mean nTPC number in mutants	nTPC T-Test p value (*0.001*)	Significance
ace – drg11	14.4 (± 0.83)	17.4 (± 0.92)	0.081	none
noi – drg11	8.8 (± 0.33)	11.9 (± 0.80)	0.01	**
ace – isl1	16.5 (± 0.92)	18.6 (± 0.65)	0.153	none
noi – isl1	11.6 (± 0.52)	12.3 (± 0.65)	0.398	none

(B)

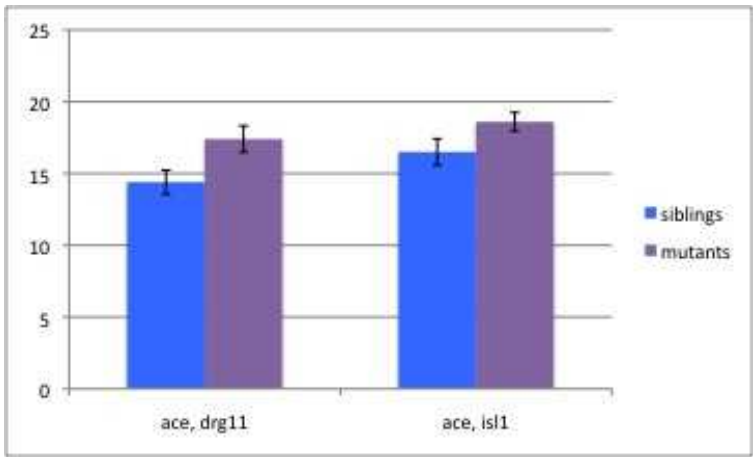

(C)

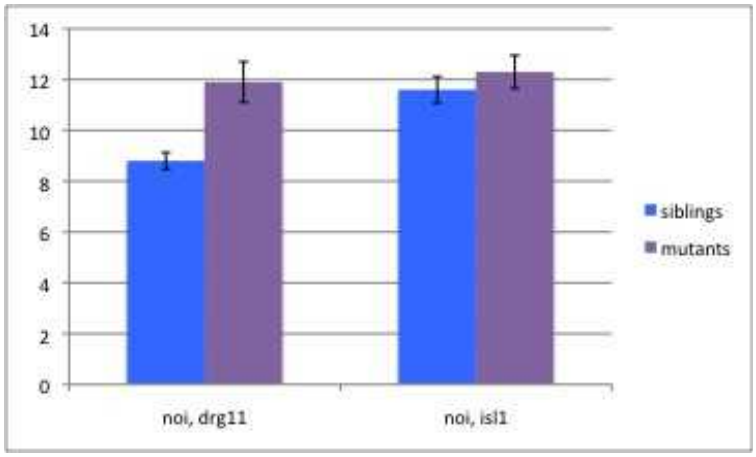

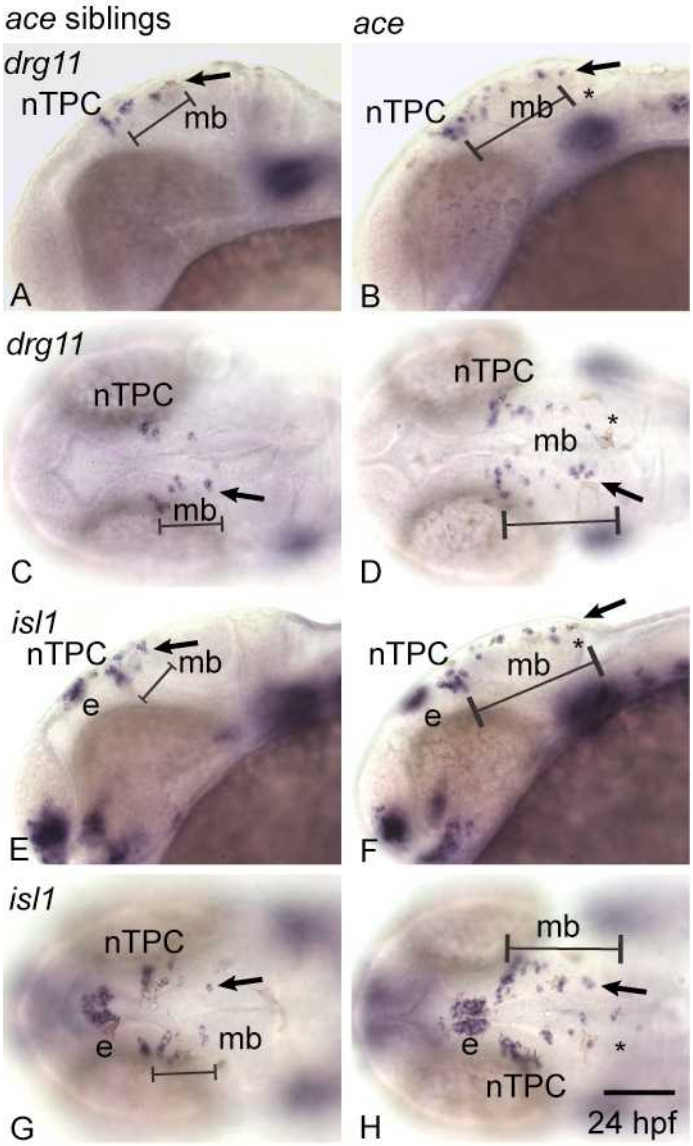

Figure 4.2.3.3 – Down-regulation of the Fgf signalling pathway in *ace* mutants causes an increase in the number of MTN neurons

Relative to WT animals (A, C, E, G), *ace* mutants (B, D, F, H) display more neurons expressing *drg11* (B, D) or *isl1* (F, H) in the mesencephalon. Brackets indicate the distance of furthest MTN neurons from the nucleus of the posterior commissure (nTPC). e, epiphysis. mb, midbrain. nTPC, nucleus of the tract of the posterior commissure.

Scale bar = 100 μm

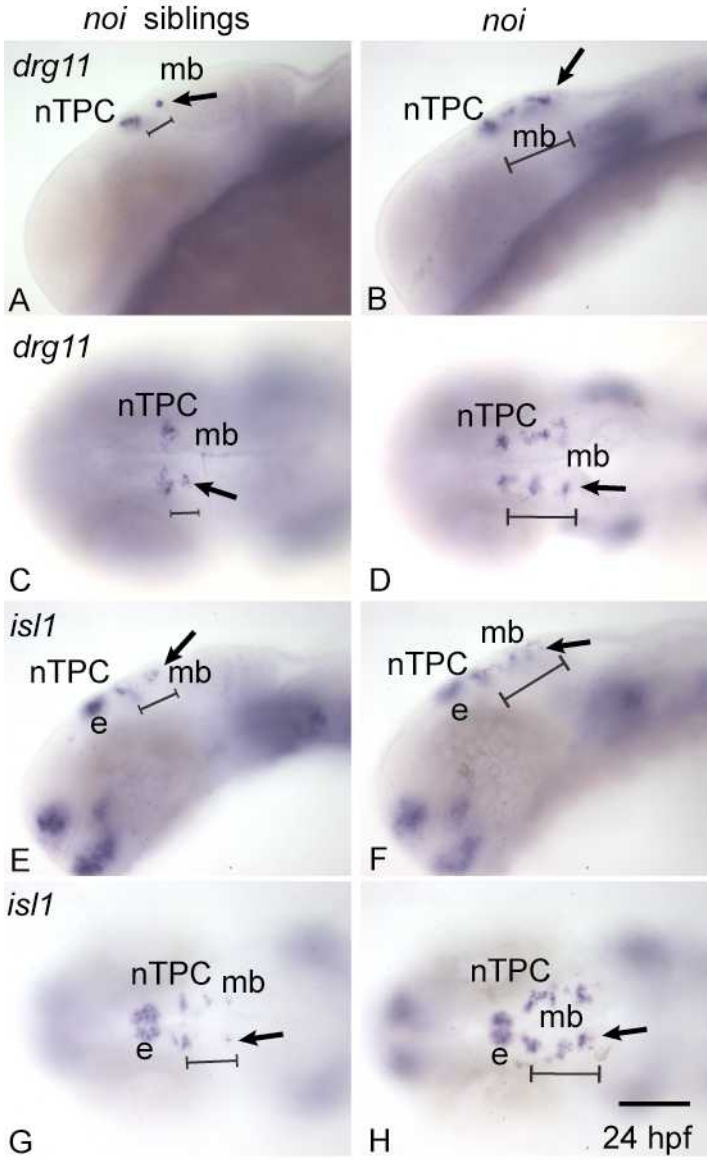

Figure 4.2.3.4 – Down-regulation of the Fgf signalling pathway in *noi* mutants causes an increase in the number of MTN neurons.

Relative to WT animals (A, C, E, G), noi mutants (B, D, F, H) display more neurons expressing drg11 (B, D) or isl1 (F, H) in the mesencephalon. Brackets indicate the distance of furthest MTN neurons from the nucleus of the tract of the posterior commissure (nTPC). e, epiphysis. mb, midbrain. nTPC, nucleus of the tract of the posterior commissure.

Scale bar = 100 μm

4.2.4 – Down-regulation of Fgf signalling by either treatment with SU5402 from 10 ss, or in *ace* and *noi* does not result in a change in the forebrain-midbrain fate

To ascertain if the forebrain midbrain boundary was posteriorly shifted when Fgf is down-regulated, expression of forebrain and midbrain markers was analysed. A change of cell fate from midbrain to forebrain could have caused the posterior expansion in the location of MTN neurons, and the increase in their numbers.

Forebrain and midbrain were labelled with *pax6* and *pax7* respectively (red) relative to MTN labelled by *drg11* (purple). In *ace* mutants, *pax6* expression in the forebrain is unchanged relative to wild type siblings (Figure 4.2.4.1A-D). However in *noi* mutants, while the dorsal *pax6* expression in the forebrain is also unchanged relative to wild type siblings, ventral *pax6* expression is extended into presumptive midbrain territory as previous studies have shown (Scholpp et al., 2003; Figure 4.2.4.2B). In *ace* and *noi*, the dorsal posterior border of the *pax6* expression appears to be in a similar region to that in the wild type zebrafish. (Figure 4.2.4.1A – D and 4.2.4.2A – D). In both mutant and wild type, nTPC neurons are located at the posterior boundary of *pax6* expression at the forebrain midbrain boundary (Figure 4.2.4.1A, B and Figure 4.2.4.2A, B). In *ace* and *noi*, MTN neurons are positioned in the midbrain region posterior to *pax6* expression.

pax7 expression in the midbrain in *ace* and animals treated by SU5402, was unchanged relative to wild type (Figure 4.2.4.1E – D; Figures 4.2.4.3A – D). In *noi* however, the area of *pax7* expression was reduced in the midbrain, revealing the loss of posterior midbrain, but the anterior boundary of expression was similar to its location in wild type (Figure 4.2.4.2E – H). MTN neurons are restricted to the region of *pax7* expression in the midbrain in *ace*, *noi* and animals treated by SU5402, similar to wild type.

These results reveal that there is not a posterior shift in the forebrain midbrain boundary.

Figure 4.2.4.1 – Down-regulation of the Fgf signalling pathway in *ace* mutants does not affect forebrain – midbrain boundary fate

(A) Lateral and (C) dorsal views of *ace* wild type siblings at 24 hpf, showing *drg11* (purple) expression in MTN cell bodies, in the dorsal mesencephalon, and the nucleus of the tract of the posterior commissure (nTPC). Expression of *pax6* (red) in the forebrain is also seen. (B) Lateral and (D) dorsal views of *ace* mutant zebrafish at 24 hpf, displaying an increase in the number of *drg11* expressing MTN cell bodies in the dorsal mesencephalon. The expression of forebrain marker *pax6* is unchanged relative to the *ace* siblings in A and C. (E) Lateral and (G) dorsal views of *ace* wild type siblings at 24 hpf, showing *drg11* (purple) expression in MTN cell bodies of the dorsal mesencephalon and the nTPC. Expression of *pax7* (red) in the midbrain is also shown. (F) Lateral and (H) dorsal views of *ace* mutant zebrafish at 24 hpf, displaying an increase in the number of *drg11* expressing MTN cell bodies in the dorsal mesencephalon. The expression of midbrain marker *pax7* is unchanged relative to the DMSO control in A and C. dd, dorsal diencephalon. nTPC, nucleus of the tract of the posterior commissure. t, tectum. tel, telencephalon.

Scale bar = 100 μm

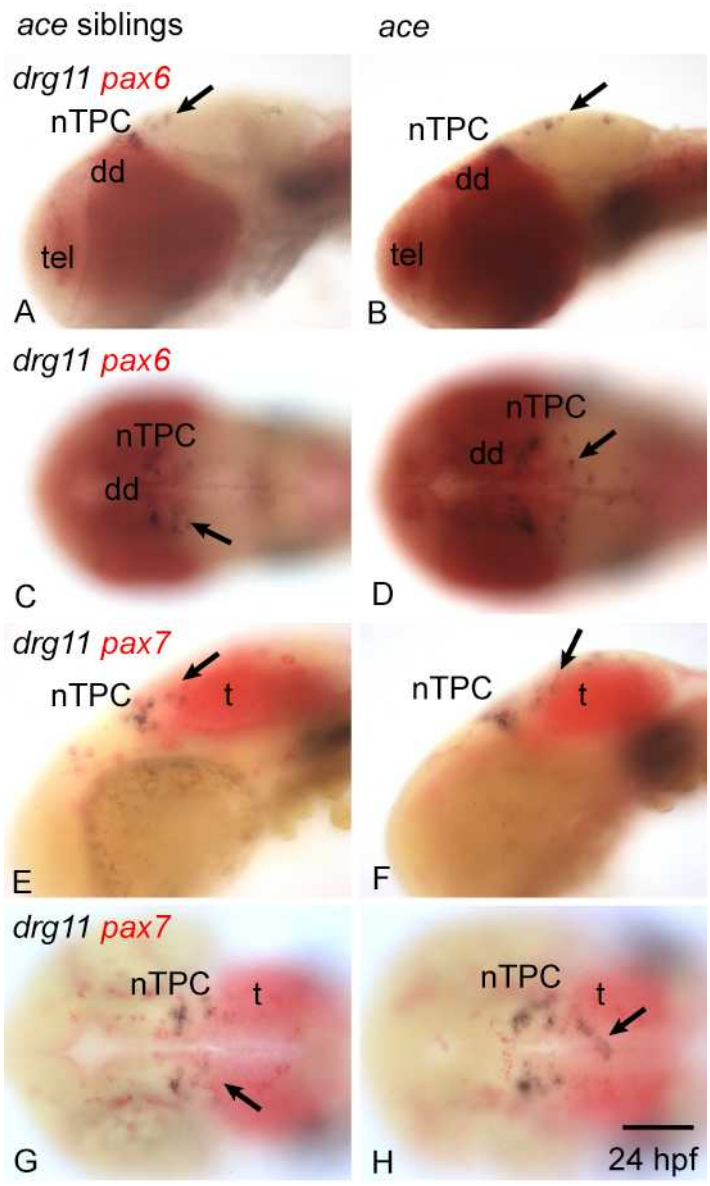
ace siblings
ace
drg11 pax6
nTPC
dd
tel
A
B
drg11 pax6
nTPC
dd
C
D
drg11 pax7
nTPC
t
E
F
drg11 pax7
nTPC
t
G
H
24 hpf

Figure 4.2.4.2 – Down-regulation of the Fgf signalling pathway in *noi* mutants causes a reduction in midbrain size

(A) Lateral and (C) dorsal views of *noi* wild type siblings at 24 hpf, showing *drg11* (purple) expression in MTN cell bodies of the dorsal mesencephalon and the nucleus of the tract of the posterior commissure (nTPC). Expression of *pax6* (red) in the forebrain is also seen. (B) Lateral and (D) dorsal views of *noi* mutant zebrafish at 24 hpf, displaying an increase in the number of *drg11* expressing MTN cell bodies in the dorsal mesencephalon. The expression of forebrain marker *pax6* is expanded ventrally into presumptive midbrain territory (asterisk). (E) Lateral and (G) dorsal views of *noi* wild type siblings at 24 hpf, showing *drg11* (purple) expression in MTN cell bodies, of the dorsal mesencephalon, and the nTPC. Expression of *pax7* (red) in the midbrain is also shown. (F) Lateral and (H) dorsal views of *noi* mutant zebrafish at 24 hpf, displaying an increase in the number of *drg11* expressing MTN cell bodies in the dorsal mesencephalon. The region of *pax7* expression is reduced in the midbrain. dd, dorsal diencephalon. nTPC, nucleus of the tract of the posterior commissure. t, tectum. tel, telencephalon.

Scale bar = 100 μm

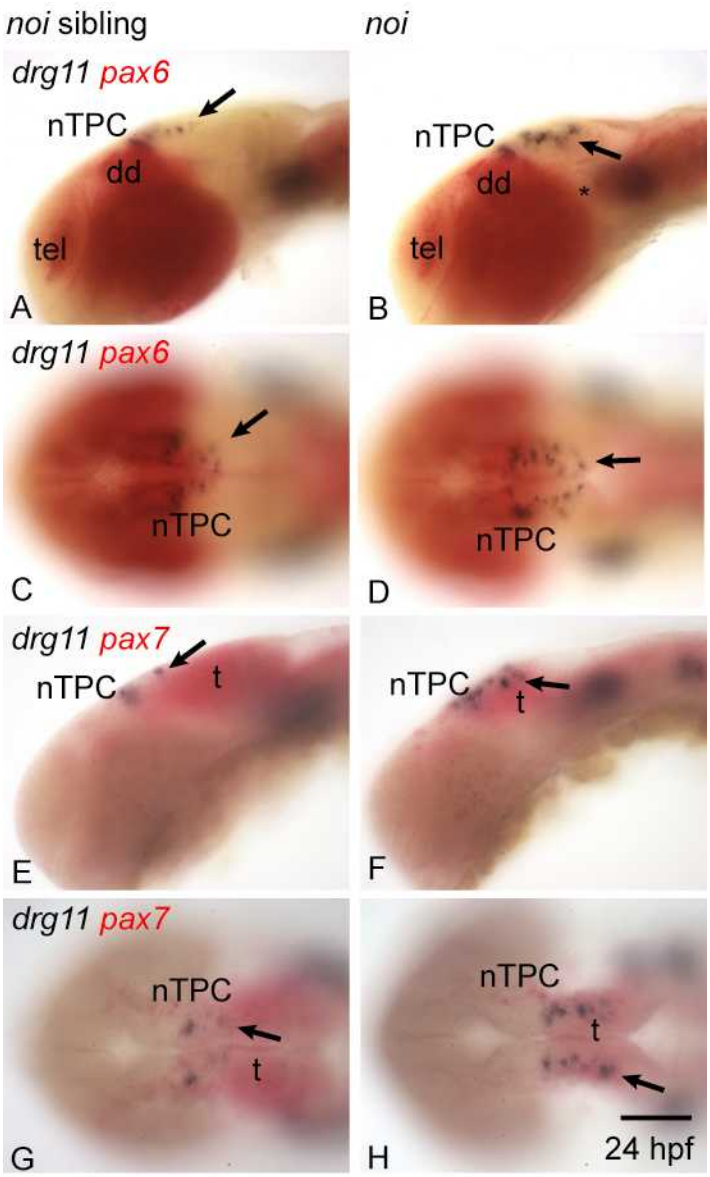
noi sibling
noi
drg11 pax6
nTPC
dd
tel
A
drg11 pax6
nTPC
dd
*
tel
B
drg11 pax6
nTPC
C
drg11 pax6
nTPC
D
drg11 pax7
nTPC
t
E
nTPC
t
F
drg11 pax7
nTPC
t
G
nTPC
t
24 hpf
H

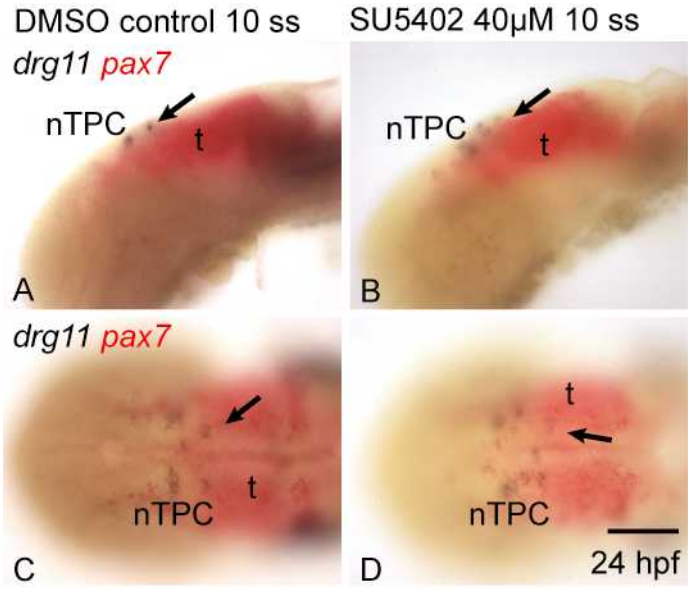

Figure 4.2.4.3 – Inhibition of the Fgf signalling pathway by SU5402 drug treatment from 5 ss to 24 hpf does not affect forebrain – midbrain boundary fate

(A) Lateral and (C) dorsal views of DMSO control treated zebrafish from 10 ss to 24 hpf, showing *drg11* (purple) expression in MTN cell bodies, in the dorsal mesencephalon, and the nucleus of the posterior commissure (nTPC). The expression of *pax7* (red) in the midbrain is also shown. (B) Lateral and (D) dorsal views of SU5402 treated zebrafish from 5 ss to 24 hpf, displaying an increase in the number of *drg11* expressing MTN cell bodies in the dorsal mesencephalon. The expression of midbrain marker *pax7* is unchanged relative to the DMSO control in A and C. nTPC, nucleus of the tract of the posterior commissure. t, tectum.

Scale bar = 100 µm

4.2.5 – Axonal tracts in SU5402 treated fish and controls

To assess if axons grow from all the MTN cells bodies that form in SU5402 treated fish, including ectopic MTN neurons in the dorsal posterior mesencephalon, acetylated tubulin was used to label axons.

Axons could be seen extending from some MTN cell bodies in the midbrain in SU5402 treated fish (Figure 4.2.5); Only a few MTN neurons appeared to have axonal projections (arrowheads, Figure 4.2.5D), these were more anterior in their location. These axons appeared to follow a similar path to those in DMSO controls (Wilson et al., 1990; Chitnus and Kuwada, 1990). The axons followed a descending path in the periphery, towards the medial longitudinal fasciculus, adjacent to the TPC, as I have previously described in chapter 3. No axons were labelled by acetylated tubulin in the more posterior located MTN. This may be because of temporal differences in development; the axons of posterior MTN neurons are observed to develop later than anterior MTN neurons in the *Tg(huC:eGFP)* transgenic line (Sub-section 3.2.14).

Figure 4.2.5 – Axons can be seen growing from a few anterior MTN cell bodies in the dorsal mesencephalon in SU5402 treated zebrafish

Dorsal views of a DMSO control zebrafish treated from 10 ss to 24 hpf showing (A) Isl1 expression, (B) acetylated tubulin (a-tub) labelling, and (C) a merge of A and B. MTN cell bodies are labelled in the dorsal anterior mesencephalon by Isl1 (white arrow). Axons can be seen projecting from MTN cell bodies in a posterior direction and towards the periphery (white arrowhead). Dorsal views of an SU5402 treated zebrafish from 10 ss to 24 hpf showing (D) Isl1 expression, (E) acetylated tubulin labelling, and (F) a merge of D and E. More MTN cell bodies expressing Isl1 are present in the dorsal mesencephalon than in wild type (white arrows). Axons can be seen projecting from some anterior MTN cell bodies in a comparable direction and orientation to the control animals. e, epiphysis. nTPC, nucleus of the tract of the posterior commissure (nTPC).
Scale bar = 50 μm

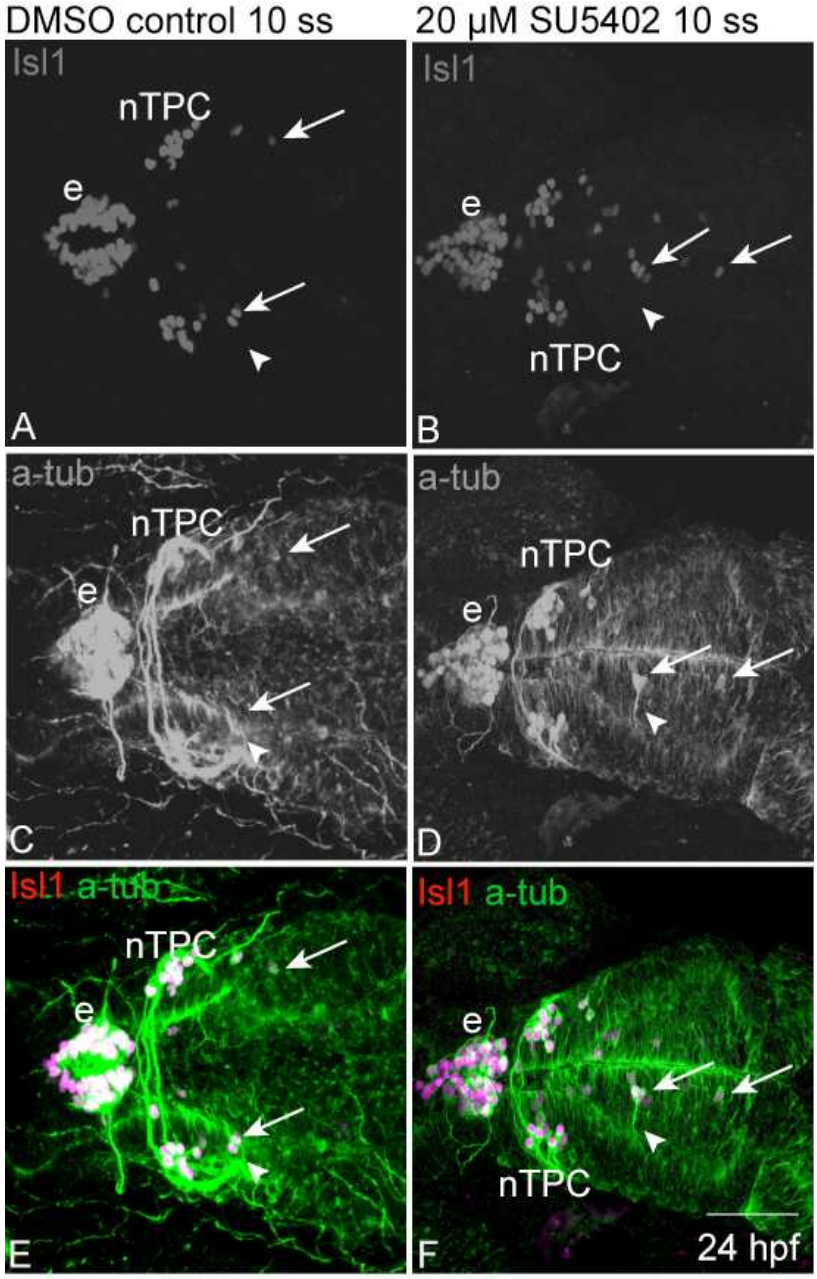
DMSO control 10 ss
20 μM SU5402 10 ss
Isl1
nTPC
e
A
Isl1
e
nTPC
B
a-tub
nTPC
e
C
a-tub
nTPC
e
D
Isl1 a-tub
nTPC
e
E
Isl1 a-tub
e
nTPC
24 hpf
F

4.2.6 – Up-regulation of the Wnt signalling pathway results in an increase in the number of MTN cell bodies

Wnt signalling is critical for maintaining the isthmus and midbrain patterning. To assess the role of Wnt during MTN development, BIO, an ATP competitive inhibitor of GSK3β, was used to up-regulate Wnt. GSK3β is an important molecule that is part of the complex which targets β-catenin for ubiquitination (Heisenberg et al., 2001). BIO prevents this complex from forming, enabling β-catenin to enter the nucleus and cause the translation of Wnt target genes. Therefore BIO treatment results in an up-regulation of β-catenin activated genes. This results in a typical Wnt over-expression phenotype where the telencephalon is reduced in size, and eyes are smaller or absent (Heisenberg, 1996; Kim et al., 2000; Figure 4.2.6.1).

Figure 4.2.6.1 – Schematic of the Wnt signalling pathway

Diagrammatic representation of the Wnt signalling pathway, showing the binding of a Wnt ligand to its frizzled receptor which leads to the activation of the GSK3β complex preventing the degradation of β-catenin, enabling it to enter the nucleus and cause the translation of Wnt target genes. Taken from Alberts et al., 2002.

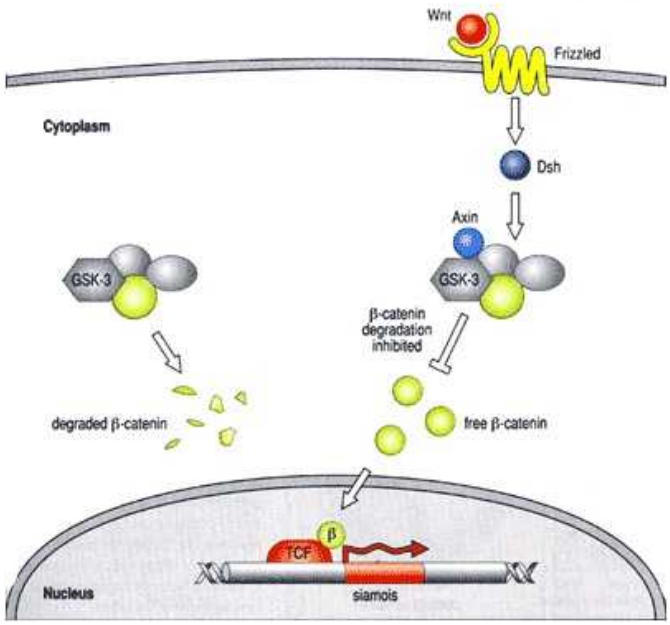

Fish were treated with 4μM BIO at 5 ss and 10 ss until 24 hpf. Treatments were carried out at these two stages due to the same reasoning described in the previous section, where fish were treated with SU5402, as the border between diencephalon and mesencephalon is established by 10 ss. Treatments in zebrafish from 5 ss proved to be toxic as necrosis occurred in the head and animals died by 24 hpf. Fish treated at 10 ss did not cause neurosis, but showed an increase in the size of the diencephalon (asterisk, Figure 4.2.6.4B and D).

BIO treated animals were labelled with *axin2*, a reporter gene of Wnt signalling. *axin2* is a negative regulator of the Wnt signalling pathway (Jho et al., 2002). When Wnt is up-regulated, so *axin2* expression is increased. In the 4μM BIO treatments there was an increase in *axin2* expression (Figure 4.2.6.4F), showing successful up-regulation of Wnt signalling relative to DMSO controls (Figure 4.2.6.4E).

In the DMSO controls labelled with *drg11* or *isl1*, normal expression was seen (Figure 4.2.6.4A and C; Figure 4.2.6.5A and C). When fish were treated with BIO at 10 ss, there appeared to be an increase in the number of MTN, and a slight posterior expansion in their location (brackets, Figure 4.2.6.4B and D; Figure 4.2.6.5B and D). This posterior spread from the boundary of the diencephalon and mesencephalon, was not as obvious as that which occurred in fish where Fgf was down-regulated. The numbers of nTPC in treated animals were similar to the numbers in DMSO controls.

MTN and nTPC neurons expressing *drg11* and *isl1* were counted, and the mean numbers for each condition were plotted onto graphs (MTN table and graph, Figure 4.2.6.2; nTPC table and graph, Figure 4.2.6.3; Raw data tables Appendices 2.1A and 2.2A; see materials and methods). The mean number of *drg11+* MTN neurons per fish (± S.E.M.) was 15.7 ± for fish treated with BIO from 10 ss (n=10), significantly higher than the 5.8 ± seen for DMSO controls (n=10) ($p < 0.0000010$; Student's t-test; Graph 4.2.6). Similarly the mean number of *isl1+* MTN neurons per fish (± S.E.M.) was 13.3 ± for fish treated with BIO from 10 ss (n=10) significantly higher than the 6.9 ± seen for DMSO controls (n=10) ($p< 0.0000110$; Student's t-test; Figure 4.2.6.2).

Alsterpaullone was also tested for its ability to up-regulate Wnt signalling in zebrafish. Alsterpaullone is an ATP competitive inhibitor of gsk3β, similar to BIO. It inhibits tau phosphorylation at sites that are normally phosphorylated by gsk3β (Leost et al., 2000). Solubility of Alsterpaullone in water made applying it to embryos

problematic. Injections into the yolk failed to provide convincing phenocopies of Wnt over expression phenotypes. Due to these problems, BIO treatments proved to be better at pharmacologically up-regulating Wnt.

Up-regulation of the Wnt signalling pathway by BIO drug treatments at 10 ss resulted in an increase in the numbers of MTN neurons in the dorsal anterior mesencephalon. This indicates that MTN development is positively regulated by Wnt signalling.

Figure 4.2.6.2 – Up-regulation of the Wnt signalling pathway using BIO causes an increase in the number of MTN cell bodies expressing *drg11* and *isl1*

(A) Table showing the mean numbers of MTN cell bodies counted per zebrafish in DMSO controls compared to BIO treated zebrafish (n = 10), and the p values showing the difference is statistically different (*0.001*). (B) Graph showing the differences in MTN numbers, and standard error of the mean, in DMSO controls (blue) compared to BIO treated animals (purple).

A)

Condition	Mean MTN number in wild type	Mean MTN number in mutants	MTN T-Test p value (*0.001*)	Significance
BIO 4µM – *drg11*	5.8 (± 0.51)	15.7 (± 0.78)	0.000001	***
BIO 4µM – *isl1*	6.9 (+/- 0.43)	13.3 (+/- 0.7)	0.000011	***

B)

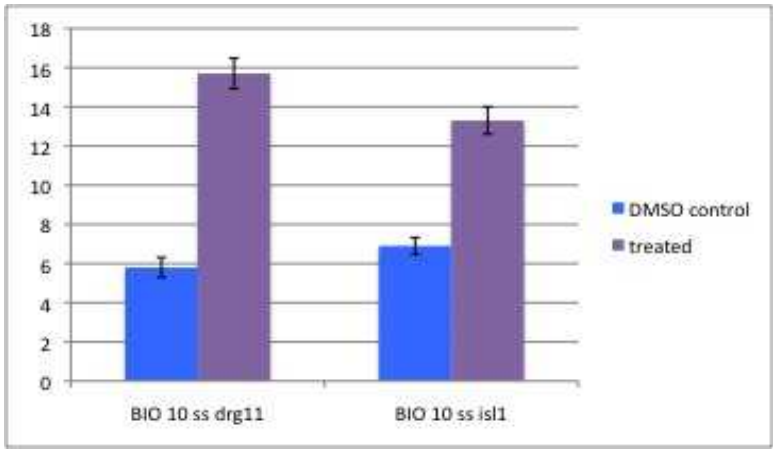

Figure 4.2.6.3 – Up-regulation of the Wnt signalling pathway using BIO does not cause a significant increase in the number of nTPC cell bodies expressing *drg11* and *isl1*.

(A) Table showing the mean number of nTPC cell bodies counted per zebrafish in DMSO control compared to BIO treated zebrafish (n = 10), and the p values showing no significant difference (*0.001*). (B) Graph showing the differences in nTPC numbers, and standard error of the mean, in DMSO controls (blue) compared to mutants or BIO treated animals (purple).

(A)

Condition	Mean MTN number in wild type	Mean MTN number in mutants	MTN T-Test p value (*0.001*)	Significance
BIO 4µM – *drg11*	12.7 (± 0.45)	10.7 (± 1.15)	0.1226	none
BIO 4µM – *isl1*	15.5 (± 0.83)	14.2 (± 0.89)	0.44	none

(B)

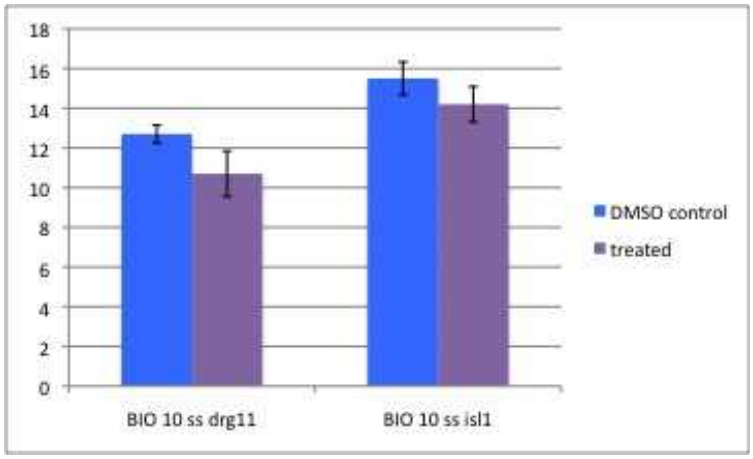

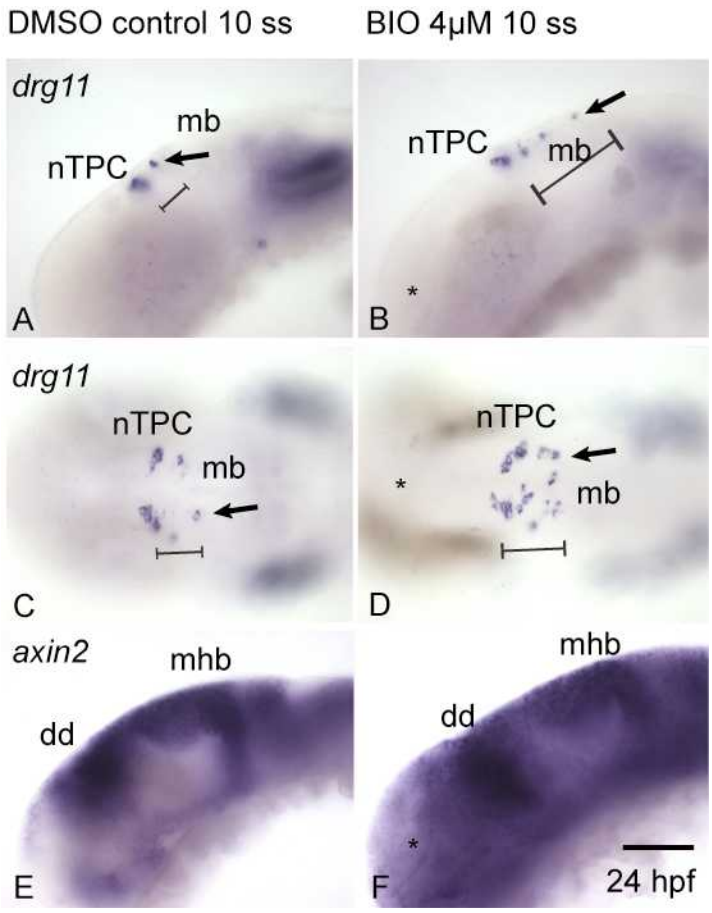

Figure 4.2.6.4 – Activating canonical Wnt signalling by application of BIO at 10 ss results in an increase in the number of MTN neurons expressing *drg11*

(A) Lateral and (C) dorsal views of a DMSO control treated zebrafish from 10 ss to 24 hpf, showing *drg11* expression in MTN in the dorsal anterior mesencephalon (bracket; black arrows), nucleus of the tract of the posterior commissure (nTPC) and trigeminal ganglia. (B) Lateral and (D) dorsal views of a BIO treated zebrafish from 5 ss to 24 hpf, revealing ectopic MTNs (black arrows) expressing *drg11* in the dorsal mesencephalon. Brackets indicate the posterior extension in the location of furthest MTN cell bodies from the nTPC. *drg11* expression is lost from the trigeminal ganglia (tg). Asterisk indicates the enlarged telencephalon. (E) Lateral view of a DMSO treated zebrafish from 10 ss to 24 hpf showing *axin2* expression, while (F) a lateral view of a BIO treated zebrafish shows an increase in *axin2* expression, indicating an up-regulation of Wnt signalling. dd, dorsal diencephalon. mb, midbrain. mhb, midbrain-hindbrain boundary. Scale bar = 100 µm

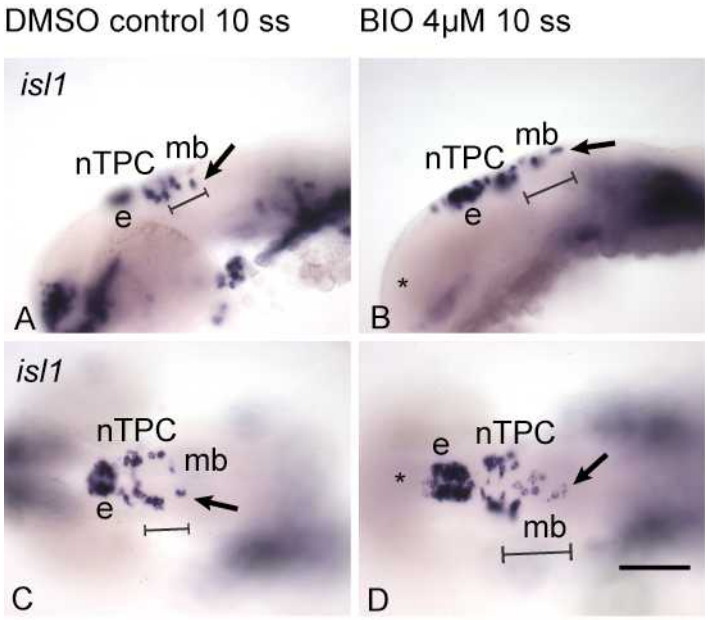

Figure 4.2.6.5 – Activating canonical Wnt signalling by application of BIO at 10 ss results in an increase in the number of MTN neurons expressing *isl1*

(A) Lateral and (C) dorsal views of a DMSO control treated zebrafish from 10 ss to 24 hpf, showing *isl1* expression in MTN in the dorsal anterior mesencephalon (bracket; black arrows), nucleus of the tract of the posterior commissure (nTPC) and trigeminal ganglia. (B) Lateral and (D) dorsal views of a BIO treated zebrafish from 5 ss to 24 hpf, revealing an increase in the number of MTN (black arrows) expressing *isl1* in the dorsal mesencephalon. Brackets indicate the posterior spread of MTN neuronal cell bodies from the boundary of the mesencephalon and diencephalon. Asterisk indicates the enlarged telencephalon. e, epiphysis. mb, midbrain.

Scale bar = 100 μm

4.2.7 – Up-regulation of Wnt signalling in *axin1* mutant *masterblind* also results in an increase in MTN numbers

To show that inhibition of GSK-3β by BIO treatments were not affecting signalling pathways other than Wnt, the development of MTN was analysed in *masterblind* (*mbl*) mutants. *mbl* mutants have a mutation in the gsk3β binding domain of the scaffolding protein *axin1* (Heisenberg et al., 2001). This mutation prevents the gsk3β destruction complex from forming so β-catenin cannot be targeted for degradation, and Wnt is up-regulated.

mbl mutants have a more extreme phenotype relative to embryos treated with BIO at 10 ss, because the eye completely fails to develop and the epiphysis in the diencephalon expands anteriorly (Van De Water et al., 2001; Masai, 1997). Similar to BIO treated embryos the telencephalon is reduced or absent (Heisenberg et al., 1996).

mbl mutants were easily distinguished from their wild type siblings by the loss of eye phenotype. There is also an increase in the size of the forebrain at the expense of the eyes. *mbl* mutants and siblings were labelled with *drg11* or *isl1*. *drg11* and *isl1* expression in siblings were similar to wild type. In the *mbl* mutants an increase in MTN and nTPC numbers was seen, with a slight posterior expansion in the location of MTN neurons (Figure 4.2.7.3B and D). The epiphysis also appeared to be enlarged and was no longer located centrally along the dorsal diencephalon, a phenotype characteristic of Wnt up-regulation (Masai et al., 1997; Heisenberg et al., 1996) (Figure 4.2.7.3H).

MTN and nTPC neurons expressing *drg11* or *isl1* were counted, and the mean numbers for each condition were plotted onto graphs (MTN graph and table, Figure 4.2.7.1; nTPC graph and table, Figure 4.2.7.2; Raw data tables Appendices 2.1B and 2.2B; see materials and methods). The mean number of *drg11+* MTN neurons per fish (± S.E.M.) was 12.1 ± for *mbl* mutant fish (n=10), significantly higher than the 7.9 ± seen for *mbl* siblings (n=10) ($p < 0.001212$; Student's t-test; Figure 4.2.7.1). Similarly the mean number of *isl1*+ MTN neurons per fish (± S.E.M.) was 11.3 ± for *mbl* mutant fish (n=10) significantly higher than the 7.8 ± seen for *mbl* siblings (n=10) ($p< 0.000088$; Student's t-test; Figure 4.2.7.1).

Analyses of MTN development following Wnt up-regulation by drug treatment or in mutant fish reveals that MTN number is positively regulated by Wnt signalling. However, an increase in the number of nTPC in *mbl* mutants and the change

in location of epiphysal neurons, implies that Wnt signalling regulates the development of dorsal neurons in general.

Figure 4.2.7.1 – Up-regulation of the Wnt signalling pathway causes an increase in the number of MTN cell bodies expressing *drg11* and *isl1*

(A) Table showing the mean numbers of MTN cell bodies counted per zebrafish in wild type siblings compared to mutant zebrafish (n = 10), and the p values showing the difference is statistically different (*0.001*). (B) Graph showing the differences in MTN numbers, and standard error of the mean, in wild type (blue) compared to mutants (purple).

A)

Condition	Mean MTN number in wild type	Mean MTN number in mutants	MTN T-Test p value (*0.001*)	Significance
mbl – drg11	7.9 (± 0.43)	12.1 (± 0.74)	0.001212	**
mbl – isl1	7.8 (+/- 0.47)	11.3 (+/- 0.45)	0.000088	***

B)

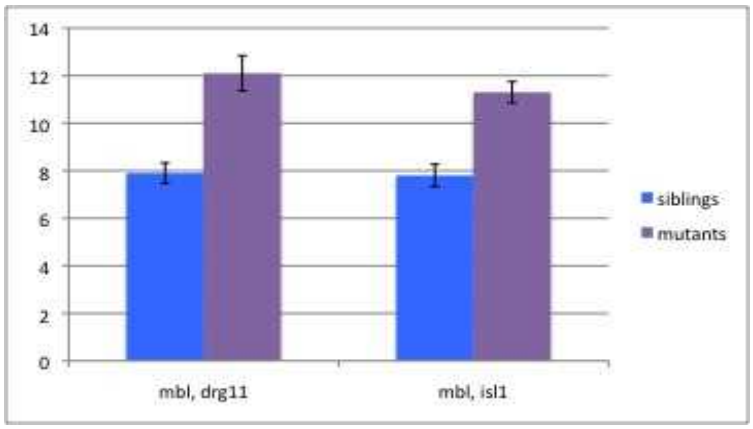

Figure – 4.2.7.2 – Up-regulation of the Wnt signalling pathway does not cause a significant increase in the number of nTPC cell bodies expressing *drg11* and *isl1.*

(A) Table showing the mean number of MTN cell bodies counted per zebrafish in wild type siblings compared to *mbl* zebrafish (n = 10), and the p values showing no significant difference (*0.001*). (B) Graph showing the differences in nTPC numbers, and standard error of the mean, in wild type siblings (blue) compared to *mbl* mutants (purple).

(A)

Condition	Mean MTN number in wild type	Mean MTN number in mutants	MTN T-Test p value (*0.001*)	Significance
mbl – drg11	14.8 (± 0.42)	20.7 (± 0.79)	0.004	**
mbl – isl1	14.5 (± 0.83)	17.1 (± 0.48)	0.02	**

(B)

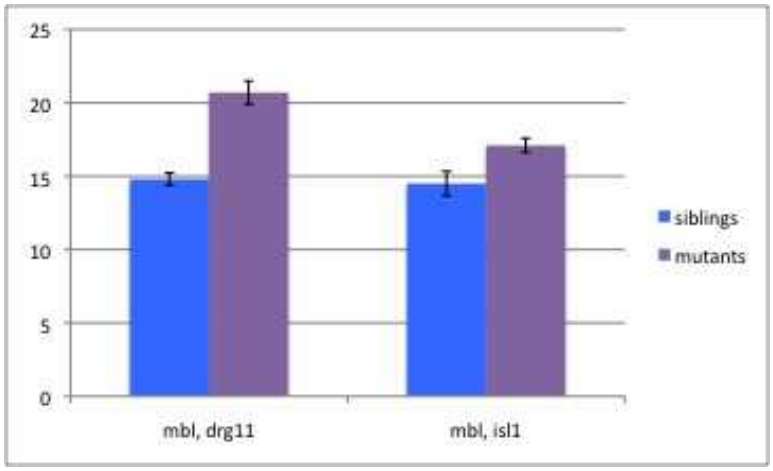

Figure 4.2.7.3 – Up-regulation of the Wnt signalling pathway in *mbl* mutants causes an increase in the number of MTN neurons

(A) Lateral and (C) dorsal views of WT at 24 hpf, showing *drg11* expression in MTN in the dorsal anterior mesencephalon (bracket; black arrows), nucleus of the posterior commissure (nTPC) and trigeminal ganglia. (B) Lateral and (D) dorsal views of *mbl* at 24 hpf, revealing an increase in the number of MTN (black arrows) expressing *drg11* in the dorsal mesencephalon. Brackets indicate the posterior extension in the location of furthest MTN cell bodies from the nTPC. (E) Lateral and (G) dorsal view of WT at 24 hpf, showing *isl1* expression in MTN in the dorsal anterior mesencephalon, nTPC and trigeminal ganglia. (F) Lateral and (H) dorsal view of *mbl* at 24 hpf, revealing an increase in the number of MTN (black arrows) expressing *isl1* in the dorsal mesencephalon. Brackets indicate the posterior extension in the location of furthest MTN cell bodies from the nTPC. e, epiphysis. mb, midbrain. Scale bar = 100 μm

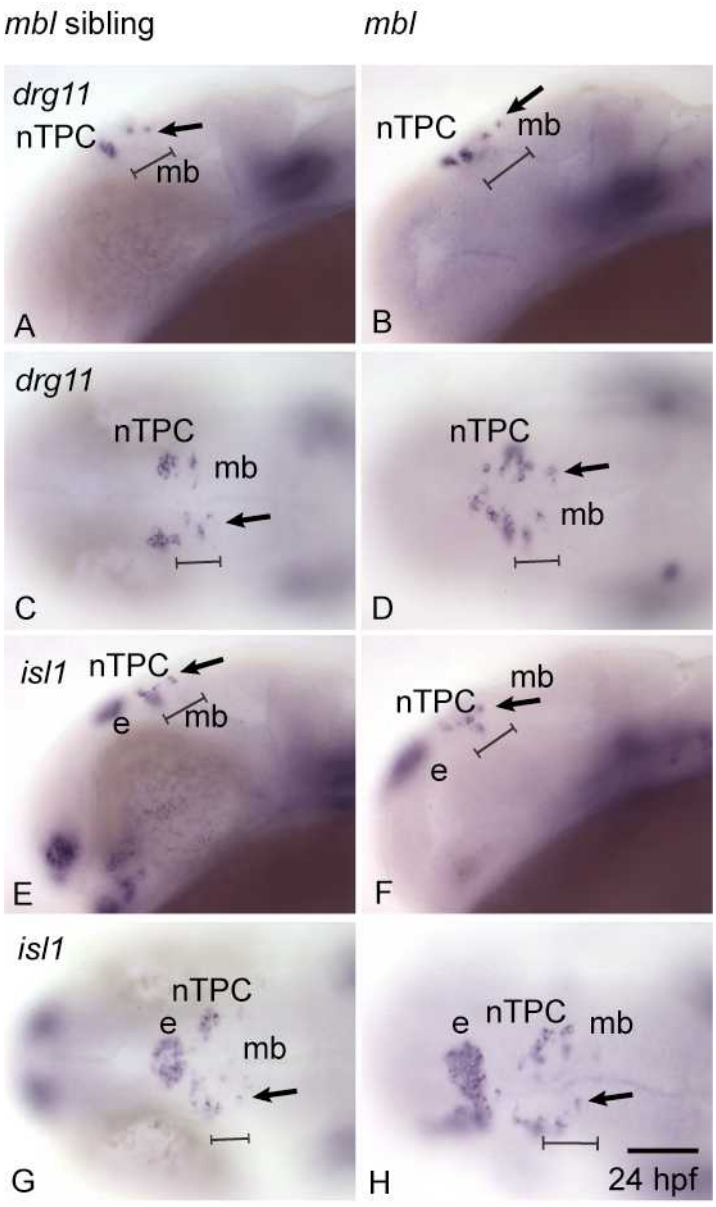
mbl sibling
mbl
drg11
nTPC
mb
A
nTPC
mb
B
drg11
nTPC
mb
C
nTPC
mb
D
isl1
nTPC
e
mb
E
mb
nTPC
e
F
isl1
nTPC
e
mb
G
e
nTPC
mb
H
24 hpf

4.2.8 – Up-regulation of Wnt signalling results in an increase in the size of the forebrain, but does not affect the position of the midbrain boundary

Wnt is required for normal brain development, and in particular it plays an important role in forebrain development. Up-regulation of Wnt signalling can result in an increase in diencephalic fate at the expense of the eyes (Heisenberg et al., 2001). An increase in forebrain may also result in a loss of anterior midbrain and therefore a change in fate and position of forebrain/midbrain boundary (Kim et al., 2000). Alternatively the midbrain may also have increased in size, as Wnt signalling acts as a proliferation factor (Van De Water et al., 2001). Such changes could results in a general proliferation of all cell types, rather then the up-regulation of wnt signalling itself directly affecting MTN specification.

To determine whether there was a change in identity of midbrain relative to forebrain following up-regulation of Wnt, midbrain was labelled with *pax7* (red). MTN was labelled by molecular marker *drg11* (purple). *pax7* expression in the midbrain is unchanged in BIO treated animals relative to control animals, similar to previous published data (Heisenberg et al., 2001; Figure 4.2.8). This implies that an increase in MTN number does not result from an expansion of the forebrain.

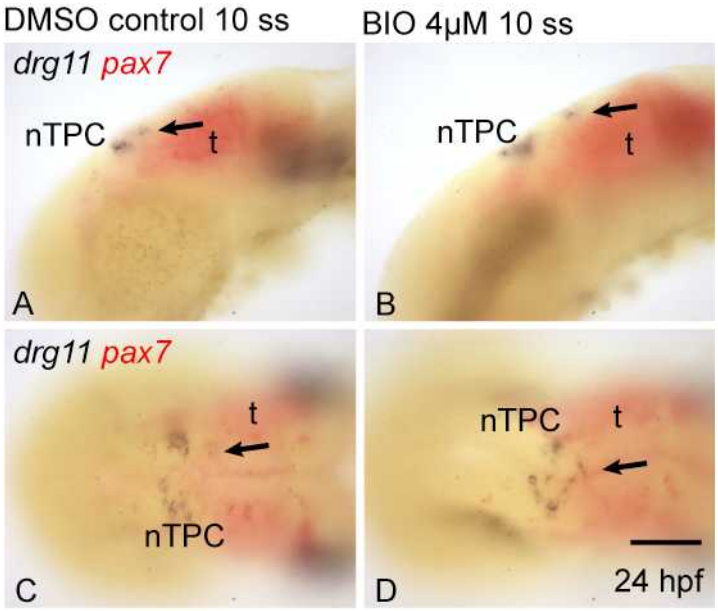

Figure 4.2.8 – Up-regulation of the Wnt signalling pathway in BIO treatments does not affect forebrain – midbrain boundary fate

(A) Lateral and (C) dorsal views of WT at 24 hpf, showing *drg11* (purple) expression in MTN cell bodies of the dorsal mesencephalon and the nucleus of the tract of the posterior commissure (nTPC), and expression of *pax7* (red) in the midbrain. (B) Lateral and (D) dorsal views of BIO treatments at 24 hpf, showing an increase in the number of *drg11* expressing MTN cell bodies in the dorsal mesencephalon. The expression of midbrain marker *pax7* is unchanged relative to DMSO control in A and C. t, tectum. Scale bar = 100 µm

4.2.9 – Down-regulation of the Wnt signalling pathway results in a decrease in the number of MTN cell bodies

To determine the requirements for Wnt signalling during MTN development a *Tg(hsp70:dkk1-GFP)* fish line was used (Stoick-Cooper et al., 2007). *dkk1* inhibits the the Wnt/β-catenin pathway extracellularly by binding to a component of the Wnt receptor complex, therefore when *dkk1* is induced by heat-shock, Wnt signalling is down-regulated (Glinka et al., 1998; Kuwano and Kypta, 2003). The *Tg(hsp70:dkk1-GFP)* fish were heat-shocked at varying stages, but heat-shock at 15 ss proved to be less toxic to the fish because they were able to survive to 24 hpf (see materials and methods).

Tg(hsp70:dkk1-GFP) fish were distinguished from wild type siblings by the presence of GFP expression. In *Tg(hsp70:dkk1-GFP)* GFP+ fish, in which Wnt signalling was down-regulated, a reduction in the number of MTN neurons expressing *drg11* and *isl1* was seen, in contrast to animals exposed to up-regulated Wnt signalling (Figure 4.2.9.3). The few MTN neurons present in the GFP+ fish are located close to the nTPC (Figure 4.2.9.3D). Numbers of the nTPC in *Tg(hsp70:dkk1-GFP)* also appeared to be reduced relative to WT, however the location and size of the epiphysis appeared to be unchanged (Figure 4.2.9.3E – H).

MTN and nTPC neurons expressing *drg11* or *isl1* were counted, and the mean numbers for each condition were plotted onto graphs (MTN table and graph, Figure 4.2.9.1; nTPC table and graph, Figure 4.2.9.2; Raw data tables Appendices 3A, and B; see materials and methods). The mean number of *drg11+* MTN neurons per fish (± S.E.M.) was 1.8 ± for *Tg(hsp70:dkk1-GFP)* GFP+ fish (n=10), significantly lower than the 4.6 ± seen for *Tg(hsp70:dkk1-GFP)* GFP- fish (n=10) ($p < 0.0000014$; Student's t-test; Figure 4.2.9.1). Similarly the mean number of *isl1*+ MTN neurons per fish (± S.E.M.) was 3 ± for *Tg(hsp70:dkk1-GFP)* GFP+ fish (n=10) significantly lower than the 5.3 ± seen for *Tg(hsp70:dkk1-GFP)* GFP- fish (n=10) ($p< 0.00636$; Student's t-test; Figure 4.2.9.1).

Analyses of MTN numbers following the down-regulation of Wnt signalling indicates that Wnt is required for the specification of dorsal neurons MTN and nTPC.

Figure 4.2.9.1 – Down-regulation of the Wnt signalling pathway causes a decrease in the number of MTN cell bodies expressing *drg11* and *isl1*.

(A) Table showing the mean numbers of MTN cell bodies counted per zebrafish in wild type siblings compared to *Tg(hsp70:dkk1-GFP)* zebrafish (n = 10), and the p values showing the difference is statistically different (*0.001*). (B) Graph showing the differences in MTN numbers, and standard error of the mean, in wild type siblings (blue) compared to GFP+ *dkk1* induced animals (purple).

A)

Condition	Mean MTN number in siblings	Mean MTN number in mutants	MTN T-Test p value (*0.001*)	Significance
HS:dkk *-drg11*	4.6 (± 0.27)	1.8 (± 0.25)	0.000001	***
HS:dkk - *isl1*	5.3 (± 0.42)	3 (± 0.63)	0.00636	**

B)

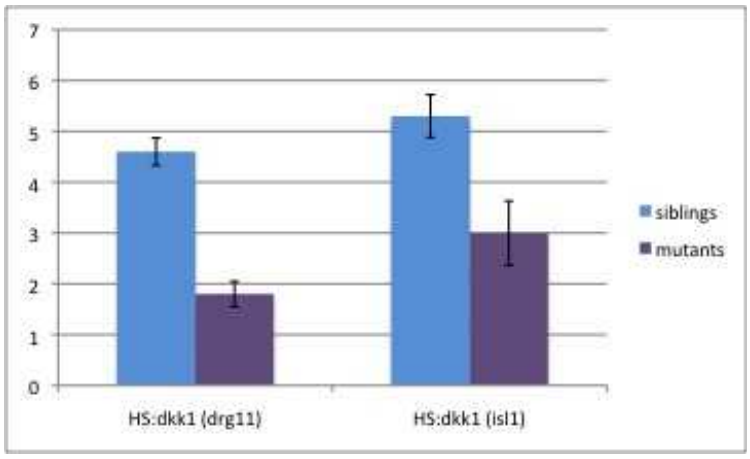

Figure 4.2.9.2 – Down-regulation of the Wnt signalling pathway does not cause a significant increase in the number of nTPC cell bodies expressing *drg11* and *isl1.*

(A) Table showing the mean numbers of nTPC cell bodies counted per zebrafish in wild type siblings compared to *Tg(hsp70:dkk1-GFP)* zebrafish (n = 10), and the p values showing the difference is statistically different (*0.001*). (B) Graph showing the differences in MTN numbers, and standard error of the mean, in wild type siblings (blue) compared to GFP+ *dkk1* induced animals (purple).

(A)

Condition	Mean nTPC number in siblings	Mean nTPC number in mutants	nTPC T-Test p value (*0.001*)	Significance
HS:dkk *-drg11*	13.4 (± 0.31)	11.1 (± 1.02)	0.04	*
HS:dkk *isl1*	14.2 (± 0.98)	12.6 (± 0.6)	0.16	none

(B)

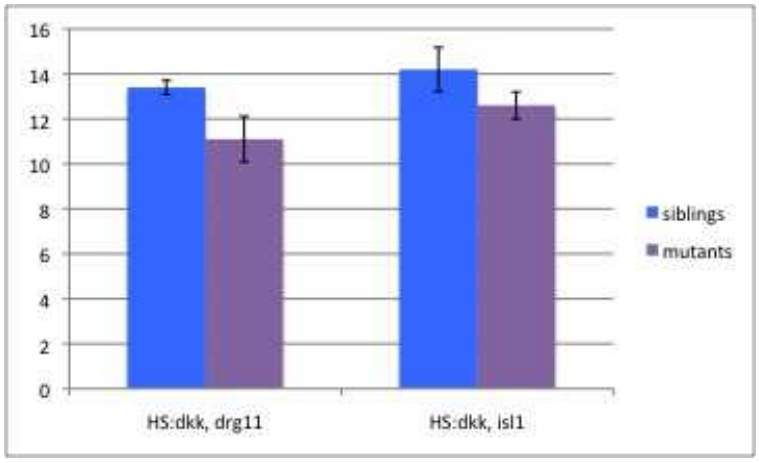

Figure 4.2.9.3 – Down-regulation of the Wnt signalling pathway by heat shock induction of *dkk1* at 15 ss causes a decrease in the number of MTN neurons

(A) Lateral and (C) dorsal views of WT at 24 hpf, showing *drg11* expression in MTN in the dorsal anterior mesencephalon (bracket; black arrows), nucleus of the tract of the posterior commissure (nTPC) and trigeminal ganglia. (B) Lateral and (D) dorsal views of a *Tg(hsp70:dkk1-GFP)* zebrafish at 24 hpf, revealing a decrease in the number of MTN (black arrows) expressing *drg11* in the dorsal mesencephalon. Brackets indicate the reduced distance from the nTPC, in the location of posterior MTN cell bodies. (E) Lateral and (G) dorsal view of WT at 24 hpf, showing *isl1* expression in MTN in the dorsal anterior mesencephalon, nTPC and trigeminal ganglia. (F) Lateral and (H) dorsal view of *Tg(hsp70:dkk1-GFP)* at 24 hpf, revealing a decrease in the number of MTN (black arrows) expressing *isl1* in the dorsal mesencephalon. Brackets indicate the closer proximity of MTN cell bodies to the nTPC. e, epihysis. mb, midbrain.

Scale bar = 100μm

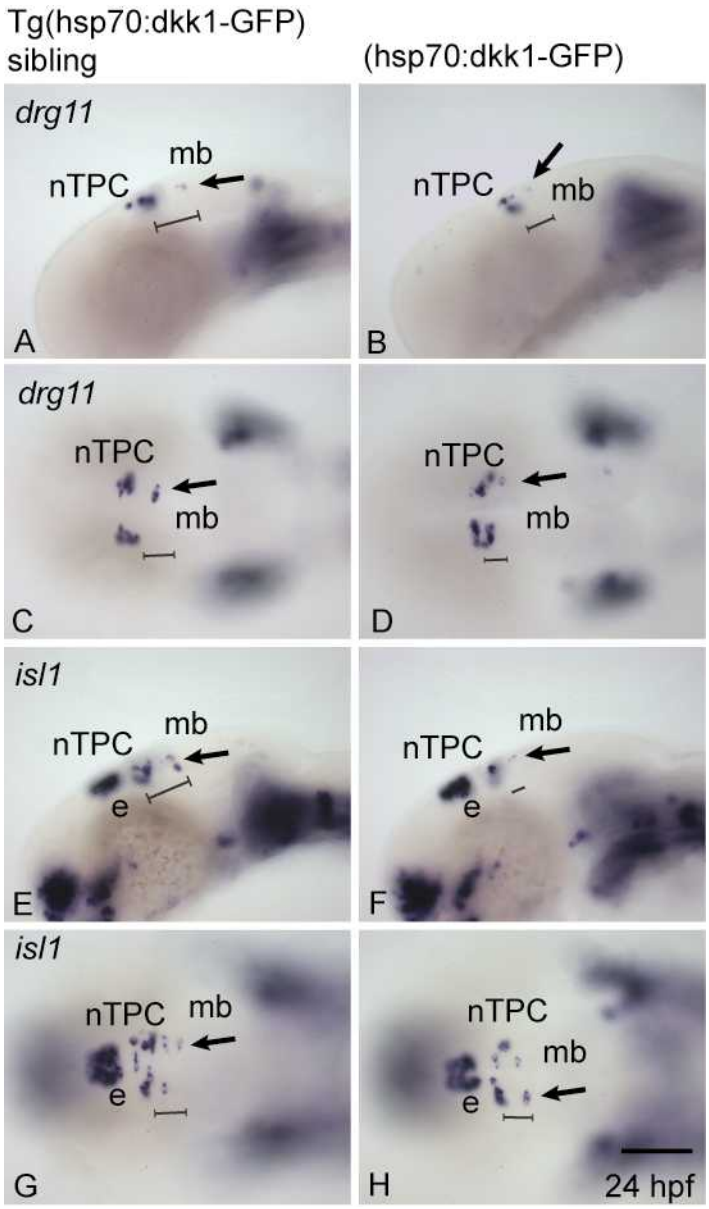
Tg(hsp70:dkk1-GFP)
sibling
(hsp70:dkk1-GFP)
drg11
nTPC
mb
A
B
drg11
nTPC
mb
C
D
isl1
nTPC
mb
e
E
F
isl1
nTPC
mb
e
G
H
24 hpf

4.2.10 – Altering Fgf and Wnt signalling by drug treatments affects the development of the trigeminal ganglia and Rohon Beard neurons.

To assess similarities and differences between other sensory neurons and MTN during development, I analysed the effects on the development of the trigeminal ganglia, and RB neurons after manipulation of Fgf and Wnt signalling.

drg11 expression in animals treated by either SU5402 or DMSO from 10 ss was analysed (Figure 4.2.10A – D). There is a complete loss of *drg11* expression in the trigeminal ganglia in the SU5402 treated fish (Figure 4.2.10A, B). This suggests that Fgf is required for the development of the trigeminal ganglia, which has previously been documented in chick (Canning et al., 2008). In the trunk there also appears to be a reduction in the number of RB cells expressing *drg11* compared to the DMSO controls opposite to that seen with the MTN (Figure 4.2.10C, D). In contrast, in the *ace* and *noi* mutants where Fgf is down-regulated, there is little change in the expression of *drg11* in the trigeminal ganglia, which is comparable to controls (Figure 4.2.10E, F, I and J).

Comparison of *drg11* expression in the trigeminal ganglia of BIO treated zebrafish and DMSO controls, where Wnt is up-regulated, reveals no difference in expression in this tissue (Figure 4.2.10M, N). Numbers of RB cells in the trunk appear to be reduced (Figure 4.2.10O and P), similar to when zebrafish are treated with SU5402. However, in both these drug treatment conditions trunk development is slightly retarded, so the affects on RB formation may be due to toxicity. Analysis of *drg11* expression in *mbl*, where Wnt is up-regulated, shows there is little change in the expression of *drg11* in the trigeminal ganglia (Figure 4.2.10Q, R) and RB neuron numbers appear to also be comparable to wild type siblings (Figure 4.2.10S, T).

Figure 4.2.10 – *drg11* expression is reduced in the trigeminal ganglia, and Rohon-Beard neurons when the Fgf and Wnt signalling pathways are altered

(A) Lateral view of DMSO control treated embryo, showing *drg11* expression in the trigeminal ganglia (tg). (B) A lateral views of an SU5402 treated zebrafish from 10 ss, revealing a loss of *drg11* expression in the trigeminal ganglia (tg). (C) A lateral view of the trunk in a DMSO control treated from 10 ss, showing RB neurons expressing *drg11*. (D) A lateral view of the trunk in SU5402 treated animals from 10 ss revealing a reduction in the number of RB neurons. (E) Lateral views in an *ace* sibling and (F) *ace* mutant, revealing *drg11* expression is unchanged in the trigeminal ganglia. (G) Lateral views of the trunk in an *ace* sibling and (H) *ace* mutant, revealing similar numbers of RB neurons. (I) Lateral views of a *noi* sibling, and (J) *noi* mutant, revealing similar *drg11* expression in the trigeminal ganglia. (K) Lateral views of the trunk in *noi* sibling, and (L) *noi* mutant, revealing similar numbers of RB neurons. (M) Lateral views of a DMSO control treated and (N) BIO treated zebrafish at 10 ss, revealing similar *drg11* expression in the trigeminal ganglia. (O) A lateral view of the trunk in a DMSO control zebrafish showing RB neurons. (P) A lateral view of the trunk in a BIO treated zebrafish, revealing a reduction in the number of RB neurons. (Q) Lateral views of *mbl* sibling and (R) *mbl* mutant, revealing similar expression in the trigeminal ganglia. (S) Lateral views in the trunk of *mbl* sibling and (T) *mbl* mutant, showing comparable numbers of RBs.

Scale bar = 100 μm

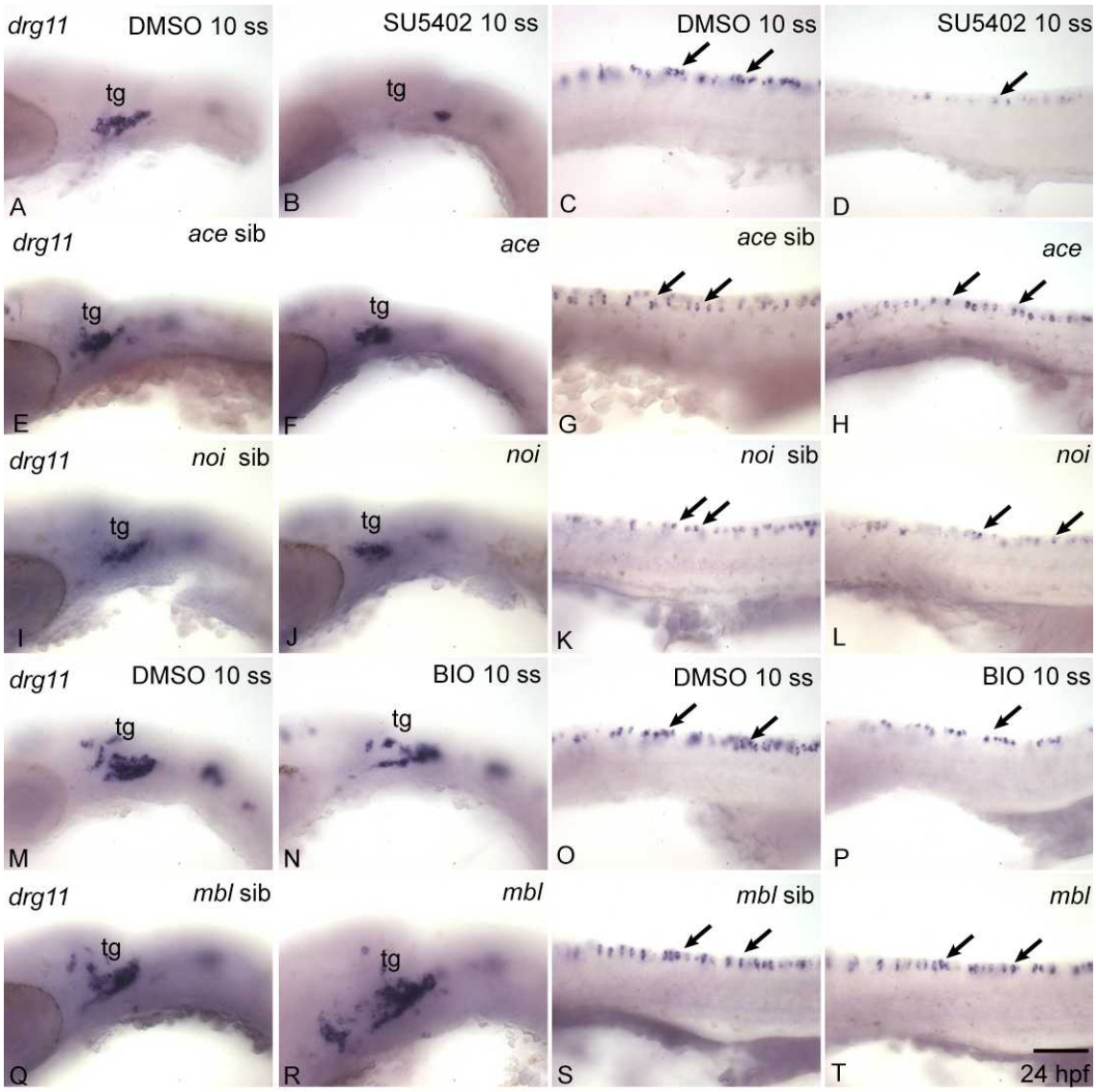
drg11
DMSO 10 ss
SU5402 10 ss
DMSO 10 ss
SU5402 10 ss
tg
A
B
C
D
drg11
ace sib
ace
ace sib
ace
E
F
G
H
drg11
noi sib
noi
noi sib
noi
I
J
K
L
drg11
DMSO 10 ss
BIO 10 ss
DMSO 10 ss
BIO 10 ss
M
N
O
P
drg11
mbl sib
mbl
mbl sib
mbl
Q
R
S
T
24 hpf

4.2.11 – Down-regulation of the Fgf signalling pathway causes a loss of *fgf8* and *wnt1* expression at the midbrain hindbrain boundary

In section 4.2.2 and 4.2.3 I showed that when Fgf is down-regulated, either chemically or genetically, there is an increase in the number of MTN cells. From these experiments we cannot be sure whether the increase in MTN is specific to the down-regulation of Fgf or from an indirect effect on other signalling pathways such as Wnt and Shh.

To assess the effects on Wnt and Shh signalling pathways when Fgf is down-regulated, *wnt1* and *shh* expression patterns and their corresponding reporter genes *axin2* and *ptc2*, were analysed. The expression patterns of *fgf8* and reporter gene *pea3* were also analysed to show that Fgf signalling is down-regulated in SU5402 treatments, *ace* mutants and *noi* mutants.

Fgf and Wnt are required for normal brain development as I have previously described. *Shh* is important for patterning and maintaining ventral brain development, and *ptc2* is a molecular reporter of *shh* signalling (Strähle and Blader, 1994; Lewis et al., 1999). *Pea3* is an ETS transcription factor and is a target gene of Fgf signalling (Molina et al., 1997). *Axin2* is a negative regulator of Wnt signalling, and therefore *axin2* expression increases when Wnt is up-regulated.

In situ hybridisation was carried out on SU5402 treatments and DMSO controls, *ace* and *noi* mutants and wild type siblings. In treated/mutants labelled with *fgf8*, there was a loss of *fgf8* expression at the midbrain hindbrain boundary as previously documented in *ace* and *noi* mutants (Scholpp and Brand, 2003; Brand et al., 1996) ; Figures 4.2.11.1A – D, 4.2.11.2A – D, and 4.2.11.3A – D). However *fgf8* is only slightly reduced in *noi* mutants. *fgf8* expression is lost in this region because the isthmus is absent in these mutants (Brand et al., 1996).

fgf8 expression can still be seen in the dorsal diencephalon in SU5402 treated embryos and mutants, but the region of expression is reduced compared to controls (Figures 4.2.11.1B, D, 4.2.11.2B, D, and 4.2.11.3B, D). Ectopic *fgf8* expression can also be seen in the dorsal anterior diencephalon in SU5402 treatments (Figure 4.2.11.1B; asterisk). Expression of the Fgf reporter gene *pea3* is lost in SU5402 treatments and *ace* mutants, and slightly reduced in *noi* mutants, consistent with data from previous studies in which fgf signalling is down-regulated (Figures 4.2.11.1F, H, 6.2.2.2F, H, and 4.2.11.3F, H) (Scholpp et al., 2003).

wnt1 expression was also lost in the treated/mutants at the midbrain hindbrain boundary similar to that seen with the *fgf8* expression (Figures 4.2.11.1I – L, 4.2.11.2I – L, and 4.2.11.3I – L). This is consistent with results from previous studies showing that *fgf8* is required to maintain *wnt1*, similarly *wnt1* maintains *fgf8*, in a positive regulatory feedback loop (Canning et al., 2008). *wnt1* expression is also lost in the dorsal diencephalon in SU5402 treatments and *ace* mutants, and reduced in *noi* mutants. *wnt1* also appears as a continuous line from the midline expression rather then ending in a circular region (Figure 4.2.11.1J and 4.2.11.2J; arrowhead). Expression along the midline is slightly reduced too. Expression of the Wnt reporter gene *axin2* is comparable between the treated/mutants and controls, with the exception of expression at the midbrain hindbrain boundary that is lost in the treated/mutants.

Finally the effects on Shh signalling were examined. *shh* is required for development of the ventral brain and the ZLI, an organising centre in the diencephalon (Kiecker and Lumsden, 2005; Scholpp et al., 2006). *shh* expression was comparable between treated/mutants and controls (Figures 4.2.11.1Q – T, 4.2.11.2Q – T, and 4.2.11.3Q – T). *ptc2* expression was also comparable between the two conditions (Figures 4.2.11.1U – W, 4.2.11.2U – W, and 4.2.11.3U – W).

Figure 4.2.11.1 – The effects on the expression of *fgf8*, *wnt1*, *shh* and their reporter genes when Fgf signalling is inhibited by SU5402 drug treatment

Images are of DMSO controls and SU5402 treated (10 ss) zebrafish at 24 hpf. (A) Lateral and (C) dorsal views of a DMSO control showing *fgf8* expression in the dorsal diencepalon (dd), telencephalon (t) and isthmus. (B) Lateral and (D) dorsal views of a SU5402 treated animal, revealing a loss of *fgf8* expression at the midbrain hindbrain boundary (mhb), and ectopic expression in the anterior diencephalon. (E) Lateral and (G) dorsal views of a DMSO treated control showing *pea3* expression in the isthmus and eye. (F) Lateral and (H) dorsal views of a SU5402 treated animal, revealing a complete loss of *pea3* expression. (I) Lateral and (K) dorsal views of a DMSO treated control showing *wnt1* expression in the dorsal diencephalon, isthmus and along the dorsal midline of the mesencephalon. (J) Lateral and (L) dorsal views of an SU5402 treated animal, revealing a reduction in *wnt1* expression along the dorsal midline of the mesencephalon, and a loss of expression in the dorsal diencephalon and the isthmus. (M) Lateral and (O) dorsal views of a DMSO treated control showing *axin2* expression in the diencephalon, isthmus and along the dorsal midline. (N) Lateral and (P) dorsal views of an SU5402 treated animal revealing *axin2* expression similar to the control in M and O, except for a slight reduction in expression in the isthmus. (Q) Lateral and (S) dorsal views of a DMSO treated control showing *shh* expression in the ventral brain and ZLI. (R) Lateral and (T) dorsal views of a SU5402 treated animal showing *shh* expression similar to the DMSO controls in Q and S. (U) Lateral and (W) dorsal views of a DMSO treated control showing *ptc2* expression in the ventral brain and ZLI. (V) Lateral and (X) dorsal views of a SU5402 treated animal showing *ptc2* expression similar to the DMSO controls in U and W.

Scale bar = 100 μm

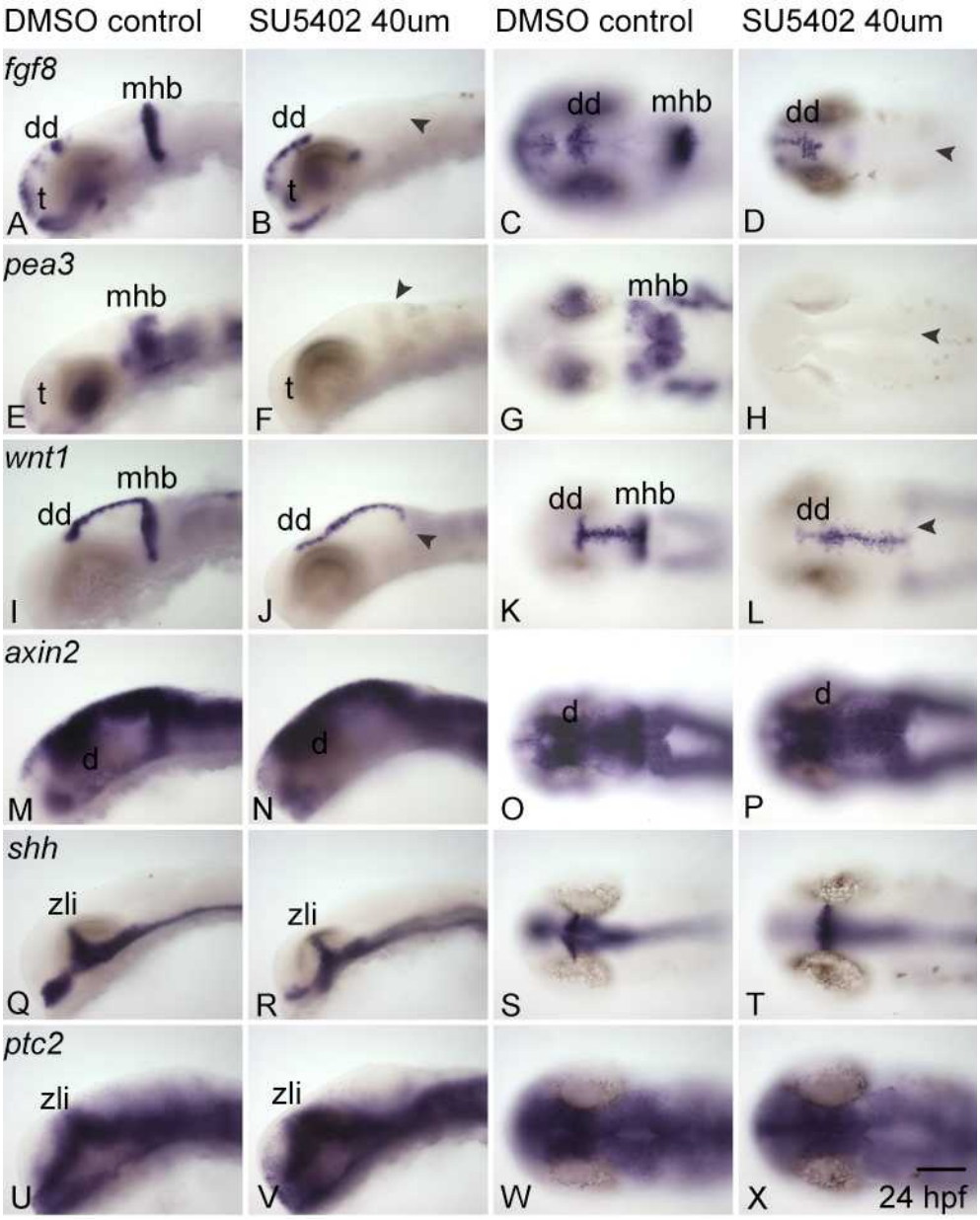
DMSO control
SU5402 40um
DMSO control
SU5402 40um
fgf8
mhb
dd
t
A
B
C
D
pea3
E
F
G
H
wnt1
I
J
K
L
axin2
d
M
N
O
P
shh
zli
Q
R
S
T
ptc2
U
V
W
X
24 hpf

Figure 4.2.11.2 – The effects on the expression of *fgf8*, *wnt1*, *shh* and their reporter genes when Fgf signalling is down-regulated in *ace* mutants

Images are of WT and *ace* mutant zebrafish at 24 hpf. (A) Lateral and (C) dorsal views of WT showing *fgf8* expression in the dorsal diencephalon (dd), telencephalon (t) and isthmus. (B) Lateral and (D) dorsal views of *ace* mutants, revealing a loss of *fgf8* expression at the midbrain hindbrain boundary (mhb). (E) Lateral and (G) dorsal views of WT showing *pea3* expression in the isthmus and eye. (F) Lateral and (H) dorsal views of *ace* mutants, revealing a complete loss of *pea3* expression in the isthmus and reduced expression in the eye. (I) Lateral and (K) dorsal views of WT showing *wnt1* expression in the dorsal diencephalon, isthmus and along the dorsal midline of the mesencephalon. (J) Lateral and (L) dorsal views of *ace* mutants, revealing a loss of *wnt1* expression in the isthmus. (M) Lateral and (O) dorsal views of WT showing *axin2* expression in the diencephalon (d), isthmus and along the dorsal midline. (N) Lateral and (P) dorsal views of *ace* mutants revealing *axin2* expression similar to the WT siblings in M and O. (Q) Lateral and (S) dorsal views of WT showing *shh* expression in the ventral brain and ZLI. (R) Lateral and (T) dorsal views of *ace* mutants showing *shh* expression similar to the wild type siblings in Q and S. (U) Lateral and (W) dorsal views of WT showing *ptc2* expression in the ventral brain and ZLI. (V) Lateral and (X) dorsal views of *ace* mutants revealing *ptc2* expression similar to the WT siblings in U and W.

Scale bar = 100 μm

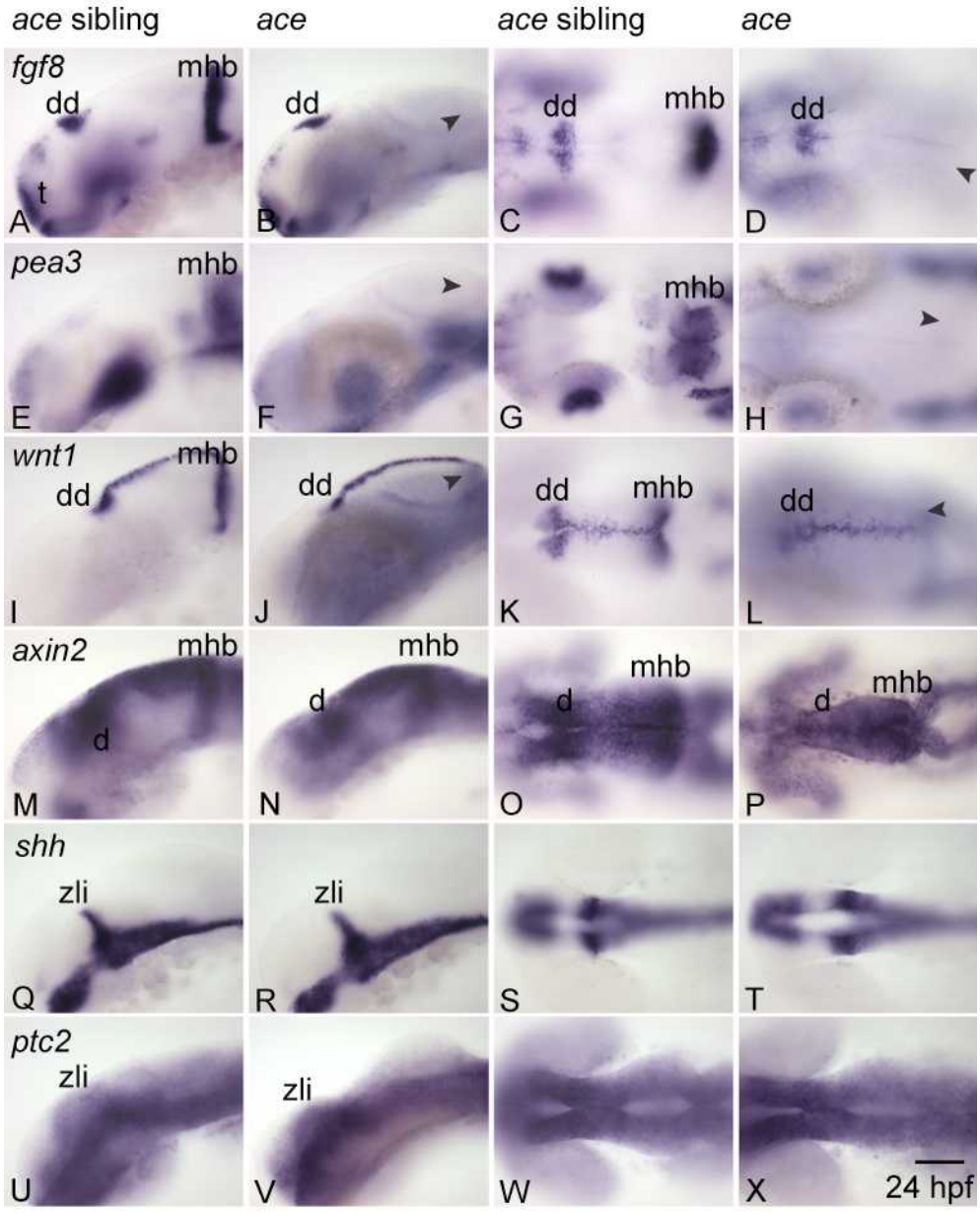
ace sibling
ace
ace sibling
ace
fgf8
mhb
dd
t
A
dd
B
dd
mhb
C
dd
D
pea3
mhb
E
F
mhb
G
H
wnt1
mhb
dd
I
dd
J
dd
mhb
K
dd
L
axin2
mhb
d
M
mhb
d
N
mhb
d
O
mhb
d
P
shh
zli
Q
zli
R
S
T
ptc2
zli
U
zli
V
W
X
24 hpf

Figure 4.2.11.3 – The affects on *fgf8*, *wnt1*, *shh* and their reporter genes when Fgf signalling is down-regulated in *noi* mutants

Images are of WT and *noi* mutant zebrafish at 24 hpf. (A) Lateral and (C) dorsal views of WT showing *fgf8* expression in the dorsal diencephalon (dd), telencephalon (t) and isthmus. (B) Lateral and (D) dorsal views of *noi* mutants, revealing a reduction of *fgf8* expression at the midbrain hindbrain boundary (mhb). (E) Lateral and (G) dorsal views of *noi* siblings showing *pea3* expression in the isthmus and eye. (F) Lateral and (H) dorsal views of *noi* mutants, revealing a reduction in *pea3* expression in the isthmus and eye. (I) Lateral and (K) dorsal views of WT showing *wnt1* expression in the dorsal diencephalon, isthmus and along the dorsal midline of the mesencephalon. (J) Lateral and (L) dorsal views of *noi* mutants, revealing a reduction of *wnt1* expression in the isthmus. (M) Lateral and (O) dorsal views of WT showing *axin2* expression in the diencephalon (d), isthmus and along the dorsal midline. (N) Lateral and (P) dorsal views of *noi* mutants revealing *axin2* expression similar to the WT siblings in M and O. (Q) Lateral and (S) dorsal views of WT showing *shh* expression in the ventral brain and ZLI. (R) Lateral and (T) dorsal views of *noi* mutants revealing a reduction of *shh* expression in the ZLI. (U) Lateral and (W) dorsal views of WT showing *ptc2* expression in the ventral brain and ZLI. (V) Lateral and (X) dorsal views of *noi* mutants revealing a reduction in *ptc2* expression.

Scale bar = 100 μm

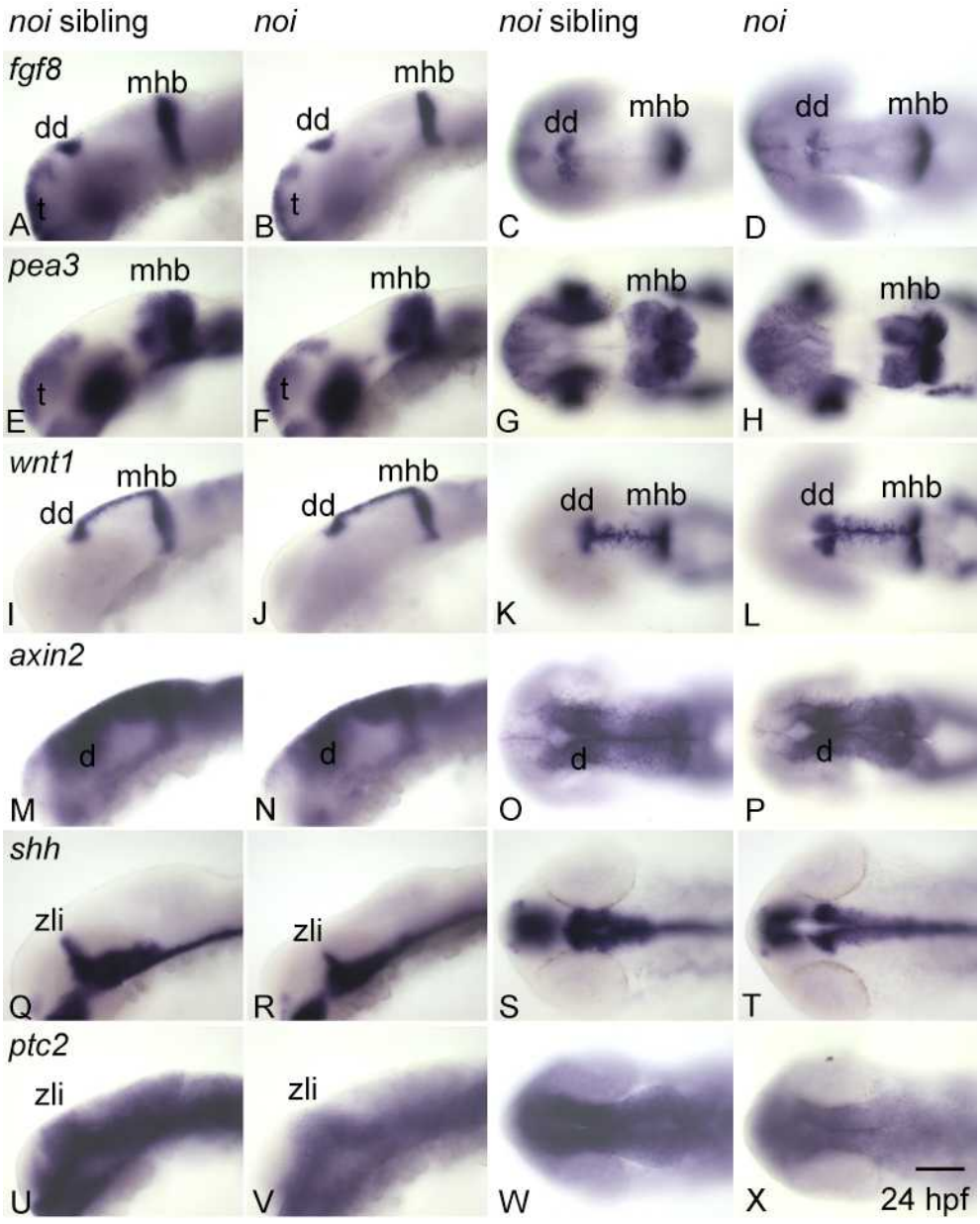
noi sibling
noi
noi sibling
noi
fgf8
mhb
dd
t
A
B
C
D
pea3
mhb
t
E
F
G
H
wnt1
mhb
dd
I
J
K
L
axin2
d
M
N
O
P
shh
zli
Q
R
S
T
ptc2
zli
U
V
W
X
24 hpf

4.2.12 – Effects on the expression of *fgf8*, *wnt1*, *shh* and reporter genes when Wnt signalling is up-regulated

In section 4.2.6 I showed that when the Wnt pathway is up-regulated, an increase in MTN neurons can be seen. This increase may be an indirect effect via the Fgf signalling pathway. To assess the affects on Fgf and Shh signalling pathways when Wnt is up-regulated, the expression patterns of *fgf8*, *shh* and corresponding reporter genes were analysed. *Wnt1* and *axin2* were also analysed to show that Wnt is being up-regulated in the BIO treatments and *mbl* mutants compared to controls.

Wnt1 expression in *mbl* mutants compared to siblings was comparable (Figure 4.2.12.2I - J). In the BIO treated embryos however there was a loss of *wnt1* expression along the midline (Figure 4.2.12.1J, L), and expression at the midbrain hindbrain boundary was not as strong. It is unclear why up-regulating Wnt results in a loss of *wnt1* expression along the dorsal midline. Expression of the reporter gene *axin2* was increased in treated/mutants compared to controls, and a higher background level could be observed (Figure 4.2.12.1M – P, and 4.2.12.2M – P).

In BIO treated embryos there is an increase in *fgf8* expression at the midbrain hindbrain boundary (Figure 4.2.12.1B, D), but in *mbl* mutants *fgf8* expression is comparable to siblings (Figure 4.2.12.2A – D). *fgf8* expression in the dorsal diencephalon in BIO treated animals extends more anteriorly. This is consistent with the phenotype where Wnt is up-regulated, because the epiphysis in the dorsal diencephalon becomes anteriorised (Van der Water et al., 2001). However in the *mbl* mutants *fgf8* expression is completely lost in the dorsal diencephalon, while expression in the telencephalon is comparable to siblings (Figure 4.2.12.2B, D).

In contrast to the anterior extension of *fgf8* expression in the dorsal diencephalon of BIO treated embryos, there is no expression of the *fgf8* reporter gene *pea3* in the forebrain that is present in the DMSO controls. *pea3* expression is lost in the pharyngeal arches in the BIO treated embryos, and reduced at the midbrain hindbrain boundary in both treated and mutant embryos (Figures 4.2.12.1F, H and 4.2.12.2F, H). Reduction of pea3 expression after BIO treatment implies that activating canonical Wnt signalling reduces FGF signalling, i.e., relieves the inhibitory effect of Fgf signalling on MTN formation, consistent with the Fgf pathway manipulations.

Finally the effects on the Shh signalling pathway were examined. *shh* expression was comparable between treated/mutants and controls, with the exception of some loss of expression in the ventral telencephalon (Figures 4.2.12.1Q – R, and

4.2.12.2Q - R). This data is consistent with previous studies that describe a loss of telencephalon when Wnt signalling is upregulated (Heisenberg, 1996). *ptc2* expression was increased in BIO treatments (Figure 4.2.12.1V, X), while expression in *mbl* mutants were comparable to siblings (Figure 4.2.12.2U – X).

Figure 4.2.12.1 – The effects on *fgf8*, *wnt1*, *shh* and their reporter genes when Wnt signalling is up-regulated by BIO drug treatment

Images are of DMSO controls and BIO treated (10 ss) zebrafish at 24 hpf. (A) Lateral and (C) dorsal views of a DMSO control showing normal *fgf8* expression in the dorsal diencephalon (dd), telencephalon (t) and isthmus. (B) Lateral and (D) dorsal views of a BIO treated animal, showing an increase in *fgf8* expression at the midbrain hindbrain boundary (mhb), and ectopic expression in the anterior diencephalon. (E) Lateral and (G) dorsal views of a DMSO treated control showing normal *pea3* expression in the isthmus and eye. (F) Lateral and (H) dorsal views of a BIO treated animal, showing a reduction of *pea3* expression at the midbrain hindbrain boundary. (I) Lateral and (K) dorsal views of a DMSO treated control showing normal *wnt1* expression in the dorsal diencephalon, isthmus and along the dorsal midline of the mesencephalon. (J) Lateral and (L) dorsal views of a BIO treated animal, showing a loss of *wnt1* expression along the dorsal midline of the mesencephalon, and a reduction in expression in the dorsal diencephalon and the isthmus. (M) Lateral and (O) dorsal views of a DMSO treated control showing normal *axin2* expression in the diencephalon (d), isthmus and along the dorsal midline. (N) Lateral and (P) dorsal views of a BIO treated animal showing increased *axin2* expression. (Q) Lateral and (S) dorsal views of a DMSO treated control showing *shh* expression in the ventral brain and ZLI. (R) Lateral and (T) dorsal views of a BIO treated animal showing a loss of *shh* expression in the ZLI. (U) Lateral and (W) dorsal views of a DMSO treated control showing *ptc2* expression in the ventral brain and ZLI. (V) Lateral and (X) dorsal views of a BIO treated animal showing *ptc2* expression comparable to the DMSO controls in U and W.

Scale bar = 100 μm

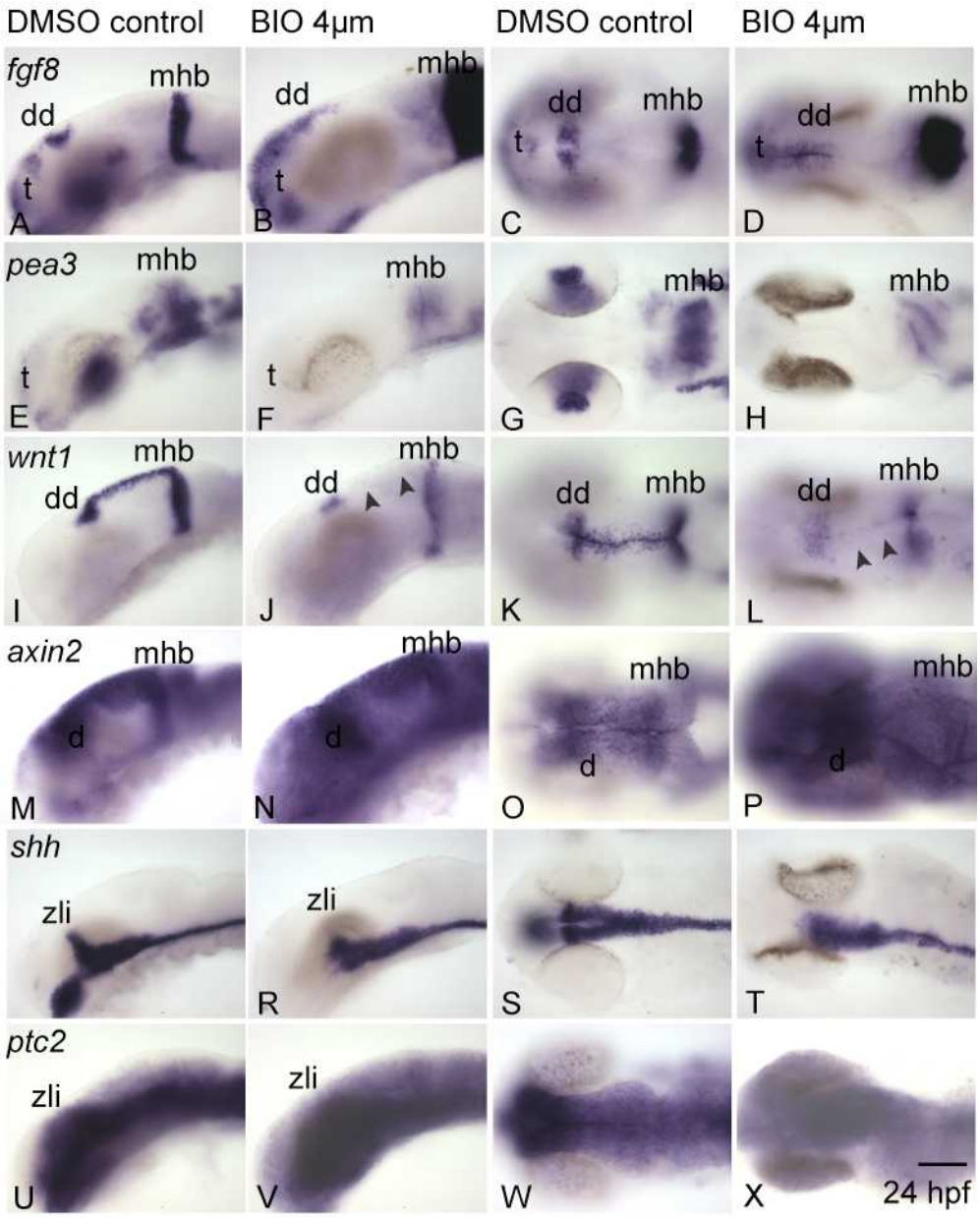
DMSO control
BIO 4µm
DMSO control
BIO 4µm
fgf8
mhb
dd
t
A
B
C
D
pea3
E
F
G
H
wnt1
I
J
K
L
axin2
d
M
N
O
P
shh
zli
R
S
T
ptc2
U
V
W
X
24 hpf

Figure 4.2.12.2 – The effects on *fgf8*, *wnt1*, *shh* and their reporter genes when Wnt signalling is up-regulated in *mbl* mutants

Images are of WT and *mbl* mutant zebrafish at 24 hpf. (A) Lateral and (C) dorsal views of *mbl* siblings showing *fgf8* expression in the dorsal diencephalon (dd), telencephalon (t) and isthmus. (B) Lateral and (D) dorsal views of *mbl* mutants, revealing similar *fgf8* expression at the midbrain hindbrain boundary (mhb) to WT in A and C, but a loss of *fgf8* expression in the dorsal diecephalon. (E) Lateral and (G) dorsal views of WT showing *pea3* expression in the isthmus and eye. (F) Lateral and (H) dorsal views of *mbl* mutants, revealing a reduction of *pea3* expression at the midbrain hindbrain boundary and a complete loss of expression in the eye. (I) Lateral and (K) dorsal views of WT showing *wnt1* expression in the dorsal diencephalon, isthmus and along the dorsal midline of the mesencephalon. (J) Lateral and (L) dorsal views of *mbl* mutants, revealing *wnt1* expression in the isthmus similar to WT in I and K, but a reduction in expression along the dorsal midline. (M) Lateral and (O) dorsal views of WT showing *axin2* expression in the diencephalon (d), isthmus and along the dorsal midline. (N) Lateral and (P) dorsal views of *mbl* mutants revealing an increase in *axin2* expression. (Q) Lateral and (S) dorsal views of WT showing *shh* expression in the ventral brain and ZLI. (R) Lateral and (T) dorsal views of *mbl* mutants revealing *shh* expression similar to WT in Q and S. (U) Lateral and (W) dorsal views of WT showing *ptc2* expression in the ventral brain and ZLI. (V) Lateral and (X) dorsal views of *mbl* mutants revealing *ptc2* expression similar to WT siblings in U and W.

Scale bar = 100 μm

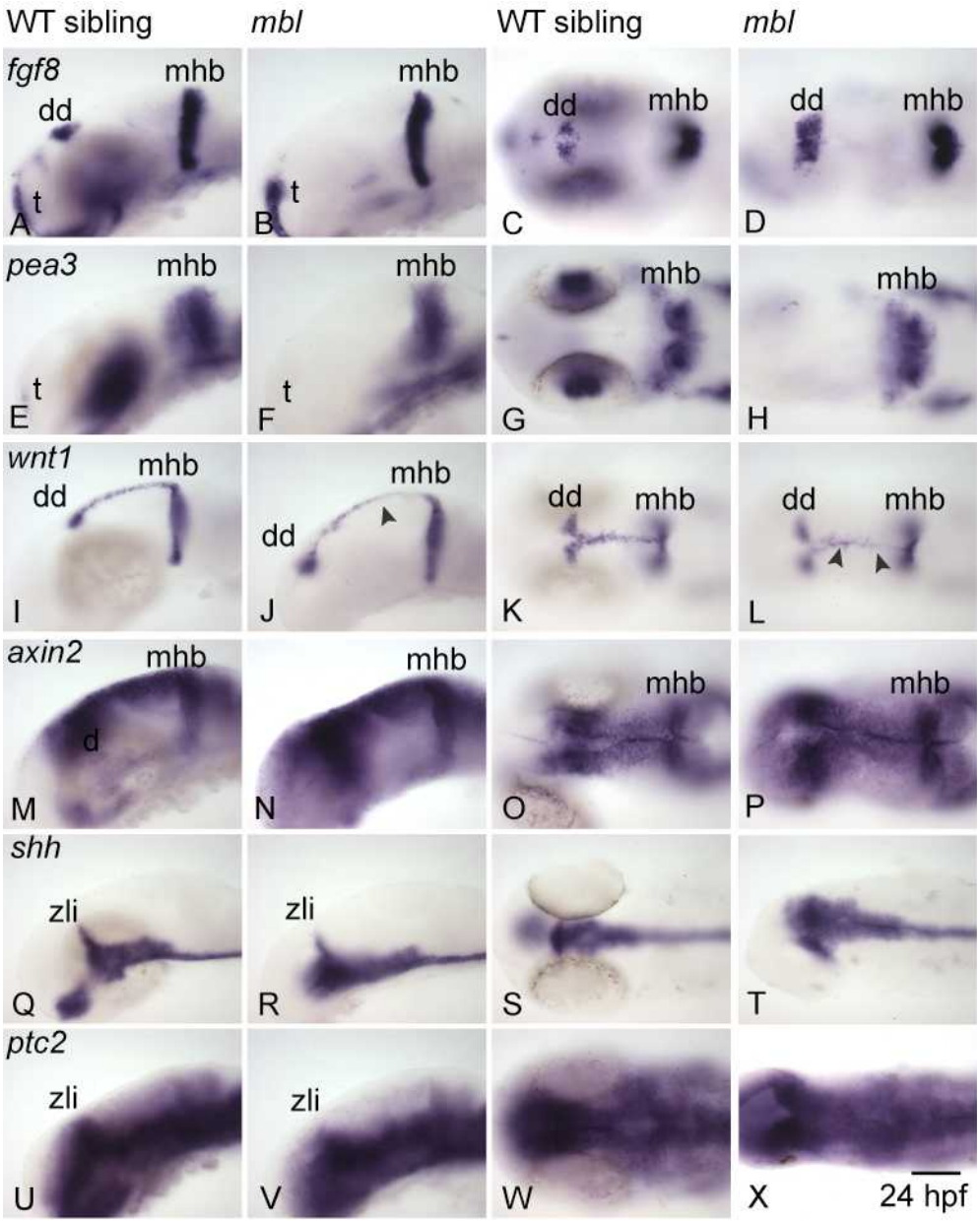
WT sibling
mbl
WT sibling
mbl
fgf8
mhb
dd
t
A
mhb
t
B
dd
mhb
C
dd
mhb
D
pea3
mhb
t
E
mhb
t
F
mhb
G
mhb
H
wnt1
mhb
dd
I
mhb
dd
J
dd
mhb
K
dd
mhb
L
axin2
mhb
d
M
mhb
N
mhb
O
mhb
P
shh
zli
Q
zli
R
S
T
ptc2
zli
U
zli
V
W
X
24 hpf

4.3 – Summary

In this chapter I have investigated the role of Fgf and Wnt signalling during MTN specification. Fgf and Wnt signals from the isthmic organiser and anterior neural plate are required for normal forebrain, midbrain and hindbrain development.

drg11 and *isl1* were used to label MTN neurons. Fgf down-regulation via chemical drug treatments, or genetically, resulted in an increase in the number of MTN cell bodies are seen. Conversely when the Wnt signalling pathway is up-regulated there is an increase in MTN numbers. Interestingly there were greater numbers of *isl1* labelled MTN in both mutants and siblings compared to when *drg11* was used to show MTN. *isl1* may be expressed first in developing MTN as it is a post-mitotic marker (Hunter et al., 2001), and then shortly afterwards *drg11* also starts to be expressed.

In general, the greatest increase in MTN numbers was seen in the *ace* and *noi* mutants compared to wild type siblings. In the SU5402 drug treatments, while there was an increase in MTN numbers, this was not as great compared to the mutants. Interestingly the increase in number was larger in the SU5402 treatments at 10 ss to 24 hpf than in those treated at 5ss – 24 hpf. The increases in MTN numbers in Wnt mutants and control were not as great as the increases seen in any of the Fgf conditions. The increase in MTN numbers, however for all the Fgf anf Wnt conditions are statistically significant ($p < 0.001$).

These results imply that Fgf signalling from the isthmus at the midbrain hindbrain boundary plays an inhibitory role in MTN specification, particularly in the posterior midbrain. Conversely the Wnt signalling pathway is required to promote MTN specification, indicated by the reduction in MTN numbers when Wnt signalling is down-regulated.

Chapter 5: Origin of MTN neurons

5.1 – Introduction

The aim of this chapter is to investigate the cellular origin of MTN neurons as this is relatively obscure. Previous studies have resulted in conflicting results regarding the origin of MTN. Early studies where prospective quail mesencephalic neural crest cells from underlying neuro-epithelium were grafted into duck hosts, have shown that MTN are neural crest derived (Narayanan and Narayanan, 1978). More recent grafting studies where quail mesencephalic migratory neural crest cells (NCC) were transplanted into chick did not find a neural crest contribution to the MTN. (Baker et al., 1997a). Analysis of genes that label neural crest in chick also revealed no expression in the MTN (Hunter et al., 2001). However gene expression data alone does not indicate lineage.

Neural crest is an embryonic cell population derived from ectoderm, which arises at the border of the neural plate and non-neural ectoderm (Trainor et al., 2003; Arduini et al., 2009). In the trunk neural crest cells (NCC) arise from an equivalence group with Rohon Beard (RB) neurons (Cornell and Eisen, 2000). As the neural plate folds to form the neural tube, NCCs become localised within the dorsal portion and undergo an epithelial to mesenchymal transition and delaminate from the neuro-epithelium of the neural tube (Barembaum and Bronner-Fraser, 2005; Santagati and Rijli, 2003). They then migrate and differentiate to form many diverse cell types such as sensory neurons (DRGs), glia, connective tissues and bone to name a few (Gammill and Bonner-Fraser 2003; Arduini et al., 2009).

Cranial neural crest cells (CNCC) play a major role in head development. They arise from the diencephalon, midbrain and hindbrain and migrate in three phases (Santagati and Rijli, 2003). Like NCCs in the trunk, CNCCs form melanocytes, neurons and glia, while only CNCCs differentiate to form cartilage and bone (Santagati and Rijli, 2003). NCC induction at the neural plate border requires expression of genes required for specification of the neural crest, and these are important in forming the neural crest sub-lineages (Sauka-Spengler and Bronner-Fraser, 2008; Betancur et al., 2010). Examples of these genes are: *foxd3*, *tfap2a*, *sox10* and *sox9*.

To test whether gene expression data might support a neural crest origin for MTN neurons (*foxd3*, *snail2*, and *sox10*), I used in situ hybridisation to assess their

expression relative to MTN neurons. I also analysed *Tg(sox10:eGFP)* and *Tg(foxd3:eGFP)* transgenic fish using immunohistochemistry to assess neural crest contribution to MTN neurons, as GFP expression in MTN would suggest a neural crest origin.

To determine if neural crest are important for MTN neuron development, I analysed MTN neurons in a mutant lacking populations of neural crest derived sensory neurons (*colourless*), and in zebrafish larvae where neural crest was genetically ablated by morpholino injection.

In summary I present data that provides evidence that MTN are not neural crest derived and furthermore, that primary sensory neuron development in the brain and neural crest specification are linked processes.

5.2 – Results

5.2.1 - Genes *drg11* and *isl1* are not co-expressed with neural crest markers in MTN cell bodies

The cellular origin of MTN neurons is unclear. To assess whether MTN are neural crest derived, I tested whether zebrafish MTN express genes that are expressed in the neural crest (*foxd3*, *snail2* and *sox10*). *foxd3* is a winged helix/forkhead transcription factor (Kaestner et al., 2000). *foxd3* is required for the development of many neural crest derivatives such as jaw cartilage, peripheral neurons and glia (Lister et al., 2006). *sox10* is a Sry-related HMG box transcription factor required for the development of sensory neurons and pigment cell derivatives of the neural crest (Kelsh, 2006; Carney et al., 2006). *snail2* is a zinc-finger transcriptional repressor and is specific to pre-migratory neural crest and appears to be required for specification and migration of the neural crest (Barembaum and Bronner-Fraser, 2005; Aybar et al., 2002). These are expressed by neural crest progenitors and are required for the early development of neural crest. *foxd3* and *sox10* transcription factors appear to be important for mediating initial specification of neural crest sub-lineages (Arduini et al., 2009).

drg11 and *isl1* were used to visualise MTN cell bodies, as described in the previous chapters. Zebrafish at embryonic stage 20 hpf (22 ss) were assessed for co-expression between *drg11* or *isl1* in MTN neurons and genes that label the neural crest. 20 hpf was determined as the most appropriate stage to compare expression because this

is when MTN neurons begin to differentiate (shown in chapter 3, by timelapse imaging of *Tg(huC:GFP)*). By 24 hpf MTN are specified and have undergone differentiation. Therefore any expression in MTN neurons at 24 hpf of genes normally seen in neural crest may not imply neural crest form MTN.

drg11 and *isl1* expression were labelled using fast red and show the same expression patterns as described previously in chapter 3. Both *foxd3* and *sox10* are expressed in the epiphysis and migratory neural crest in the midbrain, but *sox10* appears to be expressed in more cells than *foxd3* (Figure 5.2.1.1A, C, D, F, and Figure 5.2.1.2A, C, D, F). Co-expression of *isl1* with both *foxd3* and *sox10* can be seen in the epiphysis (Figures 5.2.1.2A, C). Co-expression can also be seen between *sox10* and *isl1* or *drg11* in some nTPC neurons, but no co-expression was seen in MTN cell bodies expressing *drg11* or *isl1* (Figure 5.2.1.1I, and Figure 5.2.1.2I).

At higher magnification, there does appear to be some co-localisation in the expression of *foxd3/sox10*, and *drg11/isl1* in MTN neurons (Figure 5.2.1.1G, I, Figure 5.2.1.2G, I). However, the NCCs expressing *sox10* and *foxd3* appear to lie more dorsal relative to the MTN neurons expressing *drg11* or *isl1*. This juxtaposition of neural crest and MTN creates the illusion of co-expression. At 20 hpf, *snail2* expression is restricted to the ventral brain, therefore it could not be used as a mesencephalic neural crest marker and compared to MTN neurons.

The lack of co-localisation between *drg11* or *isl1* in MTN, and genes that mark neural crest, suggests that MTN are not neural crest derived. However, *sox10* and *foxd3* expression in neural crest cells are rapidly lost following neural crest migration; therefore it is possible that neural crest derived cells no longer express these genes at the 20 hpf stage examined.

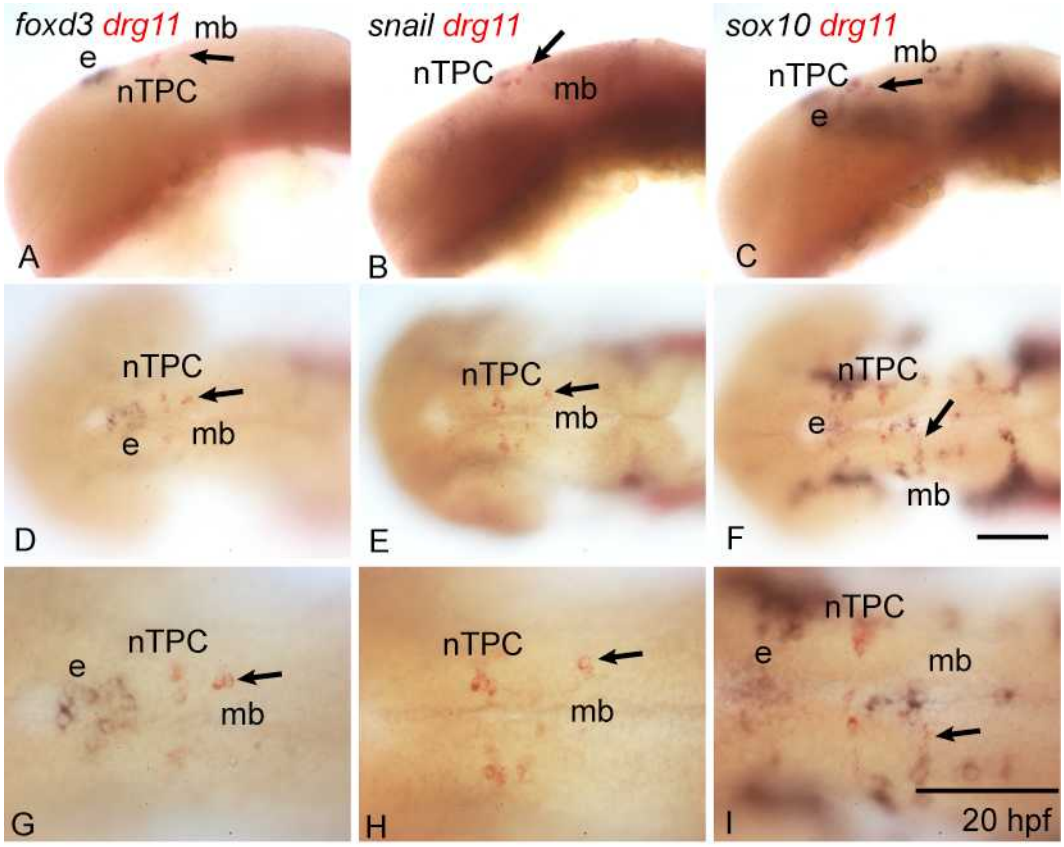

Figure 5.2.1.1 – *drg11* does not co-express with neural crest markers in MTN cell bodies

Lateral views in zebrafish at 20 hpf showing *drg11* (red) expression in MTN neurons compared to neural crest markers (A) *foxd3*, (B) *snail2* and (C) *sox10* (purple). Dorsal views in zebrafish at 20 hpf showing *drg11* expression compared to neural crest markers (D) *foxd3* (E) *snail2* and (F) *sox10*. (G) A higher magnification of D, showing *foxd3* expression in cells of the dorsal mesencephalon, but *foxd3* is not co-expressed with *drg11*. (H) A higher magnification of E, again showing *drg11* expression in MTN cell bodies. *Snail2* is only expressed ventrally. (I) Higher magnification of F, showing *sox10* expression in cells of the dorsal mesencephalon, but *sox10* is not co-expressed with *drg11*. e, epiphysis. mb, midbrain. nTPC, nucleus of the tract of the posterior commissure

Scale bars = 100 μm

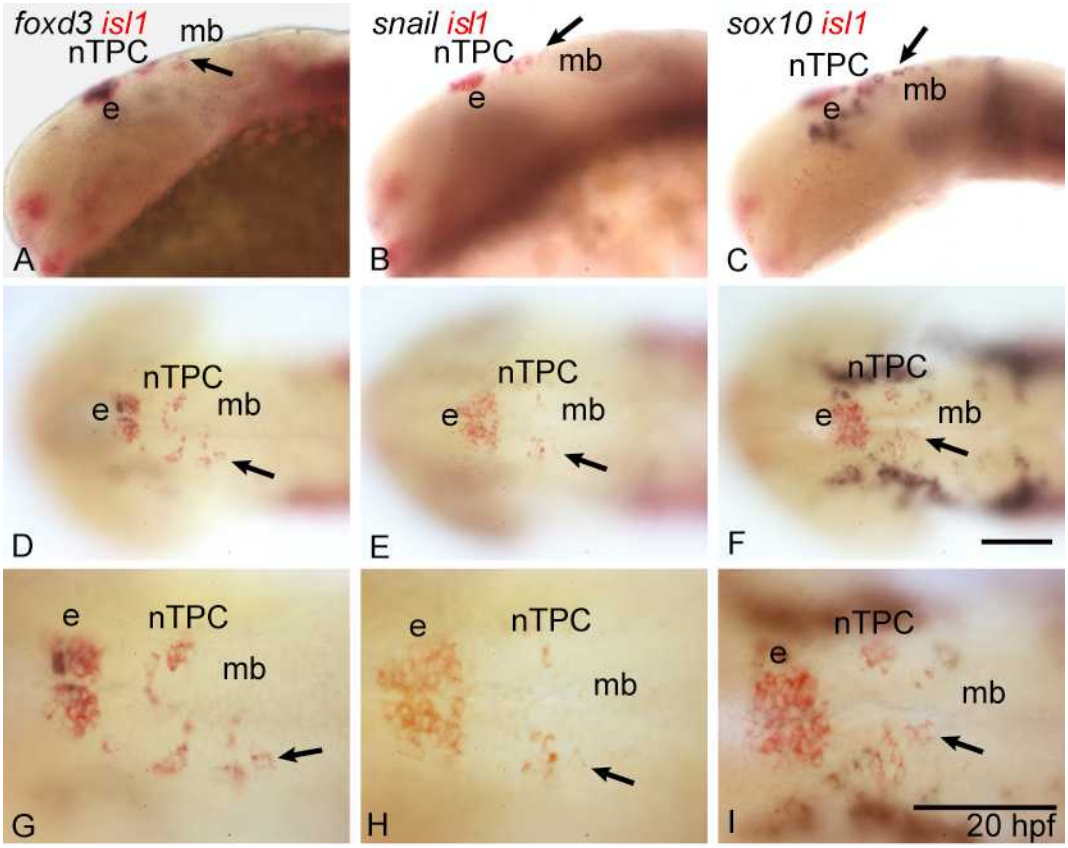

Figure 5.2.1.2 – *isl1* does not co-express with neural crest markers in MTN cell bodies

Lateral views in zebrafish at 20 hpf showing *isl1* (red) expression in MTN neurons compared to neural crest markers (A) *foxd3*, (B) *snail2* and (C) *sox10* (purple). Dorsal views in zebrafish at 20 hpf showing *isl1* expression compared to neural crest markers (D) *foxd3* (E) *snail2* and (F) *sox10*. (G) A higher magnification of D, showing *foxd3* expression in cells of the dorsal mesencephalon, but *foxd3* is not co-expressed with *isl1*. (H) A higher magnification of E, again showing *isl1* expression in MTN cell bodies. *Snail2* is only expressed ventrally. (I) Higher magnification of F, showing *sox10* expression in cells of the dorsal mesencephalon, but *sox10* is not co-expressed with *isl1*. e, epiphysis. mb, midbrain. nTPC, nuclei of the tract of the posterior commissure.
Scale bars = 100µm

5.2.2 – Fluorescent labelling of *Tg(sox10:eGFP)* reveals some co-expression with *drg11* and *isl1*

Perdurance of GFP allows for more robust mapping of cell fate than gene expression, which is often transient. The *Tg(foxd3:GFP)* and *Tg(sox10:eGFP)* transgenic lines label all mesencephalic neural crest and were used to assess neural crest contribution to MTN (Carney et al., 2006; Gilmour et al., 2002).

Tg(foxd3:GFP) and *Tg(sox10:eGFP)* were co-labelled with either Isl1 antibody or *drg11* antisense RNA to label MTN cell bodies. In the *Tg(sox10:eGFP)* line GFP (green) expression can be seen in most/all MTN cell bodies labelled with Isl1 (magenta; white arrowheads, Figure 5.2.2.1F, I). In the *Tg(sox10:GFP)* labelled with *drg11* there also appears to be co-labelling in some MTN cell bodies (green; white arrowhead; Figure 5.2.2.1C). Co-expression could also be seen between GFP and *isl1* and *drg11* in the nTPC (Figure 5.2.2.1C, F, I). These data contradict what is seen in the RNA expression patterns in sub-section 5.2.1 in which analysis showed no co-localisation in MTN.

Recent studies reveal that GFP in the *Tg(sox10:eGFP)* is transiently expressed in non-neural crest cells; oligodendrocytes and the otic vesicle (Antonellis et al., 2008). GFP expression in *Tg(sox10:eGFP)* transgenic fish has also been reported in some CNS neurons, including RB neurons (Dutton et al., 2008). Therefore the *Tg(sox10:eGFP)* line is not the most appropriate tool to examine neural crest contribution to MTN. The *Tg(foxd3:GFP)* line may be more appropriate for lineage analysis of mesencephalic neural crest, as its expression appears more restricted to neural crest cells (Gilmour et al., 2002). GFP expression also persists for longer in the *Tg(foxd3:GFP)* line compared to *Tg(sox10:eGFP)* where GFP expression is lost quite quickly after it first appears. In the *Tg(foxd3:GFP)* line, no co-expression with either Isl1 or *drg11* can be seen in MTN cell bodies, which implies MTN are not neural crest derived (Figure 5.2.2.2C, F, I). Co-expression in the epiphysis between Isl1 and GFP is seen, similar to that seen in the double in situ hybridisation (Figure 5.2.1.2).

The different results obtained when using the *Tg(foxd3:GFP)* and *Tg(sox10:eGFP)* lines causes some ambiguity as to whether or not MTN are neural crest derived.

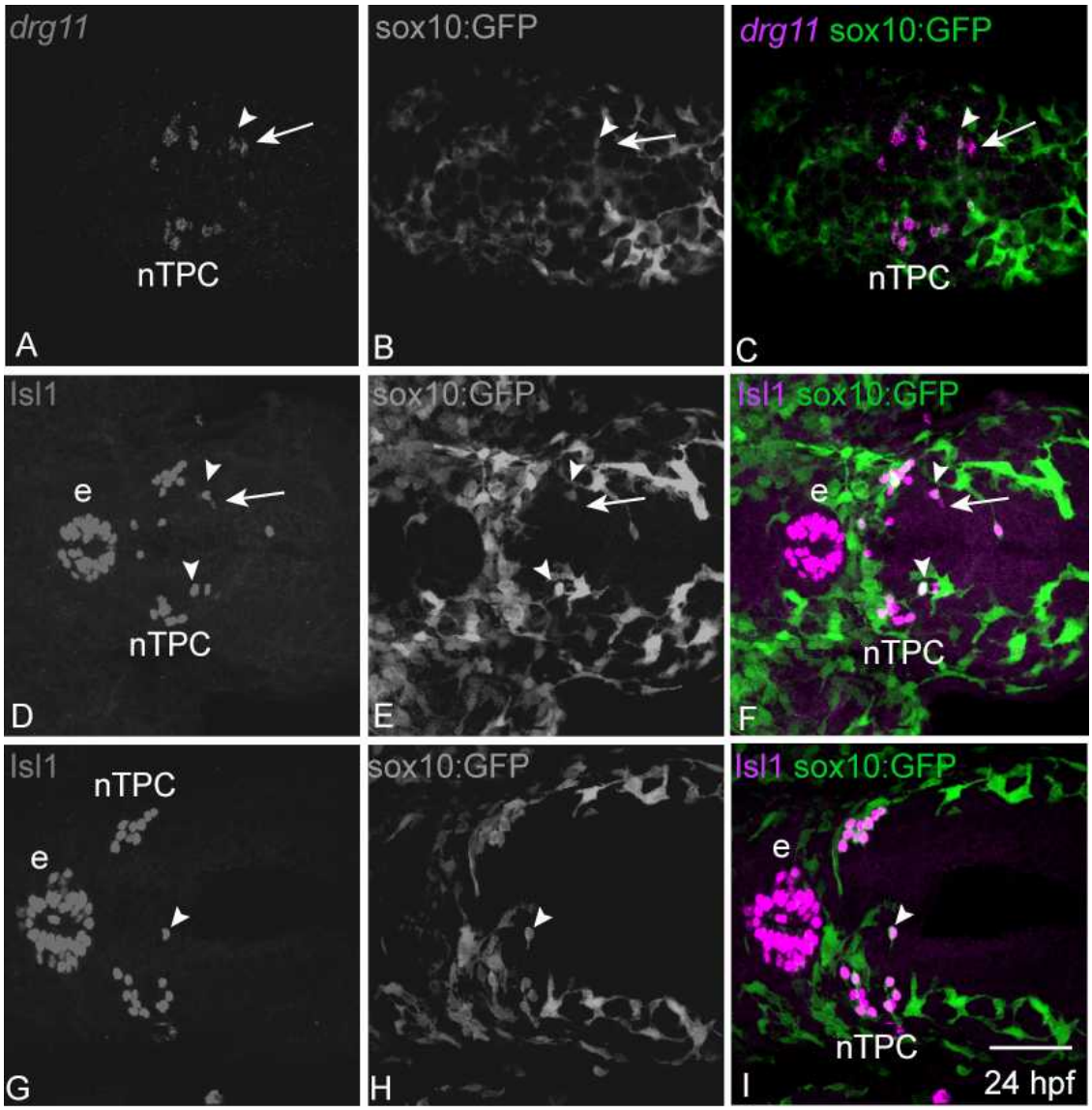

Figure 5.2.2.1 – *drg11* and Isl1, molecular markers of MTN, co-label with some GFP+ cells in the dorsal mesencephalon in *Tg(sox10:eGFP)* transgenic zebrafish

Dorsal views of *Tg(sox10:eGFP)* transgenic fish at 24 hpf, showing (A) *drg11* expression, (B) GFP+ cells showing transient expression in neural crest cells, and (C) a merge of A and B. MTN cell bodies are labelled by *drg11* expression (white arrows). Some GFP+ cells in the dorsal mesencephalon are co-labelled with *drg11* (white arrowhead). Dorsal views of *Tg(sox10:eGFP)* transgenic fish at 24 hpf, showing (D,G) Isl1 expression, (E,H) GFP+ cells, and (F,I) a merge of D,E, and G,H respectively. MTN cell bodies are labelled by Isl1 expression (white arrowhead). The majority of Isl1 expressing MTN cell bodies in the dorsal anterior mesencephalon are co-labelled with GFP+ cells (white arrowhead); White arrows in F indicate the exceptions where Isl1 is solely expressed. e, epiphysis. nTPC, nucleus of the tract of the posterior commissure. Scale bar = 50 μm

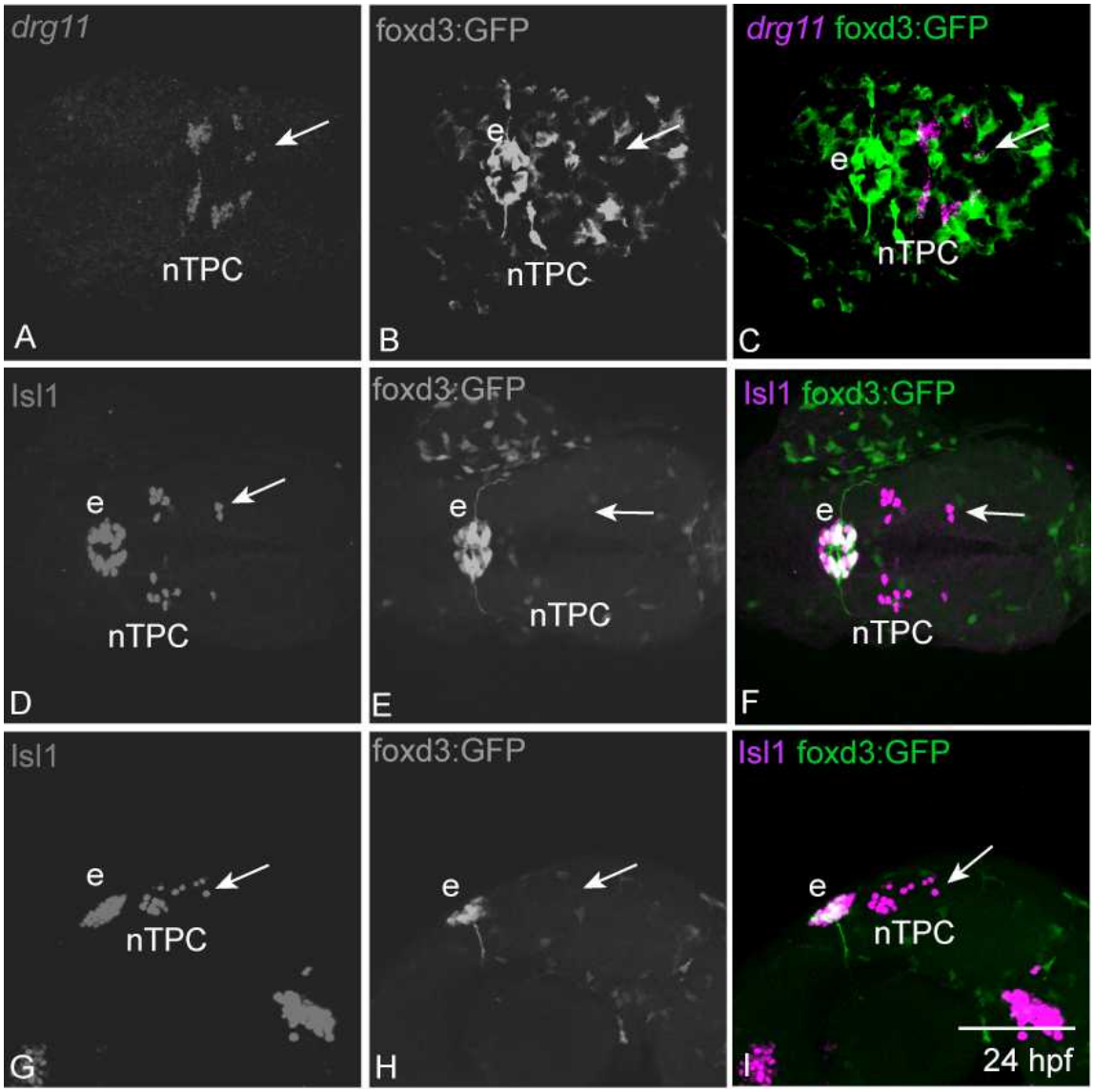

Figure 5.2.2.2 – *drg11* and Isl1 do not co-label with GFP+ cells in the dorsal mesencephalon of *Tg(foxd3:GFP)* transgenic zebrafish

Dorsal views of *Tg(foxd3:GFP)* transgenic fish at 24 hpf, showing (A) *drg11* expression, (B) GFP+ cells showing transient expression in neural crest cells, and (C) a merge of A and B. MTN cell bodies in the dorsal mesencephalon expressing *drg11* (white arrows) are not co-labelled with GFP. Dorsal views of *Tg(foxd3:GFP)* transgenic fish at 24 hpf, showing (D) Isl1 expression, (E) GFP+ cells, and (F) a merge of D, and E. MTN cell bodies expressing Isl1 (white arrows) are not co-labelled with GFP. Lateral views of *Tg(foxd3:GFP)* transgenic fish at 24 hpf, showing (G) Isl1 expression, (H) GFP+ cells, and (I) a merge of G, and H. MTN cell bodies expressing Isl1 (white arrows) do not exhibit co-labelling with GFP. e, epiphysis. nTPC, nucleus of the tract of the posterior commissure.

Scale bar = 50 µm

5.2.3 – There is no significant difference in the number of MTN neurons in the *sox10* mutant *colourless*

Potentially ambiguous results regarding MTN origin from neural crest due to the co-expression between *drg11* and GFP+ cells in *Tg(sox10:eGFP)* fish, led me to further examine the potential role of neural crest in MTN development. A *sox10* mutant, *colourless* (*cls*), was used to determine whether MTN cell bodies fail to develop in an absence of neural crest derived sensory neurons and glia (Kelsh et al., 1996). Expression of *sox10* in *cls* mutants is lost, as described by Kelsh et al. (1996) (Figure 5.2.3I, J). *sox10* has a primary role in the specification of non-ectomesenchymal fates (Dutton et al., 2001). In *cls* mutants there is a loss of melanophore pigment cells (Kelsh et al., 2000), enteric nervous system, and a large reduction in sensory and sympathetic neurones (Kelsh and Eisen, 2000). *cls* mutants were analysed due to the important role *sox10* has in sensory neuron development.

Ectomesenchymal NCC derivatives, such as craniofacial skeleton and fin mesenchyme, are not affected in *cls* mutants. While there are no craniofacial defects in *cls* mutants, because the NCC-derived craniofacial skeleton is not affected, cls mutants were analysed due to the important role *sox10* has in sensory neuron development.

cls mutants were identified based on their loss of pigment at 26 hpf (when pigment cells begin to form (Minchin and Hughes, 2008)). *drg11* and *isl1* expression in MTN neurons and nTPC were similar in the mutant and wild type siblings (Figure 5.2.3). MTN cell bodies and nTPC were counted in *cls* mutants and siblings (Figure 5.2.6.5; raw data table Appendices 6.4.1 and 6.4.2; for nTPC graphs see Appendices 9.1 and 9.2). The mean number of *drg11*+ MTN neurons per fish (± S.E.M.) was 9.2 ± 0.68 for *cls* mutants fish (n=10) which was not significantly different to the 7.7 ± 0.54 seen for *cls* siblings (n=10) ($p < 0.160$; Student's t-test; Figure 5.2.6.5). Similarly the mean number of *isl1*+ MTN neurons per fish (± S.E.M.) was 8.7 ± 0.496 for *cls* mutant fish (n=10) which was not significantly different to the 9.2 ± 0.680 seen for *cls* siblings (n=10) ($p < 0.626$; Student's t-test; Figure 5.2.6.6).

These data reveal that a loss of *sox10* function does not affect the development of MTN.

Figure 5.2.3 – *cls* mutants show normal numbers of MTN and nTPC neurons

(A) Lateral and (C) dorsal views of a *cls* sibling at 26 hpf, showing wild type *drg11* expression in MTN (black arrow). (B) Lateral and (D) dorsal views of a *cls* mutant zebrafish at 26 hpf, revealing *drg11* expression similar to the cls sibling in A and C. (E) Lateral and (G) dorsal views of a *cls* wild type sibling at 26 hpf, showing wild type *isl1* expression. (F) Lateral and (H) dorsal views of a *cls* mutant zebrafish at 26 hpf, revealing *isl1* expression similar to the *cls* sibling in E and G. (I) A Lateral view of a *cls* sibling showing wild type *sox10* expression, and (J) a *cls* mutant revealing a loss of *sox10* expression.

Scale bar = 100μm

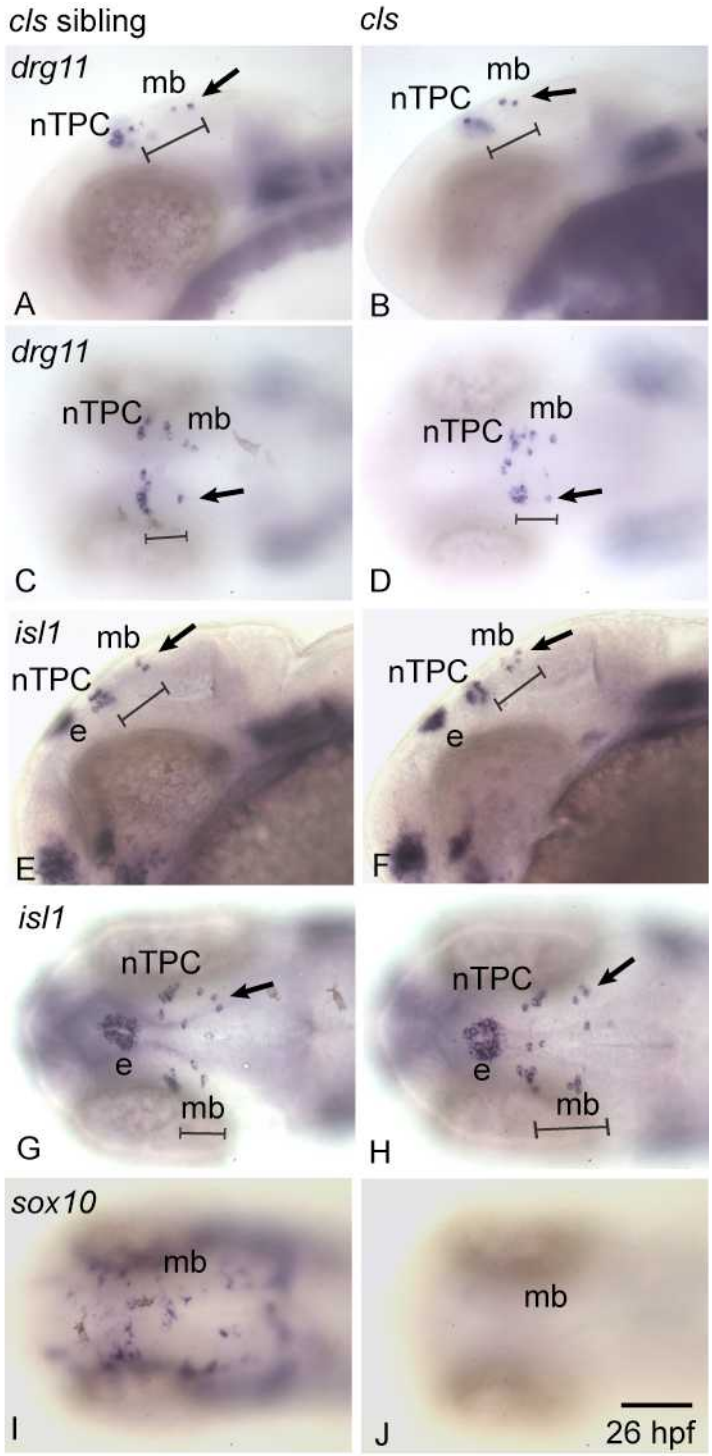
cls sibling
cls
drg11
mb
nTPC
A
B
drg11
nTPC
mb
C
D
isl1
mb
nTPC
e
E
F
isl1
nTPC
e
mb
G
H
sox10
mb
I
J
26 hpf

5.2.4 – Genetic ablation of neural crest causes an increase in MTN neurons

sox10 is required for normal development of a sub population of neural crest, forming non-ectomesenchymal derivatives (Kelsh and Eisen, 2000; Dutton et al., 2001). Other neural crest populations may give rise to MTN, or may compensate for the loss of *sox10* and therefore rescue MTN development.

To further investigate the role of neural crest in MTN formation, neural crest was genetically ablated by *tfap2c* morpholino injection into *tfap2a* mutant *lockjaw* (*low*, Knight et al., 2003), and double morpholino injections of *tfap2a* and *tfap2c* (O'Brien et al., 2004; Li et al., 2007). *tfap2a* is orthologous to mammalian *tfap2a* and is expressed in non-neural ectoderm during gastrulation and is up-regulated in premigratory neural crest. *tfap2a* is required for the formation of a subset of neural crest derived cell types; sensory neurons, cartilage and pigment cells. *tfap2c* is expressed in non-neural ectoderm and transiently in pre-migratory neural crest, and acts redundantly with *tfap2a*, to specify neural crest and the development of non-neural ectodermal derivatives (Li et al., 2007).

Initially *tfap2c* morpholino was injected into *low* mutants and siblings (see materials and methods). *low* mutants could be distinguished from their wild type siblings as they exhibited a reduction in pigmentation (Arduini et al., 2009; Knight et al., 2003). A previous study by Li et al., 2001 describes the *tfap2a-/tfap2c* MO double knockdown phenotype to have a complete loss of pigmentation, absence of yolk extension, poorly extended tail and oedema ventral to hindbrain. None of the *low* injected with *tfap2c* morpholino, in my study, resulted in this strong phenotype as only a reduction in pigmentation was noted and this coincided with poor survival of the injected animals.

To visualise whether neural crest was successfully ablated, and to analyse the affects on MTN development, double in situ hybridisation was carried out. Expression of the distal-less homeobox gene *dlx2* in the arches, was used to show loss of neural crest, and *drg11* was used to label MTN cell bodies.

Wild type siblings were easily distinguished from *low* mutants and *low/tfap2c* morpholino injected animals by *dlx2* expression in the mandibular and hyoid pharyngeal arches. *Tfap2c* injection into wild type revealed unaffected *dlx2* expression. In all the *tfap2c* morpholino injected *low* mutants, only a partial knockdown of *dlx2* was seen. In the 'double' knockdowns, *dlx2* was expressed normally in the mandibular, the first pharyngeal arch, and dramatically decreased in the hyoid arches. This *dlx2* expression

pattern is the same at that described in previous studies for single *tfap2a* knockdown (Li et al. 2007; Knight et al., 2003). A complete loss of *dlx2* in the arches, which has previously been documented to occur in double knockdowns, was not seen (Li et al., 2007).

Controls and injected embryos were grown to 3 dpf, and stained with alcian blue to label cartilage (Kimmel et al., 1998). Non-injected *low* siblings, and *tfap2c* morpholino injected KWT fish, stained with alcian blue (Figure 5.2.4A, B), showed the wild type phenotype of normal cartilage development (Figure 5.2.4A). Non-injected *low* mutants, labelled with alcian blue, showed the cartilages of the hyoid to be absent, a reduction in ventral ceratobranchial cartilages, and a normal or slightly reduced mandibular cartilage and jaw (Knight et al., 2003) (Figure 5.2.4C). In the double knock-down (*low/tfap2c*), an even greater reduction in hyoid cartilage was seen in the few larvae that survived, and a more noticeable reduction in the mandibular cartilage (Figure 5.2.4E, F); different to that previously reported, when a complete loss of all ventral craniofacial cartilages was seen (Li et al., 2007). The lack of phenocopy suggests that neural crest was not completely ablated, but the survival rate in *low/tfap2c*- double knock-downs was low, therefore this approach was not the most appropriate to use to ablate neural crest.

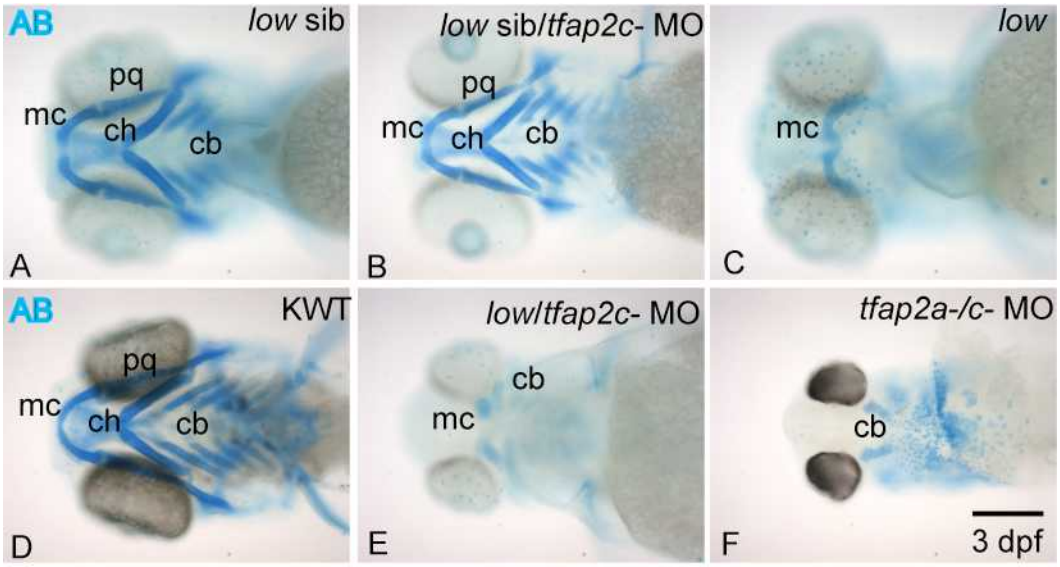

Figure 5.2.4 – Genetic ablation of neural crest affects the development of cartilage in the head

Ventral views of 3 dpf zebrafish of; (A) *low* sibling, (B) *low* sibling/wild type injected with *tfap2c*- morpholino, and (D) wild type, labelled with Alcian Blue (AB), showing wild type development of cartilage. Ventral views of 3 dpf zebrafish of; (C) *low* mutant, (E) *low* mutant injected with *tfap2c*-, and (F) wild type injected with *tfap2a-/tfap2c*- double morpholino, showing the progressive loss of head cartilage. cb, ceratobranchial, ch. ceratohyal, hs. hyosymplectic, mc. Meckel's cartilage, pq. palatoquadrate

Scale bar = 100 μm

5.2.5 – Genetic ablation of neural crest in double morphants causes an increase in MTN neurons

A more efficient and reliable way of completely ablating neural crest was by injecting double morpholinos to *tfap2a* and *tfap2c*. Double morphants and controls were grown to 26 hpf and fixed. *tfap2a-/c-* morphants exhibited the phenotype previously described (Li et al., 2007); a complete loss of pigmentation, absence of yolk extension, poorly extended tail and oedema of the heart. Labelling of neural crest in the pharyngeal arches with *dlx2*, confirmed a loss of neural crest in the double morphants, as studies have previously shown (Li et al., 2007; Figure 5.2.5.1J).

Morphants and controls were labelled with *drg11* and *isl1* (Figure 5.2.5.1A - H). In *tfap2a-/c-* morphants there was an increase in the number of MTN cell bodies expressing *drg11* and *isl1* relative to non-injected controls (Figure 5.2.5.1B, D, F, H). MTN cell bodies in *tfap2a-/c-* morphants, also appeared to span a wider area of the dorsal midbrain and were positioned more medially. MTN furthest away from the nTPC were located more posteriorly, compared to the most posterior position of MTN cell bodies in non-injected controls (brackets, Figure 5.2.5.1A - H). nTPC also appeared to be increased in number in *tfap2a-/c-* morphants.

drg11 and *isl1* expression in the trigeminal ganglia was lost in the *tfap2a-/c-* morphants (Figure 5.2.5.1B, F; Figure 5.2.5.2D). *drg11* expression in the trigeminal ganglia was greatly reduced, but expression in the anterior lateral line ganglia appeared similar to the non-injected controls (Figure 5.2.5.2D). Most cells in the ganglia are derived from neurogenic placodes of embryonic ectoderm (Graham and Begbie, 2000). Therefore the loss of *drg11* and *isl1* expression in the ganglia implies that a loss of *tfap2a-/c-* not only ablates neural crest, but may also affect neural ectoderm. There are also defects in the development of the epiphysis in the *tfap2a-/c-* double morphants. *isl1* expression is reduced in the epiphysis, and it is no longer symmetrically situated along the midline in the dorsal diencephalon. Instead, epiphysal cells are located more peripherally either side of the midline (Figure 5.2.5.1H).

In the trunk, *drg11* and *isl1* labels the dorsal RB neurons (McCormick et al., 2007; Sun et al., 2008). RB cells are derived from the neural plate border (Cornell and Eisen, 2000). Expression of *drg11* and *isl1* in RB neurons in the trunk, is comparable to non-injected controls (Figure 5.2.5.2). The number of RB neurons were assessed by counting *drg11*+ RB neurons in *tfap2a-/c-* double morphants and controls. Statistical analysis using Student's t-test revealed no significant difference in the number of RB

neurons between double morphants and controls (data not shown).

The number of MTN cell bodies and nTPC were separately counted in morphants and controls (MTN tables and graphs, Figure 5.2.6.5 (*drg11*) and Figure 5.2.6.7 (*isl1*); nTPC tables and graphs, Figure 5.2.6.6 (*drg11*) and Figure 5.2.6.8 (*isl1*): Raw data table Appendices 4.1 and 4.2). The mean number of *drg11*+ MTN neurons per fish (± S.E.M.) was 18.1 ± 0.91 for *tfap2a-/c-* double morphants (n=10) which was significantly higher than the 6.8 ± 0.71 seen for non-injected controls (n=10)(*p< 0.000013,* Student's t-test; Figure 5.2.6.5). Similarly the mean number of *isl1* MTN neurons per fish (± S.E.M.) was 19.2 ± 0.81 for *tfap2a-/c-* double morphants (n=10) which was significantly higher than the 8.5 ± 0.86 seen for non-injected controls (n=10)(*p<0.000032* Student's t-test; Figure 5.2.6.7). Statistical analysis using Student's t-test shows that the increase in nTPC neurons in *tfap2a-/c-* morphants is significantly different too (Figure 5.2.6.6).

These results imply that MTN is not neural crest derived, and that neural crest may actually inhibit MTN development. However, *tfap2a* and *tfap2c* are also required for development of non-neural ectoderm (Li et al., 2007). Therefore the increase in numbers of MTN and nTPC may be due to the loss of derivatives from non-neural ectoderm, causing a change in cell fate. To test this hypothesis an alternative approach was used to ablate neural crest that does not perturb ectodermal development.

Figure 5.2.5.1 – Neural crest ablation by double morpholino injection of *tfap2a-* and *tfap2c-* causes an increase in MTN numbers expressing *drg11* and *isl1*

(A) Lateral and (C) dorsal views of a non-injected control zebrafish at 26 hpf, showing *drg11* expression in MTN in the dorsal anterior mesencephalon (bracket; black arrows), nucleus of the tract of the posterior commissure (nTPC) and trigeminal ganglia (tg). (B) Lateral and (D) dorsal views of a *tfap2a-/tfap2c-* morphant zebrafish at 26 hpf, revealing an increase in the number of MTN (black arrows) expressing *drg11* in the dorsal mesencephalon. Brackets indicate the posterior extension in the location of furthest MTN cell bodies from the nTPC. *drg11* expression is lost from the tg. (E) Lateral and (G) dorsal views of a non-injected control zebrafish at 26 hpf, showing *isl1* expression in MTN in the dorsal anterior mesencephalon (bracket; black arrows), nTPC, tg and epiphysis (e). (F) Lateral and (H) dorsal views of a *tfap2a-/tfap2c-* morphant zebrafish at 26 hpf, revealing an increase in the number of MTN (black arrows) expressing *isl1* in the dorsal mesencephalon. Brackets indicate the posterior extension in the location of furthest MTN cell bodies from the nTPC. *isl1* expression is reduced in the tg, and the organisation in the epiphysis (e) is disrupted. (I) A lateral view of a non-injected control, showing wild type *dlx2* expression in the pharyngeal arches, and (J) a *tfap2a-/tfap2c* morphant, revealing the loss of *dlx2* expression. allg, anterior lateral line ganglia.

Scale bar = 100 μm

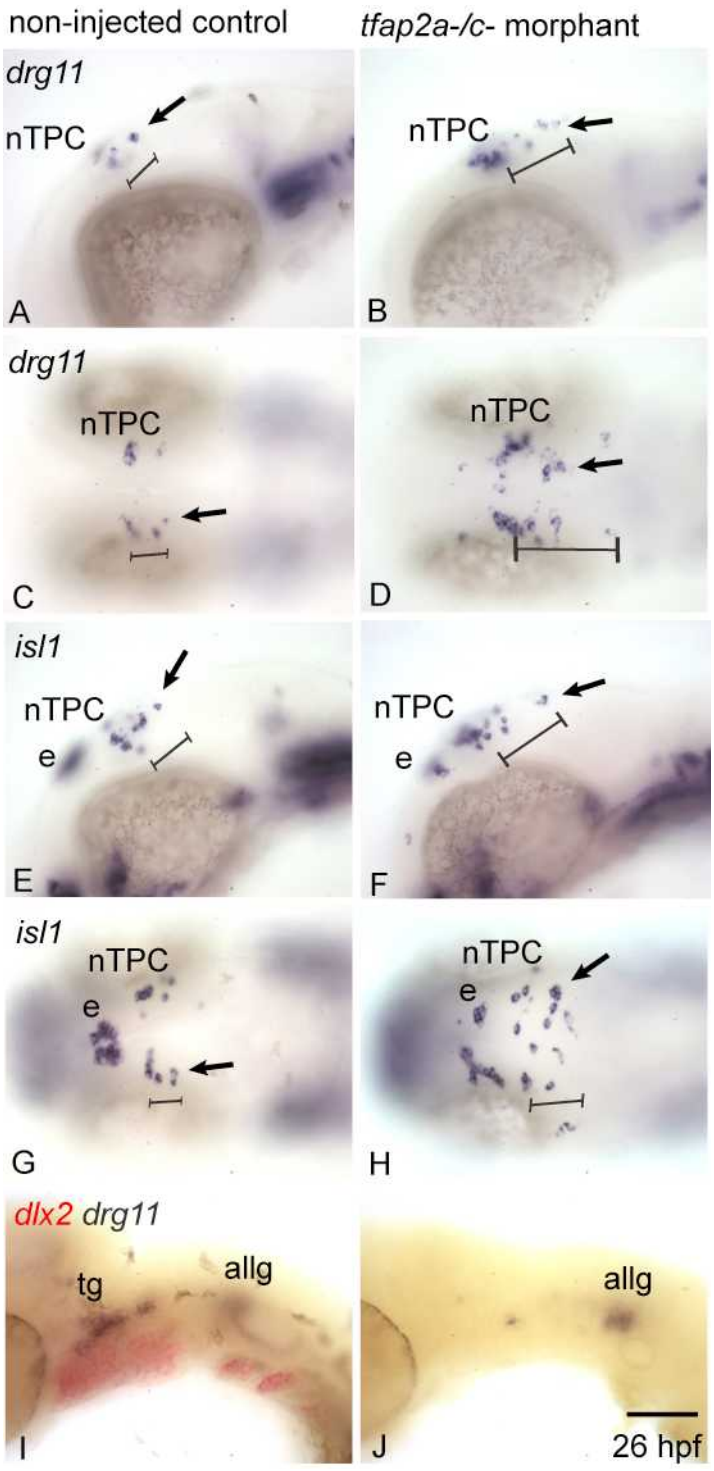
non-injected control
tfap2a-/c- morphant
drg11
nTPC
A
B
drg11
nTPC
C
D
isl1
nTPC
e
E
F
isl1
nTPC
e
G
H
dlx2 drg11
tg
allg
I
allg
J
26 hpf

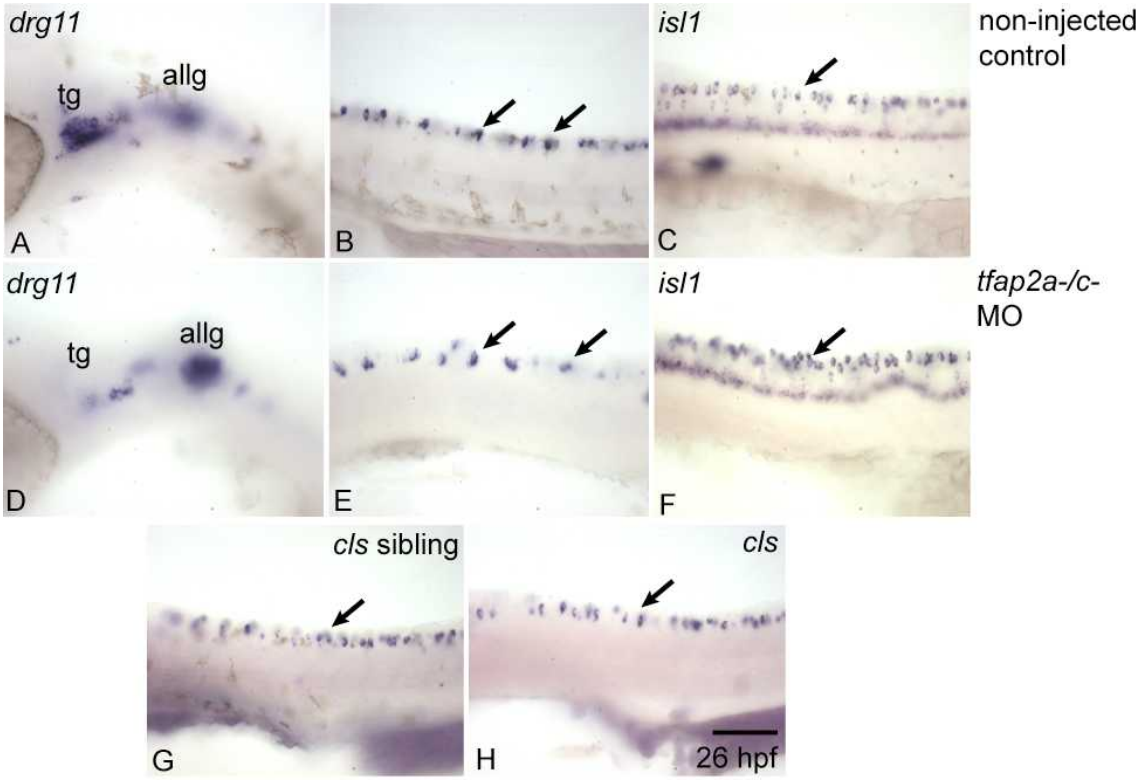

Figure 5.2.5.2 – Genetic ablation of neural crest affects the development of the trigeminal ganglia, but there is no major change in the number of RB neurons

Lateral views of a non-injected control at 26 hpf, showing; (A) wild type *drg11* expression in the trigeminal ganglia (tg), and anterior lateral line ganglia (allg). (B) *drg11* expression and (C) *isl1* expression in RB neurons in the trunk. Lateral views of a *tfap2a-/tfap2c-* morphant at 26 hpf revealing; (D) a loss of *drg11* expression in the Tg, (E) *drg11* expression in RB neurons in the trunk similar to the control in B, and (F) *isl1* expression in RB neurons in the trunk similar to the control in C. (G) A lateral view of *cls* sibling at 26 hpf, showing wild type *drg11* expression in RB neurons. (H) A lateral view of *cls* mutant at 26 hpf, revealing *drg11* expression in RB neurons, similar to the wild type in G.

Scale bar = 100 μm

5.2.6 – Knockdown of *foxd3* and *tfap2a* function results in an increase in MTN cell body numbers

Ablation of the neural crest using *tfap2a* and *tfap2c* morpholinos may also perturb non-neural ectoderm, as well as neural crest. Double *foxd3* and *tfap2a* mutants completely lack differentiated neural crest derived cells, but neural plate border patterning and RB neuron formation occur normally (Arduini et al., 2009). *foxd3* a forkhead transcription factor, is required for the development of many neural crest derivatives such as jaw cartilage, peripheral neurons and glia. Together *foxd3* and *tfap2a* are required to specify and differentiate all major neural crest sub-lineages (Arduini et al., 2009). Therefore morpholino knock-down of foxd3 and tfap2a function was used to ablate neural crest and test the contribution of neural crest to MTN development.

foxd3-/tfap2a- double morphants and controls were labelled with *dlx2*, *drg11* and *isl1* to label neural crest derivatives in the arches, MTN neurons and nTPC neurons. A loss of *dlx2* in the arches of *foxd3-/tfap2a-* morphants, indicated a loss of neural crest derived cells. Similar to the *tfap2a-/c-* double morphants, in *foxd3-/tfap2a-* morphants there was an increase in the number of MTN, and nTPC (Figure 5.2.6.1B, D, F, H; brackets). MTN neurons showed a more posterior distribution compared to control animals, similar to *tfap2a-/tfap2c-* morphants. There was also a reduction in *drg11* and *isl1* expression in the trigeminal ganglia but this was not as reduced compared to the *tfap2a-/c-* morphants.

MTN neurons and nTPC neurons were quantified in *foxd3-/tfap2a-* morphants and non-injected controls. The mean numbers for *drg11* and *isl1* can be seen in Figure 5.2.6.5A and 5.2.6.6A and mean numbers of MTN were plotted onto a graph (MTN tables and graphs, Figure 5.2.6.5 (*drg11*) and Figure 5.2.6.7 (*isl1*); nTPC tables and graphs, Figure 5.2.6.6 (*drg11*) and Figure 5.2.6.8 (*isl1*): Raw data table Appendices 4.1 and 4.2). The mean number of *drg11*+ MTN neurons per fish (± S.E.M.) was 16.1 ± 0.92 for *foxd3/tfap2a-* double morphants (n=10) which was significantly higher than the 7.4 ± 0.52 seen for non-injected controls (n=10)(*p< 0.000003,* Student's t-test; Figure 5.2.6.5). Similarly the mean number of *isl1* MTN neurons per fish (± S.E.M.) was 23.6 ± 1.29 for *foxd3/tfap2a-* double morphants (n=10) which was significantly higher than the 6.6 ± 0.43 seen for non-injected controls (n=10) (*p<0.000002* Student's t-test; Figure 5.2.6.7). Statistical analysis using Student's t-test shows that the increase in nTPC neurons in *foxd3/tfap2a-* morphants is significantly different too (Figure 5.2.6.6).

To determine if there was an intermediate affect on the increase of MTN numbers when neural crest was partially ablated, single morpholino injections using *foxd3-*, *tfap2a-* or *tfap2c-* were carried out (Figures 5.2.6.2, 5.2.6.3 and 5.2.6.4). The mean number of *drg11+* MTN neurons per fish (± S.E.M) was; 6.3 ± 0.68 for *tfap2a-*, 4.6 ± 0.27 for *tfap2c-*, and 4.9 ± 0.23 for *foxd3-,* which was not significantly different to the 6.3 ± 0.54, 5.2 ± 0.39, and 5.4 ± 0.43 respectively, for non-injected controls (n=10)(Student's t-test; *tfap2a p<1*; *tfap2c- p<0.111*; *foxd3- p< 0.14*; Figure 5.2.6.5). The mean number of *isl1+* MTN neurons per fish (± S.E.M) was; 7 ± 0.58 for *tfap2a-*, 6.4 ± 0.52 for *tfap2c-*, and 7.9 ± 0.35 for *foxd3-* which was not significantly different to the 6.6 ± 0.45, 6.1 ± 0.31, and 8.1 ± 0.43 respectively, for non-injected controls (n=10)(Student's t-test; *tfap2a p< _0.494*; *tfap2c- p<0.576*; *foxd3- p< 0.716*; Figure 5.2.6.7).

These results imply that MTN is not neural crest derived, and that neural crest may actually inhibit MTN development, but in order to affect neuronal numbers neural crest needs to be completely ablated.

Figure 5.2.6.1 – The specific ablation of neural crest by double morpholino injection still causes an increase in MTN numbers expressing *drg11* and *isl1*

(A) Lateral and (C) dorsal views of a non-injected controls at 26 hpf, showing *drg11* expression in MTN in the dorsal anterior mesencephalon (bracket; black arrows), nucleus of the tract of the posterior commissure (nTPC) and trigeminal ganglia (Tg). (B) Lateral and (D) dorsal views of a *foxd3-/tfap2a-* morphant at 26 hpf, revealing an increase in the number of MTN (black arrows) expressing *drg11* in the dorsal mesencephalon. Brackets indicate the posterior extension in the location of furthest MTN cell bodies from the nTPC. *drg11* expression is lost from the Tg. (E) Lateral and (G) dorsal views of a non-injected controls at 26 hpf, showing *isl1* expression in MTN in the dorsal anterior mesencephalon (bracket; black arrows), nTPC, Tg and epiphysis (e). (F) Lateral and (H) dorsal views of a *foxd3-/tfap2a-* morphant at 26 hpf, revealing an increase in the number of MTN (black arrows) expressing *isl1* in the dorsal mesencephalon. Brackets indicate the extent of MTN neurons relative to the nTPC.

Scale bar = 100 μm

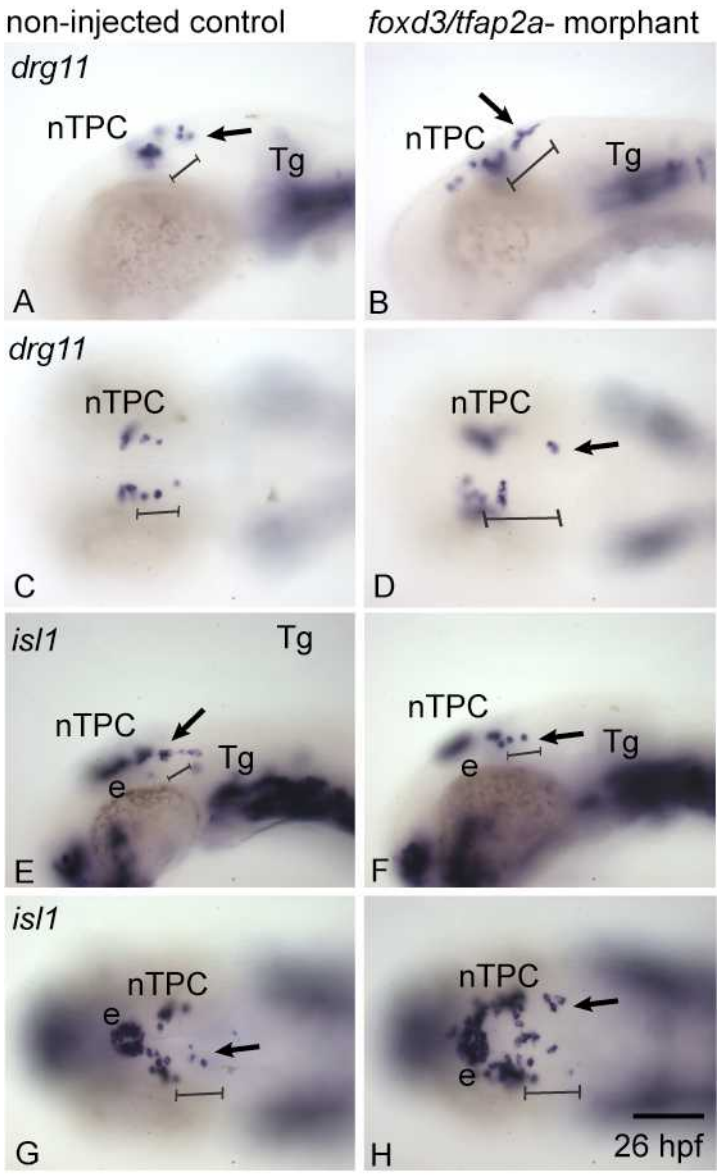
non-injected control
foxd3/tfap2a- morphant
drg11
nTPC
Tg
A
B
drg11
nTPC
C
D
isl1
Tg
nTPC
e
E
F
isl1
nTPC
e
G
H
26 hpf

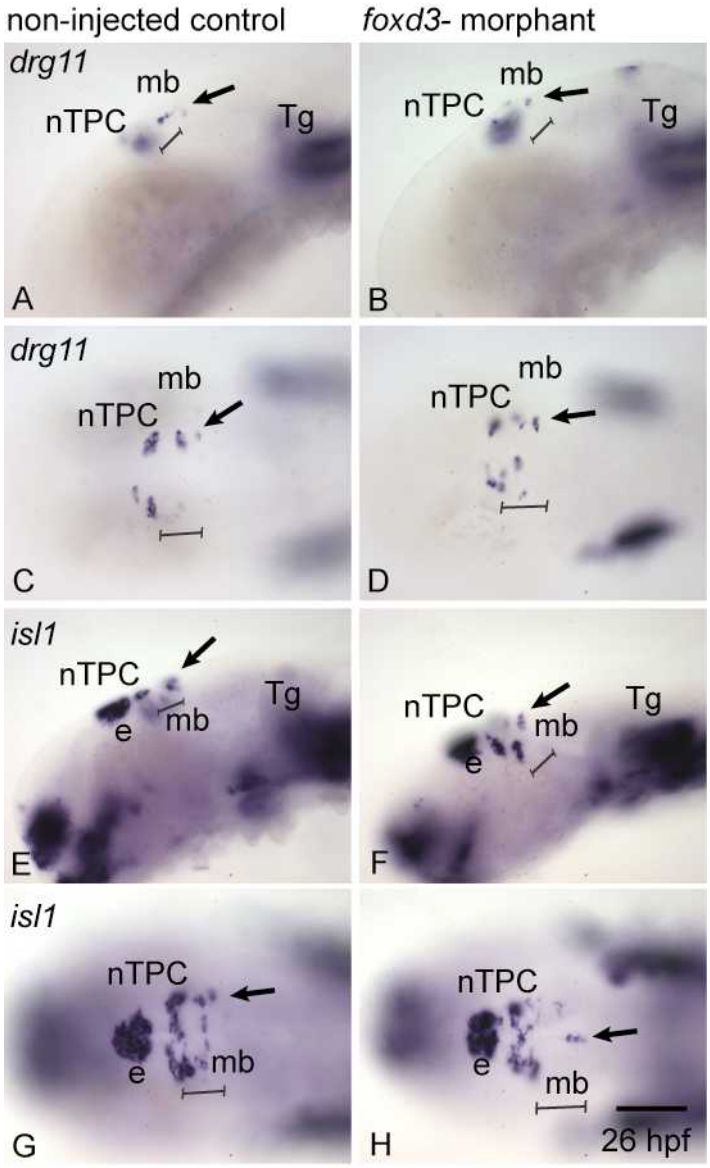

Figure 5.2.6.2 – Partial ablation of neural crest by single morpholino injection of *foxd3*- does not affect MTN numbers

(A) Lateral and (C) dorsal views of a non-injected control at 26 hpf, showing wild type *drg11* expression in MTN (black arrow). (B) Lateral and (D) dorsal views of a *foxd3*- morphant at 26 hpf, revealing *drg11* expression similar to the non-injected control in A and C. (E) Lateral and (G) dorsal views of a non-injected control at 26 hpf, showing *isl1* expression. (F) Lateral and (H) dorsal views of a *foxd3*- morphant at 26 hpf, revealing *isl1* expression similar to the non-injected control in E and G. e, epiphysis. mb, midbrain. nTPC, nucleus of the tract of the posterior commissure. Tg, trigeminal ganglia.

Scale bar = 100 μm

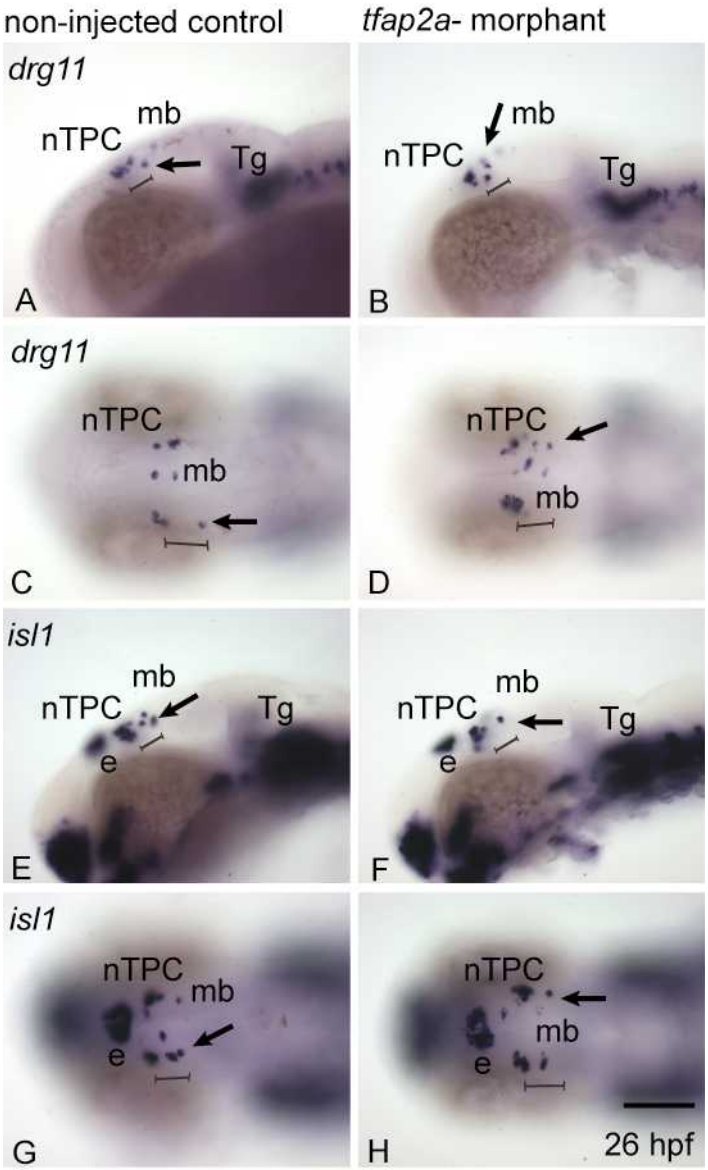

Figure 5.2.6.3 – Partial ablation of neural crest by single morpholino injection of *tfap2a*- does not cause a change in MTN numbers

(A) Lateral and (C) dorsal views of a non-injected control at 26 hpf, showing wild type *drg11* expression in MTN (black arrow). (B) Lateral and (D) dorsal views of a *tfap2a*- morphant at 26 hpf, revealing *drg11* expression similar to the non-injected control in A and C. (E) Lateral and (G) dorsal views of a non-injected control at 26 hpf, showing *isl1* expression. (F) Lateral and (H) dorsal views of a *tfap2a*- morphant at 26 hpf, revealing *isl1* expression similar to the non-injected control in E and G. e, epiphysis. mb, midbrain. nTPC, nucleus of the tract of the posterior commissure. Tg, trigeminal ganglia.

Scale bar = 100 μm

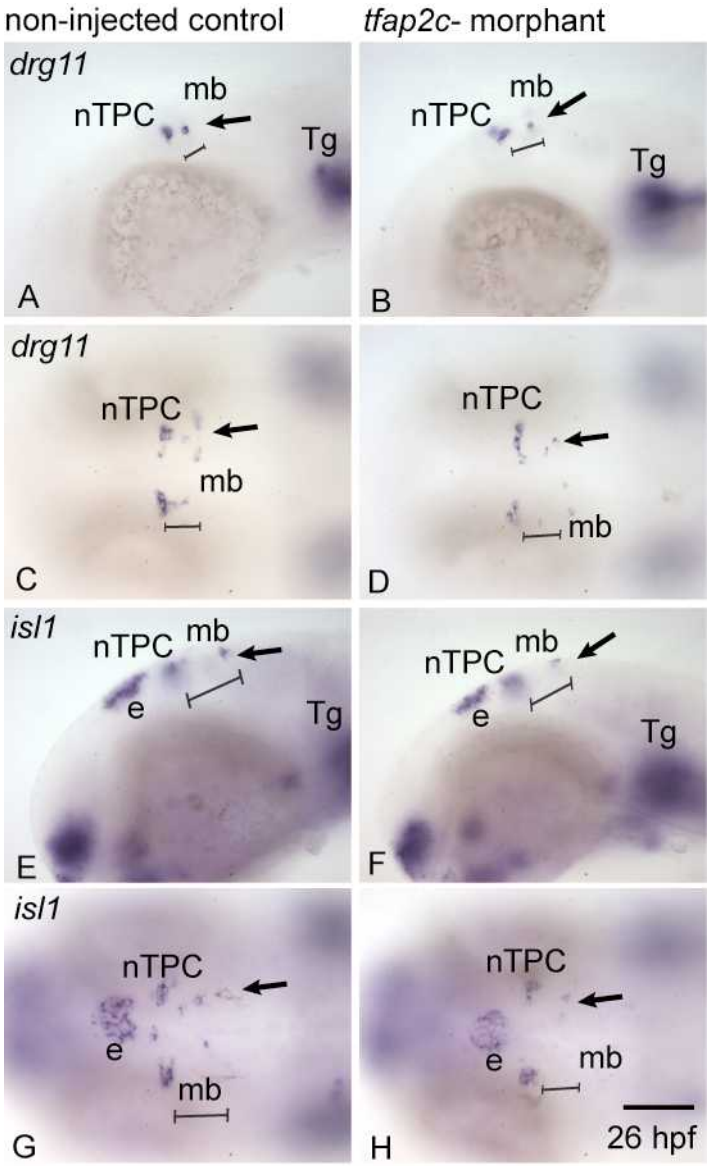

Figure 5.2.6.4 – Partial ablation of neural crest by single morpholino injection of *tfap2c*- does not affect MTN numbers

(A) Lateral and (C) dorsal views of a non-injected control at 26 hpf, showing wild type *drg11* expression in MTN (black arrow). (B) Lateral and (D) dorsal views of a *tfap2c*- morphant at 26 hpf, revealing *drg11* expression similar to the non-injected control in A and C. (E) Lateral and (G) dorsal views of a non-injected control at 26 hpf, showing *isl1* expression. (F) Lateral and (H) dorsal views of a *tfap2c*- morphant at 26 hpf, revealing *isl1* expression similar to the non-injected control in E and G. e, epiphysis. mb, midbrain. nTPC, nucleus of the tract of the posterior commissure. Tg, trigeminal ganglia.

Scale bar = 100 μm

Figure 5.2.6.5 – Genetic ablation of the neural crest by double morpholino injection causes an increase in the number of MTN cell bodies expressing *drg11*

(A) Table showing the average numbers of MTN cell bodies counted per zebrafish in non-injected controls/siblings compared to morphant/mutant zebrafish (n = 10), and the p values indicating how statistically significant the differences are (*0.001*). (B) Graph showing the differences in MTN numbers, and standard error of the mean, in controls (blue) compared to morphants (purple).

A)

Condition	Mean MTN number in non-injected controls labelled with *drg11*	Mean MTN number in morphants labelled with *drg11*	MTN T-Test p value	Significance (*0.001*)
cls	7.7 ± 0.54	9.2 ± 0.68	0.160	none
tfap2a-/tfap2c-	6.8 ± 0.71	18.1 ± 0.91	0.000013	***
tfap2a-	6.3 ± 0.54	6.3 ± 0. 68	1	none
tfap2c-	5.2 ± 0.39	4.6 ± 0.27	0.111	none
foxd3-/tfap2a-	7.4 ± 0.52	16.1 ± 0.92	0.000003	***
foxd3-	5.4 ± 0.43	4.9 ± 0.23	0.14	none

B)

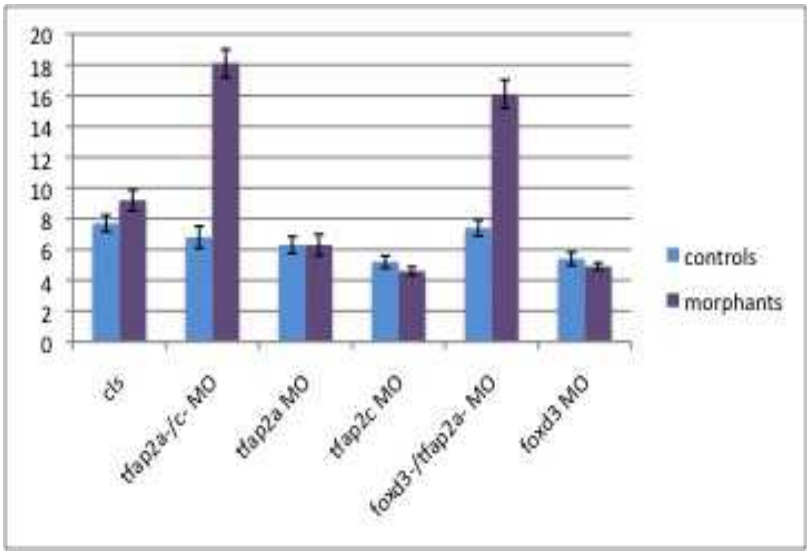

Figure 5.2.6.6 – Genetic ablation of the neural crest by double morpholino injection causes a significant increase in the number of nTPC cell bodies expressing *drg11*.

(A) Table showing the mean number of nTPC cell bodies counted per zebrafish in non-injected controls/siblings compared to morphant/mutant zebrafish (n = 10), and the p values showing a significant difference in *tfap2a-/tfap2c-* and *foxd3/tfap2a-* morphants only (*0.001*). (B) Graph showing the differences in nTPC numbers, and standard error of the mean, in controls (blue) compared to morphants (purple).

(A)

Condition	Mean nTPC number in non-injected controls labelled with *drg11*	Mean nTPC number in morphants labelled with *drg11*	nTPC T-Test p value (*0.001*)	Significance
cls	13.3 (± 0.3)	12.6 (± 0.476)	0.226	*
tfap2a-/tfap2c-	13.6 (± 0.909)	24.7 (± 0.92)	0.000003	***
tfap2a-	13.4 (± 1.077)	16.3 (± 0.761)	0.106	*
tfap2c-	13.5 (± 0.654)	12.8 (± 0.712)	0.406	*
foxd3-/tfap2a-	16.4 (± 1.077)	22.8 (± 0.964)	0.001	***
foxd3-	12.8 (± 0.389)	12.5 (± 0.543)	0.604	none

(B)

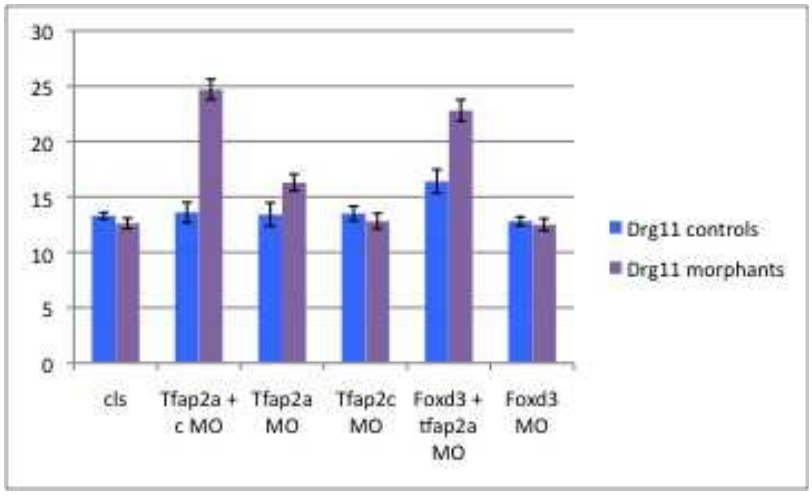

Figure 5.2.6.7 – Genetic ablation of the neural crest by double morpholino injection causes a significant increase in the number of MTN cell bodies expressing *isl1*.

(A) Table showing the average numbers of MTN cell bodies counted per zebrafish in non-injected controls/siblings compared to morphant/mutant zebrafish (n = 10), and the p values indicating how statistically significant the differences are (*0.001*). (B) Graph showing the differences in MTN numbers, and standard error of the mean, in controls (blue) compared to morphants (purple).

A)

Condition	Mean MTN number in non-injected controls labelled with *isl1*	Mean MTN number in morphants labelled with *isl1*	MTN T-Test p value (*0.001*)	Significance
cls	9.2 ± 0.68	8.7 ± 0.5	0.626	none
tfap2a-/tfap2c-	8.5 ± 0.86	19.2 ± 0.81	0.000032	***
tfap2a-	6.6 ± 0.45	7 ± 0.58	0.494	none
tfap2c-	6.1 ± 0.31	6.4 ± 0.52	0.576	none
foxd3-/tfap2a-	6.6 ± 0.43	23.6 ± 1.29	0.000002	***
foxd3-	8.1 ± 0.43	7.9 ± 0.35	0.716	none

B)

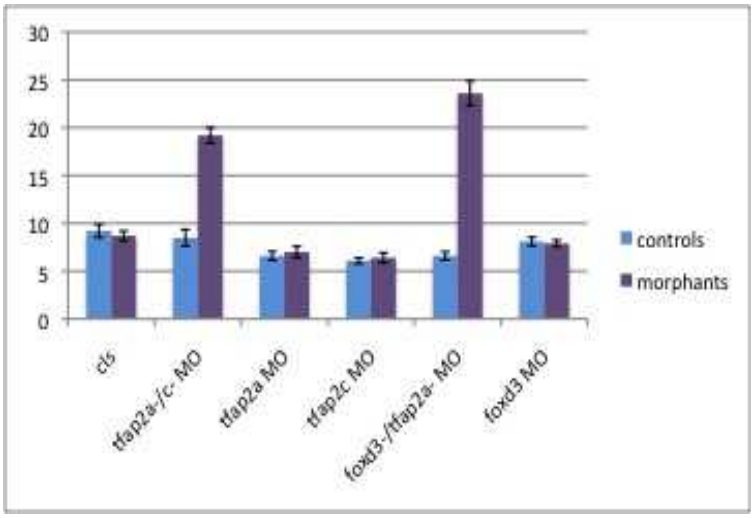

Figure 5.2.6.8 – Genetic ablation of the neural crest by double morpholino injection does not cause a significant increase in the number of nTPC cell bodies expressing *isl1*.

(A) Table showing the mean number of nTPC cell bodies counted per zebrafish in non-injected controls/siblings compared to morphant/mutant zebrafish (n = 10), and the p values showing no significant difference (*0.001*). (B) Graph showing the differences in nTPC numbers, and standard error of the mean, in controls (blue) compared to morphants (purple).

(A)

Condition	Mean nTPC number in non-injected controls labelled with *isl1*	Mean nTPC number in morphants labelled with *isl1*	nTPC T-Test p value (*0.001*)	Significance
cls	16.1 (± 0.77)	13.5 (± 0.62)	0.022	**
tfap2a-/tfap2c-	13.6 (± 0.48)	16 (± 1.63)	0.186	none
tfap2a-	18 (± 0.82)	17.7 (± 0.4)	0.713	none
tfap2c-	14 (± 0.63)	15.8 (± 0.8)	0.156	*
foxd3-/tfap2a-	17.9 (± 0.86)	22.4 (± 0.97)	0.004	**
foxd3-	15.6 (± 0.78)	14.6 (± 0.52)	0.204	none

(B)

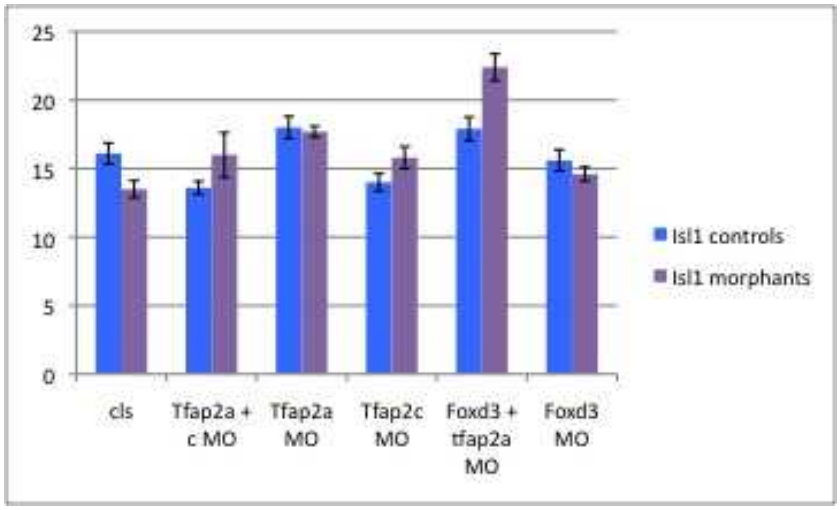

5.2.7 – The position of brain boundaries is not affected in *tfap2a-/c-* or *foxd3-/tfap2a-* double morphants

In the *tfap2a-/c-* and *foxd3-/tfap2a-* morphant conditions, it is possible that brain patterning is disrupted and this may cause the change in neuronal numbers observed. To assess patterning, *pax6* and *pax7* were used to label forebrain and midbrain respectively, to determine whether there were alterations in identity that correlated with changes in MTN and nTPC numbers in morphants.

pax6 and *pax7* expression patterns in the brain appeared similar to the non-injected controls. This shows that ablating neural crest does not affect forebrain and midbrain development, nor does it change their boundary formation (Figure 5.2.7). Therefore the increase in MTN numbers is not due to a change in the positioning of the DMB and ectopically positioned nTPC.

Figure 5.2.7 – Ablation of neural crest by double morpholino injection does not affect forebrain – midbrain boundary fate

(A) Lateral and (C) dorsal views of non-injected controls at 26 hpf, showing *drg11* (purple) expression in MTN cell bodies of the dorsal mesencephalon and the nTPC. *pax6* (red) expression in the forebrain is also seen. (B) Lateral and (D) dorsal views of *tfap2a-/tfap2c-* morphants at 26 hpf, revealing an increase in the number of *drg11* expressing MTN cell bodies in the dorsal mesencephalon. The expression of *pax6* in the forebrain, is similar to the non-injected controls in A and C. (E) Lateral and (G) dorsal views of non-injected controls at 26 hpf, showing *drg11* (purple) expression in MTN cell bodies of the dorsal mesencephalon and the nTPC. *pax7* (red) expression in the midbrain is also seen. (F) Lateral and (H) dorsal views of *tfap2a-/tfap2c-* morphants at 24 hpf, revealing an increase in the number of *drg11* expressing MTN cell bodies in the dorsal mesencephalon. The expression of *pax7* in the midbrain is similar to the DMSO control in A and C.

Scale bar = 100 um

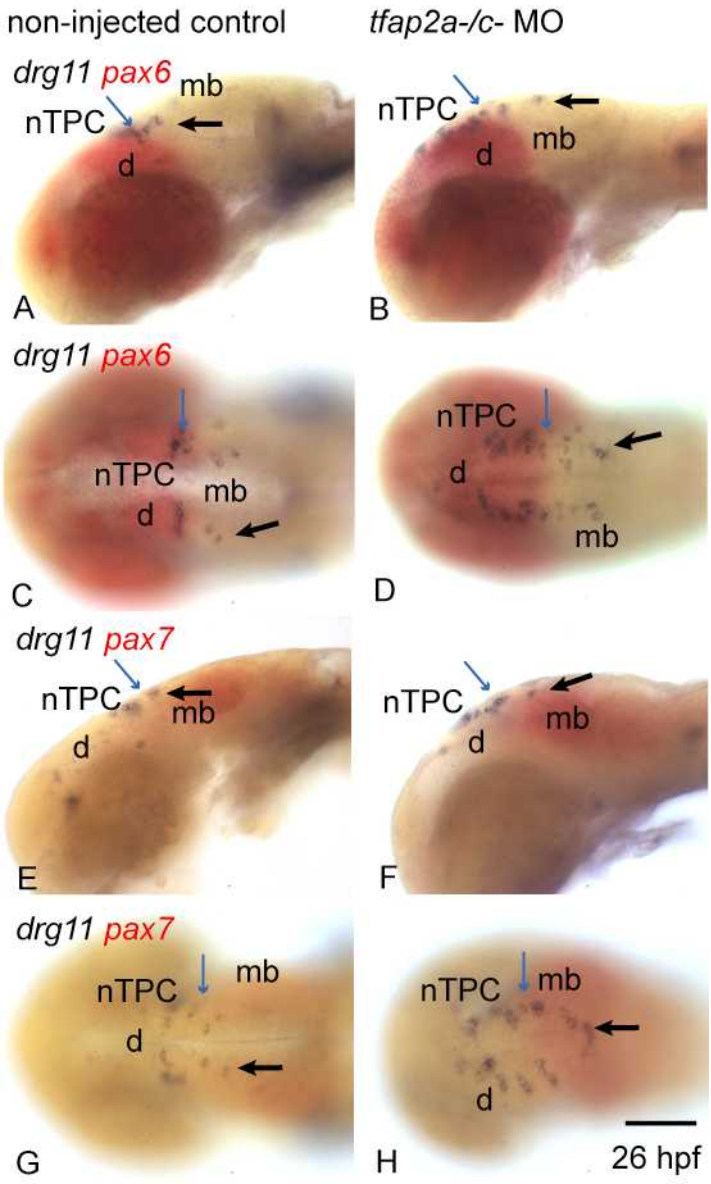
non-injected control
tfap2a-/c- MO
drg11 pax6
mb
nTPC
d
A
B
drg11 pax6
nTPC
mb
d
C
D
drg11 pax7
nTPC
mb
d
E
F
drg11 pax7
nTPC
mb
d
G
H
26 hpf

5.2.8 – MTN axons follow similar paths to wild type controls in double morphants and *cls* mutants

Ablation of neural crest causes an increase in the number of MTN cell bodies. When these morphants were labelled with *pax6* and *pax7* respectively, there was no change in boundary formation in the brain (Figure 5.2.7). To determine whether axonal development occurred in ectopic MTN at posterior positions in the mesencephalon, I next analysed the formation of axons in *tfap2a-/c-* double morphants, compared to non-injected wild type. Labelling of axons would also show if there were any anatomical changes to the brain in these double morphants.

Axons in morphants and controls were labelled with acetylated tubulin (green) and MTN cell bodies with Isl1 (magenta, Figure 5.2.8.1). In non-injected controls, axonal projections from the MTN could be seen (Figure 5.2.8.1C and F). Axons appeared to project peripherally towards the TPC and then grow ventrally towards the MLF, adjacent to the TPC (Wilson et al., 1990). In the *tfap2a-/c-* morphants, the major axon scaffolds in the zebrafish brain have developed normally. Axons can be seen projecting from most MTN cell bodies (Figure 5.2.8.1I, L), including those situated ectopically in the posterior mesencephalon (asterisk; Figure 5.2.8.1I). However, many axons from MTN in the dorsal anterior mesencephalon, now appear to follow the same path as the TPC (Figure 5.2.8.1H, K, L). The more posterior located MTN appear to send out axons ventrally, but in a more extreme manner towards the periphery, compared to controls. These axon terminals end in the medial midbrain; it is unclear whether these would have continued to grow ventrally towards the MLF, or if their growth had terminated (arrowhead, Figure 5.2.8.1I, L). The tract of the posterior commissure (TPC) is also perturbed as the axons no longer cross the midline (Figure 5.2.8.1H, I), but dorsal nTPC axons still appear to descend to the ventral tract and fasciculate with the medial longitudinal fasiculus (MLF) (Figure 5.2.8.2K, L).

In *cls* mutants and siblings, axons could be seen projecting from putative MTN cell bodies ventrally, adjacent to axons from the nTPC (Figure 5.2.8.2). The MTN axonal pathways in *cls* mutants were comparable to wild type siblings.

Figure 5.2.8.1 – MTN axons in double morphants follow similar paths to wild type controls

Dorsal views of a non-injected control at 26 hpf showing, (A) Isl1 expression, (B) acetylated tubulin (a-tub) labelling, and (C) a merge of A and B. MTN cell bodies are labelled in the dorsal anterior mesencephalon by the expression of Isl1 (white arrow). Axons can be seen projecting from MTN cell bodies in a posterior direction and towards the periphery (white arrowhead). Lateral views of a non-injected control at 26hpf showing, (D) Isl1 expression, (E) acetylated tubulin labelling, and (F) a merge of D and E. The tract of the posterior commissure (TPC) and medial longitudinal fasciculus (mlf) are clearly labelled. Dorsal views of a *tfap2a-/tfap2c-* double morphant at 26 hpf revealing (G) Isl1 expression, (H) acetylated tubulin labelling, and (I) a merge of G and H. Axons can be seen projecting from MTN cell bodies in a similar manner to wild type (arrowheads). The TPC shows some defects as the midline crossing is no longer present. Lateral views of a tfap2a-/tfap2c- double morphant at 26 hpf showing (J) Isl1 expression, (K) acetylated tubulin labelling, and (L) a merge of J and K. Axons can be seen projecting from MTN cell bodies similar to non-injected wild type controls. The major axon tracts that form; the TPC, mlf, are still present, but the TPC appears to cover a wider area relative to non-injected controls. (M) A lateral 3D projection of I, showing axonal projections from some anterior MTN cell bodies (white arrow).

Scale bar = 100 μm

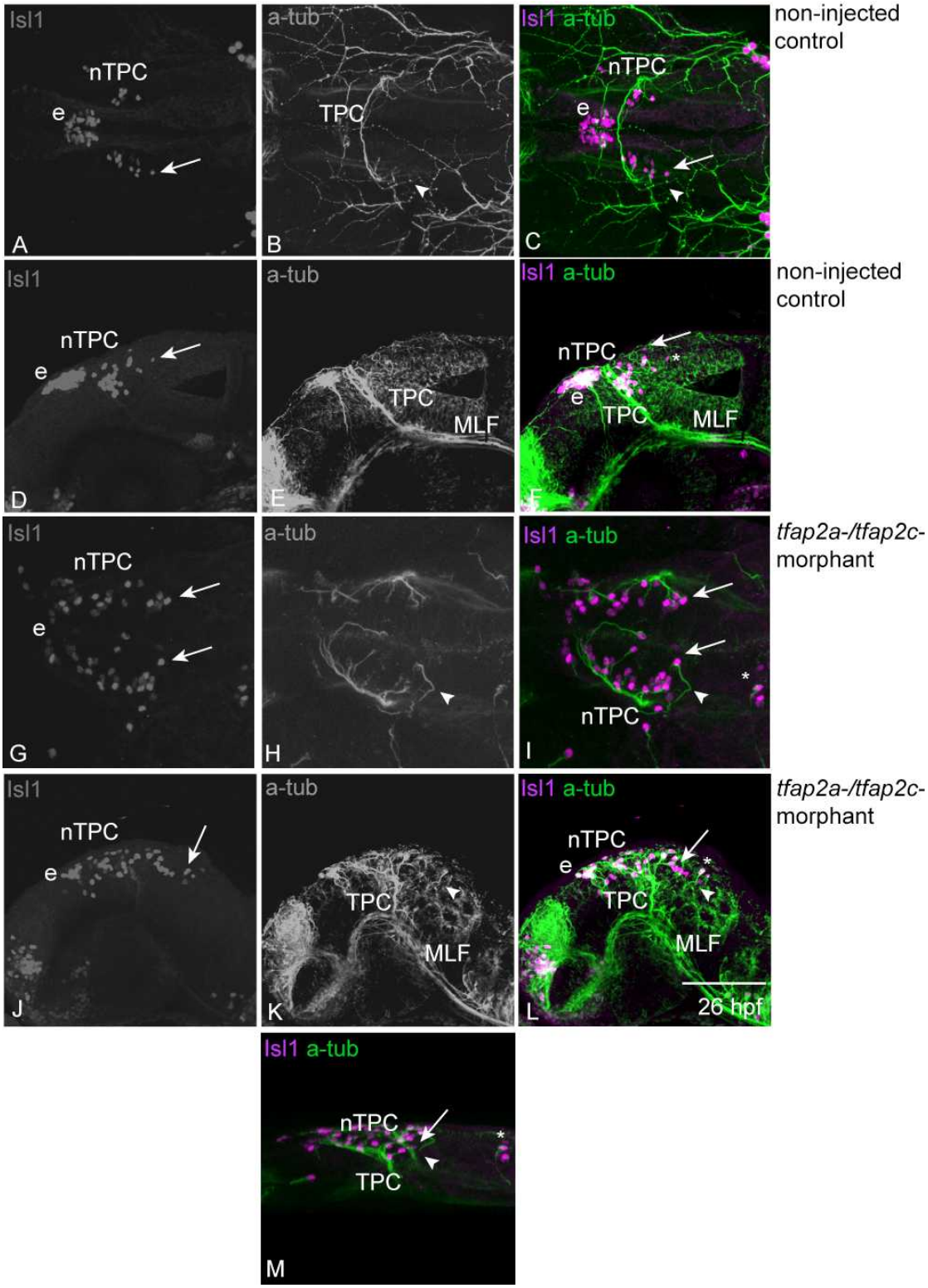
Isl1
nTPC
e
A
a-tub
TPC
B
Isl1 a-tub
nTPC
e
C
non-injected control
Isl1
nTPC
e
D
a-tub
TPC
MLF
E
Isl1 a-tub
nTPC
e
TPC
MLF
*
F
non-injected control
Isl1
nTPC
e
G
a-tub
H
Isl1 a-tub
nTPC
*
I
tfap2a-/tfap2c- morphant
Isl1
nTPC
e
J
a-tub
TPC
MLF
K
Isl1 a-tub
nTPC
e
TPC
MLF
*
26 hpf
L
tfap2a-/tfap2c- morphant
Isl1 a-tub
nTPC
TPC
*
M

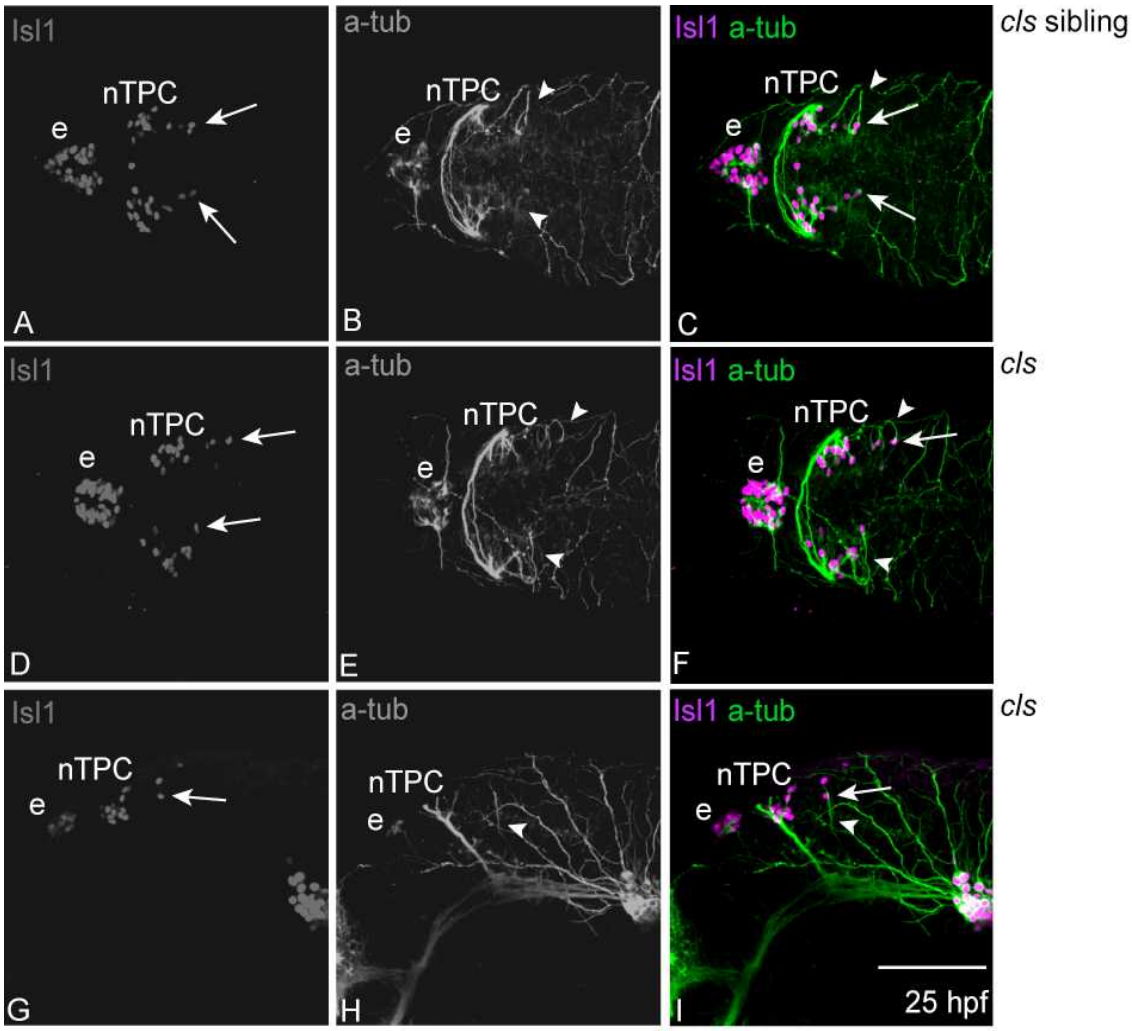

Figure 5.2.8.2 – MTN axons in *cls* mutants follow similar pathways as *cls* wild type siblings

Dorsal views of a *cls* sibling at 26 hpf showing, (A) Isl1 expression, (B) acetylated tubulin (a-tub) labelling, and (C) a merge of A and B. MTN cell bodies are labelled in the dorsal anterior mesencephalon by the expression of Isl1 (white arrow). Axons can be seen projecting from MTN cell bodies in a posterior direction and towards the periphery (white arrowhead). Dorsal views of a *cls* mutant at 26hpf revealing, (D) Isl1 expression, (E) acetylated tubulin labelling, and (F) a merge of D and E. Axons can be seen projecting from MTN cell bodies (arrowhead) similar to wild type siblings. Lateral views of a *cls* mutant zebrafish at 26 hpf revealing, (G) Isl1 expression, (H) acetylated tubulin labelling, and (I) a merge of G and H. Axons can be seen projecting from MTN cell bodies in a similar manner to wild type. The TPC and mlf are also similar to wild type controls.

Scale bar = 100 μm

5.2.9 – Ablation of neural crest by morpholino injection has no effect on Fgf signalling but reduces Wnt signalling activity

When the neural crest is ablated, there is an increase in the number of MTN cell bodies. It is unclear whether this increase in MTN was directly caused by loss of neural crest, or indirectly via change to the Fgf or Wnt pathways. To assess the affects on Fgf, Wnt and Shh signalling pathways when neural crest is ablated, the expression patterns of *fgf8*, *wnt1*, *shh* and responsive genes were analysed in *tfap2a-/c-* and *foxd3-/tfap2c-* double morphants.

In general the heads of *tfap2a-/c-*, and *foxd3-/tfap2a-* double morphants tended to be rounded and smaller, similar to the phenotype previously described (Li et al., 2007; Arduini et al., 2009). However, the expression patterns for all 6 genes studied were generally comparable between the *tfap2a-/c-*, and *foxd3-/tfap2a-* morphants and controls with some exceptions (Figure 5.2.9.1 and Figure 5.2.9.2). In the *tfap2a-/c-* morphants there was a reduction in *wnt1* expression along the dorsal midline of the midbrain, suggesting a perturbation of the midline (Figure 5.2.9.1J, L). A reduction in *wnt1* expression along the dorsal midline is also seen in *foxd3-/tfap2a-* morphants (Figure 5.2.9.2J, L). In contrast there appears to be an increase in *wnt1* in the isthmus of *tfap2a-/c-* morphants (5.2.9.1J, L). In the *tfap2a-/c-* morphants the expression of Wnt reporter gene *axin2* appeared to be reduced, suggesting that ablation of neural crest reduces Wnt activity. However, the reduction in *wnt1* and *axin2* expression may be due to morpholino toxicity effects (Gerety and Wilkinson, 2011). To test this, non-specific missense morpholinos should be injected into control animals and *wnt1* expression analysed; If *wnt1* expression is comparable to non-injected controls, this shows the reduction of *wnt1* expression along the midline is a specific effect of *foxd3-/tfap2a-* ablation.

In the *foxd3-/tfap2a-* morphants there is a loss of *shh* and *ptd* expression in the ZLI compared to non-injected controls (Figure 5.2.9.2V, X). Together these results suggest that ablation of neural crest does not effect the Fgf signalling pathway, but may effect Wnt and Shh activity.

Figure 5.2.9.1 – The effects on *fgf8*, *wnt1*, *shh* and their reporter genes when neural crest is ablated in *tfap2a-/c-* morphants

Images are of non-injected controls and *tfap2a-/c-* morpholino injected at 24 hpf. (A) Lateral and (C) dorsal views of non-injected controls showing *fgf8* expression in the dorsal diencepalon, telencephalon and isthmus. (B) Lateral and (D) dorsal views of *tfap2a-/c-* morphants, revealing *fgf8* expression similar to the control in A and C. (E) Lateral and (G) dorsal views of non-injected controls showing *pea3* expression in the isthmus and eye. (F) Lateral and (H) dorsal views of *tfap2a-/c-* morphants, revealing *pea3* expression similar to the control in E and F. (I) Lateral and (K) dorsal views of non-injected controls showing *wnt1* expression in the dorsal diencephalon, isthmus and along the dorsal midline of the mesencephalon. (J) Lateral and (L) dorsal views of *tfap2a-/c-* morphants, revealing a reduction in *wnt1* expression along the dorsal midline of the mesencephalon. An increase in *wnt1* expression in the isthmus can also be seen. (M) Lateral and (O) dorsal views of non-injected controls showing *axin2* expression in the diencephalon, isthmus and along the dorsal midline. (N) Lateral and (P) dorsal views of *tfap2a-/c-* morphants revealing reduced *axin2* expression. (Q) Lateral and (S) dorsal views of non-injected controls showing *shh* expression in the ventral brain and ZLI. (R) Lateral and (T) dorsal views of *tfap2a-/c-* morphants, revealing *shh* expression similar to the controls in Q and S. (U) Lateral and (W) dorsal views of non-injected controls showing *ptd2* expression in the ventral brain and ZLI. (V) Lateral and (X) dorsal views of *tfap2a-/c-* morphants revealing *ptd2* expression similar to the controls in U and W.

Scale bar = 100 μm

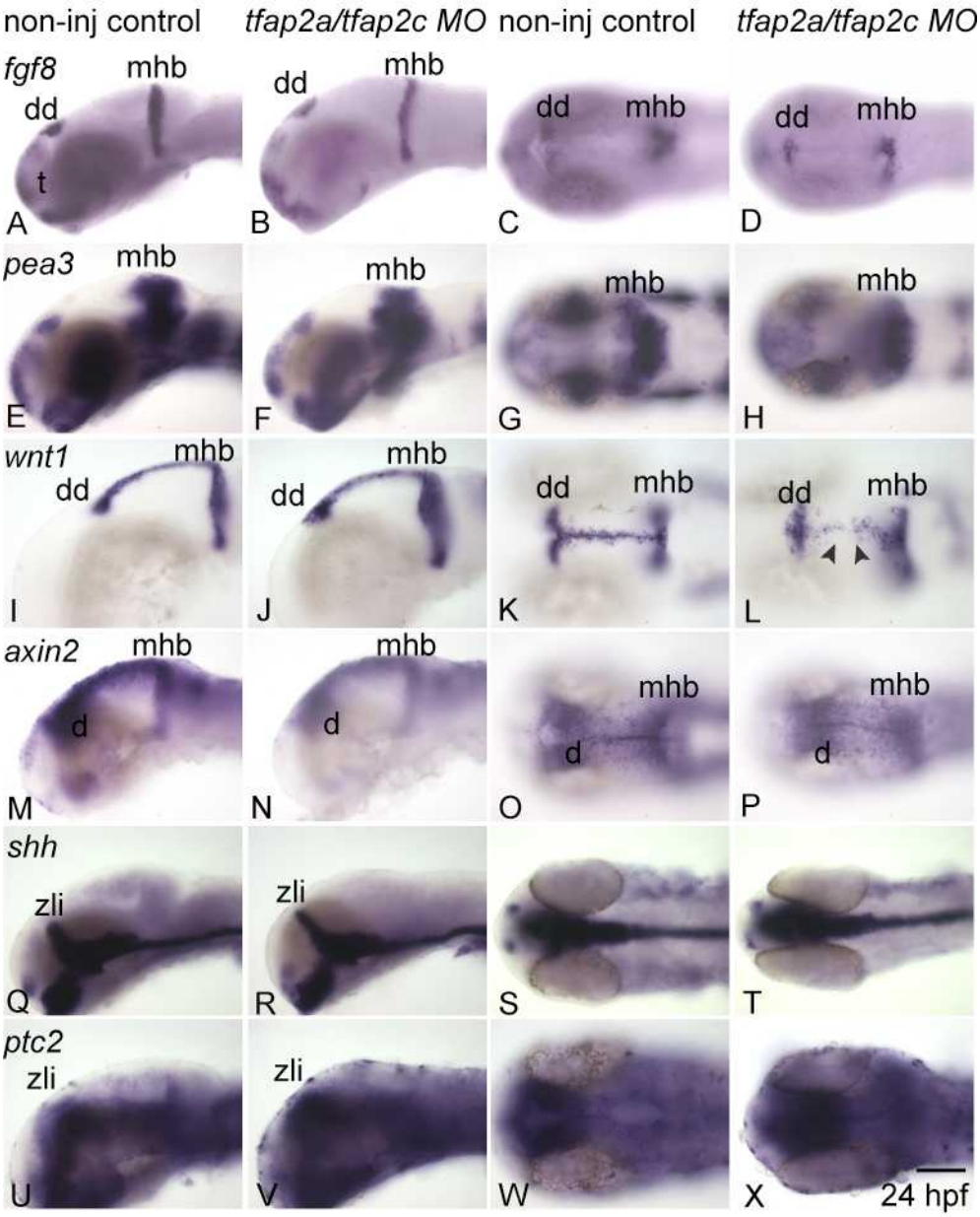
non-inj control
tfap2a/tfap2c MO
non-inj control
tfap2a/tfap2c MO
fgf8
mhb
dd
t
A
B
C
D
pea3
E
F
G
H
wnt1
I
J
K
L
axin2
d
M
N
O
P
shh
zli
Q
R
S
T
ptc2
U
V
W
X
24 hpf

Figure 5.2.9.2 – The effects on *fgf8*, *wnt1*, *shh* and their reporter genes when neural crest is ablated in *foxd3-/tfap2a-* morphants

Images are of non-injected controls and *foxd3-/tfap2a-* morpholino injected at 24 hpf. (A) Lateral and (C) dorsal views of non-injected controls showing *fgf8* expression in the dorsal diencepalon, telencephalon and isthmus. (B) Lateral and (D) dorsal views of *foxd3-/tfap2a-* morphants, revealing *fgf8* expression similar to the control in A and C. (E) Lateral and (G) dorsal views of non-injected controls showing *pea3* expression in the isthmus and eye. (F) Lateral and (H) dorsal views of *foxd3-/tfap2a-* morphants, revealing *pea3* expression similar to the control in E and F. (I) Lateral and (K) dorsal views of non-injected controls showing *wnt1* expression in the dorsal diencephalon, isthmus and along the dorsal midline of the mesencephalon. (J) Lateral and (L) dorsal views of *foxd3-/tfap2a-* morphants, revealing a slight reduction in *wnt1* expression along the dorsal midline of the mesencephalon. (M) Lateral and (O) dorsal views of non-injected controls showing *axin2* expression in the diencephalon, isthmus and along the dorsal midline. (N) Lateral and (P) dorsal views of *foxd3-/tfap2a-* morphants revealing *axin2* expression similar to the control in M and O. (Q) Lateral and (S) dorsal views of non-injected controls showing *shh* expression in the ventral brain and ZLI. (R) Lateral and (T) dorsal views of *foxd3-/tfap2a-* morphants, revealing a loss of *shh* expression in the ZLI. (U) Lateral and (W) dorsal views of non-injected controls showing *ptd2* expression in the ventral brain and ZLI. (V) Lateral and (X) dorsal views of *foxd3-/tfap2a-* morphants revealing a loss of *ptd2* expression in the ZLI.

Scale bar = 100 μm

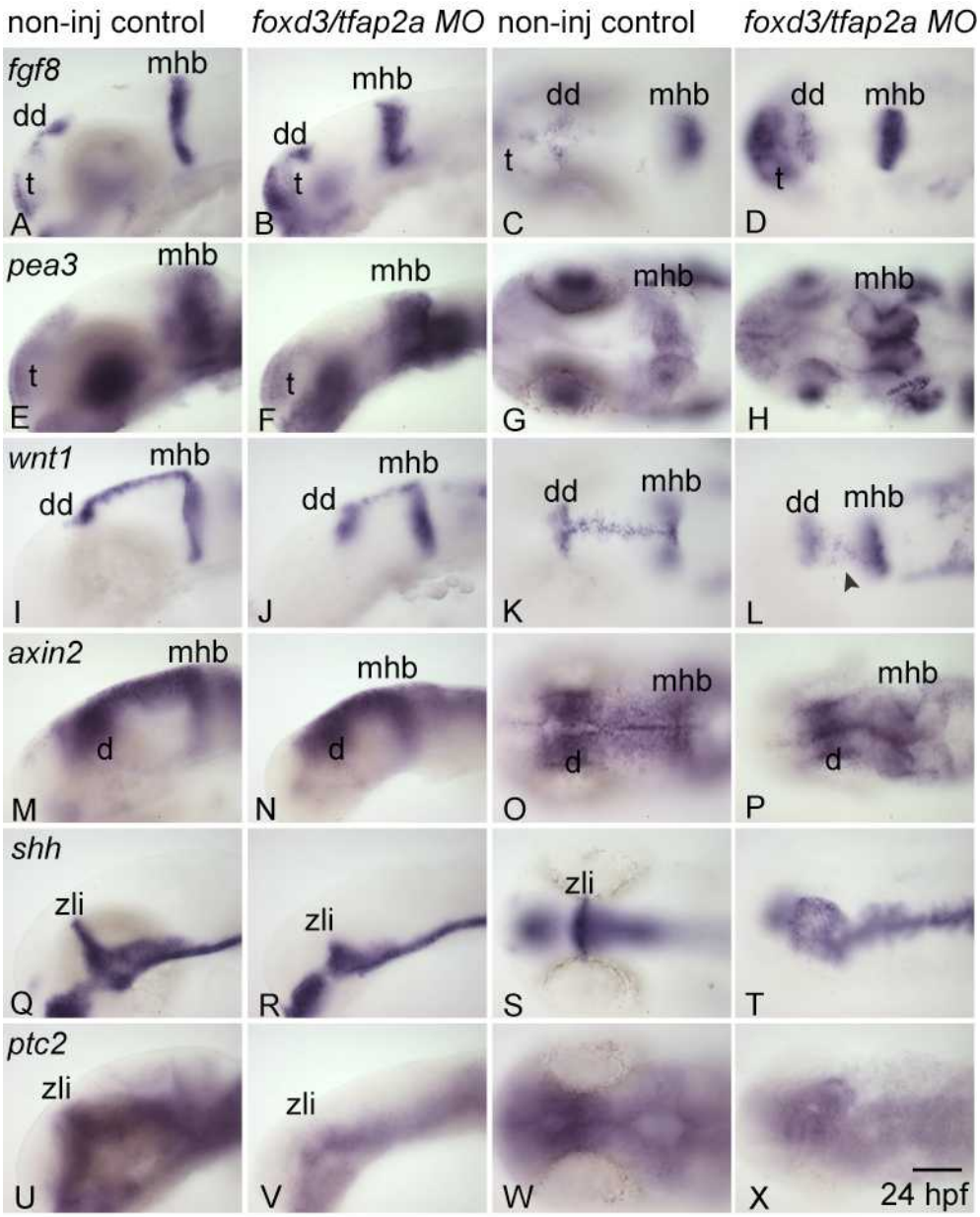
non-inj control
foxd3/tfap2a MO
non-inj control
foxd3/tfap2a MO
fgf8
mhb
dd
t
A
B
C
D
pea3
E
F
G
H
wnt1
I
J
K
L
axin2
d
M
N
O
P
shh
zli
Q
R
S
T
ptc2
U
V
W
X
24 hpf

5.2.10 – Effects on neural crest following changes to Fgf and Wnt signals

The ablation of neural crest results in an increase in the number of MTN neurons, similar to conditions in which the Fgf and Wnt signalling pathways are affected. Therefore the increase in numbers of MTN observed when these pathways are affected may be due to an indirect effect via a neural crest cells. I therefore analysed the expression patterns of neural crest markers *dlx2*, and *sox10*, in SU5402 and BIO treatments, *ace* and *mbl* mutants, to determine if there are obvious alterations to neural crest after changes to Fgf or Wnt signalling.

In animals with a loss of Fgf signalling after SU5402 treatment, *sox10* expression in the midbrain appeared to be lateralised; *sox10* is expressed further from the midline, relative to expression in the wild type (Figures 5.2.10.1A, B, E, F). Similarly when Wnt was up-regulated by BIO drug treatment, *sox10* expression was also lateralised (Figures 5.2.10.2A, B, E, F). In the *ace* and *mbl* mutants, however, the positions of neural crest cells expressing *sox10* was comparable to siblings, but their numbers appear to be increased (Figures 5.2.10.1C, D, G, H and 5.2.10.2C, D, G, H).

A complete loss of *dlx2* expression in the mandibular and hyoid pharyngeal arches, was seen in SU5402 and BIO treated animals, similar to the loss of *pea3* expression in SU5402 and BIO treated zebrafish (Figures 5.2.10.1I – P, and 5.2.10.2I – P). Interestingly *dlx2* expression in *ace* and *mbl* mutants was similar to siblings, revealing that neural crest in the arches is unaffected in these mutants.

These results suggest that numbers of MTN neurons are unlikely to be elevated indirectly via neural crest when the Fgf and Wnt signalling pathways are affected.

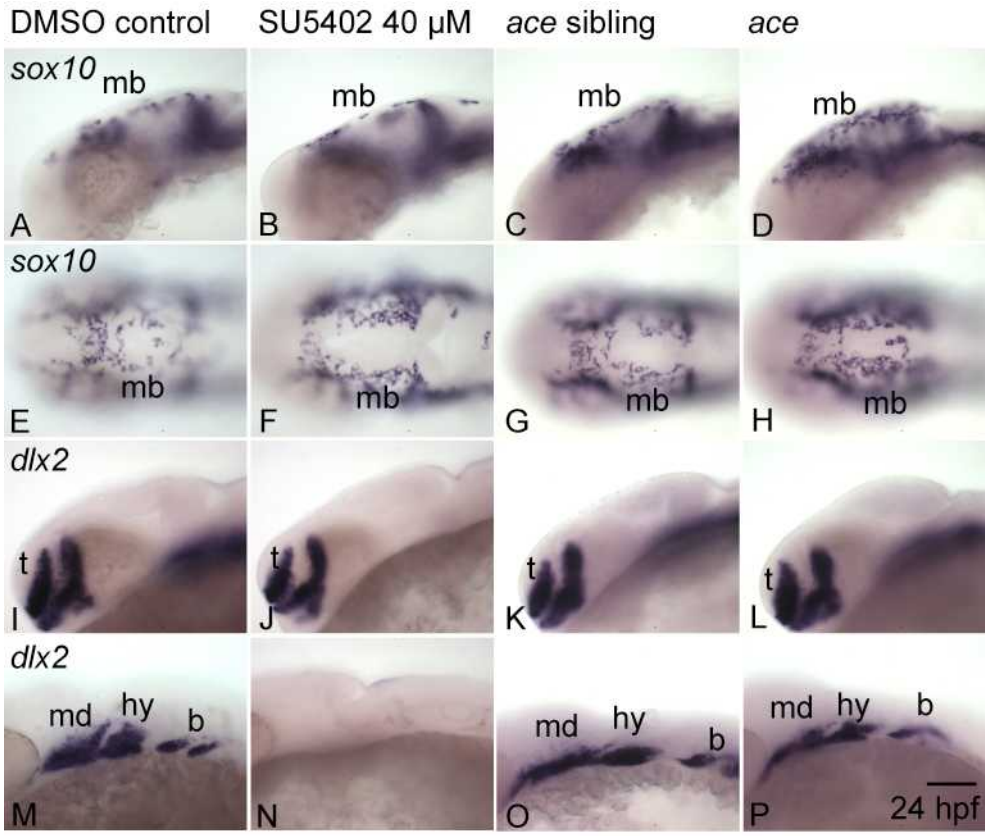

Figure 5.2.10.1 – The effects on *sox10* and *dlx2* expression when Fgf is down-regulated in SU5402 treatments and *ace* mutants compared to controls

Lateral views of (A) DMSO control showing *sox10* expression in neural crest cells, and (B) SU5402 treated zebrafish (10 ss), revealing lateralised *sox10* expression from the midline. Lateral views of (C) *ace* sibling showing *sox10* expression, and (D) *ace* mutant revealing an increase in *sox10* expression in neural crest. Dorsal views of (E) DMSO control showing *sox10* expression, and (F) SU5402 treated zebrafish (10 ss), revealing lateralised *sox10* expression in neural crest cells. Dorsal views of (G) *ace* sibling, showing *sox10* expression, and (H) *ace* mutant revealing increased *sox10* expression in neural crest. Lateral views of (I) DMSO control showing *dlx2* expression in the telencephalon, and (M) the pharyngeal arches, and (J) SU5402 treated zebrafish, revealing *dlx2* expression similar to M, and (N) loss of *dlx2* expression in the pharyngeal arches. Lateral views of (K) *ace* sibling showing *dlx2* expression in the telencephalon and (O) the pharyngeal arches, and (L) *ace* mutant revealing *dlx2* expression in the telencephalon and (P) pharyngeal arches similar to K and O. b. branchial arch, h. hyoid, mb, mandibular arch.

Scale bar = 100 µm

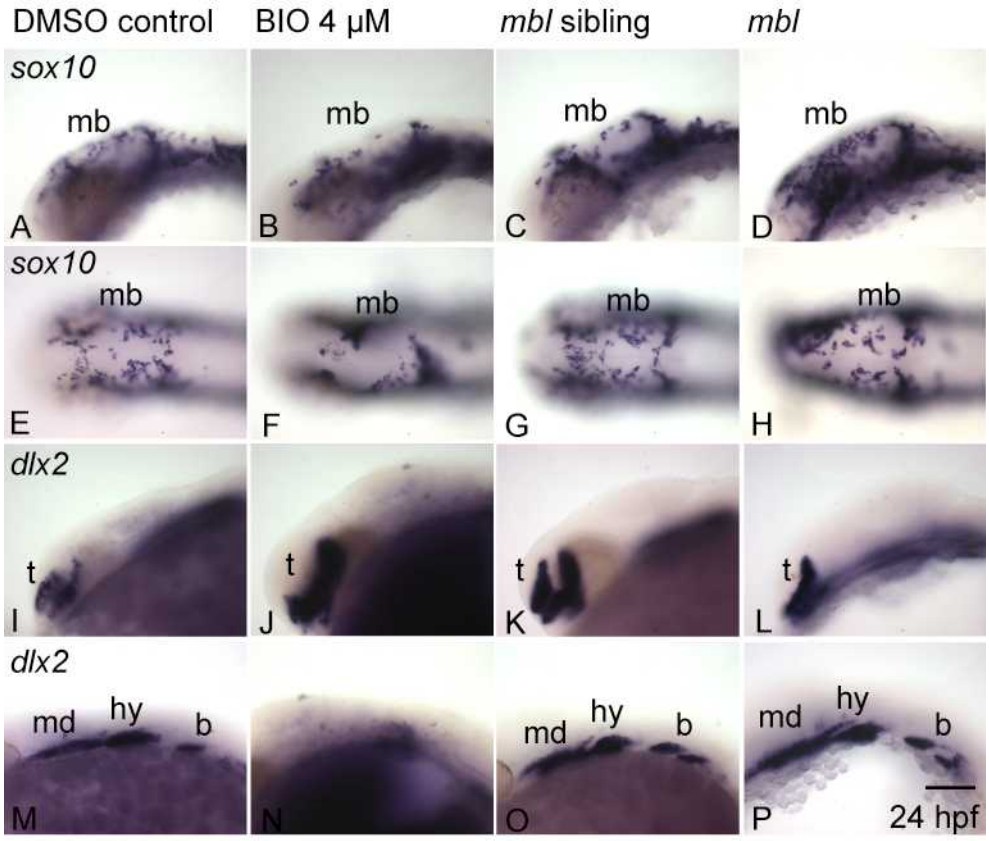

Figure 5.2.10.2 – The effects on *sox10* and *dlx2* expression when Wnt is up-regulated in BIO treatments and *mbl* mutants compared to controls

Lateral views of (A) DMSO control showing *sox10* expression in neural crest cells, and (B) BIO treated zebrafish (10 ss), revealing lateralised *sox10* expression either side of the midline. Lateral views of (C) *mbl* sibling showing *sox10* expression, and (D) *mbl* mutant revealing an increase in *sox10* expression in neural crest. Dorsal views of (E) DMSO control showing *sox10* expression, and (F) BIO treated zebrafish (10 ss), showing lateralised *sox10* expression in neural crest cells. Dorsal views of (G) *mbl* sibling, showing *sox10* expression, and (H) *mbl* mutant revealing *sox10* expression similar to G. Lateral views of (I) DMSO control showing *dlx2* expression in the telencephalon, and (M) the pharyngeal arches, and (J) BIO treated zebrafish, revealing increased *dlx2* expression in the telencephalon, and (N) loss of *dlx2* expression in the pharyngeal arches. Lateral views of (K) *mbl* sibling showing *dlx2* expression in the telencephalon and (O) the pharyngeal arches, and (L) *mbl* mutant revealing *dlx2* expression in the telencephalon and (P) pharyngeal arches similar to K and O. b. branchial arch, h. hyoid, mb, mandibular arch.

Scale bar = 100 µm

5.2.11 – There is no epistatic interaction between neural crest and Fgf signalling regulating MTN development

Ablation of neural crest and down-regulation of Fgf, results in an increase in the number of MTN forming in the zebrafish midbrain. To assess whether there are any interactions occurring between neural crest and Fgf signalling, that regulate MTN development, I have combined morpholino injections with SU5402 treatments at varying concentrations (see materials and methods). This was to determine whether the combined partial loss of neural crest and Fgf signalling enhanced the number of MTN that develop compared to ablation of neural crest or knockdown of Fgf signalling alone.

drg11 was used as before, to visualise MTN neurons. The average number of MTN in DMSO controls were comparable to numbers in previous experiments. When the neural crest was partially ablated (0.4µM *tfap2a-*/0.2µM *tfap2c-*), or the Fgf signalling pathway partially down-regulated (20uM) respectively, there was an increase in the number of MTN neurons (0.4µM *tfap2a-*/0.2µM *tfap2c-* MO, 8.4;SU5402 20µM, 6.8) compared to wild type controls (4.8) (Figure 5.2.11.1A, B, J, K, M, N; Figure 5.2.11.2). The average number of MTN neurons increased further in zebrafish where Fgf signalling alone was further down-regulated (40µM SU5402, 10.8; Figure 5.2.11.1P, Q; Figure 5.2.11.2).

When both neural crest and Fgf signalling were partially ablated within the same animal, the average number of MTN (10.2; Figure 5.2.11.1D, E) was slightly higher than the average numbers of MTN neurons observed when the neural crest alone was partially ablated (0.4µM *tfap2a-*/0.2µM *tfap2c-* MO, 8.4; Figure 5.2.11.2).

In contrast, when neural crest was partially ablated and the Fgf signalling pathway further down-regulated, the average number of MTN (8.4; Figure 5.2.11.1 G, H; Figure 5.2.11.2) was the same as the average number of MTN when neural crest alone was partially ablated (8.4). These fish were severely retarded suggesting toxicity. A Chi-Squared test of independence was used, which revealed there to be no significant support for an epistatic relationship between Fgf signalling and neural crest in directing MTN development ($p = 0.08$).

The number of MTN neurons forming in the combined partial ablation was comparable to individual partial ablation. These results suggest that Fgf signalling and neural crest are not acting epistatically to regulate MTN development.

Figure 5.2.11.1 – Neural crest and Fgf signalling interactions are not required for MTN development

(A) Lateral, and (B) dorsal views of a zebrafish head, where the neural crest has been partially ablated by *tfap2a-/c-* morpholino injection, showing slightly increased numbers of MTN cell bodies expressing *drg11*, and (C) *drg11* expression in the trunk similar to control. (D) Lateral, (E) dorsal, and (F) trunk views of zebrafish where neural crest and Fgf signalling together have been partially ablated, revealing *drg11* expression similar to animals where neural crest has been partially ablated alone in A, B and C. (G) Lateral, (H) dorsal views of zebrafish where neural crest has been partially ablated and Fgf signalling down-regulated, revealing a reduction in numbers of MTN expressing *drg11* and (I) a reduction in RBs expressing *drg11*. (J) Lateral, (K) dorsal views of a non-injected, DMSO control showing *drg11* expression in MTN neurons and nTPC, and (L) *drg11* expression in the trunk. (M) Lateral, and (N) dorsal views of zebrafish where Fgf signalling has been partially ablated by SU5402 treatments (20μM), revealing slightly increased numbers of MTN cell bodies expressing *drg11* similar to A, B and C, and (O) a reduction in RBs expressing *drg11* in the trunk. (P) Lateral, and (Q) dorsal views of zebrafish where Fgf signalling has been down-regulated, revealing an increase in numbers of MTN expressing *drg11*, and (R) reduced *drg11* expression in the trunk.

Scale bar = 100 μm

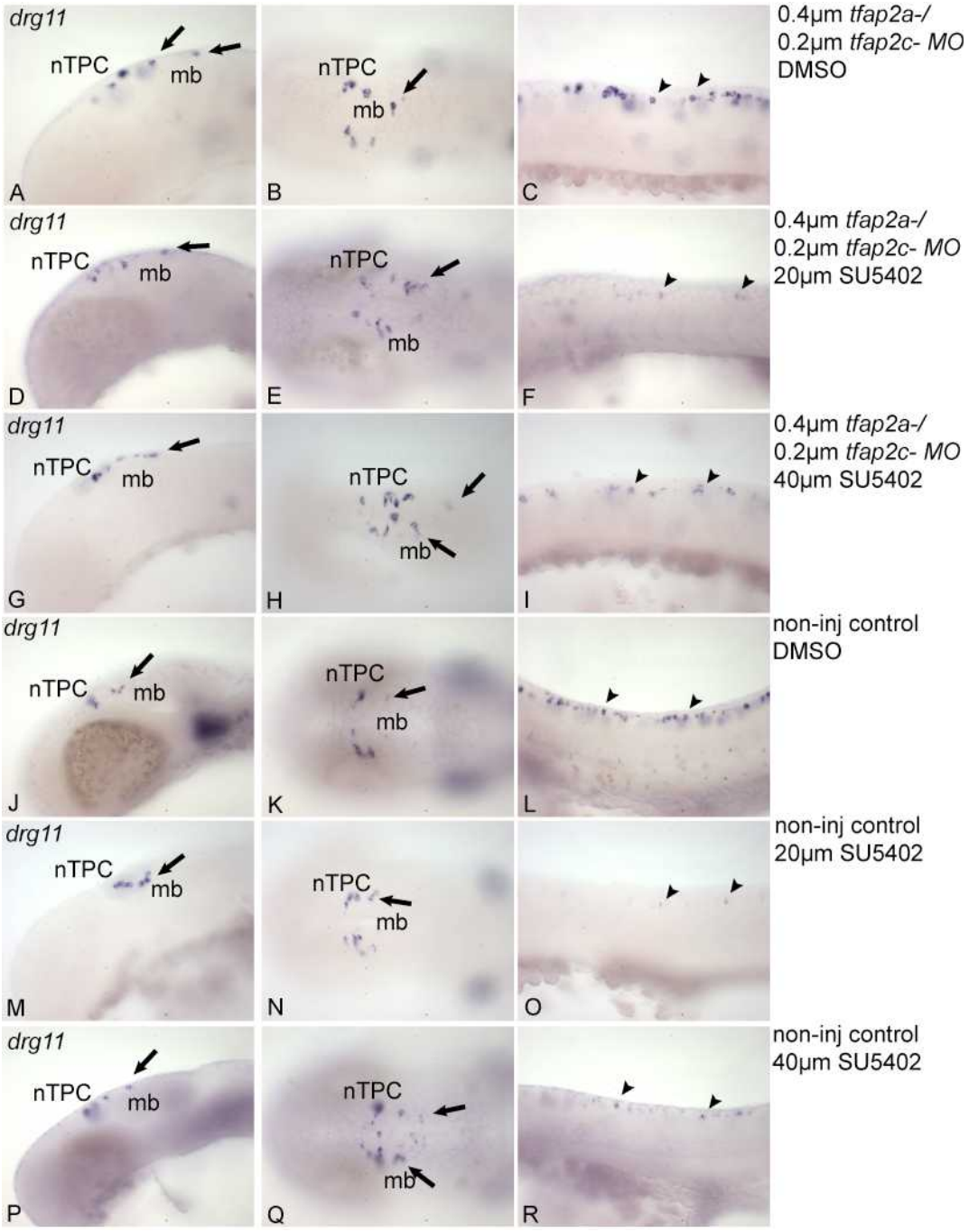
drg11
nTPC
mb
A
B
C
0.4µm tfap2a-/
0.2µm tfap2c- MO
DMSO
D
E
F
20µm SU5402
G
H
I
40µm SU5402
J
K
L
non-inj control
DMSO
M
N
O
non-inj control
20µm SU5402
P
Q
R
non-inj control
40µm SU5402

Figure 5.2.11.2 – Neural crest and Fgf signalling interactions are not required for MTN development

(A) Table showing the average numbers of MTN cell bodies counted per zebrafish in DMSO control compared to zebrafish where neural crest, and Fgf signalling is partially ablated in individual animals and within the same animal. The average numbers of MTN cell bodies in Fgf down-regulated individual animals and where neural crest has been partially ablated, is also shown (n = 10). (B) Graph showing the differences in MTN numbers, and standard error of the mean, in the various conditions.

A)

Condition	Average MTN number in morphants and treatments labelled with *drg11*
DMSO control/KWT	4.8 ± 0.25
DMSO control/*tfap2a-/c*- 0.5µM	8.4 ± 0.34
20µM SU5402/KWT	6.8 ± 0.29
20µM SU5402/*tfap2a-/c*- 0.5µM	10.2 ± 0.65
40µM SU5402/KWT	10.8 ± 0.4
40µM SU5402/ *tfap2a-/c*- 0.5µM	8.4 ± 0.51

B)

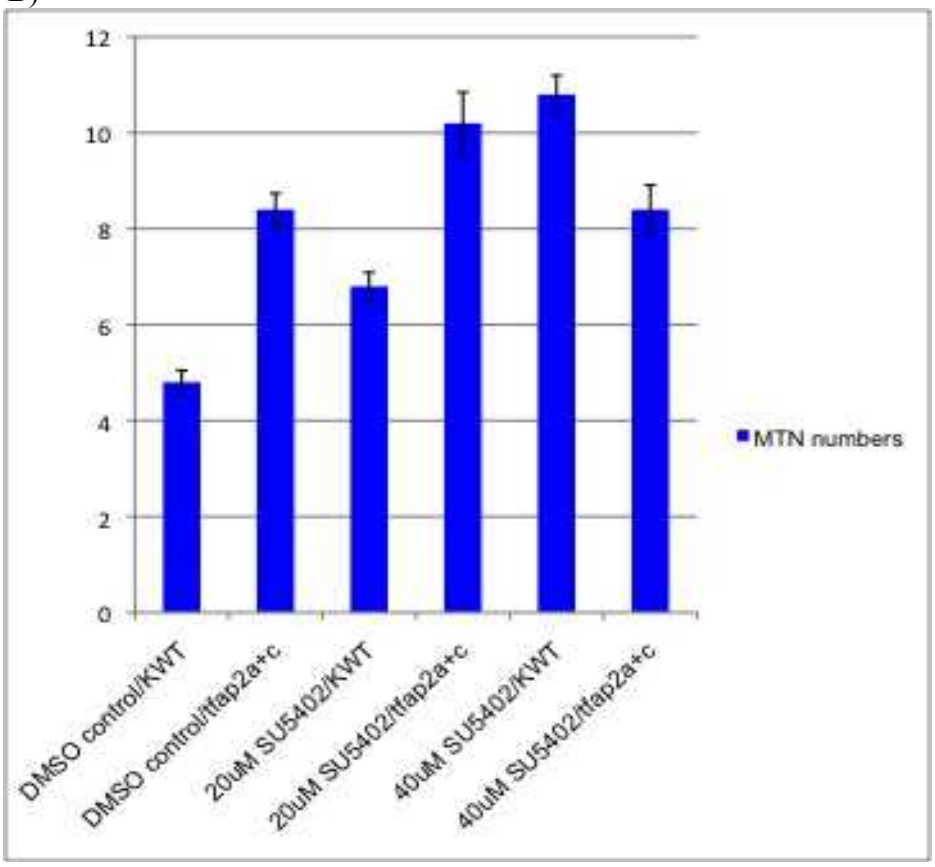

5 .3 – Summary

The neural crest is an embryonic cell population that gives rise to a diverse number of cell types. Neural crest cells play a major role in head development and form neurons, glia, cartilage and bone (in the head). Importantly, they also give rise to the peripheral sensory neurons, including the proprioceptive neurons in the DRG.

In this chapter I have assessed the role of neural crest during MTN development with the aim to determine if MTN neurons are derived from neural crest. My results support the hypothesis that MTN are not derived from neural crest, but that neural crest cells inhibit MTN development.

A comparison of *sox10* and *foxd3* expression to MTN neurons expressing *drg11* showed that there was no co-localisation, but comparison of *Tg(sox10:eGFP)* transgenic fish with *drg11* and *isl1*, revealed some co-localisation. However the *Tg(sox10:eGFP)* transgenic line is not the most reliable way to determine co-expression because the GFP is expressed in some non-neural crest cells too.

Analysis of mutants and morphants in which neural crest was ablated suggest MTN is not neural crest derived. In *cls* mutants there was no significant change in MTN number. However in *tfap2a-/c-* double morphants there was an increase in the number of MTN, similar to that seen when Fgf was down-regulated and Wnt up-regulated. Losses of non-neural ectoderm in *tfap2a-/c-* double morphants imply that the increase in MTN numbers may have been due to the loss of this tissue type rather then neural crest. Morpholinos directed against *foxd3-* and *tfap2a-* were co-injected which specifically ablates the neural crest and does not affect non-neural ectoderm. In these *foxd3-/tfap2a-* double morphants the same MTN phenotype was seen as in *tfap2a-/-c-* morphants. These results show that MTN are not neural crest derived, but NCCs may play a role in MTN specification.

Chapter 6: Discussion

The MTN is a crucial sensory nucleus in the head that conveys proprioception from the jaw muscles to the brain in mammals, and from the skin and perioral area of the jaw in vertebrates. It is evolutionarily ancient and may have evolved in conjunction with a jaw, but its molecular and cellular development has been investigated in a limited number of studies.

In this thesis, I identify and describe the anatomy of the MTN and its gene expression profile during development in zebrafish. The cellular origin of MTN has been controversial, with some studies suggesting it is derived from neural crest, while others imply it is not (Narayanan and Narayanan, 1978; Baker et al., 1997a). I present data that shows that MTN neurons are not neural crest derived, but that MTN neurons may share a common progenitor with neural crest. To determine how MTN is regulated during midbrain development, the Fgf and Wnt signalling pathways are tested for their roles in specifying or inhibiting MTN formation. This reveals that Fgf signalling negatively regulates MTN specification, and Wnt signalling positively regulates MTN development. The results of the analysis are presented in a model that shows how MTN neurons are specified in the anterior forebrain during vertebrate development.

6.1 – MTN development is conserved in vertebrates

6.1.1 – Characterisation of zebrafish MTN

Only one previous study has identified MTN neurons in the zebrafish and this only described them as located in the midbrain, similar to amniotes (mouse, Weinberg, 1928; cat, Alvarado-Mallart et al., 1975; zebrafish, Kimmel et al., 1985; chick, Hunter et al., 2001). MTN neurons have also been identified in shark (Roberts and Witkovsky, 1975; Kuratani and Horigome, 2000), and teleosts (Goldfish, Puzdrowski et al., 1988; Guppy, Pombal et al., 1997; Medaka, Ishikawa et al., 2004).

In this study, the retrograde labelling with DiI applied to the adductor mandibulae revealed MTN neurons in the dorsal anterior mesencephalon of the embryonic zebrafish brain. The location of MTN cell bodies in the midbrain of zebrafish is consistent with that of MTN cell bodies identified in other teleosts and species such as shark, mouse, chick and cat. In mammals, MTN cell bodies have also

been identified in the rostral hindbrain (Alvarado-Mallart et al., 1975; Ruggiero et al., 1982; De et al., 2005). In the zebrafish however, MTN cell bodies are more restricted to the dorsal anterior mesencephalon, caudal to diencephalic neurons of the nTPC. In mouse and chick, labelling with lipophilic dyes applied to the dorsal – lateral mesencephalon, or with cell adhesion molecules (BEN), revealed MTN are distributed throughout most of the rostrocaudal extent of the dorsal mesencephalon, though they are absent in the most caudal region in chick (Stainier and Gilbert, 1990; Stainier and Gilbert, 1991; Chedotal et al., 1995). In particular, MTN cell bodies in the embryonic mouse (from E10.0) are also located dorsally in prosomere 1 (p1), the posterior region of the diencephalon, and in the hindbrain (Mastick and Easter, 1996; De et al., 2005).

Studies of the MTN in chondrichthyes (the catshark), and teleosts (the guppy and medaka) identified MTN cell bodies restricted to the dorsal anterior mesencephalon, as in zebrafish (Pombal et al 1997; Kuratani and Horigome, 2000: Ishikawa et al., 2004). However, in another teleost the carp, MTN cell bodies are situated in a more ventral location, in the dorsal mesencephalic tegmentum (Luiten, 1979). In lungfish MTN are located in the anterior ventral tectum (von Bartheld, 1992).

The labelling of MTN neurons from DiI application to the a.m. of zebrafish suggests that the innervation of jaw muscles by MTN neurons is conserved in bony fish. In previous studies, HRP was injected into the masticatory muscles of chick and frog, and also labelled MTN (Hiscock and Straznicky, 1982; 1986; Figure 6.1). In contrast, HRP labelling studies in other teleosts have not identified any innervation of jaw muscles by the MTN. For example a study in adult carp in which the mandibular arch muscles were injected with HRP, resulted in no retrogradely labelled MTN neurons, implying they do not innervate these muscles (Luiten, 1979). MTN neurons were shown to innervate the perioral area of the jaw instead. It is possible that HRP labelling of the muscle did not label MTN neurons because MTN terminals did not come into sufficient contact with the HRP; and also only a limited number of these experiments were carried out (Nauta et al., 1974). In shark the MTN does not appear to innervate the jaw muscles either, and again appears to innervate the perioral area of the jaw (Roberts and Witkovsky, 1975; Figure 6.1A). This was shown by stimulating the jaw opening and closing muscles, which failed to cause a measured response in the MTN. The results from my DiI labelling of the mandibular muscles suggests that the MTN does innervate jaw muscles in teleosts.

Alternatively the MTN may not innervate the mandibular muscles in zebrafish, but innervate the perioral area around these muscles instead, as has been

shown in carp, goldfish, guppy, medaka (Luiten, 1979; Puzdrowski et al., 1988; Pombal et al., 1997; Ishikawa et al., 2004) and in shark (Roberts and Witkovsky,1985). The DiI applied to the mandibular muscles in this thesis may have been taken up by the MTN innervating the skin adjacent to these muscles. However when labelling the muscle with DiI, those which failed to retrogradely label the MTN (30/50) were those in which the DiI appeared to be restricted to the skin; suggesting that the MTN does innervate the muscle in zebrafish. To test this further alternative application methods could be used; such as specifically applying DiI crystals to the surface of the skin in the perioral area above the mandibular muscles, or by applying DiI crystals to cut skin of the perioral area. Anterograde labelling of MTN cell bodies to follow the axons to the regions they innervate, would also help to determine if they innervate these muscles.

HRP labelling of extraocular muscles the superior rectus, inferior rectus, medialis rectus, superior oblique and inferior oblique reveal that the MTN also innervates these muscles in some amniotes (cat, Alvarado-Mallart et al., 1975; rat, Matesz, 1981; Figure 6.1). In frog the MTN was also seen to innervate some extraocular muscles; the superior rectus, inferior rectus, and superior oblique (Hiscock and Straznicky, 1982). However no MTN neurons were labelled after HRP injections to the inferior oblique and lateral rectus extraocular muscles in frog (Hiscock and Straznicky, 1982). I only applied DiI to the mandibular arch muscles in zebrafish, therefore I am unable to conclude if MTN neurons in zebrafish also innervate the extraocular muscles.

In some DiI applications to the a.m. muscle the inferior oblique eye muscle was also labelled. In these samples the MTN cell bodies labelled were numerically comparable to those in which DiI was only applied to the a.m. This implies that the MTN does not innervate this eye muscle, similar to frog and chick (Hiscock and Straznicky, 1982; 1986). It is possible that MTN neurons in zebrafish only innervate the jaw-closing muscles.

Figure 6.1 – Targets of the MTN in vertebrates

(A) Table summarising the tissues innervated by axons of the MTN in different species. (B) Diagrammatic representation of the MTN, its axonal projections and the regions it innervate in amniotes. the mesencephalic trigeminal nucleus (MTN, purple), located in the midbrain (mb) and hindbrain (hb), the mandibular branch of the trigeminal motor nerve (nV, green) and mandibular arch muscles (am, lap, do). The MTN is also shown innervating the eye muscles together with the oculomotor motor nerve (nIII, blue; io, ir, mr, sr) and the trochlear motor nerve (nIV, red; so)(Alvarado-Mallart et al., 1975; Ruggiero et al., 1982). am, adductor mandibulae. do, dilator operculi. hb,hindbrain. io, inferior oblique. ir, inferior rectus. lap, levator arcus palatini. mb, midbrain. nIII, oculomotor motor nerve. nIV, trochlear motor nerve. nV, trigeminal motor nerve. mr, medial rectus. so, superior oblique. sr, superior rectus.

A)

	trigeminal branches			Synapses with motor nerve				tissue innervates			
	opth	max	mand	III	IV	V	VI	jaw muscle	eye muscle	skin	teeth
cat	√	√	√	√	√	√	√	√	√	√	√
mouse	√	√	√			√		√		√	√
rat	√	√	√	√	√	√	√	√	√	√	√
bird			√			√		√			
turtle (reptile)			√					√			
frog		√		√		√		√	√		
zebrafish		√				√ ?		√			
guppy		√				√				√	
goldfish	√	√	√			√				√	
carp		√				√ ?				√	
shark (dogfish)	√	√	√			√				√	√

B)

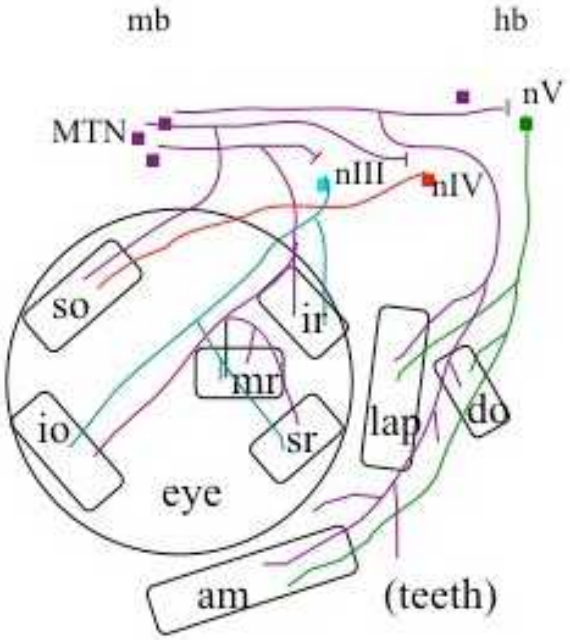

Retrograde labelling of jaw muscles by DiI in *Tg(1.4dlx4-6:GFP)* transgenic fish that labels mesencephalic neurons, revealed a proportion of these neurons were MTN. The absence of GFP in some of the DiI labelled cell bodies may be because there is mosaic expression in dorsal cells in the *Tg(1.4dlx4-6:GFP)* transgenic line, and possible variation in expression of the transgene. However it may also imply that there are sub-populations of MTN neurons. In the chick, four neuronal populations of the developing MTN have been identified. These are: a medial group located at the tectal commissure, a lateral group located more ventrally in the optic tectal hemisphere, a group outside the neural tube, and a group located at the posterior commissure (Sanchez et al., 2002; von Bartheld and Bothwell, 1993). These latter two groups emigrate from the neuroepithelium from E6 to merge with the medial and lateral populations, resulting in the MTN forming just two neuronal populations in adult chicks (von Bartheld and Bothwell, 1993). No topographic mapping to specific mandibular muscles was seen between the two groups.

It is unclear from the DiI labelling of MTN cell bodies in *Tg(1.4dlx4-6:GFP)* transgenic fish, whether there are populations of MTN neurons arising in different locations similar to in chick. However, live imaging of MTN neurons in *Tg(huC:eGFP)* transgenic zebrafish shows one population of MTN neurons that is born along the dorsal midline of the anterior mesencephalon. This is comparable to the earliest population of MTN neurons born in the midbrain in the mouse, frog and chick which is located in the rostral part of the mesencephalon (Stainier and Gilbert, 1990; Hiscock and Straznicky, 1982; Chedotal et al., 1995).

The formation of MTN neurons along the dorsal midline in zebrafish, resembles the C-division of neural plate cells during formation of the neural tube. During C-division neural plate cells divide mediolaterally along the midline of the neural keel (Clarke, 2009). As the cells divide one daughter cell remains in the ipsilateral side of the neural keel, while the other daughter cell crosses the midline and integrates into the contra-lateral neuroepithelial layer (Concha and Adams, 1998). In timelapse analysis of *Tg(huC:eGFP)* transgenic zebrafish, MTN cells also appear to divide along the dorsal midline and move in opposite directions to a more lateral position either side of the midline.

My results from the retrograde labelling of the MTN in zebrafish after applying DiI to the adductor mandibulae muscle of the jaw, suggests that the innervation of jaw muscles appears to be a conserved feature of bony vertebrates with the exception of shark and some teleosts.

6.1.2 – Conserved axonal pathways during MTN development

In amniotes MTN neurons form their own dorsal axonal tract which runs parallel to the ventral tracts formed by the mammilotegmental tract (MTT) and medial longitudinal fasciculus (mlf; Mastick and Easter, 1996). MTN neurons in shark and some teleosts (medaka and guppy) also have dorsal mesencephalic tracts (Barreiro-Iglesias et al., 2008), but it is unclear if MTN neurons in zebrafish form an individual mesencephalic tract. Analysis of the axonal pathways of zebrafish MTN neurons reveals they potentially form a dorsal tract, similar to that described in mouse and chick.

In zebrafish MTN axons grew ventrally and laterally from the dorsal midline, posterior to the adjacent tract of the posterior commissure (TPC), and rostrally towards the nV (Figure 6.2).

Figure 6.2 – MTN neurons in the zebrafish form a dorsal tract similar to in other vertebrates.

Diagrammatic representation of the axonal tracts in an embryonic zebrafish, showing that MTN neurons form a dorsal tract (purple) similar to amniotes. Image adapted from Barreiro-Iglesias et al., 2008. AC, anterior commissure. DMT, Dorsal mesencephalic tract. DVDT, dorso-ventral diencephalic tract. e, epiphysis. ha, habenula. MLF, medial longitudinal fasciculus. MTN, mesencephalic trigeminal nucleus. PC, posterior commissure. POC, postoptic commissure. SOT, supraoptic tract. THC, tract of the habenula commissure. TPC, tract of the posterior commissure. TPOC, tract of the postoptic commissure.

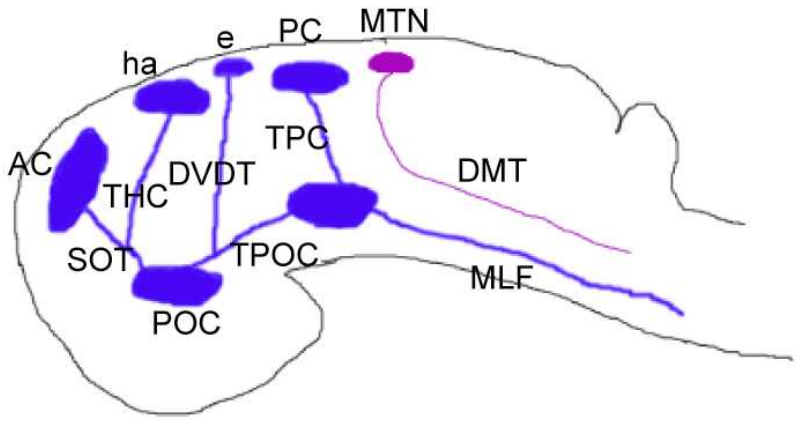

In mouse MTN neurons also project ventrally and form the descending tract of the mesencephalic nucleus of the trigeminal nerve (dtmesV). Axonal tracing studies in mouse have also revealed that while the rostral MTN axons forming the dtmesV intermix with the TPC, they form a separate tract to the TPC. They were distinguished from one another by the ascending pathway the axons of the nTPC follow (Mastick and Easter, 1996).

The rostrally forming tracts; the postoptic commissure (TPOC) and the supraoptic tract (SOT) that arise in the telencephalon in mouse have caudal trajectories that continue into the dtmesV. All these tracts project caudally to the rhomobencephalon (Easter et al., 1993). Similarly in chick the MTN projects axons ventrally in the dorsal mesencephalon and pioneers the lateral longitudinal fasciculus (LLF, Hunter et al.,

2001). The MTN axons cross the MHB into the hindbrain within the basal plate. In the hindbrain the axon branches and either synapses with the nuclei of the trigeminal nerve or follows the trigeminal motor nerve down to the mandibular arch muscles which they innervate (Molle et al., 2004; Butler and Hodos, 2005).

Previously in zebrafish only one longitudinal tract has been described, with the TPOC belonging to the ventral tract as opposed to the dorsal tract in amniotes, except at the level of the rhombencephalon where the dorsolateral tract (DLT) forms (Wilson, 1990; Ishikawa et al., 2004). In other teleosts, medaka and guppy, the MTN forms the dorsal mesencephalic tract (DMT) that is also separate to the TPC; this is located anterior to the DMT (Pombal et al., 1997; Ishikawa et al., 2004).

The MTN tracts in amniotes are dorsal to the mlf, therefore the MTN axons in zebrafish may also form their own tracts rather then merging with the more ventral mlf. In 5 dpf fish, in which MTN neurons were retrogradely labelled with DiI, the tract appears to be relatively dorsal passing through the tectum, and therefore unlikely to be following along the mlf. It is unclear from these studies, whether the MTN synapses with the nuclei of the trigeminal nerve (nV), similar to other vertebrates such as frog (Hiscock and Straznicky, 1982; Pratt et al., 2009). However, it is likely the MTN forms synapses to the nV, given the close apposition of MTN axons and nV.

These studies suggest the presence of a dorsal mesencephalic tract is conserved in vertebrates.

6.1.3 – MTN neurons and RB neurons may share a common evolutionary ancestor

MTN neurons are conserved in amniotes. However their evolutionary origin is unknown. MTN neurons are unusual because they are located in the CNS, unlike all other adult sensory neurons in jawed vertebrates. Sensory neurons of the cephalochordate amphioxus, an invertebrate chordate, are also situated in the CNS (Baker et al., 1997c; Lacalli and Kelly, 2003; Lacalli, 2004; Figure 6.3). These sensory neurons are segmentally arranged along the dorsal spinal cord and have been proposed to be primitive RB neurons (Bone, 1960; Lacalli and Kelly, 2003; Figure 6.4). After the divergence of agnathans and gnathostomes, dorsal cells (DC, homologous to RB neurons) appear to have persisted into adult stages of extant agnathan the sea lamprey (Anadon et al., 1989; Figure 6.3). The formation of the gnathostome lineage lead to the evolution of cartilaginous fishes (chondrichthyans, e.g. shark) and bony fishes

(osteichthyans). The bony fish lineage diverged further giving rise to the ray-finned fishes (actinopterygians), to which teleosts belong; and the lobe-finned fishes (sarcopterygians) to which lungfish and tetrapods belong (Cao et al., 1998). These different chordate groups have been evolving down their own separate lineages for over 500 million years, which appeared to result in the loss of RB neurons in amniotes (Baker et al., 1997c; Chen et al., 1995; Figure 6.3). All jawed vertebrates except amniotes have RB neurons which are only present in the spinal cord during early development, and are replaced by the adult sensory neurons the dorsal root ganglia (DRG) in later development (Hughes, 1957; Clarke et al., 1984; Kuratani and Horigome, 2000). In amniotes RB neurons have been lost, possibly because, unlike all other vertebrates, the larvae is protected inside the egg, so they do not need to develop a functioning larval nervous system..

Figure 6.3 – Evolution of chordates

(A) Phylogenetic tree of the chordates.

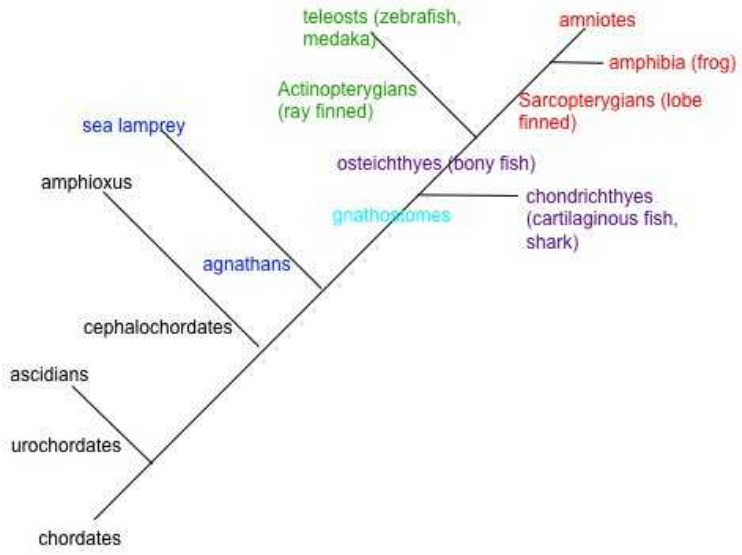

MTN neurons however, are present in most of the separate chordate lineages, which may imply they evolved from primitive RB neurons present in the mesencephalon of the common ancestor of vertebrates (Anadon et al., 1989).

MTN neurons possess similarities to RB neurons other than their CNS location. Both MTN and RB neurons convey proprioceptive information (Luiten, 1979; Clarke et al., 1984). In vivo timelapse imaging of developing neurons in *Tg(huC:eGFP)* zebrafish showed that MTN are early born neurons, as they are in amniotes (Stainier and Gilbert, 1990; Chedotal et al., 1995). Similarly RB neurons also begin to form early in development in frogs and teleosts, during late gastrulation before the neural tube as closed (Lamborghini, 1980; Bernhardt et al., 1990). Molecular characterisation of MTN neurons reveals they have a similar gene expression profile as RB neurons. MTN and RB neurons do exhibit some differences however; MTN neurons are uni-polar, as they send out a single axon, but RB neurons are bipolar with two axons projecting from their cells bodies (Bernhardt et al., 1990). This difference may have developed as MTN neurons evolved away from primitive RB neurons and became specialised.

In the agnathan vertebrate the Sea Lamprey, DCs are proposed to be a serial homologue of MTN cells (Nieuwenhuys, 1972; Anadon et al., 1989; Barreiro-Iglesias et al., 2008). These DCs have been described as homologous to MTN cell bodies because they are one of the earliest cells to arise in the brain, and they send axons through the trigeminal motor nerve (Barreiro-Iglesias et al., 2008). In amniotes 70% of MTN neurons are also positioned in the hindbrain, while the remaining 30% are located in the mesencephalon (Ruggiero et al., 1982; Lazarov 2007). It is possible that lamprey also possess MTN neurons as a small number of mesencephalic neurons were retrogradely labelled after injections of cobalt-lysine into the motor nucleus of the trigeminal nerve (Huard et al., 1999). Huard et al. (1999) did not examine this further due to the small numbers that were labelled, and instead focussed on the rhombencephalic populations which are responsible for mastication and swallowing in higher vertebrates (Huard et al., 1999). This role for rhombencephalic populations was based on studies in which the electromyographic activity was measured in masticatory muscles (Dellow and Lund, 1971; Lund, 1991). The presence of DC/RB neurons in the mesencephalon of the sea lamprey may imply that MTN neurons are DCs that have become specialised and have persisted during the evolution of jawed vertebrates (Figure 6.4).

Figure 6.4 – Locations of sensory neurons within the CNS

Diagrammatic representation showing the locations of sensory neurons within the CNS. Sensory neurons are located in the brain and dorsal spinal cord of the amphioxus, and sea lamprey. In zebrafish and frog primary sensory Rohon-Beard (RB) neurons are located in the dorsal spinal cord, and MTN neurons are positioned in the dorsal midbrain. MTN sensory neurons are positioned in the dorsal midbrain of mammals. DC, dorsal cell. MTN, mesencephalic trigeminal nucleus.

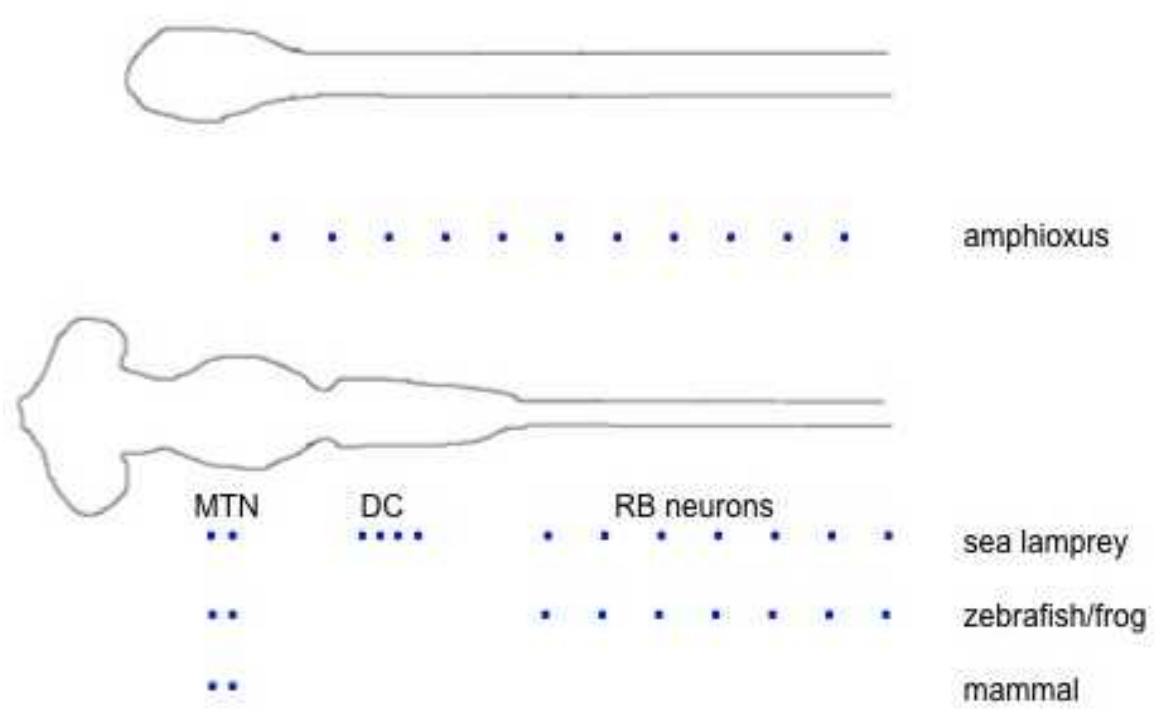

Alternatively MTN neurons may be a serial homologue of the neighbouring nTPC neurons. nTPC neurons are located in the posterior diencephalon at the forebrain midbrain boundary. It has previously been suggested that the MTN may actually be part of the nTPC (Manni et al., 1963; Azzena and Palmieri, 1967). Other studies in zebrafish have not identified these dorsal anterior cells of the mesencephalon as MTN, instead they have been identified as nTPC (Wilson et al., 1990). Previous analysis of *noi* mutant zebrafish, whose midbrain identity is disrupted (lacks tectum, isthmus and cerebellum), resulted in the observation of increased nTPC numbers, which included those I have identified as MTN neurons (Scholpp and Brand, 2003). Expression analysis of *tlx3* in zebrafish stated it was expressed only in diencephalic neurons the nTPC, which appears to include dorsal anterior cells of the midbrain (Langenau et al., 2002). Characterisation

by gene expression does not reveal whether neurons at the DMB are nTPC or MTN, but retrograde labelling with DiI, of the nTPC and MTN in mouse, showed they were two distinct populations from their different axonal trajectories, though the nuclei of both intermix within prosomere 1 of the forebrain (Mastick and Easter, 1996).

Timelapse imaging of *Tg(huC:eGFP)* transgenic fish revealed that nTPC and MTN are both early born neurons, with nTPC arising in the dorsal diencephalon from 20 ss, shortly before MTN cell bodies are born in the dorsal mesencephalon. MTN cell bodies and nTPC are also similar in size, though nTPC are slightly oval in shape compared to the more circular MTN. Molecular characterisation of MTN neurons reveal that they have a similar genetic expression profile as nTPC*; brn3a*, *drg11*, *huC*, *isl1*, *ngn1*, and *tlx3* are expressed in both MTN neurons and nTPC. nTPC neurons also respond to Fgf and Wnt signalling, and ablations of neural crest in the same way as MTN, with an increase in their number. However the response of nTPC to Fgf and Wnt signalling is not as dramatic as the response by MTN neurons.

The posterior commissure is formed from bundles of axons that originate from pre-tectal nuclei such as the nuclei of Cajal (Carpenter et al., 1970; Stanic et al., 2010;). As development proceeds so fibres from other pre-tectal nuclei form the nTPC, and contribute to the formation of the posterior commissure (Hoyo-Becerra et al., 2010). Studies in goldfish have shown that when the posterior commissure is cut pattern discrimination is affected, suggesting that the posterior commissure aides visual functioning (Mark, 1966; Hemsley and Savage, 1987).

There is some evidence that MTN also has a visual role. Studies in tadpoles have led to the suggestion that MTN neurons play an integrative, multisensory role during tadpole development (Pratt et al., 2009). Pratt et al. (2009) showed that while MTN are electrophysiologically distinct from principal tectal neurons, they receive visual input by synaptic inputs from RGC terminals, via principal tectal neurons. From their results they proposed that MTN neurons form part of a feedback loop; at which point visual information is combined with somatosensory information, to help facilitate jaw movement as the tadpoles filter feed. In some species MTN neurons have been shown to innervate extraocular muscles (cat, Alvarado-Mallart et al., 1975; rat, Matesz, 1981; frog, Hiscock and Straznicky, 1982). This implies MTN neurons have a role in eye movement, which may be a primitive function. As jaws evolved, so MTN neurons innervated the perioral area, teeth and in amniotes the jaw muscles, revealing the importance of vision in jaw reflexes for biting (Anadon et al., 1989).

6.2 – MTN neurons are derived in a spatial and temporally restricted manner in the midbrain

It is unclear how MTN neurons are specified, and why they are restricted to the dorsal anterior region of the midbrain in zebrafish. The Fgf and Wnt signalling pathways are critical for patterning the midbrain. A number of studies indicate that Fgf signalling from the isthmus acts to regulate specification of neuronal types in the midbrain (Rhinn and Brand, 2001; Wurst and Bally-Cuif, 2001; Scholpp et al., 2003). Wnt signalling is required for maintaining Fgf signalling from the isthmus (Wurst and Bally-Cuif, 2001). Therefore the Fgf and Wnt signalling pathways are likely to have a role in specifying the development of MTN neurons in the dorsal anterior midbrain. I present data that reveal MTN neuronal numbers increase, and are positioned ectopically in the posterior dorsal midbrain of zebrafish, when Fgf signalling is down-regulated. The number of MTN neurons also increase in the dorsal anterior mesencephalon when Wnt signalling is up-regulated. These results imply that MTN neurons are specified in a spatial and temporal manner in the midbrain via Fgf signalling regulating the rostrocaudal identity of the midbrain and neurogenesis. Wnt signalling may be regulating MTN development by acting as a proliferative factor along the dorsal midline, and by maintaining the organising activity of Fgf signalling from the isthmus.

6.2.1 – MTN development is inhibited by the Fgf signalling pathway to maintain rostrocaudal identity of midbrain

In amniotes, Fgf signalling from the isthmus patterns the posterior midbrain and anterior hindbrain, and is required to maintain posterior midbrain identity (Rhinn and Brand, 2001). Studies have shown that Fgf signalling has a role in conferring A-P polarity in the midbrain (Marin and Puelles, 1994; Chi et al., 2003). Therefore high Fgf signalling levels are present at the isthmus and posterior regions of the midbrain, with low levels in the anterior midbrain.

MTN neurons are located in the dorsal anterior mesencephalon of zebrafish, and it is unclear if cells at the anterior midbrain are responsive to Fgf signalling at the stage that MTN neurons arise. I have shown that loss of Fgf signalling in *ace* or *noi* mutant fish, or after drug treatments to inhibit Fgf signalling, results in an increase in the number of MTN neurons similar to that described for nTPC neurons by Scholpp et

al. (2003). Some of these MTN neurons are located more posteriorly in the dorsal midbrain compared to their relative anterior positions in wild type. This implies that MTN neurons form in low Fgf signalling areas of the brain. It also suggests that high levels of Fgf signalling have an inhibitory role during MTN formation in the anterior midbrain, in order to maintain posterior identity (Figure 6.5A). However MTN neurons do not express the Fgf target gene *pea3*, therefore they are unlikely to be responding directly to Fgf signalling (Figure 6.5B). A microarray could be carried out to identify the Fgf target genes that causes MTN neurons to indirectly respond to Fgf signalling.

Figure 6.5 – Fgf signalling indirectly inhibits specification of the MTN

A) Diagrammatic representation of a zebrafish head at 24 hpf indicating Fgf signalling (blue) from the isthmus that inhibits the formation of the MTN in the posterior midbrain. B) Schematic showing Fgf signalling effecting an intermediate Fgf target gene, which in turn inhibits the specification of the MTN. c, cerebellum. dd, dorsal diencephalon. e, epiphysis. mb, midbrain. nTPC, nucleus of the tract of the posterior commissure. tg, trigeminal ganglion. X, unknown target gene.

A)

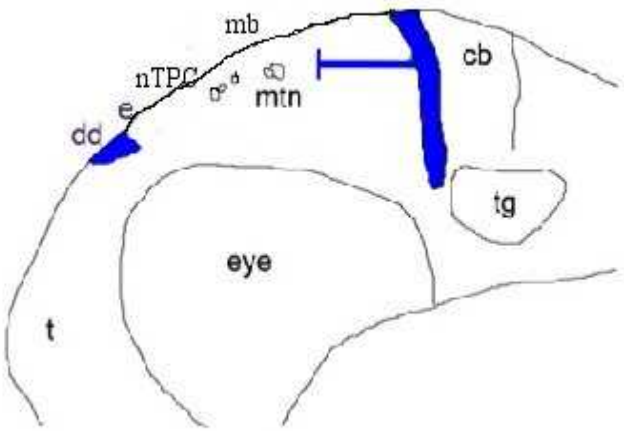

B)

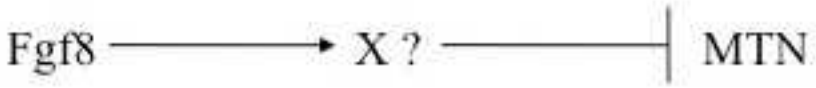

Previous studies have shown that Fgf signalling has a role in conferring A-P polarity in the midbrain. In mice when *Fgf8* was reduced by conditional gene inactivation, the posterior midbrain structures, isthmus and cerebellum failed to develop, but the rostral midbrain appeared to develop normally (Chi et al., 2003). Later studies, in which Fgf signalling was reduced by the misexpression of *Sprouty2* (*spry2*; an antagonist of the Fgf signalling pathway), showed that cell death occurred in the

rostral midbrain and the remaining posterior mesencephalic cells develop into anterior midbrain (Basson et al., 2009). This implies that low Fgf signalling is required to promote anterior midbrain development, while high levels are required to maintain the posterior midbrain (Basson et al., 2009). This supports my results which also shows that the midbrain becomes anteriorised, indicated by the posterior formation of MTN neurons that are an anterior cell population of the midbrain, when Fgf signalling is reduced.

Further evidence for Fgf signalling specifying rostrocaudal identity, has been shown in chick by inverting the midbrain with prospective isthmocerebellar tissue, which caused a transformation of caudal diencephalon into ectopic isthmus and cerebellum, and caudal midbrain structures in place of a pre-tectum (Marin and Puelles, 1994). Inversion of prospective midbrain alone, had no affect on midbrain development (Marin and Puelles, 1994). Similarly in mice, ectopic expression of the *Fgf8* in the dorsal mesencephalon resulted in a posteriorisation of much of the tectum (Lee et al., 1997).

The role of Fgf signalling in conferring A-P polarity during midbrain development has also been demonstrated by *Fgf8* over-expression in MTN analyses in the chick (Hunter et al., 2001). *Fgf8* soaked beads were implanted unilaterally into the anterior wall of the mesencephalon of the chick embryos at stage 12 (Hunter et al., 2001). This resulted in the induction of caudal midbrain shown by the increased numbers of *Brn3a* positive MTN neurons in regions of high Fgf signalling (Hunter et al., 2001). In contrast when they applied neutralizing antibodies to Fgf8 there was a decrease in the number of *Brn3a* positive MTN neurons. This contrasts with other studies in mammal and the observations in this thesis, in which MTN neurons first form furthest away from the isthmus where fgf8 is secreted. However *Brn3a* is a somatosensory marker of neural precursor cells. Therefore while these *Brn3a* cells may be fated to become MTN closest to the isthmus, it is unclear when or if they differentiate to form MTN. Mouse studies have shown that signals from the isthmus and ventral midline regulate *Brn3a* expression (Fedtsova and Turner, 2001). It is possible that *Fgf8* specifically affects *Brn3a* expression and not just MTN neurons, therefore the ectopic cells seen may be anterior cells of the mesencephalon that have been posteriorised. This is supported by studies in mouse that reveal *Fgf8* is required for formation of the posterior midbrain (Lee et al., 1997; Basson et al., 2009).

Alternatively the differing results between the chick study by Hunter et al (2001), and this thesis may reflect the different way in which the MTN develop in chick

compared to other species. Chick MTN neurons are positioned throughout the dorsal A-P axis of the midbrain. MTN neurons are also located throughout the A-P axis in mammals but, in contrast to chick, MTN neurons appear to develop first, and then more caudally as development progresses. In zebrafish, MTN neurons are a dorsal anterior midbrain cell population only, which may make them more responsive to Fgf signalling to maintain rostralcaudal identity.

6.2.2 – The ectopic formation of MTN neurons in the posterior midbrain may be due to a posterior shift in DMB when Fgf signalling is down-regulated

Previous studies in zebrafish have shown that *fgf8* suppresses forebrain fate, and therefore maintains the diencephalic – mesencephalic boundary (DMB) (Scholpp et al., 2003). In *noi* (*pax2.1*) and *ace* (*fgf8*) mutants the forebrain marker *pax6* is expanded posteriorly into the presumptive midbrain, as the midbrain loses its identity and becomes anteriorised. This occurs in conjunction with a loss of Fgf signalling in the isthmus from early somite stages (Scholpp et al., 2003). Increases in the number of nTPC neurons have also been observed in these mutants. This suggests that the ectopic formation of neurons in the posterior midbrain, after Fgf signalling is down-regulated, may be due to an anteriorisation of the midbrain into a diencephalic fate and the formation of ectopically positioned nTPC in the midbrain region.

noi mutants show a stronger change in brain identity phenotype (posterior shift in DMB) than *ace* mutants. In *ace* early development proceeds as normal, the isthmus initially is able to form at the interface of *otx2* and *gbx2* expression at the presumptive MHB, with early expression of *pax2.1*, *eng2/3* and *wnt1*. *eng2/3* is expressed in the midbrain and represses diencephalic *pax6* expression, maintaining the DMB. As development progresses from 6 ss (12 hpf) *pax2.1*, *eng2/3* and *wnt1* expression starts to decrease, as they require *fgf8* in a regulatory feedback loop to maintain their expression (Reifers et al., 1998). By this time *eng2/3* has acted to repress diencephalic *pax6*, helping to specify the DMB. While *eng2/3* expression decreases later in development, it persists enough to continue to repress *pax6* until 10 ss when the DMB is completely specified; this results in the relatively unaffected position of the DMB in *ace* mutants. It is thought that specification of the midbrain and forebrain are complete by 10 ss in zebrafish, with no cellular transfer between the boundaries (Kiecker and Lumsden, 2005). Therefore treatments with SU5402 from 10 ss should not

affect the position of the DMB. I have demonstrated this by labelling SU5402 treated animals from 10 ss with *pax6* and *pax7*, which revealed unchanged expression relative to wild type controls.

I have also shown that *pax6* expression is extended into presumptive midbrain territory in *noi* and *ace* mutants, but *pax6* expression appears to be more strongly expanded in the ventral midbrain, as previously documented (Scholpp et al., 2003). The dorsal positioning of the DMB appears similar to wild type siblings. The increase in MTN number and their ectopic positioning in the posterior midbrain is consistent between the conditions in which Fgf signalling is down-regulated, so this is unlikely to be caused by a change in DMB, and ectopically located nTPC.

Alternatively neurons of an indeterminate character that have both MTN and nTPC features may be present in the dorsal midbrain in zebrafish when Fgf signalling is down-regulated. This has been shown in another study using *ace* mutant zebrafish which shows plasticity of midbrain precursors at the anterior territory (Tallafuss and Bally-Cuif, 2003). In wild type embryos, genes (*pax6.1*, *fgfr3*) expressed in the diencephalon abut *Tg(her5:eGFP)* expressed in the midbrain. The normal formation of boundaries between the forebrain and midbrain, are required to prevent intermingling of cells fated to contribute to the different parts of the embryo (Kieckers and Lumsden, 2005). However in *ace* mutants, diencephalic genes were shown to intermix with *Tg(her5:eGFP)* in the midbrain at the anterior border. Therefore in this region where diencephalic and mesencephalic genes intermix the dorsal neurons may have an indeterminate character, in which they have both MTN and nTPC features. This could be tested by identifying genes that are normally only expressed in nTPC and MTN cell bodies and analysing for co-expression in these indeterminate cells.

6.2.3 – Wnt signalling from the dorsal mesencephalic midline may act as a proliferative factor during MTN formation within the midbrain

In vertebrates *Wnt1* is required for patterning the diencephalon and mesencephalon (Houart and Wilson, 2004). The Wnt signalling pathway is required for maintaining Fgf signalling activity in the isthmus (Wurst and Bally-Cuif, 2001). Therefore it is possible that Wnt signalling may also have a role in specifying the formation of MTN neurons. I have shown that the up-regulation of Wnt signalling causes an increase in the number of MTN neurons in the dorsal anterior midbrain. This

implies that MTN neuronal development is positively regulated by Wnt signalling that may act as a proliferative factor (Figure 6.6).

Figure 6.6 - Wnt signalling positively regulates the development of the MTN

A) Diagrammatic representation of a zebrafish head at 24 hpf indicating Wnt signalling (green) from the dorsal midline that may act as a proliferative factor during formation of the MTN in the anterior midbrain. B) Schematic showing Wnt signalling positively regulating specification of the MTN. cb, cerebellum. dd, dorsal diencephalon. e, epiphysis. mb, midbrain. nTPC, nucleus of the tract of the posterior commissure. t, telencephalon. tg, trigeminal ganglion.

A)

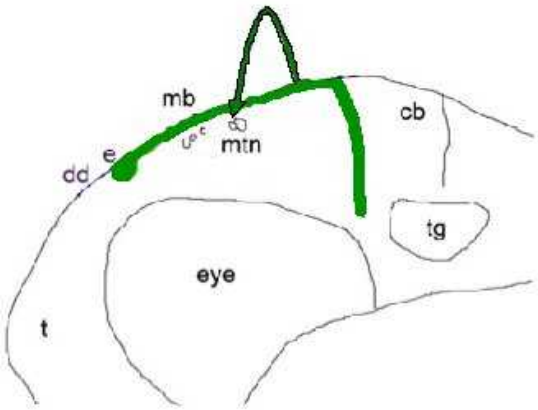

B)

Over-expression studies in chick and mice, support the hypothesis that Wnt signalling acts as a proliferative factor. In chick, over-expression of *Wnt1* resulted in an increase in the size of the tectum and cerebellum (Matsunaga et al., 2002). Similarly over-expression of *Wnt1*, by ectopic expression under the control of the *En1* promoter in mice from E8.5, caused an enlargement of the dorsal midbrain from E11.5 and an increase in proliferative cells in this region (Panhuysen et al., 2004). Before E11.5 no

proliferation was seen in the dorsal midbrain following Wnt1 over-expression. The delay in response to *Wnt1* up-regulation may be due to the time it takes for the levels of *Wnt1* to saturate and therefore have an affect on proliferation. However, this delay may also confirm the differing roles Wnt signalling has on development, with a proliferative role beginning from E11.5. In mouse an up-regulation of *CyclinD1*, which regulates cell cycle progression, was seen in the midbrain, further supporting the proliferative role of Wnt signalling from E11.5 (Panhuysen et al., 2004). When *Wnt1* function is lost in mutant mice there is a complete loss of the midbrain, indicating that Wnt signalling is permissive in patterning the midbrain by regulating proliferation (Mastick et al., 1996). A complete loss of the midbrain is also seen in zebrafish loss of function experiments in which *wnt1*, *wnt3* and *wnt10b* function is combinatorially ablated (Buckles et al., 2004). Wnt signalling regulates *fgf8* expression at the isthmus which is required for the formation and maintainance of the midbrain, therefore the loss of the midbrain in *Wnt1* mutant mice, and triple *wnt1/wnt3/wnt10b* mutant zebrafish, may be due to a loss of Fgf signalling. In these zebrafish mutants extensive apoptosis occurs from mid-somitogenesis (16-19 hpf), resulting in the absence of midbrain and cerebellum (Buckles et al., 2004). This implies that the loss of the midbrain when *wnt1* function is lost, is more likely a result of a loss of Fgf signalling, so midbrain structures are not specified.

I tested the effect of an up-regulation of Wnt signalling (BIO) in zebrafish from 10 ss (14 hpf), during the time that Wnt signalling is believed to regulate proliferation (Megason and McMahon, 2002; Panhuysen et al., 2004). This resulted in an increase in the number of MTN neurons, and the epiphysis appeared to be enlarged. Therefore it is likely that the increase in MTN cell number in the anterior midbrain is a result of a proliferative affect by Wnt signalling from the dorsal midline. This could be resolved by antibody labelling of proliferative cells, using phospho-histone 3 or BrdU, following an up-regulation of Wnt signalling and assessing if midbrain cells have an increase in their proliferation.

Wnt appears to be important for MTN formation, because in its absence there is a reduction in the number of MTN neurons. Over-expression of the Wnt inhibitor *dkk1* at 15 ss, before MTN neurons form, causes a reduction in MTN number. However, it appears that Wnt signalling is not required for specification of MTN, because some MTN neurons still form in *Tg(hsp70:dkk1-GFP)* zebrafish following heat shock induction of *dkk1* at mid somite stages. Similarly in *Wnt1-/-* mutant mice, while there is a complete loss of the midbrain, MTN neurons still form in prosomere 1 (dorsal

diencephalon in zebrafish) along with the mesV tract (Mastick et al., 1996).

The presence of MTN neurons following a reduction in Wnt signalling in this study, and in *Wnt1-/-* mutant mice, suggests that the non-canonical Wnt signalling genes may have a role in MTN formation. In BIO treated fish whilst the Wnt reporter gene *axin2* is increased, indicating that Wnt signalling is up-regulated, *wnt1* expression is reduced along the midline of the dorsal mesencphalon. This also implies that other Wnt signalling genes have a role in MTN formation. For example *wnt3a* and *wnt4* that are expressed in overlapping domains with *wnt1* along the dorsal mesencephalon from 20 ss in zebrafish (Hollyday et al., 1995; Jaszai et al., 2003). *dkk* inhibits the canonical Wnt pathway, therefore *wnt4* which signals via the non-canonical pathway is not antagonised, so it may exert a proliferative affect on MTN formation. This may also be occurring in *ace* mutants as *wnt4* expression is up-regulated along the dorsal midline of the midbrain (Jaszai et al., 2003). Together these results suggest that several Wnt genes act as a proliferative factor during the formation of MTN neurons.

6.2.4 – Fgf signalling and Wnt signalling pattern the midbrain and regulate neuronal identity in the midbrain

Fgf and Wnt signalling from the isthmus at the MHB interact in a positive cross-regulatory system (Tallafuss and Bally-Cuif, 2003). This feedback loop maintains the organising activity at the MHB, and the identity of the midbrain and anterior hindbrain. Wnt signalling from the dorsal midline of the midbrain and the isthmus promotes the expression of *fgf8*, *eng2/3* and *pax2.1*. These in turn promote the expression of *wnt1*. Conversely when *fgf8* is down-regulated, the expression of *eng2/3*, *pax2.1* and *wnt1* are also down-regulated (Reifers et al., 1998). Therefore it may be possible that MTN formation is regulated by the interaction between *wnt1* and *fgf8*. This is potentially shown in *ace* mutants and SU5402 drug treatments in which *wnt1* expression is lost in the isthmus, and reduced in the isthmus of *noi* mutants, potentially due to the reduced Fgf signalling which may not be sufficient to maintain *wnt1* expression. It has previously been implied from chick studies that this regulatory mechanism between Fgf and Wnt signalling may be involved in the development of the MTN (Canning et al., 2008). This is due to the response of MTN neurons to isthmic *Fgf8* signals, and the position of MTN in the dorsal mesencephalon close to the midline where *wnt1* is expressed (Canning et al., 2008; Hunter et al., 2001). In BIO treated

zebrafish and *mbl* mutants, where Wnt signalling is up-regulated, analysis revealed a reduction in *pea3* expression. This suggests that activating the canonical Wnt signalling reduces Fgf signalling, therefore relieving the inhibitory effect of Fgf signalling on MTN formation; consistent with the results from when Fgf is down-regulated. However Fgf target gene *pea3* is not expressed in MTN neurons suggesting that the MTN do not respond to Fgf signalling via *pea3*.

The roles of Fgf and Wnt signalling during MTN specification are likely to be unlinked. An up-regulation of Wnt by BIO treatment results in an up-regulation of *fgf8* and an increase in MTN numbers. If MTN development is regulated by the interaction of *wnt1* and *fgf8*, then the up-regulation of *fgf8* may potentially counter-act the proliferative affect of *wnt1* in the midbrain. Instead, *fgf8* continues to exert an inhibitory affect on the posterior formation of MTN in the dorsal midbrain to maintain posterior midbrain fate. This was shown by the limited number of MTN neurons forming posteriorly when canonical Wnt signalling is up-regulated, relative to their extended posterior positioning observed when Fgf is down-regulated.

It may also be possible that the increase in MTN numbers that occurs when Fgf is down-regulated from the 10 ss, is due to ectopic neurogenesis. During neurogenesis pre-pattern genes define populations of cells that express pro-neural basic helix loop helix (bHLH; i.e *ngn1*) proteins (Blader et al., 2004; Geling et al., 2004). Within these cell populations neuronal progenitors are selected by Delta/Notch signalling which causes lateral inhibition (Blader et al., 2004; Geling et al., 2004). In zebrafish *her5* acts as an inhibitor of neurogenesis in the intervening zone (IZ) that is located at the prospective area of the isthmus (Geling et al., 2003). *her5* inhibits *ngn1*, a key regulator of neurogenesis (Blader et al., 2004) During gastrulation at 70% epiboly, *her5* is expressed in the entire midbrain hindbrain anlage, which consists of precursors for the midbrain, isthmus, rhombomere 1 and rhombomere 2. During development *her5* expression in the zebrafish regresses posteriorly from 3 ss, beginning in the ventral mesencephalon, and becomes restricted to the isthmus by 24 hpf, allowing neurogenesis to occur. When Fgf signalling is down-regulated in *ace* and *noi* mutants, the regulatory processes of neurogenesis that controls the formation of neurons in the brain of vertebrates are perturbed (Geling et al., 2003). This indicates that the inhibition of neurogenesis by *her5* is regulated by Fgf signalling at the isthmus (Tallafuss and Bally-Cuif, 2003). In *ace* (*fgf8*) and *noi* (*pax2.1*) mutants *her5* expression is greatly reduced (*ace*) or lost (*noi*), so neurogenesis in the posterior midbrain is no longer inhibited (Tallafuss and Bally-Cuif, 2003).

Negative regulation by *her5* is important for normal development of pro-neural genes. Lack of *her5* expression results in the premature and accelerated differentiation of neurons in the midbrain, causing the altering of neuronal subtypes and affecting the nervous system (Kageyama and Nakanishi, 1997). Such alteration of neuronal subtypes is seen in the zebrafish when Fgf signalling is down-regulated, with an increase in MTN numbers, some of which are located in a more posterior region of the midbrain.

Wnt signalling may also have a role in regulating neurogenesis. There is no evidence that Wnt signalling has such a role within the dorsal midbrain, but studies have shown that it regulates neurogenesis in other regions of the brain. In zebrafish, ablation of *wnt1* and *wnt10* resulted in a loss of *her5* expression in the ventral MHB, and reduced *her5* expression in the dorsal MHB (Lekven et al, 2003). Wnt signalling is required to maintain Fgf signalling at the MHB, therefore Wnt signalling may be indirectly affecting *her5* expression via the regulation of Fgf (Wurst and Bally-Cuif, 2001). However *fgf8* expression in *wnt1* and *wnt10* mutants was comparable to wild type embryos, implying that Wnt signalling directly affects *her5* expression and therefore neurogenesis (Lekven et al., 2003).

In mice, the lateral to medial regression of *Wnt1* generates a Wnt signalling gradient that allows initiation of neurogenesis in the cortex (Machon et al., 2007). Wnt signalling inhibits neurogenesis by inhibiting the expression of *ngn2* in the cortex. Also in mice studies, Wnt signalling has been shown to inhibit neurogenesis in the hippocampus (Lie et al., 2005). Similarly in zebrafish Wnt signalling appears to inhibit neurogenesis in boundary cells in the hindbrain, and cells within the retina (Amoyel, 2005; Yamaguchi, 2005). These studies suggest that Wnt signalling has a specialised role in neurogenesis by inhibiting the differentiation of specific neuronal types. However, Wnt signalling is unlikely to inhibit neurogenesis of MTN neurons because *wnt1* is expressed along the dorsal midline of the mesencephalon. Timelapse analysis of *Tg(huC:GFP)* transgenic fish (expressed in differentiating cells) reveal MTN neurons arise at the dorsal midline of the anterior mesencephalon, showing that Wnt signalling from the roofplate does not inhibit their differentiation. Up-regulation of Wnt signalling causes an increase in MTN numbers. If Wnt signalling is inhibitory to neurogenesis then a decrease in MTN numbers would be predicted following an up-regulation of Wnt and this is not observed, revealing that Wnt does not inhibit neurogenesis in the midbrain.

Analysis of the post mitotic neuronal marker *huC* in the embryonic zebrafish reveals expression in many dorsal cells in the mesencephalon, similar to the location of MTN

neurons in the chick and mouse. Not all these cells undergo differentiation as the HuC protein is only expressed in anterior dorsal cells in the midbrain. This implies that the expression of *huC* is not a readout of differentiation. It has been suggested that micro RNA's (miR-9) block the translation of MHB specific genes (*fgf8*) during early development, which in turn reduces *her5* expression, to promote neurogenesis (Leucht et al., 2008; Coolen and Bally-Cuif, 2009). miR-9 is also believed to inhibit *her5* directly (Coolen and Bally-Cuif, 2009). When miR-9 is over-expressed, immunostaining to detect HuC revealed an increase in HuC positive cells in the midbrain hindbrain domain (Leucht et al., 2008). Over-expression of miR-9 promotes neurogenesis via the down-regulation of *fgf8* and inhibition of *her5*, causing a loss of MHB phenotype, similar to *ace* (*fgf8*) mutants (Leucht et al., 2008). Conversely when miR-9 is down-regulated, a reduction in HuC positive cells are seen (Leucht et al., 2008). This suggests *huC* translation in posterior dorsal cells of the mesencephalon may be blocked as there is only a low level expression of miR-9 in this region, and *her5* cannot be inhibited to promote neurogenesis. In the anterior dorsal cells however, there may be higher levels of miR-9 which antagonise the inhibitory affect of *her5* on neurogenesis, promoting differentiation of MTN neurons.

These results have been used to present a regulatory model of MTN development whereby *fgf8* and *wnt1* affect MTN development differently. This model suggests that Fgf signals repress MTN formation in the posterior mesencephalon, despite the potential for neurons to form as indicated by *ngn1* and *huC* expression (Figure 6.3). Loss of *fgf8* from the isthmus, after brain regionalisation into forebrain and midbrain domains has finished, reveals the potential for these cells to form ectopic posteriorly located MTN neurons. Posteriorly located MTN neurons are able to form as neurogenesis in the midbrain is no longer inhibited during early development when Fgf signalling is down-regulated. *wnt1* drives the proliferation of MTN neurons, in addition to other cells within the forebrain and midbrain (Figure 6.7).

Figure 6.7 – Fgf and Wnt signalling regulates the formation of MTN neurons in the dorsal anterior midbrain.

The formation of MTN neurons (purple) is spatially regulated by inhibitory Fgf signalling (black) from the isthmus. Wnt signalling (blue) has a proliferative effect on MTN development. MTN neuronal precursors have the potential to form in the posterior midbrain, but are inhibited by Fgf signalling. Green indicates a Fgf signalling gradient regulating *her5* expression which in turn inhibits posterior neurogenesis.

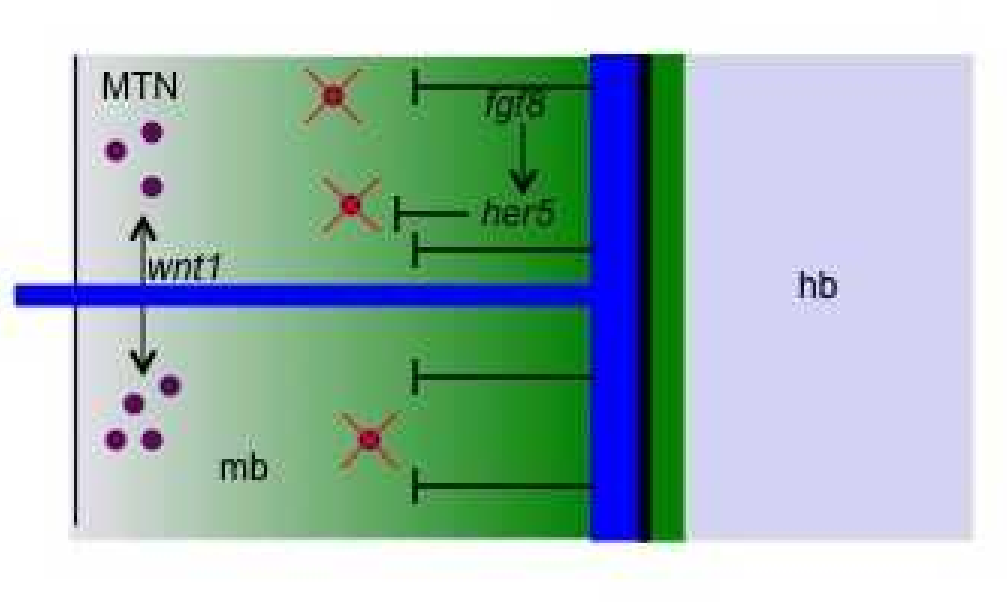

6.3 – Neural crest is required to maintain MTN development

6.3.1 – MTN neurons are not derived from neural crest

MTN neurons share several similarities, in their expression of genes during development and their function, with sensory neurons in the DRG. This implies that MTN may have a similar cellular origin as DRG neurons which are neural crest derived. In order to determine whether MTN neurons are derived from neural crest, I have analysed whether the genes (*foxd3*, *snail2*, and *sox10*) that are expressed in neural crest are also expressed in MTN neurons. I have also genetically ablated neural crest by morpholino injection. Results from these experiments revealed that MTN is not neural crest derived, in agreement with recent studies investigating the origin of MTN neurons.

When quail mesencephalic neural crest cells (NCCs) were transplanted into chick, no contribution of neural crest to MTN neurons was seen (Baker et al., 1997a). Similarly genetic analysis of neural crest markers, to examine whether they are expressed in MTN neurons, revealed no co-expression (Hunter et al., 2001). These studies and my own, contradict the results from early grafting experiments which suggested that MTN is neural crest derived (Narayanan and Narayanan, 1978). Therefore it is possible that MTN cells originate from the dorsal neural tube similar to primary sensory neurons like RB neurons.

6.3.2 – MTN neurons and NCCs may form from a common progenitor in the head

Previous studies in *tfap2a-/c-* double morphant zebrafish, suggest that putative NCCs are trans-fated into neural plate cells in the head of these morphants (Li and Cornell, 2007). This was shown by an absence in the space between the neural plate and pre-placodal region that pre-migratory NCCs occupy, as expression of *sox2* (expressed in the neural plate) expands into this space (Li and Cornell, 2007). An increase in neural plate cells may differentiate into MTN neurons, resulting in the increased numbers of MTN neurons I observe in *tfap2a-/c-* and *tfap2a-/foxd3-* double morphants. This suggests that MTN neurons arise from the neural plate in the dorsal neural tube, similar to primary sensory neurons RB neurons.

RB neurons are not derived from neural crest, instead they arise from a common progenitor pool in an equivalence domain at the lateral edge of the neural plate (Knecht and Bronner-Fraser, 2002). Delta/Notch signalling is required to segregate neural crest and RB neurons from their common progenitor pool, via a lateral inhibition mechanism (Cornell and Eisen, 2000). It may also be possible that MTN precursor cells and NCCs are derived from a common progenitor, similar to neural crest and RB neurons in the trunk. During early development in zebrafish, these common progenitors respond to signals that specify them to form neural crest (and subsequently DRGs), or alternatively RB neurons (Cornell and Eisen, 2000). The Notch/Delta signalling pathway provides cues for this specification, and the response to these cues are dependent on the genes that they express (Cornell and Eisen, 2002). High *deltaA* expression on progenitor cells causes the activation of the Notch signalling pathway in neighbouring cells, inhibiting the expression of neurogenic genes (i.e. *ngn1*, Cornell and Eisen 2002). These neighbouring cells are unable to differentiate into RB sensory

neurons, therefore become neural crest. In *deltaA* mutant zebrafish, more RB neurons form at the expense of neural crest as neurogenesis in neighbouring cells are no longer inhibited by the Notch/Delta signalling pathway (Cornell and Eisen, 2000). These studies have only examined the specification of NCC versus RB neurons in the trunk, as RB neurons are not found in the brain of jawed vertebrates. It is unclear if similar principles apply to NCC and cells at the neural plate border, which are fated to become neurons in the brain. To begin to determine if MTN and NCCs form from a common progenitor in the head, it would be useful to examine if a loss of *deltaA* function or the inhibition of Notch in a temporal manner in zebrafish, results in more MTN neurons at the expense of neural crest. Fate mapping of MTN neurons in a neural crest transgenic line would also help to identify which cell type they are derived from.

The increases in MTN neurons in double morphants may be a result of neuronal perturbations when *tfap2a*, *tfap2c* and *foxd3* are lost. In *Foxd3* null mutant mice cranial NCC form non-neural cells during migration, and the differentiation of NCC derived mesenchymal cells was accelerated (Mundell and Labosky, 2011). This suggests that normal expression of *foxd3*, expressed in pre-migratory and early migratory NCC, prevents neural crest from differentiating (Mundell and Labosky, 2011). *foxd3* expression is absent in *tfap2a-/c-* double morphant zebrafish (Li and Cornell, 2007). Therefore the loss of function of neural crest specifying genes *tfap2a-/c-* and *tfap2a-/foxd3-* may allow the NCC progenitors to respond to neurogenic signals instructing them to differentiate into MTN neurons, as opposed to forming neural crest. This would imply that MTN precursor cells and NCCs form from a common progenitor, similar to NCCs and RB neurons in the trunk.

Alternatively NCCs may inhibit MTN formation in the developing embryo. Evidence for neural crest acting as an inhibitor on cellular development is sparse, but some studies have suggested that neural crest inhibits induction of the lens of the eye, the heart, and kidneys (Jacobson and Slater, 1988; Vaglia and Hall, 1999; Grocott et al., 2011). This data suggests that in some cases neural crest acts as an inhibitor of cellular development. However studies have shown that in order for neural crest to inhibit lens induction, Wnt signalling is also required (Grocott et al., 2011). Neural crest may inhibit neurogenesis and therefore inhibit MTN formation. During formation of DRGs in the trunk, the Delta/Notch signalling pathway determines which NCC undergo neurogenesis by lateral inhibition (Wakamatsu et al., 2000). Similarly in the head, the presence of NCCs may cause the lateral inhibition of neurogenesis in MTN neurons in the midbrain. Therefore any inhibition of the differentiation of putative MTN neurons by NCC are

abrogated in *tfap2a-/c* and *tfap2a-/foxd3*- double morphants as NCCs are ablated.

6.3.3 – NCC may interact with Fgf and Wnt signalling to specify MTN neurons

NCC has an important role in regulating patterning in the brain. Studies in chick have shown that when NCC was surgically ablated in the brain, at neurula stage before the onset of cranial neural crest migration, a loss of Fgf8 expression in the anterior neural ridge (ANR) and branchial arches occurs (Creuzet, 2009). This caused a loss of the telencephalon, dorsal brain structures and an absence of facial structures. They also showed that there was a complete loss of *wnt1* along the dorsal midline of the midbrain (Creuzet et al., 2006). From their results Creuzet et al. (2006) proposed a model in which neural crest is required to induce and maintain the expression of *Fgf8* in the ANR. In turn *Fgf8* signals from the ANR promote the migration and proliferation of these neural crest cells, contributing to normal brain formation, in a positive regulatory feedback loop (Creuzet et al., 2006). Many other studies have also suggested that *Fgf8* is a key factor for neural crest survival (Santagati and Rijli, 2003).

This may imply that interactions are occurring between neural crest and the Fgf and Wnt signalling pathways in order for MTN to develop. I have shown that when neural crest is ablated there is an increase in MTN numbers, similar to when Fgf signalling has been down-regulated and Wnt signalling up-regulated. This may suggest that disrupting different pathways required for normal brain development causes the same premature neurogenesis. However it may alternatively support the hypothesis of an interaction between neural crest, and the Fgf and Wnt signalling pathways.

To determine whether neural crest indirectly inhibits MTN formation via Fgf and Wnt signalling, *fgf8*, *pea3*, *wnt1* and *axin2* expression was analysed in *tfap2a-/c*- and *tfap2a-/foxd3*- double morphants. This revealed reduced *wnt1* expression along the dorsal midline in *tfap2a-/c*- and *tfap2a-/foxd3*- double morphants relative to controls, which may account for the medial position of MTN cell bodies in these double morphants. Alternatively the reduction in *wnt1* expression may indicate morpholino toxicity affects (Gerety and Wilkinson, 2011).. A loss of *fgf8* and *pea3* expression in the pharyngeal arches is also seen in *tfap2a-/c*- and *tfap2a-/foxd3*- double morphants, but normal expression is seen in the ANR, dorsal diencephalon and isthmus, revealing neural crest is not affecting Fgf signalling in these regions. The absence of *fgf8* expression in the pharyngeal arches of *tfap2a-/c*- zebrafish, supports the model by

Creuzet et al. (2006) in which neural crest is required to induce and maintain *fgf8* expression in the ANR. Similarly the absence of *dlx2* in the pharyngeal arches, when Fgf is down-regulated, support their model in which *fgf8* promotes migration and proliferation of NCCs. However normal expression of *fgf8* seen in the ANR of *tfap2a-/c-* morphants, indicates neural crest is not required for the induction of *fgf8* in the ANR of zebrafish. The more severe effects (loss of the telencephalon, dorsal brain and facial structures) observed in the studies in which chick neural crest was ablated could be because they may have removed other cells types such as non-neural ectoderm as well as neural crest.

It is possible that Fgf and Wnt signalling may indirectly affect MTN cell numbers through neural crest by affecting the formation of NCCs. Both BIO and SU5402 drugs were applied to embryos from 10ss, during the time that NCCs are migrating away from the neural tube, therefore effecting their migration. Analysis of *sox10* (a molecular marker of neural crest) showed that NCCs were more laterally located in the dorsal midbrain in BIO and SU5402 treated zebrafish than in wild type controls. Therefore any inhibitory effects neural crest cells may have on MTN are reduced, as they are further away from the regions where MTN form or can potentially form in the context of a reduction in Fgf signalling.

Studies have previously shown that Fgf signalling at the isthmus plays a role in neural crest plasticity and pre-patterning (Trainor et al, 2003). In particular *fgf2* is regulated by TGFβ and is required for proliferation of neural crest (Kulesa et al., 2010). It would be interesting to test whether down-regulation of *fgf2* in zebrafish results in a similar increase in MTN cell numbers, to determine if the interaction occurring between Fgf signalling and neural crest affects MTN number. It is also known that Wnts are required for neural crest migration (Curtin et al, 2010). Therefore the up-regulation of Wnt may cause NCCs to migrate faster, alleviating the potential inhibitory affects by neural crest in the dorsal midbrain. However NCCs are not laterally restricted in the Wnt and Fgf mutants (*mbl*, *ace*), suggesting that the Fgf and Wnt signalling pathways do not have a major affect on NCC development in the midbrain.

6.4 – Conclusions

In this thesis I have shown that MTNs are located in the dorsal anterior mesencephalon in zebrafish similar to other vertebrates. Orthologues of mammalian molecular markers of MTN are also expressed in zebrafish MTN, indicating a conservation of MTN neuronal specification in teleosts and amniotes. Similarly a comparison of MTN anatomy, such as their location in the midbrain and the axonal pathways they take, also shows conservation with other vertebrates.

The cellular origin of MTN has been controversial, with some studies suggesting it is derived from neural crest, while others suggest it is not. I have demonstrated by gene expression studies and genetic ablation of neural crest that MTN neurons are not derived from neural crest. In contrast, genetic ablation of neural crest indicates that neural crest may actually inhibit MTN formation, as loss of neural crest results in an increase in MTN numbers. Alternatively, MTN neurons and NCC in the midbrain may have a common progenitor.

My results from analysing the roles of Fgf and Wnt signalling pathways during MTN formation have been used to present a regulatory model for MTN development. This model suggests that Fgf signalling from the isthmus regulates the formation of MTN neurons in a spatial and temporal manner to maintain posterior midbrain identity. This inhibition is maintained by the continuous regulatory feedback loop between Fgf and Wnt signalling. Wnt signals from the dorsal roof plate putatively function to induce proliferation of MTN precursor cells.

While more MTN neurons form when Fgf signalling is down-regulated, or Wnt signalling up-regulated, the potential effects of this is not understood. It would be interesting to determine if the ectopic MTN neurons that form are able to innervate the jaw and survive into adults. DiI labelling of the jaw region could be carried out in Fgf or Wnt mutants, to analyse whether posterior MTN cell bodies are retrogradely labelled. Further analysis of the axon tracts using acetylated tubulin should also be carried out.

Future research into the origin of MTN by analysing the Notch/Delta signalling pathway will help to determine whether MTN are specified from a common progenitor that also gives rise to the neural crest, similar to RB neurons in the trunk. A better understanding of MTN development and function, can be used to determine if MTN neurons evolved from a primitive RB neuron that became specialised in conjunction with eye and jaw evolution, to integrate visual input and jaw responses.

References

Alberts, B., Johnson, A., Lewis, J., Raff, M., Roberts, K., and Walter, P. (2002). Molecular biology of the cell, 4th edition. New York: Garland Science.

Alexandrowicz, J. S. and Whitear, M. (1957). Receptor elements in the coxal region of Decapoda Crustacea. *J Mar Biol Ass UK* **36**, 602-628.

Alvarado-Mallart, M. R., Batini, C., Buisseret-Delmas, C. and Corvisier, J. (1975) Trigeminal representations of the masticatory and extraocular proprioceptors as revealed by horseradish peroxidase retrograde transport. *Exp Brain Res* **23**, 167–179.

Amoyel, M., Cheng, Y. C. Jiang, Y. J. and Wilkinson, D. G. (2005). Wnt1 regulates neurogenesis and mediates lateral inhibition of boundary cell specification in the zebrafish hindbrain. *Development* **132**, 775-85

Anadón, R., De Miguel, E., Gonzalez-Fuentes, M. J. and Rodicio, C. (1989). HRP study of the central components of the trigeminal nerve in the larval sea lamprey: organization and homology of the primary medullary and spinal nucleus of the trigeminus. *J Comp Neurol* **283**, 602-10.

Andermann, P., Ungos, J. and Raible, D. W. (2002). Neurogenin1 defines zebrafish cranial sensory ganglia precursors. *Dev Biol* **251**, 45-58.

Anderson, R. B., Jackson, S. C., Fujisawa, H. and Key, B. (2000). Expression and putative role of neuropilin-1 in the early scaffold of axon tracts in embryonic *Xenopus* brain. *Dev Dyn* **219**, 102-108.

Ang, S. L., Jin, O., Rhinn, M., Daigle, N., Stevenson, L. and Rossant, J. (1996). A targeted mouse *Otx2* mutation leads to severe defects in gastrulation and formation of axial mesoderm and to deletion of rostral brain. *Development* **122**, 243–252.

Antonellis, A. Huynh, J. L. Lee-Lin, S. Q. Vinton, R. M. Renaud, G. Loftus, S. K. Elliot, G. Wolfsberg, T. G. Green, E. D. McCallion, A. S. and Pavan, W. J. (2008). Identification of neural crest and glial enhancers at the mouse *Sox10* locus through transgenesis in zebrafish. *PloS Genet* **4**, e1000174

Arber, S., Ladle, D. R., Lin, J. H., Frank, E. and Jessell, T. M. (2000). ETS gene *Er81* controls the formation of functional connections between group Ia sensory afferents and motor neurons. *Cell* **101**, 485-98

Arduini, B. L., Bosse, K. M. and Henion, P. D. (2009). Genetic ablation of neural crest cell diversification. *Development* **136**, 1987-94.

Artavanis-Tsakonas, S., Matsuno, K. and Fortini, M. E. (1995). Notch signalling. *Science* **268**, 225-232.

Artinger, K. B., Chitnis, A. B., Mercola, M. and Driever, W. (1999). Zebrafish *narrowminded* suggests a genetic link between formation of neural crest and primary sensory neurons. *Development* **126**, 3969-79.

Aybar, M. J., Glavic, A. and Mayor, R. (2002) Extracellular signals, cell Interactions and transcription factors involved in the induction of the neural crest cells. *Biol Res* **35**, 267-75.

Aybar, M. J., Nieto, M. A. and Mayor, R. (2003). Snail precedes slug in the genetic cascade required for the specification and migration of the *Xenopus* neural crest. *Development* **130**, 483–94.

Azzena, G. B. and Palmieri, G. (1967). A trigeminal monosynaptic reflex in brids. *Exp Neurol* **18**, 184-93.

Bae, Y. C., Nakagawa, S., Yasuda, K., Yabuta, N. H., Yoshida, A., Pil, P. K., Moritani, M., Chen, K., Nagase, Y., Takemura, M. and Shigenaga, Y. (1996). Electron microscopic observation of synaptic connections of jaw-muscle spindle and periodontal afferent terminals in the trigeminal motor and supratrigeminal nuclei in the cat. *J Comp Neurol* **374**, 421–435.

Baker, C.V., Bronner-Fraser, M., Le Douarin, N. M. and Teillet, M. A. (1997a). Early- and late-migrating cranial neural crest populations have equivalent developmental potential in vivo. *Development* **124**, 3077-87.

Baker, C. V. H. and Bronner-Fraser, M. (1997b). The origins of the neural crest. Part I: embryonic induction. *Mech Dev* **69**, 3-11.

Baker, C. V. H. and Bronner-Fraser, M. (1997c). The origins of the neural crest. Part II: An evolutionary perspective. *Mech Dev* **69**, 13-29.

Baker, C. V. H. and Bronner-Fraser, M. (2001). Vertebrate Cranial Placodes I. Embryonic Induction. *Dev Biol* **232**, 1-61.

Baker, C. V. H. (2008). The evolution and elaboration of vertebrate neural crest cells. *Curr Opin Genet Dev* **18**, 536-43.

Ballintijn, C. M. and Bamford, O. S. (1975). Proprioceptive motor control in fish respiration. *J. Exp. Biol.* **62**, 99-114.

Barembaum, M. and Bronner-Fraser, M. (2005). Early steps in neural crest specification. *Semin Cell Dev Biol* **16**, 642-6.

Barreiro-Iglesias, A., Villar-Cheda, B., Abalo, X. M., Anadón, R. and Rodicio, M. C. (2008). The early scaffold of axon tracts in the brain of a primative vertebrate, the sea lamprey. *Brain Res Bull* **75**, 42-52.

Basson, A. M., Echevarria, D., Ahn, C. P., Sudarov, A., Alexandra L. Joyner, A. L.,

Mason, I. J., Martinez, S. and Gail R. Martin, G. R. (2009). Specific regions within the embryonic midbrain and cerebellum require different levels of FGF signaling during development. *Development* **135**, 889-898.

Beddington, R. S. (1994). Induction of a second neural axis by the mouse node. *Development* **120**, 613-20.

Beddington, R. S. and Robertson E. J. (1998). Anterior patterning in mouse. *Trends Genet* **14**, 277-84.

Begbie, J., Ballivet, M. and Graham, A. (2002). Early steps in the production of sensory neurons by the neurogenic placodes. *Mol Cell Neurosci* **21**, 502-11.

Bernhardt, R. R., Chitnis, A. B., Lindamer, L. and Kuwada, J. Y. (1990). Identification of spinal neurons in the embryonic and larval zebrafish. *J Comp Neurol* **302**, 603-616.

Bianco, I. H., Carl, M., Russell, C., Clarke, J. D. and Wilson, S. W. (2008). Brain asymmetry is encoded at the level of axon terminal morphology. *Neural Dev* **3**, 9.

Blader, P., Fischer, N., Gradwohl, G., Guillemot, F. and Strähle, U. (1997). The activity of *Neurogenin1* is controlled by local cues in the zebrafish embryo. *Development* **124**, 4557-4569.

Blader, P., Plessy, C. and Strähle, U. (2003). Multiple regulatory elements with spatially and temporally distinct activities control *neurogenin1* expression in primary sensory neurons of the zebrafish embryo. *Mech Dev* **120**, 211-18.

Blader, P., Lam, C. S., Rastegar, S., Scardigli, R., Nicod, J. C., Simplicio, N., Plessy, C., Fischer, N., Schuurmans, C., Guillemot, F. and Strähle, U. (2004). Conserved and acquired features of *neurogenin1* regulation. *Development* **131**, 5627-37.

Blentic, A., Chambers, D., Skinner, A., Begbie, J. and Graham, A. (2011). The formation of the cranial ganglia by placodally-derived sensory neuronal precursors. *Mol Cell Neurosci* **46**, 452-9.

Boettger, T., Knoetgen, H., Wittler, L. and Kessel, M. (2001). The avian organiser. *Int J Dev Biol* **45**, 281-7.

Bone, Q. (1960). The central nervous system in amphioxus. *J Comp Neurol* **115**, 27-51.

Brand, M., Heisenberg, C. P., Jiang, Y. J., Beuchle, D., Lun, K., Furutani-Seiki, M., Granato, M., Haffter, P., Hammerschmidt, M., Kane, D. A., Kelsh, R. N., Mullins, M. C., Odenthal, J., van Eeden, F. J. and Nusslein-Volhard, C. (1996). Mutations in zebrafish genes affecting the formation of the boundary between midbrain and hindbrain. *Development* **123**, 179-90.

Bräunig, P. and Hustert, R. (1980). Proprioceptors with central cell bodies in insects.

Nature **283**, 768-770.

Broccoli, V., Boncinelli, E. and Wurst, W. (1999). The caudal limit of *Otx2* expression positions the isthmic organizer. *Nature* **401**, 164–168.

Buckles, G. R., Thorpe, C. J., Ramel, M. C. and Lekven, A. C. (2004). Combinatorial Wnt control of zebrafish midbrain-hindbrain boundary formation. *Mech Dev* **121**, 437-47.

Butler, A. B. and Hodos, W. (2005). Advent of jaws. In Comparative vertebrate neuroanatomy: evolution and adaptation. pp. 655-657. 2nd Edition, Wiley Interscience.

Byers, M. R., O'Connor, T. A., Martin, R. F. and Dong, W. K. (1986). Mesencephalic trigeminal sensory neurons of cat: axon pathways and structure of mechanoreceptive endings in periodontal ligament. *J Comp Neurol* **250**, 181–191.

Cao, Y., Waddell, P. J., Okada, N. and Hasegawa, M. (1998). The complete mitochondrial DNA sequence of the shark *Mustelus manazo*: evaluating rooting contradictions to living bony vertebrates. *Mol Biol Evol* **15**, 1637-46.

Campos-Ortega, J. A. (1993). Mechanisms of early neurogenesis in *Drosophila melanogaster*. *J Neurobiol* **24**, 1305-27.

Canning, C. A., Lee, L., Irving, C., Mason, I. and Jones C. M. (2007). Sustained interactive Wnt and Fgf signalling is required to maintain isthmic identity. *Dev Biol* **305**, 276-86.

Canning, C. A., Lee, L., Luo, S. X., Graham, A. and Jones, C. M. (2008). Neural tube derived Wnt signals cooperate with FGF signalling in the formation and differentiation of the trigminal placodes. *Neural Dev* 3, 35.

Carney, T. J., Dutton, K. A., Greenhill, E., Delfino-Machin, M., Dufourcq, P., Blader, P. and Kelsh, R. N. (2006). A direct role for Sox10 in specification of neural crest-derived sensory neurons. *Development* **133**, 4619-30.

Carpenter, M. B., Harbison, J. W. and Peter, P. (1970). Accessory oculomotor nuclei in the monkey: Projections and effects of discrete lesions. *J Comp Neur* **140**, 131-54.

Chandrasekhar, A. (2004). Turning heads: development of vertebrate branchiomotor neurons. *Dev Dyn* **229**, 143-61.

Chedotal, A., Pourquie, O. and Soltelo, C. (1995). Initial tract formation in the brain of the chick embryo: selective expression of the BEN/SC1/DM-GRASP cell adhesion molecule. *Eur J Neurosci* **7**, 198-212.

Cheesman, S. E. and Eisen, J. S. (2004). *gsh1* demarcates hypothalamus and intermediate spinal cord in zebrafish. *Gene Expr Patterns* **5**, 107-12.

Chen, J. Y., Dzik, J., Edgecombe, G. D., Ramskold, L. and Zhou., G. Q. (1995). A possible early cambrian chordate. *Nature* **377**, 720-2.

Chen, H. H. and Frank, E. (1999). Development and specification of muscle sensory neurons. *Curr Opin Neurobiol* **9**, 405-9.

Chen, Z. F., Rebelo, S., White, F., Malmberg, A. B., Baba, H., Lima, D., Woolf, C. J., Basbaum, A. I. and Anderson, D. J. (2001). The paired homeodomain protein DRG11 is required for the projection of cutaneous sensory afferent fibers to the dorsal spinal cord. *Neuron* **31**, 59-73.

Chen, H. H., Hippenmeyer, S., Arber, S. and Frank, E. (2003). Development of the monosynaptic stretch reflex circuit. *Curr Opin Neurobiol* **13**, 96-102.

Chi, C. L., Martinez, S., Wurst, W. and Martin, G. R. (2003). The isthmic organizer signal FGF8 is required for cell survival in the prospective midbrain and cerebellum. *Development* **130**, 2633-44.

Chilton, J. K. and Guthrie, S. (2004). Development of oculomotor axon projections in the chick embryo. *J Comp Neurol* **472**, 308-17

Chitnis, A. (1999). Control of neurogenesis – lessons from frogs, fish and flies. *Curr Opin Neurobiol* **9**, 18-25.

Chitnis, A. B. and Kuwada, J. Y. (1990). Axongenesis in the brain of zebrafish embryos. *J Neurosci* **10**, 1892-905.

Ciruna, B., Jenny, A., Lee, D., Mlodzik, M. and Schier, A. F. (2006). Planar cell polarity signalling couples cell division and morphogenesis during neurulation. *Nature* **439**, 220-4.

Clarke, J. D. W., Hayes, B. P., Hunt, S. P. and Roberts, A. (1984). Sensory physiology, anatomy and immunohistochemistry of Rohon-Beard neurones in embryos of Xenopus leavis. *J Physiol* **348**, 511-25.

Clarke, J. (2009). Role of polarized cell divisions in zebrafish neural tube formation. *Curr Opin Neurobiol* **19**, 134-8.

Close, R., Toro, S., Martial, J. A. and Muller M. (2002). Expression of the zinc finger Egr1 gene during zebrafish embryonic development. *Mech Dev* **118**, 269-72.

Coen, L., Osta, R., Maury, M. and Brûlet,, P. (1997). Construction of hybrid proteins that migrate retrogradely and transynaptically into the central nervous system. *Proc Natl Acad Sci USA* **19**, 9400-5.

Colas, J. F. and Schoenwolf, G. C. (2001). Towards a cellular and molecular understanding of neurulation. *Dev Dyn* **221**, 117-45.

Colin, S. P. (1981). A proprioceptor with central cell bodies in the cockroach,

Periplaneta americana (Insecta). *Zoomorph* **98**, 227-31.

Concha, M. L., and Adams, R. J. (1998). Oriented cell divisions and cellular morphogenesis in the zebrafish gastrula and neurula: a time-lapse analysis. *Development* **125**, 983-94.

Coolen, M. and Bally-Cuif, L. (2009). MicroRNAs in brain development and physiology. *Curr Opin Neurobiol* **19**, 461-70.

Copp, A. J., Greene, N. D. and Murdoch, J. N. (2003). The genetic basis of mammalian neurulation. *Nat Rev Genet* **4**, 784-93.

Copray, J. C., Ter Horst, G. J., Liem, R., S. and van Willigen, J. D. (1990). Neurotransmitters and neuropeptides within the mesencephalic trigeminal nucleus of the rat: an immunohistochemical analysis. *Neuroscience* **37**, 399-411.

Cornell, R. A. and Eisen, J. S. (2000). Delta/Notch signalling mediates segregation of neural crest and spinal sensory neurons from zebrafish lateral neural plate. *Development* **127**, 2873-82.

Cornell, R. A. and Eisen, J. S. (2002). Delta/Notch signalling promotes formation of zebrafish neural crest by repressing Neurogenin1 function. *Development* **129**, 2639-48.

Creuzet, S. E., Martinez, S. and Le Douarin, N. M. (2006) The cephalic neural crest exerts a critical effect on forebrain and midbrain development. *Proc Natl Acad Sci U S A* **103**, 14033-8.

Creuzet, S. E. (2009). Regulation of pre-otic brain development by the cephalic neural crest. *Proc Natl Acad Sci U S A* **106**, 15774-9.

Crossley, P. H., Martinez, S. and Martin, G. R. (1996). Midbrain development induced by FGF8 in the chick embryo. *Nature* **380,** 66-68.

Crossley, P. H., Martinez, S., Ohkubo, Y. and Rubenstein, J. L. (2001). Coordinate expression of *Fgf8*, *Otx2*, *Bmp4*, and *SHH* in the rostral prosencephalon during development of the telencephalic and optic vesicles. *Neuroscience* **108**, 183-206.

Curtin, E., Hickey, G., Kamel, G., Davidson, A. J. and Liao, E. C. (2011). Zebrafish *wnt9a* is expressed in pharyngeal ectoderm and is required for palate and lower jaw development. *Mech Dev* **128**, 104-15.

Dault, S. H. and Smith, D. H. (1969). A quantitative study of the nucleus of the mesencephalic tract of the trigeminal nerve of the cat. *Anat Rec* **165**, 79-88.

De, S., Nguyen, A. Q., Shuler, C. F. and Turman, J. E. Jr. (2005a). Mesencephalic trigeminal nucleus development is dependent on Krox-20 expression. *Dev Neurosci* **27**, 49-58.

De, S. and Turman, J. E. Jr. (2005b). Krox-20 gene expression: Influencing

hindbrain-craniofacial developmental interactions. *Arch Histol Cytol* **68**, 277-234.

Dellow P. G. and Lund J. P. (1971) Evidence for central timing of rhythmical mastication. *J. Physiol.* **215,** 1–13.

Dutton, K. A., Pauliny, A., Lopes, S. S., Elworthy, S., Carney, T. J., Rauch, J., Geisler, R., Haffter, P. and Kelsh, R. N. (2001). Zebrafish *colourless* encodes *sox10* and specifies non-ectomesenchymal neural crest fates. *Development* **128**, 4113-25.

Dykes, I. M., Lanier, J., Eng, S. R. and Turner, E. E. (2010). Brn3a regulates neuronal subtype specification in the trigeminal ganglion by promoting Runx expression during sensory differentiation. *Neural Dev* **5**, 3.

Easter, S. S. Jr. and Taylor, J. S. H. (1989). The development of the *Xenopus* retinofugal pathway: optic fibers join a pre-existing tract. *Development* **107**, 553-73.

Easter, S. S. Jr., Ross, L. S. and Frankfurter, A. (1993) Initial tract formation in the mouse brain. *J Neurosci* **13**, 285-99.

Ellies, D. L., Stock, D. W., Hatch, G., Giroux, G., Weiss, K. M. and Ekker, M. (1997). Relationship between the genomic organization and the overlapping embryonic expression patterns of the zebrafish *dlx* genes. *Genomics* **45**, 580-90.

Eng, S., Gratwick, K., Rhee, J., Fedtsova, N., Gan, L. and Turner, E. (2001). Defects in sensory axon growth precede neuronal death in Brn3a deficient mice. *J Neurosci* **21**, 541-549.

Eng, S. R., Lanier, J., Fedtsova, N. and Turner, E. E. (2004). Coordinated regulation of gene expression by Brn3a in developing sensory ganglia. *Development* **131**, 3859-70.

Ensor, E., Smith, M. D. and Latchman, D. S. (2001). The BRN-3A transcription factor protects sensory but not sympathetic neurons from programmed cell death/apoptosis. *J Biol Chem* **276**, 5204-12.

Ericson, J., Thor, S., Edlund, T., Jessell, T. and Yamada, T. (1992). Early stages of motor neuron differentiation revealed by expression of homeobox gene *Islet-1*. *Science* **256**, 1555-1560.

Fan, G., Copray, S., Huang, E. J., Jones, K., Yan, Q., Walro, J., Jaenisch, R. and Kucera, J. (2000) Formation of a full complement of cranial proprioceptors requires multiple neurotrophins. *Dev Dyn* **218**, 359-70

Fedtsova, N. and Turner, E. E. (1997). Inhibitory effects of ventral signals on the development of Brn-3.0 – expressing neurons in the dorsal spinal cord. *Dev Biol* **190**, 18-31.

Fedtsova, N. and Turner, E. E. (2001). Signals from the ventral midline and isthmus regulate the development of Brn3.0 – expressing neurons in the midbrain. *Mech Dev*

105, 129-44.

Foote, S. L., Bloom, F. E. and Aston-Jones, G. (1983). Nucleus locus coeruleus: new evidence of anatomical and physiological specificity. *Physiol Rev* **63**, 844–914.

Gammill, L. S. and Bronner-Fraser, M. (2003). Neural crest specification: migrating into genomics. *Nat Rev Neurosci* **4**, 795-805.

Gamse, J. and Sive, H. (2000). Vertebrate anteroposterior patterning: the *Xenopus* neuroectoderm as paradigm. *Bioessays* **22**, 976-86.

Geling, A., Itoh, M., Tallafuss, A., Chapouton, P., Tannhäuser, B., Kuwada, J. Y., Chitnis, A. B. and Bally-Cuif, L. (2003). bHLH transcription factor Her5 links patterning to regional inhibition of neurogenesis at the midbrain-hindbrain boundary. *Development* **130**, 1591-604.

Geling, A., Plessy, C., Rastegar, S., Strahle, U., Bally-Cuif, L. (2004). Her5 acts as a prepattern factor that blocks *neurogenin1* and *coe2* expression upstream of Notch to inhibit neurogenesis at the midbrain-hindbrain boundary. *Development* **131**, 1993-2006.

Gerety, S. S. and Wilkinson, D. G. (2011). Morpholino artifacts provide pitfalls and reveal a novel role for pro-apoptotic genes in hindbrain boundary development. *Dev Biol* **350**, 279-289.

Gilmour, D. T., Maischein, H. M. and Nusslein-Volhard C. (2002). Migration and function of a glial subtype in the vertebrate peripheral nervous system. *Neuron* **34**, 577-88.

Glinka, A., Wu, W., Delius, H., Monaghan, A. P., Blumenstock, C. and Niehrs, C. (1998). Dickkopf-1 is a member of a new family of secreted proteins and functions in head induction. *Nature* **391**, 357-62.

Grocott, T., Johnson, S., Bailey, A. P. and Streit, A. (2011). Neural crest cells organize the eye via TGF-ß and canonical Wnt signalling. *Nat Commun* **2**, 265.

Graham, A. and Begbie, J. (2000). Neurogenic placodes: a common front. *Trends Neurosci* **23**, 313-6.

Haddon, C., Smithers, L., Schneider-Maunoury, S., Coche, T., Henrique, D. and Lewis, J (1998). Multiple delta genes and lateral inhibition in zebrafish primary neurogenesis. *Development* **125**, 359-370.

Hamburger, V., Hamilton, H. L. (1951). A series of normal stages in the development of the chick embryo. *J Morphol* **88**, 49-52.

Hatta, K., Tsujii, H. and Omura, T. (2006). Cell tracking using a photoconvertible fluorescent protein. *Nat Protoc* **1**, 960-67

Hatton, G. I. and Yang, Q. Z. (1989). Supraoptic nucleus afferents from the main

olfactory bulb-II. Intracellularly recorded responses to lateral olfactory tract stimulation in rat brain slices. *Neuroscience* **31**, 289-97.

Hayakawa, T. and Zyo, K. (1989). Retrograde double-labelling study of the mammillothalamic and the mammillotegmental projections in the rat. *J Comp Neurol* **284**, 1-11

Hayar, A., Poulter, M. O., Pelkey, K., Feltz, P. and Marshall, K.C. (1997). Mesencephalic trigeminal neuron responses to $-aminobutyric acid. *Brain Res* **753**, 120–127.

He, X., Treacy, M. N., Simmons, D. M., Ingraham, H. A., Swanson, L. W. and Rosenfeld, M. G. (1989). Expression of a large family of POU-domain regulatory genes in mammalian brain development. *Nature* **340**, 35-41.

Heisenberg, C. P., Brand, M., Jiang, Y. J., Warga, R. M., Beuchle, D., van Eeden, F. J., Furutani-Seiki, M., Granato, M., Haffter, P., Hammerschmidt, M., Kane, D. A., Kelsch, R. N., Mullins, M. C., Odenthal, J. and Nusslein-Volhard, C. (1996). Genes involved in forebrain development in the zebrafish, *Danio rerio*. *Development* **123,** 191-203

Heisenberg, C. P., Houart, C., Take-Uchi, M., Rauch, G. J., Young, N., Coutinho, P., Masai, I., Caneparo, L., Concha, M. L., Geisler, R., Dale, T. C., Wilson, S. W. and Stemple, D. L. (2001). A mutation in the GSK3-binding domain of zebrafish *masterblind*/Axin1 leads to a fate transformation of telencephalon and eyes to diencephalon. *Genes Dev* **15**, 1427-34

Hemmati-Brivanlou, A. and Melton, D. (1997) Vertebrate neural induction. *Annu Rev Neurosci* **20**, 43-60.

Hemsley, J. P. and Savage, G. E. (1987). Interocular transfer of shape discrimination in the goldfish – a reassessment of the role of the posterior commissure. *Exp Neurol* **98**, 664-672.

Hernandez-Lagunas, L., Choi, I. F., Kaji, T., Simpson, P., Hershey, C., Zhou, Y., Zon, L., Mercola, M. and Artinger, K. B. (2005). Zebrafish *narrowminded* disrupts the transcription factor *prdm1* and is required for neural crest and sensory neuron specification. *Dev Biol* **278**, 347-57.

Higashijima, S., Okamoto, H., Ueno, N., Hotta, Y. and Eguchi, G. (1997). High-frequency generation of transgenic zebrafish which reliably express GFP in whole muscles or the whole body by using promoters of zebrafish origin. *Dev Biol* **192**, 289-99.

Higashijima, S., Hotta, Y. and Okamoto, H. (2000). Visualization of cranial motor

neurons in live transgenic zebrafish expressing green fluorescent protein under the control of the *islet-1* promoter/enhancer. *J Neurosci* **20**, 206-18.

Hinrichsen, C. F. L. and Larramendi, L. M. H. (1969). Features of trigeminal mesencephalic nucleus structure and organization. I. light microscopy. *Am J Anat* **126**, 497-506.

Hippenmeyer, S., Vrieseling, E., Sigrist, M., Portmann, T., Laengle, C., Ladle, D., R. and Arber, S. (2005). A developmental switch in the response of DRG neurons to ETS transcription factor signalling. *PloS*, **3**, e159.

Hippenmeyer, S., Huber, R. M., Ladle, D. R., Murphy, K. and Arber, S. (2007). ETS transcription factor *Erm* controls subsynaptic gene expression in skeletal muscles. *Neuron* **55**, 726-40.

Hiscock, J. and Straznicky, C. (1982). Peripheral and central terminations of axons of the mesencephalic trigeminal neurons in Xenopus. *Neurosci Lett* **32**, 235-40.

Hiscock, J. and Straznicky, C. (1986). The formation of axonal projections of the mesencephalic trigeminal neurones in chick embryos. *J Embryol Exp Morphol* **93**, 281-90

Holland, N. D., Panganiban, G., Henyey, E. L. and Holland, L. Z. (1996). Sequence and developmental expression of *AmphiDll*, an amphioxus Distal-less gene transcribed in the ectoderm, epidermis and nervous system: insights into evolution of craniate forebrain and neural crest. *Development* **122**, 2911–920.

Holland, L. Z. (2009). Chordate roots of the vertebrate nervous system: expanding the molecular toolkit. *Nat Rev Neurosci* **10**, 736-46.

Hollyday, M., McMahon, J. A. and McMahon, A. P. (1995). *wnt* expression patterns in chick embryo nervous system. *Mech Dev* **52**, 9-25.

Hong, E. and Brewster, R. (2006). N-cadherin is required for the polarized cell behaviors that drive neurulation in the zebrafish. *Development* **19**, 3895–3905.

Honig, M. G. and Hume, R. I. (1986). Fluorescent Carbocyanine dyes allow living neurons of identified origin to be studied in long-term cultures. *J Cell Biol* **103**, 171-87.

Hooiveld, M. H., Morgan, R., In Der Rieden, P., Houtzager, E., Pannese, M., Damen, K., Boncinelli, E. and Durston, A., J. (1999). Novel interactions between vertebrate Hox genes. *Int J Dev Biol* **43**, 665-674.

Houart, C., Westerfield, M. and Wilson, S. W. (1998). A small population of anterior cells patterns the forebrain during zebrafish gastrulation. *Nature* **391**, 788-92.

Hoyo-Becerra, C., López-Avalos, M. D., Cifuentes, M., Visser, R., Fernández-Llebrez, P. and Grondona, J. M. (2010). The subcommissural organ and the

development of the posterior commissure in chick embryos. *Cell Tissue Res* **339**, 383-95.

Huang, E. J., Zang, K., Schmidt, A., Saulys, A., Xiang, M. and Reichardt, L. F. (1999). POU domain factor Brn-3a controls the differentiation and survival of trigeminal neurons by regulating Trk receptor expression. *Development* **126**, 2869-82.

Huang, X. and Saint-Jeannet, J. P. (2004). Induction of the neural crest and the opportunities of life on the edge. *Dev Biol* **275**, 1-11.

Huard, H., Lund, J. P., Veilleux, D. and Dubuc, R. (1999). An anatomical study of brainstem projections to the trigeminal motor nucleus of lampreys. *Neuroscience* **91**, 363-78.

Hughes, A. (1957). The development of the primary sensory system in *Xenopus laevis* (Daudin). *J Anat* **91**, 323-38.

Hunt, C. C. (1990). Mammalian muscle spindle: peripheral mechanisms. *Physiol Rev* **70,** 643–663.

Hunter, E., Begbie, J., Mason, I. and Graham, A. (2001). Early development of the mesencephalic trigeminal nucleus. *Dev Dyn* **222**, 484-93.

Ichikawa, H., Qiu, F., Xiang, M. and Sugimoto, T. (2005). *Brn-3a* is required for the generation of proprioceptors in the mesencephalic trigeminal tract nucleus. *Brain Res* **1053**, 203-6.

Iida, C., Oka, A., Moritani M., Kato, T., Haque, T., Sato, F., Nakamura, M., Uchino, K., Seki, S., Bae, Y. C., Takada, K. and Yoshida, A. (2010). Corticofugal direct projections to primary afferent neurons in the trigeminal mesencephalic nucleus of rats. *Neuroscience* **169**, 1739-57.

Inoue, K., Shiga, T. and Ito, Y. (2008). Runx transcription factors in neuronal development. *Neural Dev* **3**, 20.

Ishikawa, Y., Kage, T., Yamamoto, N., Yoshimoto, M., Yasuda, T., Matsumoto, A., Maruyama, K. and Ito, H. (2004). Axongenesis in the medaka embryonic brain. *J Comp Neurol* **476**, 240-53.

Jacobson, A. G. and Sater, A. K. (1988). Features of embryonic induction. *Development* **104**, 341-359.

Jarman, A. P. and Ahmed, I. (1998). The specificity of proneural genes in determining *Drosophila* sense organ identity. *Mech Dev* **76**, 117-25.

Jarman, A. P. (2002). Studies of mechanosensation using the fly. *Hum Molec Genet* **11**, 1215-18.

Jaszai, J., Reifers, F., Picker, A., Langenberg, T. and Brand, M. (2003). Isthmus-to-

midbrain transformation in the absence of midbrain-hindbrain organiser activity. *Development* **130**, 6611-23.

Jho, E. H., Zhang, T., Domon, C., Joo, C. K., Freund, J. N. and Costantini, F. (2002). Wnt/beta-catenin/Tcf signalling induces the transcription of Axin2, a negative regulator of the signalling pathway. *Mol Cell Biol* **22**, 1172-83.

Joyner, A. L., Liu, A. and Millet, S. (2000). *Otx2*, *Gbx2* and *Fgf8* interact to position and maintain a mid-hindbrain organizer. *Curr Opin Cell Biol* **12**, 736-41.

Jüch, P. J. W. (1981). Mechanoreceptive signals processed by mesencephalic trigeminal neurons in the carp. *J Comp Physiol* **141**, 157-62.

Kageyama, R. and Nakanishi, S. (1997). Helix-loop-helix factors in growth and differentiation of the vertebrate nervous system. *Curr Opin Genet Dev* **7**, 659-665.

Kaestner, K. H., Knochel, W. and Martinez, D. E. (2000). Unified nomenclature for the winged helix/forkhead transcription factors. *Genes Dev* **14**, 142-6.

Kawano, Y. and Kypta, R. (2003). Secreted antagonists of the Wnt signalling pathway. *J Cell Sci* **116**, 2627-34.

Keller, R,, Shih, J. and Sater, A. (1992). The cellular basis of the convergence and extension of the Xenopus neural plate. *Dev Dyn* **193**, 199–217.

Kelsh, R. N., Brand, M., Jiang, Y. J., Heisenberg, C. P., Lin, S., Haffter, P., Odenthal, J., Mullins, M. C., van Eeden, F. J., Furutani-Seiki, M., Granato, M., Hammerschmidt, M., Kane, D. A., Warga, R. M., Beuchle, D., Vogelsang, L. and Nusslein-Volhard, C. (1996). Zebrafish pigmentation mutations and the processes of neural crest development. *Development* **123**, 369-89.

Kelsh, R. N. and Eisen, J. S. (2000). The zebrafish *colourless* gene regulates development of non-ectomesenchymal neural crest derivatives. *Development* **127**, 515-25.

Kelsh, R. N., Schmid, B. and Eisen, J. S. (2000). Genetic analysis of melanophore development in zebrafish embryos. *Dev Biol* **225**, 277-93.

Kelsh, R. N. (2006). Sorting out Sox10 functions in neural crest development. *Bioassays* **28**, 788-98.

Kiecker, C. and Lumsden, A. (2005). Compartments and their boundaries in vertebrate brain development. *Nat Rev Neurosci* **6**, 553-64.

Kiecker, C. and Lumsden, A. (2004). Hedgehog signalling from the ZLI regulates diencephalic regional identity. Nat Neurosci **7**, 1242-9.

Kikuta, H., Kanai, M., Ito, Y. and Yamasu, K. (2003). *gbx2* homeobox gene is required for the maintenance of the isthmic region of the zebrafish embryonic brain.

Dev Dyn **228**, 433-450.

Kim, C. H., Ueshima, E., Muraoka, O., Tanaka, H., Yeo, S. Y., Huh, T. L. and Miki, N. (1996). Zebrafish *elav*/HuC homologue as a very early neuronal marker, *Neurosci Lett* **216**, 109–112.

Kim, C. H., Bae, Y. K., Yamanaka, Y., Yamashita, S., Shimizu, T., Fujii, R., Park, H. C., Yeo, S. Y., Huh, T. L., Hibi, M. and Hirano, T. (1997). Overexpression of *neurogenin* induces ectopic expression of HuC in zebrafish. *Neurosci Lett* **239**, 113-6.

Kim, J. D., Chun, H. S., Kim., S. H., Kim., H. S., Kim, Y. S., Kim, M. J., Shin, J., Rhee, M., Yeo, S. Y. and Huh, T. L. (2009). Normal forebrain development may require continual Wnt antagonism until mid-somitogenesis in zebrafish. *Biochem Biophys Res Commun* **381**, 717-21.

Kimmel, C. B., Metcalfe, W. K. and Schabtach, E. (1985). T reticular interneurons: a class of serially repeating cells in the zebrafish hindbrain. *J Comp Neurol* **233**, 365-376.

Kimmel, C. B., Warga, R. .M. and Kane, D. A. (1994). Cell cycles and clonal strings during formation of the zebrafish central nervous system. *Development* **120**, 265–276.

Knecht, A. K. and Bronner-Fraser, M. (2002). Induction of the neural crest: a multigene process. *Nat Rev Genet* **3**, 453-61.

Knight, R. D., Nair, S., Nelson. S. S., Afshar, A., Javidan, Y., Geisler, R., Rauch, G. J., Schilling, T. F. (2003). *lockjaw* encodes a zebrafish *tfap2a* required for early neural crest development. *Development* **130**, 5755-68.

Kollros, J. J. and Thiesse, M. L. (1985) Growth and death of cells of the mesencephalic fifth
nucleus in *Xenopus laevis* larvae. *J Comp Neurol* **233**, 481–489.

Korzh, V., Edlund, T. and Thor, S. (1993). Zebrafish primary neurons initiate expression of the LIM homeodomain protein Isl-1 at the end of gastrulation. *Development* **118**, 417-25

Korzh, V., Sleptsova, I., Liao, J., He, J. and Gong, Z. (1998). Expression of zebrafish bHLH genes *ngn1* and *nrd* defines distinct stages of neural differentiation. *Dev Dyn* **213**, 92-104.

Kramer, I., Sigrist, M., de Nooij, J. C., Taniuchi, I., Jessell, T. M. and Arber, S. (2006). A role for Runx transcription factor signalling in dorsal root ganglion sensory neuron diversification. *Neuron* **49**, 379-93.

Kulesa, P. M., Bailey, C. M., Kasemeier-Kulesa, J. C. and McLennan, R. (2010). Cranial neural crest migration: new rules for an old road. *Dev Biol* **344**, 543-54.

Kunz, Y. W. (2004). Developmental biology of teleost fishes. *Springer*.

Kuratani, S. and Horigome, N. (2000). Developmental morphology of branchiomeric nerves in a cat shark, *Scyliorhinus torazame*, with special reference to rhombomeres, cephalic mesoderm, and distribution patterns of cephalic crest cells. *Zoolog Sci* **17**, 893-909.

Lacalli, T. C. and Kelly, S. J. (2003). Sensory pathways in amphioxus larvae II. Dorsal tracts and translumenal cells. *Acta Zool* **84**, 1-13.

Lacalli, T. C. (2004). Sensory systems in amphioxus: a window on the ancestral chordate condition. *Brain Behav Evol* **64**, 148-62.

Lagutin, O. V., Zhu, C. C., Kobayashi, D., Topczewski, J. Shimamura, K., Puelles, L., Russell, H. R., Russell, H. R., McKinnon, P. J., Solnica-Krezel, L. and Oliver, G. (2003). *Six3* repression of Wnt signalling in the anterior neuroectoderm is essential for vertebrate forebrain development. *Genes Dev* **17**, 368–379.

Lamborghini, J. E. (1980). Rohon-Beard cells and other large neurons in *Xenopus* embryos originate during gastrulation. *J Comp Neurol* **189**, 323-33.

Langenau, D. M., Palomero, T., Kanki, J. P., Ferrando, A. A., Zhou, Y., Zon, L. I. and Look, A. T. (2002). Molecular cloning and developmental expression of *Tlx* (*Hox11*) genes in zebrafish (*Danio rerio*). *Mech Dev* **117**, 243-8.

Larsen., C. W., Zeltser, L. M. and Lumsden, A. (2001). Boundary formation and compartition in the avian diencephalon. *J Neurosci* **21**, 4699-4711.

Lazarov, N. and Usunoff, K. (2003). Descending projections from the trigeminal ganglion and mesencephalic trigeminal nucleus. *Trakia J Sci* **1**, 5-14.

Lazarov, N. (2007) Neurobiology of orofacial proprioception. *Brain Res Rev* **56**, 362-383.

Lee, S. M., Danielian, P. S., Fritzsch, B. and McMahon, A. P. (1997). Evidence that *FGF8* signalling from the midbrain-hindbrain junction regulates growth and polarity in the developing midbrain. *Development* **124**, 959-969.

Lekven, A. C., Buckles, G. R., Kostakis, N. and Moon, R. T. (2003). *wnt1* and *wnt10b* function redundantly at the zebrafish midbrain-hindbrain boundary. *Dev Biol* **254**, 172-87.

Leost, M., Schultz, C., Link, A., Wu, Y. Z., Biernat, J., Mandelkow, E. M., Bibb, J. A., Snyder, G. L., Greengard, P., Zaharevitz, D. W., Gussio, R., Senderowicz, A. M., Sausville, E. A., Kunick, C. and Meijer, L. (2000). Paullones are potent inhibitors of glycogen synthase kinase-3beta and cyclin-dependent kinase 5/p25. *Eur J Biochem* **267**, 5983-94.

Leucht, C., Stigloher, C., Wizenmann, A., Klafke, R., Folchert, A. and Bally-Cuif,

L. (2008). MicroRNA-9 directs late organizer activity of the midbrain–hindbrain boundary. *Nat Neurosci***11**, 641-648.

Lewis, J. (1996). Neurogenic genes and vertebrate neurogenesis. *Curr Opin Neurobiol* **6**, 3-10.

Lewis, K. E., Concordet, J. P. and Ingham, P. W. (1999). Characterisation of a second *patched* gene in the zebrafish *Danio rerio* and the differential response of *patched* genes to Hedgehog signalling. *Dev Biol* **208**, 14-29.

Li, W. and Cornell, R. A. (2007). Redundant activities of Tfap2a and Tfap2c are required for neural crest induction and development of other non-neural ectoderm derivatives in zebrafish embryos. *Dev Biol* **304**, 338-54.

Lie, D. C., Colamarino, S. A., Song, H. J., Désiré, L., Mira, H., Consiglio, A., Lein, E. S., Jessberger, S., Lansford, H., Dearie, A. R. and Gage FH. Wnt signalling regulates adult hippocampal neurogenesis. *Nature* **437**, 1370-5.

Linker, C. and Stern, C. D. (2004). Neural induction requires BMP inhibition only as a late step, and involves signals other than FGF and Wnt antagonists. *Development* **131**, 5671-81.

Lister, J. A., Cooper, C., Nguyen, K., Modrell, M., Grant, K. and Raible, D. W. (2006). Zebrafish Foxd3 is required for the development of a subset of neural crest derivatives. *Dev Biol* **290**, 92-104.

Livet, J., Sigrist, M., Stroebel, S., De Paola, V., Price, S. R., Henderson, C. E., Jessell, T. M. and Arber, S. (2002). ETS gene *Pea3* controls the central position and terminal arborization of specific motor neuron pools. *Neuron* **35**, 877-92.

Logan, C., Wingate, R. J., McKay, I. J. and Lumsden, A. (1998). *Tlx-1* and *Tlx-3* homeobox gene expression in cranial sensory ganglia and hindbrain of the chick embryo: markers of patterned connectivity. *J Neurosci* **18**, 5389-402

Lowery, L. A. and Sive, H. (2004). Strategies of vertebrate neurulation and a re-evaluation of teleost neural tube formation. *Mech Dev* **121**, 1189-97

Luiten, P. G. (1979). Proprioceptive reflex connections of head musculature and the mesencephalic trigeminal nucleus in the carp. *J Comp Neurol* **183**, 903-12.

Luiten, P. G. and van der Pers, J. N. (1977). The connections of the trigeminal and facial motor nuclei in the brain of the carp (*Cyprinus carpio L.*) as revealed by anterograde and retrograde transport of horseradish peroxidase. *J Comp Neurol* **174**, 575-90.

Lumsden, A. and Krumlauf, R. (1996). Patterning the vertebrate neuraxis. *Science* **274**, 1109-15.

Lun, K. and Brand, M. (1998). A series of *no isthmus* (*noi*) alleles of the zebrafish *pax2.1* gene reveals multiple signalling events in development of the midbrain-hindbrain boundary. *Development* **125**, 3049-62.

Lund, J. P. (1991) Mastication and its control by the brainstem. *Crit Rev Oral Biol Med* **2,** 33–64.

Luo, P., Zhang, J., Yang, R. and Pendlebury, W. (2006). Neuronal circuitry and synaptic organisation of trigeminal proprioceptive afferents mediating tongue movement and jaw-tongue coordination via hypoglossal premotor neurons. *Eur J Neurosci* **23**, 3269-83.

Ma, Q., Kintner, C. and Anderson, D. (1996). Identification of *neurogenin*, a vertebrate neuronal determination gene. *Cell* **87**, 43–52.

Ma, Q., Fode, C., Guillemot, F. and Anderson, D. J. (1999). NEUROGENIN1 and NEUROGENIN2 control two distinct waves of neurogenesis in developing dorsal root ganglia. *Genes Dev* **13**, 1717-28.

Macara, I. G. (2004) Parsing the polarity code. *Nature Rev Mol Cell Biol* **5**, 220-231.

Machon, O., Backman, M., Machonova, O., Kozmik, Z., Vacik, T., Andersen, L. and Krauss, S. (2007). A dynamic gradient of Wnt signalling controls initiation of neurogenesis in the mammalian cortex and cellular specification in the hippocampus. *Dev Biol* **311**, 223-37.

Maeda, N., Miyoshi, S. and Toh, H. (1983). First observation of a muscle spindle in fish. *Nature* **302**, 61-62.

Mallatt, J. (1996). Ventilation and the origin of jawed vertebrates: a new mouth. *Zool J Linn Soc* **117**, 329-404.

Mameli, O., Stanzani, S., Mulliri, G., Pellitteri, R., Caria, M. A., Russo, A. and De Riu, P. (2010). Role of the trigeminal mesencephalic nucleus in rat whisker pad proprioception. *Behav Brain Funct* **6**, 69.

Manni, E., Bortolami, R. and Azzena, G. B. (1965). Jaw muscle proprioception and mesencephalic trigeminal cells in birds. *Exp Neurol* **12**, 320-28.

Marin, F. and Puelles, L. (1994). Patterning of the embryonic avian midbrain after experimental inversions: a polarising activity from the isthmus. *Dev Biol* **163**, 19-37.

Mark, R. F. (1966). The tectal commissure and interocular transfer of pattern discrimination in cichlid fish. *Exp Neurol* **16**, 215-25.

Marmigère, F. and Ernfors, P. (2007). Specification and connectivity of neuronal subtypes in the sensory lineage. *Nat Rev Neurosci* **8**, 114-27.

Martin, S. C., Sandell, J. H. and Heinrich, G. (1998). Zebrafish TrkC1 and TrkC2

receptors define two different cell populations in the nervous system during the period of axonogenesis. *Dev Biol* **195**, 114-30

Martinez, S., Crossley, P. H., Cobos, I., Rubenstein, J. L. and Martin, G. R. (1999) *FGF8* induces formation of an ectopic isthmic organizer and isthmocerebellar development via a repressive effect on *Otx2* expression. *Development* **126**, 1189-200.

Masai, I., Heisenberg, C. P., Barth, K. A., Macdonald, R., Adamek, S. and Wilson, S. W. (1997) *floating head* and *masterblind* regulate neuronal patterning in the roof of the forebrain. *Neuron* **18**, 43-57.

Mastick, G. S. and Easter, S. S. Jr. (1996). Initial organization of neurons and tracts in the embryonic mouse fore- and midbrain. *Dev Biol* **173**, 79-94.

Mastick, G. S., Fan, C. M., Tessier-Lavigne, M., Serbedzija, G. N., McMahon, A. P., Easter, S. S. Jr. (1996). Early deletion of neuromeres in *Wnt-1-/-* mutant mice: evaluation by morphological and molecular markers. *J Comp Neurol* **374**, 246-58.

Mastick, G. S., Davis, N. M., Andrew, G. L. and Easter, S. S. J. (1997). *Pax-6* functions in boundary formation and axon guidance in the embryonic mouse forebrain. *Development* **124**, 1985–1997.

Matesz, C. (1981). Peripheral and central distribution of fibres of the mesencephalic trigeminal root in the rat. *Neurosci Lett* **27**, 13-17.

Matsunaga, E, Katahira, T. and Nakamura, H. (2002). Role of Lmx1b and Wnt1 in mesencephalon and metencephalon development. *Development* **129**, 5269-77.

Matsuo, S., Ichikawa, H., Silos-Santiago, I., Arends, J. J., Henderson, T. A., Kiyomiya, K., Kurebe, M. and Jacquin, M.F. (2000). Proprioceptive afferents survive in the masseter muscle of trkC knockout mice. *Neuroscience* **95**, 209-16.

McCormick, L. J., Hutt, J. A., Hazan, J., Houart, C. and Cohen, J. (2006). The homeodomain transcription factor *drg11* is expressed in primary sensory neurons and their putative CNS targets during embryonic development of the zebrafish. *Gene Expr Patterns* **7**, 289-296.

Meek, J. and Schellart, N. A. (1978). A golgi study of goldfish optic tectum. *J Comp Neurol* **182**, 89-122.

Megason, S. G. and McMahon, A. P. (2002). A mitogen gradient of dorsal midline Wnts organizes growth in the CNS. *Development* **129**, 2087-98.

Meijer, L., Flajolet, M. and Greengard, P. (2004). Pharmacological inhibitors of glycogen synthase kinase 3. *Trends Pharmacol Sci* **25**, 471-80.

Mill, P. J. (1976). Structure and Function of proprioceptors in the invertebrates, first edition. *Chapman and Hall*.

Millet, S., Campbell, K., Epstein, D. J., Losos, K., Harris, E. and Joyner, A. L. (1999). A role for *Gbx2* in repression of *Otx2* and positioning the mid/hindbrain organizer. *Nature* **401**, 161–164.

Minchin, J. E. and Hughes, S. M. (2008). Sequential actions of Pax3 and Pax7 drive xanthophore development in zebrafish neural crest. *Dev Biol* **317**, 508-22.

Mohammadi, M., McMahon, G., Sun, L., Tang, C., Hirth, P., Yeh, B. K., Hubbard, S. R. and Schlessinger, J. (1997). Structures of the tyrosine kinasse domain of fibroblast growth factor receptor in complex with inhibitors. *Science* **276**, 955-60.

Molina, G. A., Watkins, S. C. and Tsang, M. (2007). Generation of FGF reporter transgenic zebrafish and their utility in chemical screens. *BMC Dev Biol* **7**, 62-75.

Molle, K. D., Chédotal, A., Rao, Y., Lumsden, A. and Wizenmann, A. (2004). Local inhibition guides the trajectory of early longitudinal tracts in the developing chick brain. *Mech Dev* **121**, 143-56.

Mundell, N. A. and **Labosky,** P. A. (2011). Neural crest stem cell multipotency requires Foxd3 to maintain neural potential and repress mesenchymal fates. *Development* **138**, 641-52.

Narayanan, C. H. and Narayanan, Y. (1978). Determination of the embryonic origin of the mesencephalic nucleus of the trigeminal nerve in birds. *J Embryol Exp Morphol* **43**, 85-105.

Nauta, H. J. W, Pritz, M. B. and Lasek, R. J. (1974). Afferents to the rat caudoputamen studied with horseradish preoxidase. An evaluation of a retrograde neuroanatomical research method. *Brain Res* **67**, 219-238.

Nieuwenhuys, R. (1972). Topological analysis of the brain stem of the lamprey, *Larnpetra fluuiatilis*. *J Comp Neurol* **145**, 165-178.

Ninkovic, J., Tallafuss, A., Leucht, C., Topczewski, J., Tannhäuser, B., Solnica-Krezel, L, and Bally-Cuif, L. (2005). Inhibition of neurogenesis at the zebrafish midbrain-hindbrain boundary by the combined and dose-dependent activity of a new hairy/E(spl) gene pair. *Development* **132**, 75-88.

Northcutt, R. G. (1979). Experimental determination of the primary trigeminal projections in lampreys. *Brain Res* **163**, 323-327.

Nozue, A. T. (1988). Relationships between neural crest cells and mast cells in newborn mice. *Anat Anz* **166**, 219-25.

Nural, H. F. and Mastick, G. S. (2004). Pax6 guides a relay of pioneer longitudinal axons in the embryonic mouse forebrain. *J Comp Neurol* **479**, 399-409.

Nguyen, V. H., Trout, J., Connors, S. A., Andermann, P., Weinberg, E. and

Mullins, M. C. (2000). Dorsal and intermediate neuronal cell types of the spinal cord are established by a BMP signalling pathway. *Development* **127**, 1209-1220.

Oakley, R. A. and Karpinski, B. A. (2002). Target-independent specification of proprioceptive sensory neurons. *Dev Biol* **249**, 255-69.

O'Brien, E. K., d'Alencon, C., Bonde, G., Li, W., Schoenebeck, J., Allende, M. L., Gelb, B. D., Yelon, D., Eisen, J. S. and Cornell, R. A. (2004). Transcription factor Ap-2alpha is necessary for development of embryonic melanophores, autonomic neurons and pharyngeal skeleton in the zebrafish. *Dev Biol* **265**, 246-61.

Okafuji, T., Funahashi, J. and Nakamura, H. (1999). Roles of *Pax-2* in initiation of the chick tectal development. *Brain Res Dev Brain Res* **116**, 41-9.

Olesnicky, E., Hernandez-Lagunas, L. and Artinger, K. B. (2010). *prdm1* regulates *sox10* and *islet1* in the development of neural crest and Rohon-Beard sensory neurons. *Genesis* **48**, 656-66.

Paik, S. K., Kwak, M. K., Ahn, D. K., Kim, Y. K., Kim, D. S., Moon, C., Moritani, M., Yoshida, A. and Bae, Y. C. (2005) Ultrastructure of jaw muscle spindle afferents within the rat trigeminal mesencephalic nucleus. *NeuroReport* **16**, 1561–1564.

Panhuysen, M., Vogt Weisenhorn, D. M., Blanquet, V., Brodski, C., Heinzmann, U., Beisker, W. and Wurst, W. (2004). Effects of *Wnt1* signalling on proliferation in the developing mid-/hindbrain region. *Mol Cell Neurosci* **26**, 101-11.

Papan, C. and Campos-Ortega, J. A. (1994). On the formation of the neural kell and neural tube in the zebrafish Danio (Brachydanio) rerio. *Dev Biol* **203**, 178-186.

Park, H., Yamada, K., Kojo, A., Sato, S., Onozuka, M. and Yamamoto, T. (2009). Drebrin (developmentally regulated brain protein) is associated with axo-somatic synapses and neuronal gap junctions in rat mesencephalic trigeminal nucleus. *Neurosci Lett* **461**, 95-9.

Park, B. Y. and Saint-Jeannet, J. P. (2010). Expression analysis of Runx3 and other Runx family members during *Xenopus* development. *Gene Expr Patterns* **10**, 159-66.

Park, H. C., Kim, C. H., Bae, Y. K., Yeo, S. Y., Kim, S. H., Hong, S. K., Shin, J., Yoo, K. W., Hibi, M., Hirano, T., Miki, N., Chitnus, A. B. and Huh, T. L. (2000). Analysis of upstream elements in the HuC promoter leads to the establishment of transgenic zebrafish with fluorescent neurons. *Dev Biol* **227**, 279-93.

Partsalis, A. M., Highstein, S. M. and Moschovakis, A. K. (1994). Lesions of the posterior commissure disable the vertical neural integrator of the primate oculomotor system. *J Neurophysiol* **71**, 2582-85.

Pfaff, S. L., Mendelsohn, M., Stewart, C. L., Edlund, T. and Jessell, T. M. (1996).

Requirement for LIM homeobox gene *Isl1* in motor neuron generation reveals a motor neuron-dependent step in interneuron differentiation. *Cell* **84**, 309-20.

Pelkey, K. A. and Marshall, K. C. (1998). Actions of excitatory amino acids on mesencephalic trigeminal neurons. *Can J Physiol Pharm* **76**, 900–908.

Perrin, F. E. and Stoeckli, E. T. (2000). Use of lipophilic dyes in studies of axonal pathfinding in vivo. *Microsc Res Tech* **48**, 25-31.

Peters, A. and Vaughn, J. E. (1967). Microtubules and filaments in the axons and astroctyes of early potsnatal rat optic nerves. *J Cell Biol* **32**, 113-9.

Picker, A., Brennan, C., Reifers, F., Clarke, J., Holder, N. and Brand, M. (1999). Requirement for the zebrafish mid-hindbrain boundary in midbrain polarisation, mapping and confinement of the retinotectal projection. *Development* **126,** 2967-2978.

Piperno, G. and Fuller, M. T. (1985). Monoclonal antibodies specific for an acetylated form of α-tubulin recognize the antigen in cilia and flagella from a variety of organisms. *J Cell Biol* **101**, 2085–94.

Pombal, M. A., Alvarez-Otero, R., Rodicio, M. C. and Anadon, R. (1997). A tract-tracing study of the central projections of the mesencephalic nucleus of the trigeminus in the guppy (*Lebistes reticuatus*, teleostei), with some observations on the descending trigeminal tract. *Brain Res Bull* **42**, 111-8.

Pough, H., Janis, C. and Heiser, J. (2009). Vertebrate life. *San Franciso, CA: Pearson Education, Inc.*

Pratt, K. G. and Aizenman C. D. (2009). Multisensory integration in mesencephalic trigeminal neurons in *Xenopus* tadpoles. *J Neurophysiol* **102**, 399-412.

Pritz, M. B. (2010). Forebrain and midbraib fiber tract formation during early development in *Alligator* embryos. *Brain Res* **1313**, 34-44.

Puelles, L. and Rubenstein, J. L. (2003). Forebrain gene expression domains and the evolving prosomeric model. *Trends Neurosci* **26**, 469-476.

Puzdrowski, R. L. (1988). Afferent projections of the trigeminal nerve in the goldfish, Carassius auratus. *J Morphol* **198**, 131-147.

Purves, D., Augustine, G. J. and Fitzpatrick, D. (2001). Neuroscience. 2nd edition. Sunderland (MA): *Sinauer Associates*

Raible, F. and Brand, M. (2001). Tight transcriptional control of the ETS domain factors Erm and Pea3 by Fgf signalling during early zebrafish development. *Mech Dev* **107**, 105-17.

Raible, D. W. and Ungos, J. M. (2006). Specification of sensory neuron cell fate from the neural crest. In neural crest induction and differentiation (ed. Saint-Jeannet, J. P.).

pp.170-180. *Landes Bioscience and Springer Science.*

Rebelo, S., Chen, Z. F., Anderson, D. J. and Lima, D. (2006). Involvement of DRG11 in the development of the primary afferent nociceptive system. *Mol Cell Neurosci* **33**, 236-46.

Reifers, F., Bohli, H., Walsh, E. C., Crossley, P. H., Stainier, D. Y. and Brand, M. (1998). *Fgf8* is mutated in zebrafish *acerebellar* (*ace*) mutants and is required for maintenance of midbrain-hindbrain boundary development and somitogenesis. *Development* **125**, 2381-95.

Rhinn, M. and Brand, M. (2001). The midbrain-hindbrain boundary organizer. *Curr Opin Neurobiol* **11**, 34-42.

Rhinn, M., Lun, K., Amores, A., Yan, Y. L., Postlethwait, J. H. and Brand, M. (2003). Cloning, expression and relationship of zebrafish *gbx1* and *gbx2* genes to Fgf signalling. *Mech Dev* **120**, 919-36.

Rhinn. M., Lun, K., Ahrendt, R., Geffarth, M. and Brand, M. (2009). Zebrafish *gbx1* refines the midbrain-hindbrain boundary border and mediates the Wnt8 posteriorization signal. Neural Dev **4**, 12.

Roberts, B. L. and Witkovsky, P. (1975). A functional analysis of the mesencephalic trigeminal nucleus of the fifth nerve in the selachian brain.

Rokx, J. T. M. and van Willigen, J. D. (1988). Organization of neuronal clusters in the mesencephalic trigeminal nucleus of the rat: fluorescent tracing of temporalis and masseteric primary afferents. *Neurosci Lett* **86**, 21–26.

Ronan, M. (1988). The sensory trigeminal tract of Pacific hagfish. Primary sensory afferent projections and neurons of the tract nucleus. *Brain Behav Evol* **32**, 169-180.

Ross, L. S., Parrett, T. and Easter, S. S. Jr. (1992). Axongenesis and morphogenesis in the embryonic zebrafish brain. *J Neurosci* **12**, 467-482.

Rossi, C. C., Kaji, T. and Artinger, K. B. (2009). Transcriptional control of Rohon-Beard sensory neuron development at the neural plate border. *Dev Dyn* **238**, 931-43.

Roussigné, M. and Blader, P. (2006) Divergence in regulation of the PEA3 family of ETS transcription factors. *Gene Expr Patterns* **6**, 777-82.

Roy, S. and Ng, T. (2004). Blimp-1 specifies neural crest and sensory neuron progenitors in the zebrafish embryo. *Curr Biol* **14**, 1772–1777.

Rubenstein, J. L., Martinez, S., Shimamura, K. and Puelles, L. (1994). The embryonic vertebrate forebrain: the prosomeric model. *Science* **266**, 578–80

Rubenstein, J. L., Shimamura, K., Martinez, S. and Puelles, L. (1998). Regionalization of the prosencephalic neural plate. *Annu Rev Neurosci* **21**, 445-77.

Ruggiero, D. A., Ross, C. A., Kumada, M. and Reis, D. J. (1982). Reevaluation of projections from the mesencephalic trigeminal nucleus to the medulla and spinal cord: New projections. A combined retrograde and anterograde horseradish peroxidase study. *J Comp Neurol* **206**, 278-292.

Sagerström, C.G., Gammill, L.S., Veale, R. and Sive, H. (2005). Specification of the enveloping layer and lack of auto-neuralization in zebrafish embryonic explants. *Dev Dyn* **232**, 85–97.

Sanchez, V., Ferrán, J. L., Pereyra-Alfonso, S., Scicolone, G., Rapacioli, M. and Flores, V. (2002). Developmental changes in the spatial pattern of mesencephalic trigeminal nucleus (Mes5) neuron populations in the developing chick optic tectum. *J Comp Neurol* **448**, 337-48.

Santagati, F. and Rijli, F. M. (2003).. Cranial neural crest and the building of the vertebrate head. *Nat Rev Neurosci* **4**, 806-18.

Sapir, T., Geiman, E. J., Wang, Z., Velasquez, T., Mitsui, S., Yoshihara, Y., Frank, E., Alvarez, F. J. and Goulding, M. (2004). *pax6* and *engrailed1* regulate two distinct aspects of renshaw cell development. *J Neurosci* **24**, 1255-64

Sato, T., Hamaoka, T., Aizawa, H., Hosoya, T. and Okamoto, H. (2007). Genetic single-cell mosaic analysis implicates ephrinB2 reverse signaling in projections from the posterior tectum to the hindbrain in zebrafish. *J Neurosci* **27**, 5271-9.

Schoenwolf, G. C. and Smith, J. L. (1990). Mechanisms of neurulation: traditional viewpoint and recent advances. *Development* **109**, 243-270.

Schier, A. F. and Talbot, W. S. (1998). The zebrafish organizer. *Curr Opin Genet Dev* **8**, 464-71.

Schilling, T. F. and Kimmel, C. B. (1997). Musculoskeletal patterning in the pharyngeal segments of the zebrafish embryo. *Development* **124**, 2495-60.

Scholpp, S. and Brand, M. (2003) Integrity of the midbrain region is required to maintain the diencephalic-mesencephalic boundary in zebrafish no isthmus/pax2.1 mutants. *Dev Dyn* **228**, 313-22.

Scholpp, S., Lohs, C. and Brand, M. (2003). Engrailed and Fgf8 act synergistically to maintain the boundary between diencephalon and mesencephalon. *Development* **130**, 4881-93.

Scholpp, S., Wolf, O., Brand, M. and Lumsden, A. (2006). Hedgehog signalling from the zona limitans intrathalamica orchestrates patterning of the zebrafish diencephalon. *Development* **133**, 855-64.

Schwarz, M., Alvarez-Bolado, G., Dressler, G., Urbanek, P., Busslinger, M. and

Gruss, P. (1999). *Pax2/5* and *Pax6* subdivide the early neural tube into three domains. *Mech Dev* **82**, 29–39.

Seidensticker, M. J. and Behrens, J. (2000) Biochemical interactions in the Wnt pathway. *Biochem Biophys Acta* **1495**, 168-82.

Shih, J. and Fraser, S. E. (1996). Characterising the zebrafish organizer: microsurgical analysis at the early shield stage. *Development* **122**, 1313-22.

Shimamura, K. and Rubenstein, J. L. (1997). Inductive interactions direct early regionalization of the mouse forebrain. *Development* **124**, 2709–2718

Smith, J. L. and Schoenwolf, G. C. (1989). Notochordal induction of cell wedging in the chick neural plate and its role in neural tube formation. *J Exp Zool* **250,** 49-62.

Sommer, L., Ma, Q. and Anderson, D. J. (1996). *neurogenins*, a novel family of *atonal*-Related bHLH transcription factors, are putative mammalian neuronal determination genes that
reveal progenitor cell heterogeneity in the developing CNS and PNS. *Mol Cell Neurosci* **8**, 221-41.

Spemann, H. and Mangold, H. (1924). Über induction von embryonalanlagen durch implantation artfremder organisatoren. *Archiv für Mikroskopische Anatomie und Entwicklungsmechanik*, **100**, 599-638. Read in English translation by Viktor Hamburger, republished in 2001 by *Int J Dev Biol* **45**, 13-38.

Stainier, D. Y. and Gilbert, W. (1989). The monoclonal antibody B30 recognizes a specific neuronal cell surface antigen in the developing mesencephalic trigeminal nucleus of the mouse. *J Neurosci* **9**, 2468-85.

Stainier, D. Y. and Gilbert, W. (1990). Pioneer neurons in the mouse trigeminal sensory system. *Proc Natl Acad Sci USA* **87**, 923-7.

Stainier, D. Y. and Gilbert, W. (1991). Neuronal differentiation and materation in the mouse trigeminal sensory system, in vivo and in vitro. *J Comp Neurol* **11**, 300-12.

Stanic, K., Montecinos, H. and Caprile, T. (2010). Subdivisions of chick diencephalic roof plate: implication in the formation of the posterior commissure. *Dev Dyn* **239**, 2584-93.

Stoick-Cooper, C. L., Weidinger, G., Riehle, K. J., Hubbert, C., Major, M. B., Fausto, N. and Moon, R. T. (2007). Distinct Wnt signalling pathways have opposing roles in appendage regeneration. *Development* **134**, 479-89.

Storm, E. E., Rubenstein, J. L. and Martin, G. R. (2003). Dosage of *Fgf8* determines whether cell survival is positively or negatively regulated in the developing forebrain. *Proc Natl Acad Sci USA* **100**, 1757–1762.

Strahle, U. and Blader, P. (1994). Early neurogenesis in the zebrafish embryo. *FASEB J* **8**, 692-8.

Streit, A., Berliner, A. J., Papanayotou, C., Sirulnik, A. and Stern, C. D. (2000). Initiation of neural induction by FGF signalling before gastrulation. *Nature* **406**, 74-8.

Sun, Y., Dykes, I. M., Liang, X., Eng, S. R., Evans, S. M. and Turner, E. E. (2008). A central role for Islet1 sensory neuron development linking sensory and spinal gene regulatory programs. *Nat Neurosci* **11**, 1283-93.

Suzuki-Hirano, A. and Shimogori, T. (2009). The role of Fgf8 in telencephalic and diencephalic patterning. *Semin Cell Dev Biol* **20**, 719-25

Takahashi, K. and Ninomiya, T. (1987). Morphological changes of dorsal root ganglion cells in the process-forming period. Prog Neurobiol **29**, 393-410.

Takahashi, T., Shirasu, M., Shirasu, M., Kubo, K. Y., Onozuka, M., Sato, S., Itoh, K. and Nakamura, H. (2010). The locus coeruleus projects to the mesencephalic trigeminal nucleus in rats. *Neurosci Res* **68**, 103-6.

Tallafuss, A. and Bally-Cuif, L. (2003). Tracing of *her5* progeny in zebrafish transgenics reveals the dynamics of midbrain-hindbrain neurogenesis and maintenance. *Development* **130**, 4307-23.

Tanaka, H., Nojima, Y., Shoji, W., Sato, M., Nakayama, R., Ohshima, T. and Okamoto, H. (2011). Islet1 selectively promotes peripheral axon outgrowth in Rohon-Beard primary sensory neurons. *Dev Dyn* **240**, 9-22.

Tawk, M., Araya, C., Lyons, D. A., Reugels, A. M., Girdler, G. C., Bayley, p. R., Hyde, D. R., Tada, M. and Clarke, J. D. (2007). A mirror-symmetric cell division that orchestrates neuroepithelial morphogenesis. *Nature* **446**, 797-800.

Thisse C. and Thisse B. (2008). High-resolution *in situ* hybridisation to whole-mount zebrafish embryos. *Nat Protoc* **3**, 59-69.

Tian, E., Kimura, C., Takeda, N., Aizawa, S. and Matsuo, I. (2002). *Otx2* is required to respond to signals from anterior neural ridge for forebrain specification. *Dev Biol* **242**, 204-223.

Tobin, D. M. and Bargmann, C. I. (2004). Invertebrate nociception: behaviors, neurons and molecules. *J Neurobiol* **61**, 161-74.

Tourtellotte, W. G., Keller-Peck, C., Milbrandt, J. and Kucera, J. (2001). The transcription factor Egr3 modulates sensory axon-myotube interactions during muscle spindle morphogenesis. *Dev Biol* **232**, 388-99.

Trainor, P. A., Melton, K. R. and Manzanares, M. (2003). Origins and plasticity of neural crest cells and their roles in jaw and craniofacial evolution. *Int J Dev Biol* **47**,

541-53.

Turman Jr., J. E. and Chandler, S. H. (1994). Immunohistochemical localisation of glutamate and glutaminase in guinea pig trigeminal premotoneurons. *Brain Res* **634**, 49-61.

Vaglia, J. L. and Hall, B. K. (1999). Regulation of neural crest cell populations: occurrence, distribution and underlying mechanisms. *Int J Dev Biol* **43**, 95-110.

van de Water, S., van de Wetering, M., Joore, J., Esseling, J., Bink, R., Clevers, H. and Zivkovic, D. (2001). Ectopic Wnt signal determines the eyeless phenotype of zebrafish masterblind mutant. *Development* **128**, 3877-88.

Vieira, C., Pombero, A., Garcia-Lopez, R., Gimeno, L., Echevarria, D. and Martinez, S. (2010). Molecular mechanisms controlling brain development: an overview of neuroepithelial secondary organizers. *Int J Dev Biol* **54**, 7-20.

von Bartheld, C. S. (1992) Oculomotor and sensory mesencephalic trigeminal neurons in lungfishes: Phylogenetic implications. *Brain Behav Evol* **39**, 347-263.

von Bartheld, C. S. and Bothwell, M. (1993). Development of the mesencephalic nucleus of the trigeminal nerve in chick embryos: target innervation, neurotrophin receptors, and cell death. *J Comp Neurol* **328**, 185-202.

Waddington, C. H. (1933a). Induction by the primitive streak and its derivatives in the chick. *J. Exp. Biol.* **10**, 38-48.

Wakamatsu, Y., Maynard, T. M. and Weston, J. A. (2000). Fate determination of neural crest cells by NOTCH-mediated lateral inhibition and asymmetrical cell division during gangliogenesis. *Development* **127**, 2811-2821.

Wallingford, J. B., Fraser, S. E. and Harland, R. M. (2002). Convergent extension: the molecular control of polarized cell movement during embryonic development. *Dev Cell* **2**, 695–706.

Wang, C. Z., Shi, M., Yang, L. L., Yang, R. Q., Luo, Z. G., Jacquin, M. F., Chen, Z. F. and Ding, Y. Q. (2007). Development of the mesencephalic trigeminal nucleus requires a paired homeodomain transcription factor, *Drg11*. *Mol Cell Neurosci* **35**, 368-76.

Weinberg, E. (1928). The mesencephalic root of the fifith nerve. A comparative anatomical study. *J Comp Neurol* **46**, 249-405.

Williams, J. A., Barrios, A., Gatchalian, C., Rubin, L., Wilson, S. W. and Holder, N. (2000) Programmed cell death in zebrafish Rohon Beard neurons is influenced by TrkC1/NT-3 signaling. *Dev Biol* **226**, 220-30.

Wilson, S. W., Ross, L. S., Parrett, T. and Easter, S. S. Jr. (1990). The development

of a simple scaffold of axon tracts in the brain of the embryonic zebrafish, *Brachydanio rerio*. *Development* **108**, 121-45.

Wilson, P. A. and Hemmati-Brivanlou, A. (1997). Vertebrate neural induction: inducers, inhibitors, and a new synthesis. *Neuron* **18**, 699-710.

Wilson, S. W. and Houart, C. (2004). Early steps in the development of the forebrain. *Dev Cell* **6**, 167-181.

Wurst, W. and Bally-Cuif, L. (2001) Neural plate patterning: Upstream and downstream of the isthmus organiser. *Nat Rev Neurosci* **2**, 99-108.

Xiang, M., Zhou, L., Macke, J. P., Yoshioka, T., Hendry, S. H., Eddy, R. L., Shows, T. B. and Nathans J (1995). The Brn-3 family of POU-domain factors: primary structure, binding specificity, and expression in subsets of retinal ganglion cells and somatosensory neurons. J Neurosci **15**, 4762-85.

Xiang, M., Gan, L., Zhou, L., Klein, W. H. and Nathans, J. (1996). Targeted deletion of the mouse POU domain gene *Brn-3a* causes selective loss of neurons in the brainstem and trigeminal ganglion, uncoordinated limb movement, and impaired suckling. *Proc Natl Acad Sci USA* **93**, 11950-5.

Yamaguchi, M., Tonou-Fujimori, N., Komori, A., Maeda, R., Nojima, Y., Li, H., Okamoto, H. and Masai, I. (2005). Histone deacetylase 1 regulates retinal neurogenesis in zebrafish by suppressing Wnt and Notch signalling pathways. *Development* **132**, 3027-43.

Yoshihara, Y., Mizuno, T., Nakahira, M., Kawasaki, M., Watanabe, Y., Kagamiyama, H., Jishage, K., Ueda, O., Suzuki, H., Tabuchi, K., Sawamoto, K., Okano, H., Noda, T. and Mori, K. (1999). A genetic approach to visualization of multisynaptic neural pathways using plant lectin transgene. *Neuron* **22**, 33-41.

Zhang, J., Yang, R., Pendlebery, W. and Luo, P. (2005). Monosynaptic circuitry of trigeminal proprioceptive afferents coordinating jaw movement with visceral and laryngeal activities in rats. *Neuroscience* **135**, 147-505.

Zhao, C., He, X., Tian, C. and Meng, A. (2006). Two GC-rich boxes in huC promoter play distinct roles in controlling its neuronal specific expression in zebrafish embryos. *Biochem Biophys Res Commun* **31**, 214-20.

Appendix 1.1 – Data tables showing cell counts of MTN neurons and nTPC expressing *drg11*, in individual animals when Fgf signalling is down-regulated.

Cell counts of MTN neurons and nTPC expressing *drg11* in (A) SU5402 (from 5 ss) treatments and DMSO controls, (B) SU5402 (from 10 ss) treatments and DMSO controls, (C) *ace* mutants and siblings, and (D) *noi* mutants and siblings.

A)

24 hpf *drg11*	DMSO control (MTN)	SU5402 (5 ss) treated (MTN)	DMSO control (nTPC)	SU5402 (5 ss) treated (nTPC)
1	7	10	13	10
2	7	9	10	9
3	5	9	7	10
4	9	12	12	6
5	6	9	7	6
6	8	8	7	7
7	5	9	11	9
8	5	13	5	9
9	5	9	6	9
10	8	8	6	8
Total	65	96	84	83
Mean	6.5	9.6	8.4	8.3

B)

24 hpf *drg11*	DMSO control (MTN)	SU5402 (10 ss) treated (MTN)	DMSO control (nTPC)	SU5402 (10 ss) treated (nTPC)
1	5	10	12	16
2	4	13	11	12
3	4	12	13	13
4	5	10	12	14
5	5	11	10	15
6	4	9	8	13
7	6	11	13	14
8	4	13	14	10
9	5	11	11	13
10	6	8	12	13
Total	48	108	116	133
Mean	4.8	10.8	11.6	13.3

C)

24 hpf *drg11*	*ace* sibling (MTN)	*ace* mutant (MTN)	*ace* sibling (nTPC)	*ace* mutant (nTPC)
1	12	28	15	17
2	11	22	12	18
3	11	21	20	13
4	13	30	13	22
5	11	20	14	20
6	7	22	13	20
7	10	26	13	13
8	10	19	12	17
9	12	19	18	16
10	8	29	14	18
Total	105	236	144	174
Mean	10.5	23.6	14.4	17.4

D)

24 hpf *drg11*	*noi* sibling (MTN)	*noi* mutant (MTN)	*noi* sibling (nTPC)	*noi* mutant (nTPC)
1	9	20	10	10
2	8	17	8	12
3	9	26	8	9
4	5	18	9	13
5	6	22	10	14
6	4	17	9	15
7	6	17	9	11
8	7	18	10	16
9	6	17	8	9
10	8	21	7	10
Total	68	193	88	119
Mean	6.8	19.3	8.8	11.9

Appendix 1.2 – Data tables showing cell counts of MTN neurons and nTPC expressing *isl1*, in individual animals when Fgf signalling is down-regulated.

Cell counts of MTN neurons and nTPC expressing *isl1* in (A) SU5402 (from 5 ss) treatments and DMSO controls, (B) SU5402 (from 10 ss) treatments and DMSO controls, (C) *ace* mutants and siblings, and (D) *noi* mutants and siblings.

A)

24 hpf isl1	DMSO control (MTN)	SU5402 (10 ss) treated (MTN)	DMSO control (nTPC)	SU5402 (10 ss) treated (nTPC)
1	11	16	14	17
2	11	14	10	21
3	6	12	10	14
4	7	13	14	10
5	10	16	12	16
6	7	13	9	17
7	10	16	8	10
8	5	12	13	12
9	9	14	8	12
10	6	13	11	12
Total	82	139	109	141
Mean	8.2	13.9	10.9	14.1

B)

24 hpf *isl1*	*ace* sibling (MTN)	*ace* mutant (MTN)	*ace* sibling (nTPC)	*ace* mutant (nTPC)
1	10	20	15	20
2	9	22	22	15
3	7	27	17	18
4	8	22	14	21
5	8	18	14	18
6	10	14	18	17
7	8	19	16	21
8	9	15	19	21
9	8	16	18	17
10	6	19	12	18
Total	83	192	165	186
Mean	8.3	19.2	16.5	18.6

C)

24 hpf *isl1*	*noi* sibling (MTN)	*noi* mutant (MTN)	*noi* sibling (nTPC)	*noi* mutant (nTPC)
1	6	22	12	15
2	6	16	13	12
3	7	20	10	11
4	9	17	11	14
5	8	19	11	10
6	10	19	11	10
7	8	17	10	12
8	8	20	15	14
9	7	20	10	15
10	7	19	13	10
Total	76	189	116	123
Mean	7.6	18.9	11.6	12.3

Appendix 2.1 – Data tables showing cell counts of MTN neurons and nTPC expressing *drg11*, in individual animals when Wnt signalling is up-regulated.

Cell counts of MTN neurons and nTPC expressing *drg11* in (A) BIO (from 10 ss) treatments and DMSO controls, and (B) *mbl* mutants and siblings,

A)

24 hpf *drg11*	DMSO control (MTN)	BIO treated (MTN)	DMSO control (nTPC)	BIO treated (nTPC)
1	4	15	12	14
2	7	16	13	6
3	5	13	13	15
4	4	15	11	11
5	6	20	14	9
6	5	15	14	7
7	8	12	11	11
8	4	15	13	8
9	8	17	11	9
10	7	19	15	17
Total	58	157	127	107
Mean	5.8	15.7	12.7	10.7

B)

24 hpf *drg11*	*mbl* sibling (MTN)	*mbl* mutant (MTN)	*mbl* sibling (nTPC)	*mbl* mutant (nTPC)
1	9	10	15	18
2	6	13	16	21
3	9	12	16	21
4	6	16	14	22
5	7	9	16	16
6	8	9	16	21
7	8	14	14	19
8	10	13	15	21
9	7	11	12	24
10	9	14	14	24
Total	79	121	148	207
Mean	7.9	12.1	14.8	20.7

Appendix 2.2 – Data tables showing cell counts of MTN neurons and nTPC expressing *isl1*, in individual animals when Wnt signalling is up-regulated.

Cell counts of MTN neurons and nTPC expressing *isl1* in (A) BIO (from 10 ss) treatments and DMSO controls, and (B) *mbl* mutants and siblings.

A)

24 hpf *isl1*	DMSO control (MTN)	BIO treated (MTN)	DMSO control (nTPC)	BIO treated (nTPC)
1	9	17	13	18
2	7	14	18	11
3	6	17	17	15
4	8	11	13	13
5	5	12	12	15
6	7	13	18	11
7	5	12	12	19
8	8	11	17	14
9	6	12	18	11
10	8	14	17	15
Total	69	133	155	142
Mean	6.9	13.3	15.5	14.2

B)

24 hpf *isl1*	*mbl* sibling (MTN)	*mbl* mutant (MTN)	*mbl* sibling (nTPC)	*mbl* mutant (nTPC)
1	9	10	11	14
2	8	10	17	16
3	10	12	16	17
4	8	12	9	19
5	6	10	14	16
6	5	10	16	17
7	9	11	17	18
8	8	14	16	17
9	7	11	15	19
10	8	13	14	18
Total	78	113	145	171
Mean	7.8	11.3	14.5	17.1

Appendix 3 – Data tables showing cell counts of MTN neurons and nTPC expressing *drg11* and *isl1* in individual animals when Wnt signalling is down-regulated.

Cell counts of MTN neurons and nTPC expressing (A) *drg11* in *HS:dkk1* GFP+ and wild type siblings, and (B) *isl1* in *HS:dkk1* GFP+ and wild type siblings.

A)

24h *drg11*	wild type siblings (MTN)	*HS:dkk1* GFP (MTN)	wild type siblings (nTPC)	*HS:dkk* GFP (nTPC)
1	4	1	14	17
2	4	2	14	7
3	6	2	12	8
4	6	3	12	9
5	4	1	15	11
6	4	2	14	10
7	4	1	13	11
8	5	3	13	16
9	5	1	13	10
10	4	2	14	12
Total	46	18	134	111
Mean	4.6	1.8	13.4	11.1

B)

24h *isl1*	wild type siblings (MTN)	*HS:dkk* GFP (MTN)	wild type siblings (nTPC)	*HS:dkk* GFP (nTPC)
1	6	3	17	12
2	6	7	16	12
3	5	4	16	15
4	4	1	16	11
5	4	5	17	16
6	4	0	9	11
7	4	2	12	14
8	8	3	15	10
9	6	2	15	12
10	6	3	9	13
Total	53	30	142	126
Mean	5.3	3	14.2	12.6

Appendix 4.1 – Data tables showing cell counts of MTN neurons and nTPC expressing *drg11* in individual animals when neural crest is ablated.

Cell counts of MTN neurons and nTPC expressing *drg11* in (A) *cls* mutants and siblings, (B) *tfap2a-/c-* morphants, (C) *foxd3-/tfap2a-* morphants, (D) *tfap2a-* morphants alone, (E) *tfap2c-* morphants alone, and (F) *foxd3-* morphants alone and non-injected controls.

A)

26h *drg11*	*cls* sibling (MTN)	*cls* mutant (MTN)	*cls* sibling (nTPC)	*cls* mutant (nTPC)
1	8	10	13	10
2	7	9	14	13
3	10	6	14	11
4	8	7	13	12
5	8	7	14	14
6	5	12	15	14
7	10	12	12	15
8	6	8	13	12
9	6	11	13	13
10	9	10	12	12
Total	77	92	133	126
Mean	7.7	9.2	13.3	12.6

B)

26h *drg11*	non-injected control (MTN)	*tfap2a-/c-* morphant (MTN)	non-injected control (nTPC)	*tfap2a-/c-* morphant (nTPC)
1	7	18	12	28
2	6	17	14	22
3	4	21	11	23
4	7	17	18	28
5	6	15	15	25
6	12	18	17	23
7	5	25	10	26
8	9	17	10	27
9	6	16	16	19
10	6	17	13	26
Total	68	181	136	247
Mean	6.8	18.1	13.6	24.7

C)

26h *drg11*	non-injected control (MTN)	*foxd3-/tfap2a-* morphant (MTN)	non-injected control (nTPC)	*foxd3-/tfap2a-* morphant (nTPC)
1	7	12	10	24
2	7	11	15	22
3	5	16	14	25
4	6	19	16	26
5	10	20	16	19
6	6	15	21	27
7	7	15	16	18
8	10	18	18	25
9	8	17	22	21
10	8	18	16	21
Total	74	161	164	228
Mean	7.4	16.1	16.4	22.8

D)

26h *drg11*	non-injected control (MTN)	*tfap2a-* morphant (MTN)	non-injected control (nTPC)	*tfap2a-* morphant (nTPC)
1	7	8	8	18
2	6	4	10	19
3	10	9	9	17
4	5	5	16	12
5	4	8	18	15
6	6	3	12	16
7	5	8	15	15
8	8	8	16	14
9	6	6	15	20
10	6	4	15	17
Total	63	63	134	163
Mean	6.3	6.3	13.4	16.3

E)

26h *drg11*	non-injected control (MTN)	*tfap2c*-morphant (MTN)	non-injected control (nTPC)	*tfap2c*-morphant (nTPC)
1	7	5	14	12
2	4	4	11	13
3	4	4	14	14
4	5	5	14	10
5	5	5	16	12
6	7	5	11	14
7	6	4	13	15
8	6	6	14	11
9	4	3	11	10
10	4	5	17	17
Total	52	46	135	128
Mean	5.2	4.6	13.5	12.8

F)

26h *drg11*	non-injected control (MTN)	*foxd3*-morphant (MTN)	non-injected control (nTPC)	*foxd3*-morphant (nTPC)
1	7	5	11	12
2	4	5	15	11
3	6	6	13	11
4	5	4	12	13
5	4	4	12	11
6	5	5	14	15
7	4	4	12	12
8	8	6	14	16
9	5	5	12	12
10	6	5	13	12
Total	54	49	128	125
Mean	5.4	4.9	12.8	12.5

Appendix 4.2 – Data tables showing cell counts of MTN neurons and nTPC expressing *isl1* in individual animals when neural crest is ablated.

Cell counts of MTN neurons and nTPC expressing *isl1* in (A) *cls* mutants and siblings, (B) *tfap2a-/c-* morphants, (C) *foxd3-/tfap2a-* morphants, (D) *tfap2a-* morphants alone, (E) *tfap2c-* morphants alone, and (F) *foxd3-* morphants alone and non-injected controls.

A)

26h *isl1*	*cls* sibling (MTN)	*cls* mutant (MTN)	*cls* sibling (nTPC)	*cls* mutant (nTPC)
1	7	10	12	14
2	6	10	16	18
3	9	9	17	12
4	11	9	19	14
5	10	9	19	14
6	9	10	17	14
7	13	6	18	12
8	7	6	13	11
9	9	10	14	14
10	11	8	16	12
Total	92	87	161	135
Mean	9.2	8.7	16.1	13.5

B)

26h *isl1*	Non-injected control (MTN)	*tfap2a-/c-* morphant (MTN)	non-injected control (nTPC)	*tfap2a-/c-* morphant (nTPC)
1	12	17	14	9
2	8	21	15	19
3	11	15	12	13
4	6	20	12	12
5	8	20	15	18
6	9	21	11	20
7	13	18	15	13
8	5	17	15	14
9	6	19	14	27
10	7	24	13	15
Total	85	192	136	160
Mean	8.5	19.2	13.6	16

C)

26h *isl1*	non-injected control (MTN)	*foxd3-/tfap2a-* morphant (MTN)	non-injected control (nTPC)	*foxd3-/tfap2a-* morphant
1	5	27	19	21
2	6	30	17	27
3	6	21	14	19
4	5	29	17	28
5	7	22	19	20
6	9	20	22	21
7	8	24	15	21
8	6	23	20	23
9	8	17	15	20
10	6	23	21	24
Total	66	236	179	224
Mean	6.6	23.6	17.9	22.4

D)

26h *isl1*	non-injected control (MTN)	*tfap2a-* morphant (MTN)	non-injected control (nTPC)	*tfap2a-* morphant (nTPC)
1	7	5	14	16
2	5	7	18	18
3	6	8	15	20
4	8	8	18	17
5	8	8	21	19
6	9	7	21	18
7	7	10	15	16
8	5	4	20	18
9	5	5	20	17
10	6	8	18	18
Total	66	70	180	177
Mean	6.6	7	18	17.7

E)

26h *isl1*	non-injected control (MTN)	*tfap2c*-morphant (MTN)	non-injected control (nTPC)	*tfap2c*-morphant (nTPC)
1	6	6	16	14
2	6	5	17	14
3	7	7	14	14
4	6	5	12	16
5	7	5	14	18
6	5	6	15	20
7	6	5	16	13
8	5	8	12	13
9	5	7	11	18
10	8	10	13	18
Total	61	64	140	158
Mean	6.1	6.4	14	15.8

F)

26h *isl1*	non-injected control (MTN)	*foxd3*-morphant (MTN)	non-injected control (nTPC)	*foxd3*-morphant (nTPC)
1	10	10	22	17
2	10	7	15	15
3	9	7	14	13
4	7	7	14	13
5	7	8	16	13
6	8	7	14	15
7	9	9	17	14
8	6	9	15	17
9	8	7	15	13
10	7	8	14	16
Total	81	79	156	146
Mean	8.1	7.9	15.6	14.6

Appendix 5 – Data tables showing cell counts of MTN neurons expressing *drg11*, in individual animals when neural crest is partially ablated and Fgf signalling down-regulated.

Cell counts of MTN neurons expressing *drg11* in non-injected DMSO controls, non-injected animals treated with 20μM SU5402 and 40uM SU5402. Cells counts of MTN neurons expressing *drg11* in 0.4μM *tfap2a-*/0.2μM *tfap2c-* treated with DMSO, 20μM and 40μM SU5402.

		DMSO	20μM SU5402	40μM SU5402
No morpholino injected	1	5	7	6
	2	4	8	8
	3	4	6	4
	4	5	6	4
	5	5	7	4
	6	4	6	5
	7	6	6	5
	8	4	8	5
	9	5	8	6
	10	6	6	6
0.4μM *tfap2a-*/ 0.2μM *tfap2c-* injected	1	8	10	11
	2	9	12	10
	3	9	10	9
	4	7	8	8
	5	9	7	8
	6	9	10	7
	7	7	13	8
	8	7	8	6
	9	10	12	9
	10	9	12	6